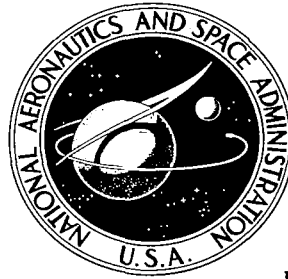


**NASA CONTRACTOR
REPORT**

NASA CR-1650



NASA CR-1650

C. 1



**LOAN COPY: RETURN TO
AFWL (DOGL)
KIRTLAND AFB, N. M.**

**AN ANALYTICAL STUDY OF HYDROGEN
COOLED PANELS FOR APPLICATION
TO HYPERSONIC AIRCRAFT**

*by W. G. Flieder, C. E. Richard, O. A. Buchmann,
and F. M. Walters*

Prepared by
THE GARRETT CORPORATION
Los Angeles, Calif.
for Langley Research Center





0060904

1. Report No. NASA CR-1650		2. Government Accession No.		3. Recipient's Catalog No.	
4. Title and Subtitle AN ANALYTICAL STUDY OF HYDROGEN COOLED PANELS FOR APPLICATION TO HYPERSONIC AIRCRAFT				5. Report Date April 1971	
				6. Performing Organization Code	
7. Author(s) W. G. Flieder, C. E. Richard, O. A. Buchmann, and F. M. Walters				8. Performing Organization Report No. 68-3667	
				10. Work Unit No.	
9. Performing Organization Name and Address AiResearch Manufacturing Company A Division of the Garrett Corporation Los Angeles, California				11. Contract or Grant No. NAS 1-5002-1	
				13. Type of Report and Period Covered Contractor Report	
12. Sponsoring Agency Name and Address National Aeronautics and Space Administration Washington, D.C. 20546				14. Sponsoring Agency Code	
15. Supplementary Notes					
16. Abstract Results of an engineering design study of flat, hydrogen-cooled, structural panels for heat fluxes up to 500 Btu/sec-ft ² (568 kN/m ²) and pressure loads up to 250 psi (1720 kN/m ²) are presented. Three basic conceptual designs with varying degrees of integration of the thermal protection and structural functions of the panel are evolved; minimum panel weights are obtained and the ranges of applicability of the various concepts are established. Included in the appendices are detailed procedures used to analyze and optimize panel design.					
17. Key Words (Suggested by Author(s)) Hydrogen-cooled, structural panels Regeneratively cooled panels Thermal protection			18. Distribution Statement Unclassified - Unlimited		
19. Security Classif. (of this report) Unclassified		20. Security Classif. (of this page) Unclassified		21. No. of Pages 202	22. Price* \$3.00



CONTENTS

	Page
FOREWORD	iii
TABLE OF CONTENTS	v
SUMMARY	1
INTRODUCTION	2
SYMBOLS AND PARAMETERS	3
STATEMENT OF PROBLEM	7
General Problem	7
Environmental Conditions and Design Constraints	7
METHOD OF ANALYSIS	8
RESULTS AND DISCUSSION	9
Concept Screening	9
Concept Evaluation	10
Tradeoff Study	12
CONCLUDING REMARKS	14
APPENDIX A CONCEPT DEFINITION AND SCREENING	17
APPENDIX B CONCEPT EVALUATION GROUND RULES	23
APPENDIX C TRADEOFF STUDY	24
APPENDIX D DESIGN LAYOUT STUDIES	28
APPENDIX E STRUCTURAL ANALYSIS	37
APPENDIX F DESIGN PROCEDURES AND SAMPLE CALCULATIONS	62
APPENDIX G MATERIAL SELECTIONS	82
REFERENCES	85
TABLES	87
ILLUSTRATIONS	121

AN ANALYTICAL STUDY OF HYDROGEN COOLED
PANELS FOR APPLICATION TO HYPERSONIC AIRCRAFT

By W. G. Flieder, C. E. Richard, O. A. Buchmann, and F. M. Walters
The Garrett Corporation
AiResearch Manufacturing Division

SUMMARY

A detailed analytical study was made of conceptual designs for hydrogen cooled flat panels. The work done in this study was part of a comprehensive investigation, comprised of various analytical and experimental studies, intended to define the problems associated with the design and fabrication of structurally efficient regeneratively cooled panels. In this program, the coolant is hydrogen, and the panel loading conditions are representative of the internal and external surfaces of hypersonic aircraft. The design and fabrication requirements of the panels and supporting structure are based on state-of-the-art materials and fabrication techniques.

The study of conceptual designs was performed for a range of heat fluxes from 10 to 500 Btu/sec-ft² (114 to 5680 kW/m²) and for pressure loads from 7 to 250 psi (48 to 1720 kN/m²). A variety of conceptual designs was screened on the basis of configuration weight and coolant consumption, and three representative designs were examined in detail. The three concepts were (1) a single-sandwich configuration in which both the structural load-carrying capability and the coolant containment and flow routing were provided; (2) a composite configuration in which the coolant-pressure-containing surface heat exchanger was metallurgically bonded to the structural load-carrying panel; and (3) a cooled shingle configuration in which the surface heat exchanger was mechanically attached to the low-temperature load-carrying structure.

Configuration weights and coolant requirements were calculated, and the ranges of application of the three concepts (based on minimum weights) were determined. The single-sandwich configuration showed to best advantage at heat fluxes below 100 Btu/sec-ft² (1140 kW/m²) and normal pressures below 50 psi (345 kN/m²). Panel weights for this concept ranged from 1.8 to 4 lb/ft² (9 to 20 kg/m²). For normal pressures greater than about 75 psi (517 kN/m²), the regeneratively cooled shingle was superior. Panel weights for this concept ranged from 5 to 8 lb/ft² (24 to 39 kg/m²). The composite configuration was lightest in the intermediate range and was competitive over a wide range of heat fluxes and pressures.

Detailed procedures used to analyze and optimize the designs are presented in the appendixes to this report. Heat transfer, fluid flow, and manifolding analyses are presented in a related study.

INTRODUCTION

In hypersonic cruise vehicles, one of the basic design problems is temperature control of the structural elements within the limits set by current material technology. For spacecraft and research aircraft that are exposed to the severe thermal environment of hypersonic speeds for a relatively short time, or that can be refurbished after each flight, temperatures have been controlled by either designing the vehicle as a heat sink or using ablative coatings. These methods of thermal protection are not attractive, however, for hypersonic cruise vehicles.

Although major portions of a hypersonic aircraft can and will be radiatively cooled, the radiation equilibrium temperatures will exceed the material limitations in some areas, and some active means of thermal protection will be necessary. A particularly severe condition occurs in the engine and inlet areas where radiation may be blocked, resulting in very high heating. Some form of active cooling is mandatory in these areas. Regenerative cooling is especially attractive for this application because cryogenic hydrogen, which has been proposed as a fuel for the hypersonic cruise vehicle, is also an excellent coolant.

Regenerative cooling has been used successfully for hydrogen-fueled rocket engines, but in contrast to the rocket engine applications that are characterized by small area, high heat fluxes, and short operating times, airbreathing hypersonic cruise aircraft will have large areas of low-to-moderate heat flux and will be expected to operate for much longer periods of time. Consequently, weight considerations and coolant conservation become paramount for these vehicles.

To investigate the problems associated with the design and fabrication of efficient regeneratively cooled structural panels, a comprehensive study program was initiated. The analytical studies described in this report and those reported in reference 1 were parallel efforts performed as part of this investigation. Reference 1 presents the results of (1) analytical studies of the heat transfer and fluid flow performance of flat, hydrogen-cooled heat exchanger panels and (2) analytical and experimental studies of associated manifolding systems. The results presented in this report are for analytical studies of a wide array of conceptual designs for flat, hydrogen-cooled structural panels. The assumed operating conditions included heat fluxes of 10 to 500 Btu/sec-ft² (114 to 5680 kW/m²) and normal pressures of 7 to 250 psi (48 to 1720 kN/m²). The studies were concerned with the structural and heat transfer design problems of the various panel concepts. Procedures were developed that were used to integrate the heat transfer and structural designs and to minimize the configuration weight.

Numerical results for three concepts are presented to indicate variations in panel weight and coolant flow rate in response to changes in heat flux, pressure load, and coolant outlet temperature. The range of applicability of each of the three concepts is indicated with minimum weight as a criterion. Although no specific applications were investigated, the data obtained can be directly useful in vehicle and engine design.

SYMBOLS AND PARAMETERS

A	~ area, ft ² (m ²)
A _f	~ flow area, ft ² (m ²)
Al	~ aluminum
a	~ length, in. (cm)
b	~ length, fin or web spacing, width, in. (cm)
C _L	~ centerline
C _{bm}	~ beam merit parameter, in. ^{4/3} /lb ^{2/3} (m ^{4/3} /N ^{2/3})
C _{pl}	~ panel merit parameter, in./lb ^{1/2} (m/N ^{1/2})
c	~ length, beam spacing, in. (cm)
D	~ diameter, in. (cm); stiffness, in. ² (m ²); OD = outside diameter
d	~ length, beam spacing, in. (cm)
E	~ elastic modulus, psi (kN/m ²)
F	~ force, lb (N)
G	~ shear modulus, psi (kN/m ²)
H	~ enthalpy, Btu/lb (J/g); hydrogen
h	~ height, spacing, in. (cm)
Inco	~ Inconel
K	~ buckling coefficient
k	~ thermal conductivity, Btu/hr-°R-ft (W/m-°K)
l, ℓ	~ panel length, in. (cm)
l _{fin}	~ effective length, in. (cm)
M, m	~ applied moment, lb-in. (N-m) or lb-in./in. (N-m/m)
N	~ number of cycles to failure, number, number of fins/unit width
P, p	~ pressure, psi or psia (kN/m ²)
Q, q	~ heat transfer rate, Btu/sec (kW)

R	~ plain rectangular fin
RA	~ reduction in area
RO	~ rectangular offset fin
r_h	~ hydraulic radius, in. (cm)
Sn	~ tin
T	~ temperature, °R (°K)
T_{DMW}	~ design maximum wall temperature = $T_{CO} + \Delta T_{fin} + 2/3 (\Delta T_{wall})$, °R (°K)
t	~ thickness, in. (cm)
\bar{t}	~ effective thickness, in. (cm)
W	~ flow rate, lb/sec (kg/s)
w	~ width, in. (cm)
X	~ general unknown variable
Y	~ general unknown variable
Z, z	~ section modulus, in. ³ (m ³) or in. ³ /in. (m ³ /m)
α	~ thermal expansion coefficient, in./in.-°F (m/m-°K)
β	~ beam and panel relative weight
γ	~ material density, lb/in. ³ (kg/m ³)
Δ	~ change in, increment of
∇	~ differential operation
δ	~ buckling coefficient ratio
ϵ	~ strain, in./in. (m/m)
η	~ plasticity reduction factor
θ	~ triangular fin angle, degrees
ν	~ Poisson's ratio
σ	~ stress, psi (kN/m ²)

τ ~ shear stress, psi (kN/m²)
 ϕ ~ stress function, lb (N)
 Ω ~ $[1/(1 - \nu)] (E \alpha T)$, psi (kN/m²)

Subscripts:

a ~ allotted, allowable
all ~ allowable
b ~ boundary
bm ~ beam
C ~ coolant
c ~ core
cc ~ critical
F ~ fin tip (location in heat exchanger most remote from aerodynamic surface), flange
f ~ face sheet, fracture
fin ~ fin
H ~ hydrogen
I ~ Inlet
min ~ minimum
O ~ outlet
op ~ operator
opt ~ optimum
p ~ plastic
pl ~ panel
R ~ recovery
ref ~ reference
T ~ total

t ~ tangent

WH ~ aerodynamic heated surface of hot wall

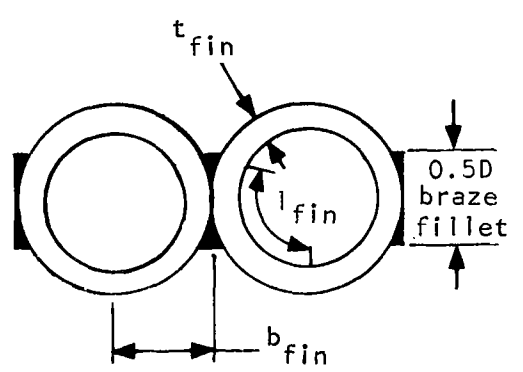
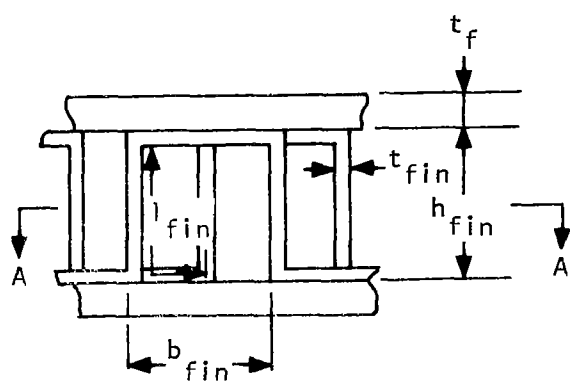
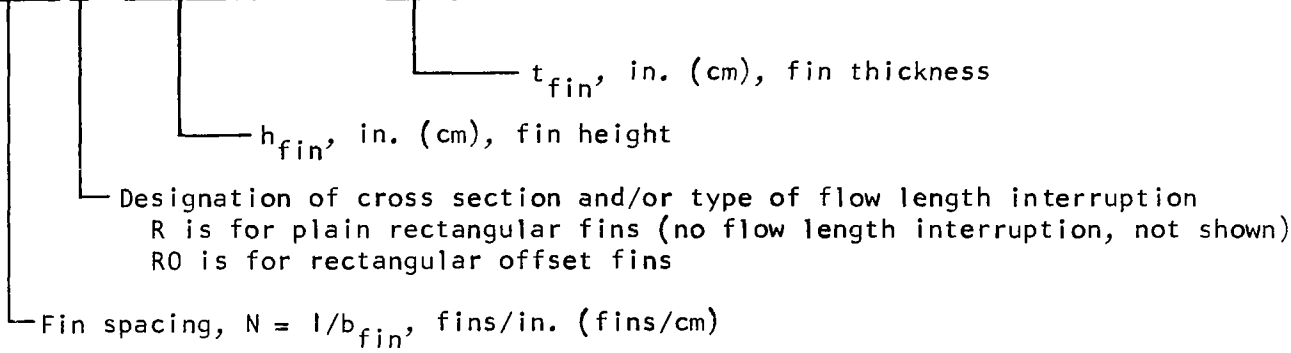
w ~ web

y ~ yield

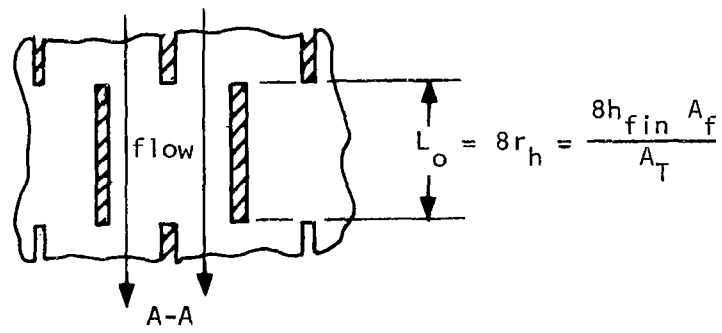
Heat exchanger geometry nomenclature:

Fin geometry is designated with a 4-part nomenclature

20(7.9)R- 0.100(0.254) - 0.004(0.010)



Tubular fins



Rectangular offset fins

STATEMENT OF PROBLEM

General Problem

This study dealt with the definition of regeneratively cooled panel concepts and with the development of supporting analysis techniques. Various configurations of the major panel elements, such as the prime structure and the heat exchanger, were defined, and their specific features and ranges of applicability were determined. The various supporting analyses used to evaluate each configuration involve practical engineering problems of material application and fabrication, structural design and analysis, and heat transfer and fluid-flow analysis. A simplified schematic detailing the considerations involved in the analyses and illustrating some of the interactions of these areas is presented in figure 1. As shown in the figure, outputs of the analyses are the detailed panel designs, panel weights, and coolant requirements.

Environmental Conditions and Design Constraints

The environmental conditions used in the course of the present study were intended to be representative of the conditions that may be experienced on both external and internal (i.e., inlet, duct, and engine wall) surfaces of hypersonic cruise vehicles. The design restraints were those that were thought to be representative of good engineering practice, and they were based on present-day materials and fabrication technology. Limiting conditions used in the study presented herein are as follows:

<u>Variable</u>	<u>Limiting conditions</u>
Static pressure, psi (kN/m ²)	0 to 250 (0 to 1720)
Dynamic pressure, psf (kN/m ²)	0 to 2000 (0 to 96)
Panel size, ft (m)	Up to 3 by 5 (0.91 by 1.52)
Panel configuration	Flat
Coolant	Hydrogen
Cooling method	Forced convection
Operating life	
Creep rupture, hrs	100
Thermal fatigue, cycles	300
Net heat flux, Btu/sec-ft ² (kW/m ²)	0 to 500 (0 to 5680)

Coolant pressure, psi (kN/m ²)	250 to 1400 (1720 to 9650)
Coolant temperature, °R (°K)	100 to 1900 (56 to 1060)

Heating condition.- For the purpose of this study, it was assumed that heating occurred from one side only. Two-sided heating may cause unacceptable thermal stresses and create special coolant control and installation requirements. The use of separate panels placed back-to-back to avoid these problems is then equivalent to one-sided heating of each panel.

Two different heating conditions, uniform and nonuniform heat flux, were considered. For the majority of cases, a uniform heat flux was assumed over the surface of the panel. Because of wall temperature variations along the length of a cooled panel, this condition is approached, for a uniform external environment, only when the recovery temperature becomes very large relative to the wall temperature. Therefore, the term infinite recovery temperature is used herein to refer to the uniform heat flux assumption. For the second heating condition, to account for varying panel surface temperatures, the panel was assumed to be exposed to a hot gas with a uniform finite recovery temperature. In this case, the maximum heat flux (which occurred at the cold end of the panel) was used to define a nominal level of heating.

Coolant pressure.- For this study, a design value of 250 psi (1720 kN/m²) coolant pressure at the exit of the outlet manifold was specified so that the pressure differential would be sufficient to inject the hydrogen into an engine combustor section. The use of supercritical outlet pressures, above 188 psia (1300 kN/m²), allows the assumption of forced-convection single-phase heat transfer coefficients throughout the study. The coolant inlet pressure used was selected to ensure that the necessary coolant flow through the heat exchanger would be produced. The upper limit on inlet pressure was usually taken to be 1000 psi (6890 kN/m²), although inlet pressures up to 1400 psi (9650 kN/m²) were considered.

Coolant temperature.- A hydrogen inlet temperature of 100°F (56°K) was used during this study. It was assumed that hydrogen would be stored at temperatures of 40°F (22°K) or less and would have a temperature increase due to heat leak and/or compressor energy input of about 60°F (33°K). A hydrogen outlet temperature of 1600°F (889°K) was usually assumed, although outlet temperatures from 1400° to 1900°R (778° to 1060°K) were considered.

METHOD OF ANALYSIS

In the initial phase of the investigation, many conceptual designs were quantitatively and qualitatively compared. The principal elements of hydrogen cooled panels were identified, and a number of concepts were selected for a more detailed evaluation. This initial screening is described in Appendix A.

The configurations selected in the initial screening were studied in greater detail at three specific baseline design points that permitted study of

important design features at widely different load/flux conditions. The three baseline design points, identified in figure 2, are indicative of the environments experienced on external and internal surfaces of a hypersonic vehicle. Calculations were carried out to determine panel weights and coolant flow requirements; ground rules for this phase of the investigation are described in Appendix B.

In the final phase of the investigation, three of the concepts were analyzed in detail to obtain tradeoff data. Calculations were carried out for the entire load spectrum considered in this investigation; panel weights and coolant flow requirements were determined with respect to various values of the parameters that affect panel design. The ranges of the calculations for the three conceptual designs are indicated in figure 2. A more detailed description of this phase of the investigation is presented in Appendix C.

Supporting analyses were developed to evaluate the various factors that affect panel design such as design layout studies, structural analysis and optimization methods, and heat transfer and fluid flow analysis. The design layout studies and structural analyses are presented in Appendixes D and E, respectively. The heat transfer and fluid flow analyses are presented in reference 1. These supporting analyses were integrated to develop design procedures that can be applied to specific applications. The development of these procedures and their application to the three baseline panel configurations are presented in Appendix F. Appendix G gives details of material and operating temperature considerations.

RESULTS AND DISCUSSION

Concept Screening

Results of the screening of the basic conceptual configurations considered in the initial phase of the investigation are summarized in tables 1 to 5. The general applicability of a concept or configuration to the overall requirements of regeneratively cooled panels is rated in the tables; the categories of the rating scale are: None, limited, and broad problem range. Table 5 indicates the combination of configurations retained as baseline concepts. Where two configurations represented solutions to the same problem, either the more efficient one was retained for further study or, if they were competitive, one configuration was arbitrarily selected. Certain subconcepts were retained to provide comparisons of heat exchanger and flow arrangement variations.

Table 1 shows five basic panel configurations that could be used with the detailed structural configurations shown in table 2. The initial screening revealed that an unsupported panel structure is always heavier than a beam and panel structure for the normal pressure range considered and that the use of sandwich-construction prime structure and I-beam stiffeners provides the minimum-weight design. Table 3 summarizes the panel flow arrangements that were considered, and table 4 indicates that a wide variety of heat exchanger geometric configurations are applicable. Of the methods studied, the only useful

flow folding arrangement was flow folding in the width dimension of the heat exchanger. It is limited in its expected range of usefulness, however, because of the short flow lengths that are required at high heat fluxes. Table 5 summarizes the configurations that were retained for the concept evaluation. These configurations are illustrated in figures 3 to 5.

Concept 1 (figure 3) utilizes a sandwich panel to provide both structural load-carrying capability and coolant flow passages. Backup I-beams are employed to transmit the loads to the vehicle structure. The flow configuration is a single-pass, straight-through heat exchanger. Concept 1a employs a folded-in-width heat exchanger geometry in which the coolant is carried in opposite directions in alternate flow channels. Concept 2 (figure 4) is a bonded concept which consists of a heat exchanger metallurgically brazed to the prime panel. Concept 2 utilizes single-pass, straight-through flow and rectangular offset-fin geometry. Concept 2a utilizes a folded-in-width heat exchanger. In concept 2b, insulation is added to the surface of a single-pass heat exchanger. Round tubes are used instead of plate fins in the heat exchanger in concept 2c. Concept 3 (figure 5) utilizes a regeneratively cooled shingle that consists of a superalloy heat exchanger surface metallurgically attached to a support panel. Spacer beams are used to mechanically fasten the shingle structure to a prime-load-bearing panel and I-beam structure. The primary panel will be cooled to temperatures that will make an aluminum alloy a suitable material. The primary panel will be protected against bypass hot-gas flow and conductive heat inputs by a metallurgically attached aluminum heat exchanger. This design represents the most clear-cut separation between the primary cooling device and the primary load-bearing structure.

Concept Evaluation

The baseline evaluations were performed at the three design points shown in figure 2 and in the following table.

Design points	Normal pressure		Heat flux		Dynamic pressure	
	psi	kN/m ²	Btu/sec-ft ²	kW/m ²	psf	kN/m ²
1. Low load/ low flux	7	48	10	114	2000	96
2. Intermediate load/inter- mediate flux	100	689	250	2840	2000	96
3. High load/ high flux	250	1720	500	5680	2000	96

Concepts 1, 1a, and 2 were compared at design point 1, and concepts 2, 2a, 2b, 2c, and 3 were compared at design points 2 and 3. The ground rules for the evaluation of these concepts and an outline of the design procedure are presented in Appendix B. The results of the evaluation are summarized in the following paragraphs.

Low-load/low-flux design point.- Table 6 lists the heat exchanger weights prime structural panel weight (concept 2 only), beam weights, manifolding weights (including piping), seal weights, total weights, and coolant flow rates for six cases considered. The results indicate that increased panel length leads to slight reductions in panel weight per unit area because of the decrease in seal and manifold weight per unit area. The influence of the 5000°R (2780°K) recovery temperature on single-pass flow (concept 1) is a reduction in coolant flow of approximately 15 to 20 percent compared with the case for infinite recovery temperature. This reduction in coolant flow rate reflects the lower average heat flux associated with the finite recovery temperature. The assumption of an infinite recovery temperature (uniform heat flux), however, results in only a small change in panel weight.

Intermediate-load/intermediate-flux design point.- The pertinent component weights, total weights, and coolant flow rates are summarized in table 7 for the nine cases considered at the intermediate-load/intermediate-flux design point. As can be seen from the table, concept 3 (nonintegral concept) results in the lowest total weight. Use of round tubes (concept 2c) in place of the plate-fin heat exchanger surface results in a higher heat exchanger weight and up to 18 percent greater coolant flow rate. These increases are due largely to the increase in exposed surface area that the tubular array presents to the hot gas stream, and to a lesser extent, to minimum gage restraints. It should be noted that some of the deficiencies of the round tubes could be alleviated through the use of tubes of other cross-sections. However, any curved surface will always result in a coolant consumption higher than that for a flat surface; and under the minimum gage restrictions of this study, a tube configuration will always be heavier than a plate fin configuration.

Consideration of a finite recovery temperature for concept 2 results in a reduced flow rate compared to the flow rates for infinite recovery temperatures. Further reductions in flow rate are accomplished by using insulation (concept 2b) or flow folding in the width direction (concept 2a).

High-load/high-flux design point.- The pertinent component weights, total weights, and coolant flow rates are summarized in table 8 for the nine cases considered at the high-load/high-flux design point. Concept 3 (nonintegral) shows a marked weight advantage in total weight compared to concept 2 (bonded). As was the case for the intermediate design point, use of a finite recovery temperature for the bonded concept leads to lower coolant flow rates, and further flow reduction is obtained by using insulation or flow folding. Comparison of the results presented in table 7 and 8 illustrates the increases in structural weight, heat exchanger weight, and coolant flow rate that result when the pressure load and heat flux are increased from intermediate to high values. The increased flow length for the high design point shows a slight increase in total weight in contrast to the slight decrease for the intermediate

design point. The net increase is due to an increased heat exchanger weight (the higher coolant flow rate required for the longer panel necessitated a taller fin to avoid excessive pressure losses) which more than offsets the reduction in seal and manifold weight per unit area.

Reference designs for tradeoff analysis.- Concepts 1, 2, and 3 (integral, bonded, and nonintegral, respectively), each with single-pass flow, were retained for the tradeoff analysis. Each of these concepts is advantageous in certain operating ranges. The remaining variations of the concepts discussed above represent refinements or involve modifications of specific design features which may be important in specific applications. Flow folding (concepts 1a and 2a) is a useful method to conserve coolant for low-flux panels. Insulation will always reduce coolant requirements for finite recovery temperatures. The tubular heat exchanger surface (concept 2c) offers lower fluid pressure drop and, hence, the possibility of longer panels for high-flux applications, but the coolant requirement per unit of panel area is increased from that needed with plate-fin construction.

Tradeoff Study

The tradeoff study evaluated the effects of normal pressure and heat flux on panel weight and coolant requirements over the entire load spectrum and investigated the effects of varying coolant outlet temperature, coolant inlet pressure, fin conductivity, and panel size. This analysis was performed on the integral, bonded, and nonintegral designs (concepts 1, 2, and 3) that were selected as the baseline reference designs. The principal results of the tradeoff study were panel weights and coolant flow rates at the specific operating conditions. Appendix C provides a detailed discussion of these results and presents related design curves.

Each of the three concepts has features that favor its use in certain operating ranges. The integral design is the simplest but is limited to a low-heat-flux/low-load environment. The bonded design is the simplest concept that can be applied over the entire heat flux and pressure range. The nonintegral design is the most complex, but it appears to be the most efficient at the high pressure loadings. In addition, thermal protection system for this design can be repaired or replaced without disturbing the basic structure. This may be an important consideration in an actual installation where the exposed surface can be damaged.

Panel weight.- The component element weights resulting from the tradeoff study are tabulated in Appendix C. Some of the resulting calculated weights are illustrated in figures 6 through 8. The weights shown in the figures include the heat exchanger; the structural panel and supporting beams; and allowances for manifolds, plumbing, and pressure seals between panels. The heat flux and the external pressure loading are assumed to be uniform over the surface of the panel.

In figure 6, the weight per unit area for each concept is shown as a function of pressure loading and heat flux. The data are based on a 2-ft by 2-ft

(0.61-m by 0.61-m) panel and are for a hydrogen outlet temperature of 1600°F (889°K). The nearly vertical constant-heat-flux lines indicate that the configuration weights are strong functions of the pressure loading, whereas the nearly horizontal constant-pressure lines indicate that the configuration weights are weak functions of heat flux. As indicated by the general slopes of the curves, the sensitivity of the weight to both of these variables changes somewhat from configuration to configuration; the integral design is the most sensitive to both variables, and the nonintegral design is the least sensitive.

The shaded areas in figure 6 indicate the regions in which a given concept provides the lightest-weight design. The choice of concept for the lightest-weight design is dependent on the particular loading conditions. At the lower pressure loadings, the integral design is indicated to be the lightest by only a small margin. At the higher pressure loadings, the optimum panel-web-faceplate material distribution for bending cannot be attained because the fin heights for this concept are limited by heat transfer considerations. The bonded concept, which is not subject to this restraint, affords the lightest weight over an intermediate pressure range. As the pressure loading increases, the weight for operating the prime structure of the bonded design at high temperatures becomes more severe. At the highest pressure loadings, this weight penalty more than offsets the weight of additional components in the nonintegral design, which then becomes the lightest design.

Plots illustrating the interrelated effects of coolant outlet temperature and external pressure loading on weight are shown in figures 7 and 8 for heat fluxes of 10 and 50 Btu/sec-ft² (114 and 568 kW/m²). As in figure 6, the results indicate that the panel weight is primarily a function of pressure loading, although for the integral and bonded designs, the effects of coolant outlet temperature become increasingly important at higher temperatures and pressures. At lower pressures, the choice of concepts for minimum weight is dependent upon temperature as well as pressure and heat flux. At higher pressure loadings, the choice of concepts is independent of outlet temperature, and the nonintegral design is the lightest. This is to be expected because the prime-load-carrying structure, the major weight factor, remains at a constant temperature regardless of the outlet temperature because it is separate from the primary heat exchanger.

Although the bonded design would be expected to be less sensitive to outlet temperature than the integral design, the data in figures 7 and 8 show similar sensitivities. The degree of sensitivity shown for the bonded design results from nonoptimum use of materials. Material selections for the three conceptual designs were made for a coolant outlet temperature of 1600°R (889°K), and the materials were not varied in the course of the tradeoff studies. At 1600°R (889°K), Inconel 718 is the superior material for a structural panel; at slightly higher temperatures, Waspaloy becomes a better choice. Accordingly, Inconel 718 was selected for the structural panel for the bonded concept because it operated at the coolant outlet temperature, and Waspaloy was selected for the integral design since the hot faceplate must operate at temperatures higher than the coolant outlet temperature. A change of materials, therefore, would improve the performance of the bonded designs at outlet temperatures higher than 1600°R (889°K), and the integral designs could be improved for maximum surface temperatures less than 1600°R (889°K).

Coolant flow rate.- Coolant flow rates shown in figure 9 were calculated from the equation

$$W = \frac{q/A}{H_{CO} - H_{CI}}$$

The coolant flow rates presented in this report are for a hydrogen inlet temperature of 100°R (56°K). The values presented are applicable to any of the concepts studied. For a fixed outlet temperature, these values are dependent solely upon the average net heat flux to which the panel is exposed.

Design tradeoffs.- The final selection of a cooled-panel concept for an actual application involves tradeoffs between panel weight, coolant flow rate, panel life, and other factors that are functions of the specific design mission requirements. Since the final concept selection depends upon the specific details of a particular application, it is beyond the scope of this study. An attempt has been made, however, to provide some of the tools required to make such selections. In particular tradeoffs between configuration weights and coolant requirements are indicated, and a typical result is shown in figure 10 (see also Appendix C).

The data indicated by symbols in figure 10 are for a coolant outlet temperature of 1600°R (889°K), and they illustrate the results of various permutations of the basic bonded design. The results for each permutation should be compared with the results for the basic configuration. By increasing the fin height from the minimum of 0.025 to 0.075 in. (0.064 to 0.191 cm), the temperature of the hot face is increased, thereby decreasing the coolant requirements for a small weight penalty. The panel life, however, is decreased due to an increased temperature difference across the fin height. Flow routing can be used to conserve coolant, and a folded-in-width case is shown in figure 10 for comparison. Although somewhat complicated manifolding is required, the weight and panel-life penalties associated with this configuration are small. The results for an insulated configuration, which also conserves coolant, are for a maximum hot-wall temperature of 2500°R (1390°K). For this configuration, both the coolant reductions and the weight penalties are relatively large. The results for the tubular heat exchanger are for 0.050-in.- (0.127 cm)-dia by 0.010-in.- (0.025-cm)-thick wall round tubes. In this case, although both the weight and the coolant consumption are higher than for the basic configuration, the pressure drop through the panel is lower.

CONCLUDING REMARKS

This report presents the results obtained from a study of hydrogen cooled structural panels. Procedures for the optimization of the design of these panels have been developed and have been applied to various conceptual designs of regeneratively cooled, flat structural panels for heat fluxes from 10 to 500 Btu/sec-ft² (114 to 5680 kW/m²) and pressure loadings from 7 to 250 psi (48 to 1720 kN/m²). Although these procedures are based on certain basic assumptions and guidelines selected for the present study, they can be readily modified to account for different assumptions and guidelines.

Screening of the various configurations considered led to the selection of three basic concepts. The simplest design is the integral concept, which consists of a single-layered sandwich panel that provides the combined function of structural load-carrying capability and fluid-flow passages for the hydrogen coolant. A more complex design is the bonded concept, which consists of a separate heat exchanger brazed to the primary load-carrying panel. The most complex design is the nonintegral concept, which consists of a heat exchanger brazed to a support panel that is in turn mechanically fastened to the primary load-carrying panel.

The three concepts were analyzed at various heat fluxes and pressure loadings and were evaluated on the basis of minimum weight. The integral concept was found to be most efficient only at low levels of heat flux and pressure load. The weight of this concept depended strongly on the pressure loading and heat flux and, to a lesser extent, on the coolant outlet temperature. The upper limit on pressure loading was about 50 psi (345 kN/m²) for a heat flux of 10 Btu/sec-ft² (114 kW/m²) and decreased to about 7 psi (48 kN/m²) as the flux was increased to 100 Btu/sec-ft² (1140 kW/m²). These conditions were also the lower limits of pressure and heat flux for which the bonded concept yielded minimum weights. The upper limit on pressure for the bonded concept was about 75 psi (517 kN/m²) for the entire range of heat flux considered. Above 75 psi (517 kN/m²), the nonintegral concept was the most efficient.

The total optimized weight (including allowances for seals, plumbing, etc.) ranged from 2.5 to 5 lb/ft² (12 to 24 kg/m²) for the integral concept, from 2.8 to 5.7 lb/ft² (14 to 28 kg/m²) for the bonded concept; and from 5.7 to 8 lb/ft² (28 to 39 kg/m²) for the nonintegral concept. The variation in weight for all three concepts depended primarily on the magnitude of the pressure loading.

The study indicates that thermal stresses are of primary concern in the design of regeneratively cooled panels. As a result, large areas of regeneratively cooled surfaces must be composed of a mosaic of panels mounted to permit individual inplane thermal expansion. Provisions must therefore be made for flexible or sliding seals between individual panels, and the design of these seals has been considered in the present investigation. To minimize inplane thermal stresses within the individual panels, the coolant must be routed to avoid nonlinear temperature gradients. This requires careful manifold design to avoid flow maldistributions that can produce large thermal stresses. In general, a single-pass, straight-through heat exchanger with an inlet and outlet manifold for each panel was the simplest design and produced the smallest thermal stresses. In-depth thermal stresses, which are unavoidable, can be minimized only through the use of small coolant passages and high fluid velocities, which in turn leads to high coolant pressure losses. For the range of coolant consumptions and pressure losses considered, the resulting in-depth temperature differentials made thermal fatigue an important problem.

A variety of coolant-passage geometries was considered. Although some differences existed in coolant consumption, configuration weight, and pressure losses, these differences were small for passages sized to provide acceptable in-depth temperature differentials. Coolant pressure containment proved to be a minor problem, and, in general, passage wall thicknesses were dictated by minimum-gage restrictions.

Various methods were considered for reducing coolant consumption including the use of insulation, increased coolant outlet temperatures, and different flow-routing schemes. Each of these methods involves a tradeoff between a weight and/or a configuration life penalty and a potential coolant savings for a particular application. The use of in-width flow folding in the heat exchanger and the application of insulation to the surface adjacent to the hot gas are attractive means of conserving coolant.

Structural optimization indicates that for the range of pressure loadings of interest, beam-panel combinations are lighter than unsupported panels. Except for panels designed for the lightest pressure loadings, panel flutter is not a significant design factor. For these panels, minimum-gage limitations are significant factors that were included in the present analysis.

Material selection is also an important consideration in the design of the regeneratively cooled panel. In addition to the usual requirement for oxidation resistance and high-temperature strength, the selected material must be compatible with the coolant (in this case hydrogen) and with the forming and joining methods employed. The heat exchanger material selection is strongly influenced by the elevated-temperature ductility which is a primary factor in determining thermal fatigue life. Uncoated nickel-base superalloys (notably Waspaloy, Inconel 625, Hastelloy X, and Inconel 718) appear to be the best materials for hydrogen cooled panels.

APPENDIX A

CONCEPT DEFINITION AND SCREENING

A wide variety of conceptual designs were reviewed during the initial phase of the program. After these designs were compared quantitatively and qualitatively, a number were selected for subsequent evaluation. The major objectives of this subtask were identification of the principal elements of regeneratively cooled panels and precise definition of distinctive concepts.

Various configurations were rated in terms of general applicability and specific design features. The configurations that were obviously inferior for the range of study variables were eliminated without reference to specific values of heat flux and applied pressure loading. This approach was not applicable to all configurations, however, and some analysis was necessary at specific design values to complete the screening.

Candidate Configurations

The composite panel structure consists of three distinct functional elements:

- Protective insulation
- Actively cooled heat exchanger surfaces
- Load-carrying structure

A panel concept may include several layers of each of these elements, or, conversely, the functions may be combined. For example, a single-layered sandwich structure could be used for the dual function of carrying normal pressure and of providing hydrogen flow passages. When the structural and heat exchanger surfaces are not combined, the heat transfer surface can be either metallurgically bonded to the prime panel or separated from the prime structural surface by spacer beams.

Four typical composite panel arrangements are shown in figures 11a, b, c, and d. In figure 11a, the hydrogen flows between the webs of a sandwich panel. Figure 11b shows a design in which the heat exchanger surface is integrally bonded to the prime panel surface. Figure 11c illustrates a multilayered insulation and heat transfer surface. In figure 11d, a mechanically attached heat exchanger is shown in which the spacer beams permit large differential expansion between the heat exchanger surface and the structural panel. A secondary heat exchanger is shown in this figure which serves to protect the prime structure from bypass heat.

Insulation

Insulation configurations include a layer of low conductivity material or void space protected by a surface sheet of coated refractory metal or superalloy. Figure 12a shows a layer of insulating material with a thin refractory alloy or superalloy sheet covering, which is in turn held in place by discrete attachments. In figure 12b, an overlapping shingle array of metal plates is shown where the sheets are held in place at their corners. The attachment points consist of one fixed support point combined with a set of slotted and oversized holes to provide support and yet allow for differential expansion of the shingle relative to its hydrogen-cooled surface. Figure 12c shows a metallic plate that is set away from the hydrogen-cooled surface by pin fins. The pin fins hold the metallic sheet and provide a heat path of high thermal resistance. The face sheet can be made from many small elements where the differential expansion between the elements and the hydrogen surface can be absorbed by lateral bending of the pin fins.

Heat Exchanger Geometry

Both heat transfer conductance and coolant frictional pressure losses are important parameters to be considered in the selection of heat exchanger geometries for application to regeneratively cooled panels. High thermal conductance is desired at the higher heat fluxes since in spite of slightly increased coolant requirements, it reduces the in-depth temperature differentials between the hot surface and prime panel surface, improving the thermal fatigue life of the panel (see Appendix E). Low pressure losses are always desirable since they permit longer flow length (hence fewer manifolds) and/or lower pumping and pressure containment requirements.

Two basic types of heat exchanger surfaces are available for consideration. They are the uninterrupted flow or plain fin type; some samples of which are shown in figure 13, and the interrupted flow or offset fin type shown in figure 14. In general the heat exchanger geometries shown in figure 13 exhibit lower pressure losses and better load carrying capabilities but lower thermal conductances than the configurations of figure 14. Thermal conductances of both types of heat exchanger surfaces can be increased by reducing the passage size (thereby increasing the coolant flow velocity) at the expense of increased pressure losses or with relatively slight increases in pressure losses but significant weight increases by plating the fin material with a high conductivity material such as copper. Fabrication of the heat exchanger surfaces is accomplished by joining (usually by brazing) discrete tubes to form tube banks (figures 13a and b) or by metallurgically bounding (again usually by brazing) a preformed core material between face plates to form plate fin heat exchangers such as figure 14.

This study program has been largely centered on the use of a plate fin type heat exchanger using rectangular offset (figure 14a) or plain rectangular (not shown) fins. This choice was dictated primarily because of the versatility of the design since it is relatively easy to vary fin spacing, height, thickness, and offset length to satisfy a wide variety of problem conditions.

Manifold Geometry

Three basic manifold designs were defined during concept screening and these are shown in figure 15. Characteristics of these designs were based on the need for (1) assembly of adjacent panels, (2) the use of edge seals to prevent hot-gas flow into regions in back of the panels, (3) practical fabrication, and (4) low weight. The upper corrugation or fin is the panel fin in all of the designs shown. The flat rectangular and flat tapered configurations are shown in figures 15a and 15b, respectively. The two styles of flat manifolds will have pressure containment provided by fins. Non-uniform resistance can be added in the length of manifold between the inlet or outlet port and the heat exchanger to compensate for the variation in pressure losses that would normally be encountered in the manifold. Cylindrical manifolds of the type shown in figure 15c could be used, but this geometry inherently results in relatively large unsupported spans which must accommodate high internal pressures.

Flow Routing Arrangements

A variety of flow routing arrangements were examined to determine their potential for (1) reducing the pressure drop in the heat exchanger, or (2) reducing the coolant requirements. As indicated in table 3, only two arrangements, the single-pass and the folded-in-width arrangements were retained for further consideration. The other arrangements were discarded due to thermal stresses, complexity and increase weight, or fabrication difficulties.

Pressure drop reduction.- Pressure drop limitations can place restrictions on allowable flow length, but this difficulty can be resolved at least analytically, if the flow length is divided into submultiples of panel length by introducing two or more sets of inlet and outlet manifolds.

Figure 16a shows a design in which there are multiple sets of inlet and outlet manifolds within a single lengthwise section of panel. The hot outlet and cold inlet manifolds are located adjacent to each other, and this causes the sawtooth temperature profile depicted in figure 16a. Thermal stresses in the plane of the panel were computed (see Appendix E) for a temperature discontinuity of 1200°R (670°K) at each sawtooth and the results indicated that panel failure would be imminent after a very few cycles of operation. Thermal stresses can be reduced to acceptable levels by greatly reducing the temperature differential between the inlet and outlet fluid. The maximum permissible temperature differential is approximately 300°R (167°K). This low differential can be achieved in a single panel, however, assuming that a single inlet temperature of 100°R (56°K) (as from cryogenic storage) and a single outlet temperature of up to 2000°R (1110°K) is desired, a series of panels will be required to satisfy the initial and final temperatures. Such a series of panels would lead to weight and pressure drop penalties due to the additional manifolds. This would defeat the purpose of achieving pressure drop reductions and this manifolding approach was not given further consideration.

Figure 16b shows a flow arrangement in which alternating common inlet and outlet manifolds are used. This would produce a triangular temperature profile

along the panel axial direction. Thermal stresses were calculated for this temperature profile, and the results of the stress analysis showed that the continuous alternating triangular profile would produce excessive thermal stresses for a 1200°R (670°K) inlet to outlet temperature rise. Configurations with acceptable thermal stresses could be obtained by limiting the panels to a length to width ratio of 2 or greater and limiting the temperature to a single cycle, i.e.: using a common outlet manifold at the panel midlength with inlet manifolds at the ends or vice versa. However, even with these configurations the resultant thermal stresses would approach 25 to 50 percent of the yield stress of the material.

Stresses for the single pass arrangement are negligibly small (see appendix E). Furthermore, fluid flow calculations of reference 1 indicate that at a heat flux of 500 Btu/sec-ft² (5680 kW/m²) single-pass flow lengths of 2 feet (0.61 m) can be utilized without excessive pressure losses and at lower fluxes panel lengths of 5 feet (1.52 m) or greater are acceptable. Therefore, for the remainder of the study, the hydrogen flow length was always equal to or multiples of the panel length.

Coolant requirement reduction.- Improved cooling efficiency may be obtained by the use of folded fluid flow arrangements within a single panel length. This flow routing technique raises the average temperature of the panel hot surface, thus decreasing the ΔT between the external hot-gas and the panel surface, and thereby reducing the heat flux. Coolant savings are proportional to this reduction in ΔT regardless of the hot gas recovery temperature. However, at high recovery temperatures (above about 7000°R (3890°K)), the percentage savings achieved by use of sophisticated flow routing or insulation become so small that the weight and complexity penalties may become excessive. In addition to the basic single-pass hydrogen routing design, which achieves an average panel hot-surface of approximately 1000°R (556°K), the designs shown in figure 17, as well as variations of these, were studied to determine the increased cooling efficiency that could be attained from increased hot-panel-surface wall temperature.

Figure 17a shows a panel with multiple injection points along the panel length. Hydrogen is constantly added along the flow length to maintain the entire hot-wall temperature at an average temperature that is nearly uniform and that is close to the maximum allowable hot-surface metal temperature. It was determined that a great many injection points would be needed to keep the stress from the resulting sawtooth temperature profile within tolerable limits (similar to those of figure 15a). The potential saving in coolant was outweighed by added complexities in manifolding, flow control, and manufacturing.

Figure 17b shows a folded-in-depth design that contains an insulation layer between two heat exchanger surfaces. Heat transfer analysis has shown that the best possible cooling efficiency that can be obtained from flow folding in depth occurs when the thermal resistance between the heat exchanger layers is zero (reference 1). Therefore, no insulating layer would be used between the heat transfer surfaces. For the limiting case of a single sheet of metal separating two brazed layers of fins, the thermal stress resulting from the temperature difference between the hydrogen inlet and outlet temperatures becomes

a design limitation. If, however, the two heat exchanger surfaces are joined in such a manner as to permit independent in-plane thermal expansion at the two surfaces, the cross-sectional ΔT in each layer becomes the thermal stress limitation. Since this design has two heat transfer layers, its heat exchanger weight is at least twice that of a basic straight-through design. This added weight, combined with the added manifolding complexity, tends to offset the coolant saving advantage.

The design shown in figure 17c combines the conceptual feature of the designs illustrated in figures 17a and 17b. Calculations have shown that the injection slots between the folded flow layers would be restricted to a length of less than 0.004 in. (0.010 cm). Fluid pressure drop can be reduced and cooling efficiency increased by having an excess of cold fluid in the lower layer. This configuration possesses all of the inherent disadvantages and complexities associated with folded-in-depth and multiple-injection design, and, therefore, it is not given any further consideration in this report.

Figure 17d is a folded-in-width design, in which the counterflow hydrogen streams are interspersed across the panel width. Plain fins are required, and the coolant inlet and outlet manifolds must be located at the same end of each panel (solid flow arrows). Alternatively, an inlet and outlet manifold must be provided at both ends of each panel (dashed flow arrows). The heat transfer performance was computed by use of a four-fluid heat exchanger digital computer analysis written for this study. This design proved to be the best of the various flow routing arrangements from a performance standpoint as well as from practical fabricability considerations.

A comparison of the flow folded-in-width design with a single pass heat exchanger at a nominal heat flux of 10 Btu/sec-ft² (114 kW/m²) and for a recovery temperature of 3000°R (1670°K) is shown in figure 18. The figure shows that, for the same hydrogen inlet and outlet temperature and same coolant flow rate, the folded-in-width design cools a larger panel area than the single-pass design, and that the temperature differences through the sandwich depth are about equal. This increase in panel area is a result of the higher average hot surface temperature at which the folded-flow design operates. Since the hydrogen outlet temperature is well below the structurally allowable maximum metal temperature for the folded flow routing, more than half of the available hydrogen thermal capacitance remains. One or more additional series-connected panels, either single-pass or folded, would be used with the panel shown in figure 18 to use the remaining hydrogen thermal capacitance.

A heat transfer computation to obtain the relative cooling efficiencies of the single-pass, the folded-in-width, and the folded-in-depth heat exchanger configurations was carried out during the concept screening phase of the program. The results of this analysis are presented in table 9. The cooling efficiency term as used in table 9 is defined as the ratio of coolant flow rate that would be required for an average hot-wall temperature of 2000°R (1110°K), to that needed with each of the three flow configurations, where coolant inlet temperature is 100°R (56°K) and coolant outlet temperature is 2000°R (1110°K). At a nominal heat flux of 10 Btu/sec-ft² (114 kW/m²) and a gas recovery temperature of 3000°R (1670°K), the folded-flow designs achieve much

greater cooling efficiency than the single-pass heat exchanger. Additional calculations showed the pressure drop to attain the required coolant flow rates is less for a single-pass than a folded-in-width flow routing which in turn is less than a folded-in-depth design. Also, the cross-section ΔT 's between the face sheets of the panel are lowest for the single pass, higher for the folded-in-width, and highest for the folded-in-depth flow routings.

These relationships make the single-pass design a clear-cut choice for higher gas recovery temperatures and higher heat fluxes and for designs in which cooling efficiency is not an important requirement. For hypersonic vehicles, however, there will generally be a great incentive to conserve coolant; for these applications, the folded-in-width configuration appears to be superior to the folded-in-depth design.

Structural Configurations

Several structural designs for prime-load-bearing structures were considered. Both plain solid plates and rib-stiffened plates were rejected because they required weight well in excess of that required for sandwich configurations with the same load-bearing capability. Further consideration led to the elimination of honeycomb sandwich panels because they could not accommodate the need for coolant manifolds across the panel width at both ends. The coolant manifold requirement also eliminated the possibility of four-edged panel support, and when two-edged panel support was assumed, multiweb sandwich panels were the most efficient structural shape. Rectangular-web-core and triangular-web-core optimization analyses were performed (Appendix E). The rectangular web-core configuration proved to be the lighter of these two designs, and it was retained as the basis for all weight computation. The optimization procedure was extended to allow for the use of a combined structural arrangement that consisted of a prime panel structure and backup I-beams. This design proved to be lighter than a sandwich panel taken by itself to span specified length and width dimensions over the entire loading range.

APPENDIX B

CONCEPT EVALUATION GROUND RULES

The different panel configurations were compared on the basis of minimum panel weight and coolant flow rate at a specified design point. Metal temperatures and temperature gradients, coolant inlet pressure, and fluid pressure drop also were important considerations. In the concept evaluation, inlet hydrogen pressure was considered only in terms of its influence on structural weight. Inlet pressures up to 1000 psia (6890 kN/m²) were acceptable. Hydrogen outlet pressure--pressure at the outlet manifold duct--was established at 250 psi (1720 kN/m²) to allow for the pressure drop that will occur at the fuel injector orifices and for combustor back pressure. Items physically removed from the immediate vicinity of the panel were designed in accordance with the following restrictions:

- (a) Weight of distribution system plumbing was not assessed beyond the panel boundaries
- (b) Weight of machinery for pump output pressures was not considered since in the range up to 1000 psi (6890 kN/m²) it is relatively insensitive to output pressure.

Three further assumptions or restrictions were imposed on the evaluation.

- (a) All panel depths were considered acceptable
- (b) A design maximum wall temperature, T_{DMW} , of 2000^oR (1110^oK) was permitted. This temperature was defined as the maximum fin temperature plus 2/3 of the ΔT through the hot faceplate and was selected to permit a realistic appraisal of the structural properties of the hot faceplate. Actual surface temperatures were somewhat hotter, up to about 2035^oR (1130^oK) at 500 Btu/sec-ft² (5680 kW/m²).
- (c) Table 10 summarizes considerations that enter manufacturing and handling limitations used in the study.

Input data necessary for a systematic solution to the design program were identified and are summarized in table 11. A complete set of results was then generated to provide panel proportions, beam proportions, and heat exchanger design and to calculate panel weight per unit area and coolant flow requirements. The design procedures for the three panel concepts are outlined in Appendix F, however, as presented, the procedures reflect later improvements which apply only to the tradeoff studies. The basic differences relate to the heat exchanger and manifold design which were not optimized or determined in a systematic way in the concept evaluation, although typical lightweight geometries were used. In addition, no weight contribution was assumed for attachment clips which were added in the tradeoff studies. Further minor weight differences can be noted between the concept evaluation and tradeoff study weights due to the effect of the clips on beam and panel weight and the improved prime panel buckling calculations.

APPENDIX C

TRADEOFF STUDY

The tradeoff study was conducted to evaluate the effects of normal pressure and heat flux on panel weight and coolant requirements over the entire load spectrum. The effects of varying coolant outlet temperature, coolant inlet pressure, fin conductivity, and panel size were also investigated. Concepts 1, 2, and 3 in the concept evaluation were selected as the reference designs for this portion of the study. Design curves of total weight and coolant rate vs several parameters, such as applied normal pressure, heat flux, and coolant outlet temperature, are provided in this appendix.

Tradeoff Study Definition

Panel pressure loading and heat flux were used as the primary variables in analyzing each of the concepts. Panel length and width, recovery temperature, coolant outlet temperature, maximum coolant inlet pressure, heat exchanger fin temperature difference, and thermal conductivity were investigated at selected values of pressure loading and heat flux. The following discussion outlines the basis for the tradeoff studies.

Concept 1.- This concept was selected for the low-load region because of its extreme simplicity and its apparent weight advantage. The straight-through, single-pass flow configuration facilitated the calculations. The following decisions were made to provide the most useful study results.

Dimensions: The hydrogen pressure drop requirements indicated by the prior analysis were not difficult to satisfy, thus permitting flexibility in the selection of panel length. The effect of variation in panel length was studied in preference to panel width to determine the influence of panel dimensions on panel weight and coolant flow rate.

Recovery temperature: A single recovery temperature (infinite) was used in the tradeoff analysis. Design features specifically aimed at reducing gas-to-surface temperature differences (e.g., flow-routing and insulation) were not investigated.

Coolant outlet temperature: Variation in coolant outlet temperature had a pronounced effect on coolant flow rate, structural operating temperature, and structural weight, and it constituted a basic design variable.

Heat exchanger fin conductivity: Two values of conductivity were used. Sandwich height for this concept was limited by fin temperature difference, and therefore conductivity represented an important variable.

Concept 2.- This concept has general applicability. Straight-through, single-pass hydrogen flow was used in this design concept.

Dimensions: Width and length were selected as variables.

Recovery temperature: Both finite and infinite recovery temperatures were used. A finite recovery temperature was used to evaluate the insulating effect of fin heights that are greater than the fin heights indicated for the minimum-weight heat exchanger design.

Coolant outlet temperature: The evaluation was identical to that of concept 1.

Heat exchanger fin height: Weight-optimized heat exchanger designs employ the minimum possible fin height that is compatible with pressure drop limitations. The resulting cross-sectional temperature difference at low heat fluxes is less than necessary to provide the required low-cycle fatigue life. Fin height was increased at finite recovery temperatures to determine both the reduction in heat flux and coolant flow rate and the weight penalty.

Heat exchanger fin thermal conductivity: The effect of conductivity was investigated as a means reducing in-depth temperature difference and raising coolant outlet temperature while maintaining the hot surface temperature at a given value.

Maximum coolant inlet pressure: Coolant inlet pressure and pressure drop can become design-limiting as heat flux increases; therefore, variation in inlet pressure was investigated to establish the effects of these variables on design.

Concept 3.- The baseline concept evaluations indicated that this configuration would show conclusive weight advantages at high loads and high heat fluxes. Single-pass, straight-through hydrogen flow was used where the coolant flowed through the prime structural panel before entering the shingle.

Design Ground Rules and Calculation Procedures

The design ground rules used in carrying out the tradeoff study were the same as those for the concept evaluation. The material choices are discussed in Appendix G. The calculation procedures used for the tradeoff study are outlined in Appendix F.

Results

A discussion of summarizing curves follows, outlining results not presented in the main text. The breakdown of the important variables and itemized weight estimates are presented in tables 12 through 14.

Comparison of concepts 1 and 2 weights vs applied pressure.- The total component weights of concepts 1 and 2 vs applied normal pressure for applied heat fluxes of 10, 50, and 100 Btu/sec-ft² (114, 568, and 1140 kW/m²) are presented in figure 19. This figure emphasizes the difference in sensitivity to

heat flux between the two concepts. The advantage of separating the coolant passages from the prime-load-carrying structure for anything but moderate heat fluxes is clearly shown.

The structural weights of concepts 1 and 2 vs applied normal pressure are shown in figure 20 for fin conductivities of 10 and 100 Btu/hr-ft-⁰R (17.3 and 173 W/m-⁰K) for the 10 Btu/sec-ft² (114 kW/m²) heat flux case. The increased conductivity lowers the maximum metal temperature and hence increases the strength of the panel material. There is a tradeoff between fin weight increase due to a coating that improves the conductivity and panel weight decrease, due to the better material properties. The fin weight is based upon an assumed copper cladding thickness that is equal to the superalloy fin thickness. Due to the operating temperature levels of the fins, the copper cladding does not contribute to fin structural strength. This calculation indicates that the fin cladding weight increase overrides the panel weight decrease at the 10 Btu/sec-ft² (114 kW/m²) heat flux used. The high conductivity fin would show an advantage at higher heat fluxes, but concept 2 would remain the lightest design where this advantage occurs.

Comparison of concepts 1 and 2 weights vs coolant outlet temperature.- The weights of concept 1 and 2 panels vs coolant outlet temperature are shown in figure 21 for 2-ft (0.61-m) flow lengths. The results show the weight advantage of concept 1 at the lower normal pressures and lower heat fluxes. Concept 1 also tends to be more competitive at the higher coolant outlet temperatures, but this is partly due to the use of the stronger Waspaloy alloy in concept 1. The use of 5-ft (1.52-m) flow lengths (see tables 12 and 13) tends to improve the concept 1 desirability, but the overall comparison of the two concepts is unchanged. The primary effect of increased length is an overall weight decrease for both concepts.

Concept 2 weight vs beam span.- The structural weight of concept 2 vs the beam span (panel width) is shown in figure 22 for three coolant outlet temperatures. This curve shows a typical variation of weight for any panel concept and is, therefore, an important curve for design. Combination of the panel structural weight with vehicle support weight will determine the beam span that would give the combined minimum weight.

Concept 2 weight vs normal pressure.- The weight of the concept 2 design vs applied normal pressure is shown in figure 23 for four coolant outlet temperatures and heat fluxes of 10 and 50 Btu/sec-ft² (114 and 568 kW/m²). This is a typical design curve for use after a panel concept has been selected and the detailed effects of variations in pressure, coolant temperature, and heat flux are to be evaluated. It can be noted that the coolant outlet temperatures have a more pronounced effect upon panel weight than the applied heat flux, particularly for coolant outlet temperatures above 1760⁰R (978⁰K).

Comparison of concepts 2 and 3 weight vs pressure.- The weights of concept 2 and 3 vs applied normal pressure are shown in figure 24 for heat fluxes of 100, 250, and 500 Btu/sec-ft² (1140, 2840, and 5680 kW/m²). The curves show that concept 3 is the lighter design for pressures above about 65 psi (448 kN/m²). The effect of heat flux is not appreciable for either design because the heat exchanger makes a small contribution to total weight.

Comparison of concepts 2 and 3 weights vs coolant outlet temperature.- The weights of concepts 2 and 3 panels vs the coolant outlet temperature are shown in figure 25 for normal pressures of 50 and 100 psi (345 and 689 kN/m²) and heat fluxes of 50, 250, and 500 Btu/sec-ft² (568, 2840, and 5680 kW/m²). The results show that the concept 3 design is less sensitive to changes in outlet temperature than the concept 2 design. The curves for 50 psi (345 kN/m²) normal pressure indicate that, even at relatively low pressures, the concept 3 design may be lighter at the higher coolant temperatures. The curves shown terminate at some value of coolant outlet temperature where no heat exchanger design is possible due to insufficient internal pressure containment strength. The 500 Btu/sec-ft² (5680 kW/m²) heat flux case did not have heat exchanger designs at 1760° and 1900°R (978° and 1060°K) outlet temperature, and the 250 Btu/sec-ft² (2840 kW/m²) case had no design at 1900°R (1060°K).

Concept 2 coolant requirements vs coolant outlet temperature and fin height.- The tradeoffs between coolant requirements and coolant outlet temperature and between coolant requirements and heat exchanger fin height were investigated for concept 2 in the 5000°R (2780°K) recovery temperature case. Figure 26 shows the coolant flow rate required vs coolant outlet temperature in the 250 Btu/sec-ft² (2840 kW/m²) heat flux case. The infinite recovery temperature line is shown for reference. The 5000°R (2780°K) recovery temperature lines shown indicate that about 15 percent less coolant is required than in the infinite case. The heat exchanger fin height was varied from the 0.025-in. (0.064-cm) minimum gage to 0.075 in. (0.191 cm) for the 5000°R (2780°K) case; a noticeable reduction in required coolant occurs at the higher fin heights. Heat exchanger maximum metal temperature vs coolant outlet temperature for values of 1800°, 1900°, and 2000°R (1000°, 1060°, and 1110°K) are included to show how any specified design limitations on maximum metal temperature could be incorporated. A maximum metal temperature limitation will then set a limit on the maximum allowable coolant outlet temperature. For example, if the maximum design metal temperature is 2000°F (1110°K), the maximum allowable coolant outlet temperatures are 1850°R (1130°K) for the 0.025-in. (0.064-cm) fin height and 1740°R (967°K) in the 0.075 in. (0.191-cm) height case.

Concept 2 coolant requirements vs fin height.- The percent reduction in coolant requirements for concept 2 has been related to the heat exchanger fin height in figure 27 for heat fluxes of 10, 100, and 250 Btu/sec-ft² (114, 1140, and 2840 kW/m²). This shows that the percentage of possible savings is greater at higher heat fluxes.

Figure 28 serves to clarify the tradeoff between coolant requirements and structural weight by showing both the percent of coolant savings and the percent of structure weight increase vs fin height. The figure shows the result for a coolant outlet temperature of 1600°R (889°K) in the 250 Btu/sec-ft² (2840 kW/m²) case. At a constant fin height and coolant outlet temperature, the magnitude of the panel weight increase is not a function of external pressure since the only weight change considered is occurring in the heat exchanger due to the varying fin height. However, the percent of weight increase is greater at the lower normal pressures because the weight of the heat exchanger relative to the entire structure is greater.

APPENDIX D

DESIGN LAYOUT STUDIES

The design layout studies were conducted to identify problem areas and to investigate potential solutions for design details such as panel interfaces, sealing, assembly, beam backup, manifolding, and temperature equalization. The design solutions warranting further study were incorporated into the concept evaluation and tradeoff study configurations. In general, the layout studies were used to guide the analytical efforts, rather than to evolve detailed mechanical design solutions, but the seal and manifold designs used in design procedures and weight estimates were a direct result of this layout study.

General Problem Areas

The general problems that were considered included

- Accommodation of thermal expansion in the plane of the panels relative to the surrounding panels and supporting structure
- Achievement of a smooth aerodynamic surface and pressure-tight seal between panels, with some undefined leakage
- Coolant manifolding between panels
- Method of attachment of panels to the supporting structure--i.e., the method of panel installation
- Method of reducing or eliminating thermal lag of panel prime structure with respect to heat exchanger surfaces

Specific Applications

Any study of panel concepts requires consideration of problems relative to installation, but solution of these problems requires definition of a specific application. The current layout studies, therefore, only evaluated these problems in a qualitative way. The problems are

- Magnitude of thrust loads and acceleration body forces acting in the plane of the panels and the need to provide axial support. These loads are related to the length of panel area under consideration.
- Type and size of allowable surface discontinuities between panels and the need to limit or control such discontinuities. An approach predicated on the acceptability of gaps at startup and closure of the gaps in operation was used in this study. Transverse gaps should close in such a way that the gas stream does not impinge on a panel edge but, rather, experiences an expansion in passing the interface. This requires that panel surfaces be offset relative to one another.

- Type of access available for panel installation, i.e., mounting and manifolding. Access to the back of the panels is the most direct approach to the problem, but this assumption may lack realism. Access only from the front of the panels becomes extremely restrictive. Access to the panels, or at least to the plumbing, at some station along the length (in a nonregeneratively cooled region, for example) represents an intermediate approach, and in defining concepts, it was generally assumed that such access was available.

Problem Area Identification

For this discussion, the general and specific problems relative to external loads are categorized according to general panel location, and then the specific areas in the panel that are affected are indicated.

Panel interfaces.- As presently envisaged, the joint between panels includes several elements of the panel. These include the seals and manifolds that must be capable of functioning in a varying temperature and geometrical environment. Other considerations specifically related to the interface are the fit-up of the panels, access to or replacement of panels, and smoothness of the joint between panels.

Manifolding.- The primary layout problems with the manifolds are related to the necessity to provide for the seals and the joint area with the panel.

Sealing: The manifold and seal design are generally intimately related due to the requirements of seal mounting and cooling the local area. The seal location in terms of the distance from the panel outer surface will affect manifold complexity and pressure drop. If the seal is located as close to the surface as possible, the manifold will have to provide for sharp turns of the coolant to avoid the seal. These turns will introduce additional joints, which considerably increase manifold complexity. On the other hand, if manifold details are simplified by placing the seal under the manifold, undesirable flow effects may result from the relatively deeper slot between the panels, and support of the seal pressure load may be more difficult.

Access: The problem of locating the manifold connections so that they may be reached for routine repairs, maintenance, or replacement is included in this category. Since the manifold will generally be welded to the panel, removal of a panel will require accessibility of the fitting connections.

Structural effects on panel and beams: Although this problem was not covered in this study, it is a design consideration. Appropriate design of the panel and manifold joint could be the key to eliminating any problems in this area.

Seal design.- The seal design will be critical to many of the panel configurations at the extreme operating conditions that may be experienced. At the higher heat fluxes, cooling of the seals becomes an important consideration. At the higher operating pressures, support of the seal and the actual sealing

mechanism may become critical. As discussed above, the manifold design is heavily affected by the seal configuration. Whatever seal design is selected, full thermal expansion of the panels must be possible. Sliding seals and bellows seals are both candidates for the panel sealing application.

Corner effects: For cases where four edge seals are required, the corners of the panel present special problems in seal design. Preventing gas leakage in such a situation can be very difficult. For sliding seals in particular, a complicated configuration may result.

Temperature control: In all but the low heat flux cases, the seal temperature must be controlled either by active or passive cooling. Active coolant schemes, such as flowing coolant along the seal (film cooling) or flowing coolant through a sandwich seal, may be required. Passive cooling could be supplied by the manifolds; this would be a preferred method because of its simplicity.

Beam backup.- Design of the beams for the external pressure load is discussed in detail as part of the structural optimization analysis. The following topics include details that are pertinent to layout studies and are not generally part of a detailed loads analysis.

Differential thermal expansion: Differential thermal growth of the beams, panels, and airframe must be considered. The thermal loads generated by constrained structural components would be prohibitive in most cases considered in this program. Therefore, growth of the panels relative to the beams and growth of the beams relative to the airframe will be accommodated by some type of sliding attachments. In general, there will be a fixed point through which acceleration and aerodynamic loads are carried, and other required attachments will be free to move in the direction of thermal growth. The design of the attachments, therefore, will be critical to the success of a panel configuration. In the design layout phase, several schemes for handling this problem were considered with the objective of determining the more reasonable arrangements in a qualitative way.

Heat leak: Depending on the specific application, flow of heat through the beams (and to them) may be undesirable. Temperature differences across the beam height may lead to thermal stress and deformation of the beams that may not be acceptable. Heating of the airframe itself or of components in the immediate area may be a serious design consideration. Insulation techniques at the panel-to-beam attachments and/or the panel-to-airframe joints would be a potential solution. In addition, active cooling of the beams, by means of either extra piping or the existing piping, is possible, as are combinations of insulation and cooling. Possible methods of insulating or cooling the beams were not included in the layout studies.

Access: Possible requirements for removal of panels or panel and beam combinations would make attachment accessibility a necessity. As mentioned above, accessibility has a qualitative influence on all of the layout studies. Access may be more desirable for the panel-to-beam attachments than for the beam-to-airframe connections because repair and inspection of coolant systems or aircraft components under the panels may be possible without removing the beams.

Orientation: To support the structural loads, the prime panels must be oriented with webs perpendicular to the directions of the beams. The orientation of the coolant flow direction in the heat exchanger for configurations in which the heat exchanger is not integral with the structural panel is somewhat more arbitrary and can be varied to suit particular application. Brief consideration has been given in the layout studies to configurations with the beams and coolant flow parallel. However, for the major portion of the present investigation, the beams have been oriented perpendicular to the coolant flow. (See figure 4.) With this arrangement, each beam operates at a uniform temperature; and although it was not done in the present study lightweight-low temperature materials could be used for the beams located at the cold end of the panel.

Additional Design Considerations

Temperature equalization.- Severe thermal stresses may occur in the panel prime structure (and beams) if proper design is not implemented. During the warmup or startup portion of the panel operation, transient thermal gradients may occur due to the nature of the heat application, i.e., on one side of the panel. One of the possible solutions to this problem is the controlled ducting of additional coolant to the prime structure portion of the panel. The general assumption made in this program was that potential transient thermal gradient problems would be solved in a specific design but that generalization to encompass all designs would not be profitable.

Layout design assumptions.- A number of layout design assumptions were made. These assumptions are listed below.

- A single panel will be 2 ft by 2 ft (0.61 m by 0.61 m).
- The temperature in the plane of each panel and in the airflow direction will increase from 500°R (278°K) at the coolant inlet end to 2000°R (1110°K) at the coolant outlet end on the hot surface. The prime structure will operate at 400°R (222°K) less than this along its entire length.
- The panel support structure (backup beams, airframe, and panel prime structure in the case where the heat exchanger is mechanically attached) will be at a temperature that is uniform and different from the integral panel prime structure temperature or the attached heat exchanger temperature.
- The panels form a circular surface, as shown in figure 29, where circle diameters are about 20 to 40 ft (6.1 to 12.2 m). Both inner surfaces, which attach directly to the airframe, and outer (cowl) surfaces, separated from the inner surfaces and forming an annulus with these, are involved.
- All panels on one surface are subjected to the same operating conditions.

The differences between configurations include the following:

- Direction of gaps between panels, i.e., longitudinal gaps only or longitudinal and transverse gaps
- The type of discontinuity in the panel surface at panel interfaces
- Sealing requirements at panel interfaces
- Panel external manifolding assembly requirements
- Thermal loading due to the type of panel interface
- Type and frequency of panel assembly axial load supports
- Method of panel or panel assembly installation

Preliminary Survey

The preliminary survey provided an opportunity to assess the design possibilities. Five preliminary configurations were investigated which consider an intermediate load of 100 psi (689 kN/m²) and intermediate heat flux of 250 Btu/sec-ft² (2840 kW/m²).

Configuration 1.- In configuration 1, shown in figure 29, panels are joined in the longitudinal direction of the vehicle leaving radial gaps between rows. This configuration implicitly assumes the existence of longitudinal backup members to provide continuous support to the thermally expanding panel assembly. In addition, the arrangement assumes the existence of a single, fixed, axial-support station for free expansion of the panels. Because both hot and cold ends of the panels are tied to adjacent hot and cold ends, a temperature-matching problem at the cold-end interface is much less severe because, in general, coolant inlet temperatures will be more predictably uniform than outlet temperatures. Such an arrangement eliminates right angle seal interfaces at the panel junction, but limitations on the frequency of axial support appear restrictive if large panel areas must be supported. In general, however, the panel area subject to high pressure and heat-flux loading and requiring smooth surfaces will be limited. Outside this high loading area, the panel area can then be transversely interrupted to permit additional axial support. Configuration 1 was dismissed from further consideration because it seemed to restrict the applicability, but modifying assumptions would make the arrangement attractive because it does simplify the sealing problem.

Configuration 2.- The layout for configuration 2 is shown in figure 30. All panels are joined to one another in a fixed relationship (for example, hoop rings at a given station connect all panels around the circumference). A single axial-support station is provided, and this arrangement allows free longitudinal expansion. A feature of the arrangement is that dynamic seals between panels are eliminated and replaced by static flexing seals. Serious potential problems include (1) the need to have closely matched metal temperatures between adjacent panels, and (2) the fact that the panels now form closed

cylinders and consequently take on a cone shape in operation. On a 20-ft (6.1-m) diameter, for example, diametral growth will be 3 in. (7.62 cm) at panel hot ends. This type of noncylindrical growth (see figure 30) appears objectionable if the panels are used as internal engine surfaces. This factor, combined with the uncertainty of the thermal loading, led to elimination of the concept from further consideration.

Configuration 3.- In the configuration shown in figure 31a, the panels are used in groups of two, with each group having its own axial support. The transverse gap present at the start of panel heating and the uncertainty of forming a smooth closure of the gap in operation are objectionable features of this configuration. In addition, it will be difficult to provide the necessary dynamic pressure seal all around the two joined panels. This type of sealing problem will probably be encountered in any application involving regeneratively cooled surfaces, however, and therefore it was worth attempting a solution. Figure 31b shows panels that are tapered in the longitudinal direction to minimize the total longitudinal gap area. Problems involved in fabricating the panels in the tapered shape do not appear to be prohibitive. The principal feature of this arrangement is that all hot or cold external manifolds and all axial-support stations are coincident (not staggered, as in configuration 3a). This configuration (3a) was selected for further investigation of design problems.

Configuration 4.- In the configuration shown in figure 32, an overlap of adjacent panels in the longitudinal direction is used to eliminate gap discontinuity. The mechanical problems associated with this configuration are the same as those encountered with configuration 3. In the area of overlap, however, an additional thermal load is imposed on the underside panel because the metal temperature will tend to experience a step change due to direct exposure to the coolant temperature. Consequently, this configuration was eliminated from further study.

Configuration 5.- Figure 33a shows an array of single panels as opposed to two panels or more rigidly joined. Features of this configuration include the elimination of thermal stresses at the interfaces of joined panels and the potential for tie-down of each individual panel to the supporting structure. The panels shown in figure 33b are tapered and installed in such a way that cold and hot ends of adjacent panels are next to each other. In both cases, the seal surfaces will be exposed to large temperature gradients, but conduction, in conjunction with a moderate amount of cooling, will reduce the potential gradients. The most attractive feature of the arrangement in figure 33b appears to be that all seals normal to the airflow will be at the same mean temperature. Consequently, a possible solution to the seal problem might be one which permits mounting of the panels directly to the support structure without precise temperature control of the seals. This configuration (5b) was selected for further investigation of design problems.

Detailed Study

Configurations 3a and 5b of the preliminary survey were selected for a more detailed study at the intermediate load and heat flux, 100 psi (689 kN/m²) and

250 Btu/sec-ft² (2840 kW/m²) design point. In addition to the general study, detailed problems peculiar to the concept 1 panel (figure 3) at the low load and flux conditions, 7 psi (48 kN/m²) and 10 Btu/sec-ft² (114 kW/m²), and to the concept 3 panel (figure 5 at the high load and flux conditions, 250 psi (1720 kN/m²) and 500 Btu/sec-ft² (5680 kW/m²), were examined.

Configuration 3a.- The basic configuration, illustrating various design considerations, including the method of installation, is shown in figure 34. It should be noted that the beam orientation retained for the concept evaluation was orientated 90 degrees from the position shown. Alternate manifolding arrangements are shown in figure 35, and a second sealing technique is illustrated in figure 36.

Manifolds: The manifold designs include provisions for location of the seal at one end of the panel; the other end is bolted to the adjacent panel in this configuration. The figures show the influence of the seal on manifold complexity. Pressure containment in flat sandwich section is provided by fins as in the heat exchanger. Flow distribution techniques for the rectangular manifolds are shown in figure 35.

Sealing: Figure 34 shows overlapping seals used at the right angle interfaces of the panels. This type of seal has some inherent leakage. Whether or not such leakage is permissible and the limits of the leakage that can be tolerated will depend on tolerances possible for the specific installation. No cooling provisions for the seals are shown based on assumption that gaps between panels will close up at operation and that this closure will effectively protect the seals. Figure 36 shows an improved seal in terms of reduced leakage, but the perpendicular seal must be maintained at aircraft structural temperature to avoid thermal loads on it and on the longitudinal seals.

Installation: Figure 34 shows a bolt connection between the backup beams and the aircraft structure. As shown, the design requires access from the rear of the panels for installation. In figure 36, the panel is installed by sliding the backup beams into a bracket attached to the aircraft structure, with the fixed attachment at one end of the two-panel assembly. This design appears suitable for installation from the front side of the panels.

Configuration 5b.- Figure 37 shows the panel assembly layout for configuration 5b, which includes a unique seal design. The use of a double set of longitudinal seal strips (see section a-a figure 37) permits the use of a continuous seal around the panel edges without constraint of the seals running in either the longitudinal or the transverse direction. Various methods of connecting the transverse seal strips are shown in figure 38. Detailed design work would be required before the best connection for the application could be selected, but the tension latch and dovetail clip connections appear attractive. This unique seal design requires the maintenance of close fit-up tolerances in both fabrication and operation.

Concept 1 panel for low-flux applications.- A concept 1 panel designed for 7 psi (48 kN/m²) normal pressure and 10 Btu/sec-ft² (114 kW/m²) heat flux was examined to determine whether sealing would be simplified at the less severe

heating level and whether bolting through the panel would be practical at the low fluxes. The panel is similar to that shown in figure 34, except that a single-layer sandwich panel is used for coolant containment and external load capability. Various methods of sealing and installing the panels were considered, but the optimum methods were the same for both high- and low-heat-flux panels. Two seal designs investigated and determined to be unsuitable are described below.

- Bellows seals around the edges. At the intersection of the transverse and longitudinal seals where four panel corners are expanding toward the intersection, there is a tendency to tear the bellows if it is tied to the panels. The problem could be eliminated by providing a cutout in this area, but it would then be necessary to cool the area (or to provide additional sealing to block flow) because hot gas would flow through the cutout.
- Skeleton-type seals with the panels attached from above. This skeleton-type of seal would be a continuous structure capable of accommodating a large number of panels (a cylinder with rectangular holes cut into it). A serious problem exists in the fit-up between the seals and the aircraft structure and between the seal and the attached panels. Panels would be installed from the outside and bolted to the backup support beams which, in turn, would be tied to the aircraft or engine. The concept was rejected because of the very tight tolerances.

Concept 3 panel for high-heat-flux/high-heat-load application.- Previous panel layouts have dealt with design concepts in which the normal pressure load is transmitted through the heat exchanger to the support structure. Figure 39 shows a concept using a regeneratively cooled shingle with an essentially zero normal pressure differential. The chief features of this concept are

- Sealing around the shingles is not required, except that baffles must be provided to minimize the leakage. Such leakage constitutes a parasitic heat load on the coolant capacity and imposes structural problems due to unpredictable heating.
- All of the pressure-bearing structures, including both the sandwich structure and the beam backup structure, operate at a low temperature throughout. Because of gas bypass leakage and radiation and conduction effects, thermal protection for this structure will probably be required. A heat exchanger panel metallurgically joined to the load-bearing panel would provide this protection. With appropriate baffling, this heat flux would be expected to be a small percentage of the total heat flux to the hot panel. Baffling involves a straightforward design problem rather than a question of basic feasibility.
- The sealing around the panel edges is accomplished by means of a flange weld. Separation of panels can be simply accomplished by grinding off the weld. This type of welded construction is frequently used on heat exchangers to provide sealing, attachment, allowance for

dimensional tolerance stack-up, and light weight. The total dimensional change involved for operation of the sandwich structure at -300°F (89°K) will be about one-fourth the differential expansion that must be considered in the shingle or in an integrated heat exchanger-structural panel and the seals appear to be capable of absorbing the differential expansion. By comparison, bolted panels would present tolerance problems and a requirement for gasketing that would also serve to shim the panel. This construction would be heavier than welded construction and would have potential leakage problems.

- The design appears to require access from the underside for installation of the structural panel and for coolant manifolding, but the heat exchanger panel can be installed and removed from the gas side or front side. After mechanical attachment of the shingle, manifold connections are required at one end to complete the installation.
- The beams that attach the shingle to the cold structure require insulation. In addition, insulation of the beam webs for protection against bypass gas flow may be required.
- Coolant flow routing at the coolant outlet end of both the structural and the heat exchanger panels appears feasible. In view of a-a figure 39, the superposition of the two manifold tubes presents a more complex picture than exists in reality. The two superimposed tubes are separated, and they break through the structural panel at different stations. Since the appropriate tubes can be preinstalled, assembly and fabrication are not expected to be impractical.

In summary, the panel concept shown in figure 39 appears to be practical. It has the advantages of relatively simple installation, relative simplicity of the structure exposed to the severe hot-gas environment, ease of sealing, and the possibility of removal of the shingle without disassembling the structural panel. These advantages are offset by the coolant penalty associated with heat bypass to the cold structure and by additional components which add complexity relative to the integrally bonded panel.

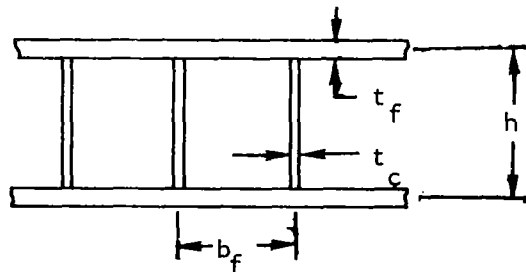
APPENDIX E
STRUCTURAL ANALYSIS

Structural analyses were conducted to provide satisfactory panel structural integrity and to develop and use techniques of minimum-weight design. The topics covered included optimization analyses for pressure loads, the effect of temperature on weight, panel in-plane thermal stresses, hot-surface thermal fatigue studies, and panel flutter considerations.

Optimization Analysis for Pure Bending

The optimum structural design approach was used to form a basis for comparing various minimum-weight structures as they perform under a pure bending moment. This approach leads to the derivation of formulas and the generation of curves in which a weight function is plotted vs a structural index. These curves show directly the minimum-weight design. The resulting derivations and curves for the rectangular web-core sandwich panel, triangular-web-core sandwich panel, I-beams, and combined panels and beam arrays are presented below.

Rectangular-web-core sandwich panel. -The weight function vs structural index curves for the case of a rectangular-web-core sandwich panel under an applied pure bending moment are developed in this section. Related expressions for the optimum stress and optimum geometrical relations of the structure vs structural index are a necessary byproduct of the analysis. The following sketch shows a typical sandwich plate element with the nomenclature for the geometric relations.



A-2365

It is assumed for this analysis that the sandwich is at a uniform temperature, that it is symmetrical, and that uniform material properties are used. The basic technique in the derivation of the formulas is to rewrite and combine the equations for panel bending stress, panel buckling stress, and weight into

forms that will permit rapid evaluation of the structure. The objective is to find the structural parameters that provide the weight function and the structural index for a sandwich panel. It will be shown in the following derivation that the weight function for the rectangular web-core sandwich panel is $\bar{t}/m^{1/2}$, where \bar{t} is the metal area per unit width, and m is the applied bending moment per unit width. The expression for \bar{t} for a rectangular-web-core panel is

$$\bar{t} = 2t_f + ht_c/b_f \quad (1)$$

The desired structural index for sandwich panels subjected to bending is m/h^2 . The equation for panel maximum bending stress is

$$\sigma = m/z \quad (2)$$

where z is the section modulus per unit width. Assuming that the faceplate moments of inertia about their own axes are negligible and that the plate thickness, t_f , is much less than the panel height, h , the moment of inertia and section modulus per unit width are given by the expressions

$$I = t_f h^2/2 + t_c h^3/12b_f$$

$$z = t_f h + t_c h^2/6b_f$$

Substituting the expression for section modulus into equation (2), the rectangular-web and faceplate maximum bending stresses are

$$\sigma = m/(t_f h + t_c h^2/6b_f) \quad (3)$$

An applied bending moment can cause local buckling in the faceplates and webs. The equations expressing the buckling criteria are

$$(\sigma_{cc})_{\text{plate}} = K_1 E \eta^{1/2} (t_f/b_f)^2 \quad (4)$$

$$(\sigma_{cc})_{\text{web}} = K_2 E \eta^{1/2} (t_c/h)^2 \quad (5)$$

where η is the plasticity reduction factor ($\eta = E_t/E$), and K_1 and K_2 are constants associated with the faceplate and rectangular-web edge fixity conditions. For the pure bending case, the particular geometrical proportions defined by the dimensions, t_f , t_c , h , and b_f , that produce the minimum-weight panel for a given applied bending moment can be readily determined. That a unique solution exists is established by the fact that there are four dimensional variables and four conditions to be satisfied--faceplate local compressive instability, rectangular-web bending instability, material allowable stress, and the minimum-weight condition. For pure bending, the optimum design was obtained by equating the applied stress to the plate and web buckling stresses. It was generally assumed that an optimum design had been achieved when the

buckling modes of the faceplates and rectangular webs, acting as plates with simple edge support, occurred simultaneously. As discussed below, there is an interaction between faceplate and rectangular-web buckling that depends on allowing one of the members to support the other in the buckling region. This buckling interaction was utilized to provide panel shear capability for the support of normal pressure forces.

For the pure bending situation, simultaneous local buckling implies that equations (4) and (5) can be rewritten in terms of a thickness ratio, t_f/t_c , and a spacing ratio, h/b_f to give

$$(t_f/t_c) (h/b_f) = \sqrt{K_2/K_1} = \delta \quad (6)$$

The equation for maximum bending stress, equation (3), can now be rearranged into a form that involves the desired grouping of the variables to express the stress in terms of the structural index, the buckling constants (K_1 and K_2), and the geometrical ratios, t_f/t_c and h/b_f . The first step is the following regrouping of equation (3)

$$\sigma = (m/h^2) / \left[(t_c/h) (t_f/t_c + \frac{1}{6} h/b_f) \right] \quad (7)$$

where m/h^2 is the structural index. Elimination of t_c/h from equations (5) and (7) gives the desired equation for optimum stress

$$\sigma = (m/h^2)^{2/3} (K_2 E)^{1/3} \eta^{1/6} / (t_f/t_c + \frac{1}{6} h/b_f)^{2/3} \quad (8)$$

from which the optimum ratios of t_f/t_c and h/b_f must be determined. The next step is to express the weight function in a form that will relate it to the structural index. Equation (1) can be rewritten into groupings of dimensionless ratios similar to those used in equation (8). By eliminating t_c/h from equations (1) and (7), \bar{t} can be expressed as a function of σ , m , h , t_f/t_c and h/b_f

$$\bar{t} = \left(\frac{2m}{h\sigma} \right) (t_f/t_c + \frac{1}{2} h/b_f) / (t_f/t_c + \frac{1}{6} h/b_f)$$

By further regrouping

$$\bar{t}/m^{1/2} = \left[(m/h^2)^{1/2} (1/\sigma) (2) (t_f/t_c + \frac{1}{2} h/b_f) \right] / \left[(t_f/t_c + \frac{1}{6} h/b_f) \right] \quad (9)$$

This form shows the evaluation of the weight function, $\bar{t}/m^{1/2}$, in terms of optimum stress, structural index, and the dimensionless geometrical ratios.

If σ in equation (8) is eliminated from the above expression, the following equation is obtained for the weight function

$$\bar{t}/m^{1/2} = 2(t_f/t_c + \frac{1}{2}h/b_f) / \left[(K_2 E)^{1/3} \eta^{1/6} (t_f/t_c + \frac{1}{\delta} h/b_f)^{1/3} (m/h^2)^{1/6} \right] \quad (10)$$

The minimum $\bar{t}/m^{1/2}$ will be obtained when that portion of equation (10) involving the dimensionless geometrical ratios is minimized. This is accomplished by using equation (6) to eliminate h/b_f from equation (10). The resulting expression is then differentiated with respect to the dimensionless ratio, t_f/t_c . Finally by setting the resulting terms equal to zero and solving it in terms of t_f/t_c , the optimum thickness ratio is obtained. This was done, and the end result showed that

$$(t_f/t_c)_{opt} = \left(\frac{2 + \sqrt{7}}{\delta} \right)^{1/2} (K_2/K_1)^{1/4} = 0.88(K_2/K_1)^{1/4} \quad (11)$$

By inserting this value for $(t_f/t_c)_{opt}$ into equation (10), the following compact formula for the weight function in terms of structural index is obtained

$$(\bar{t}/m^{1/2})_{min} = 2.81 / (K_1 K_2 \eta)^{1/6} E^{1/3} (m/h^2)^{1/6} \quad (12)$$

With the aid of equations (8), (11), and (12), σ_{opt} and $\bar{t}/m^{1/2}$ may be plotted vs m/h^2 on a single curve for any material. This has been done in figure 40, and it can be seen that $\bar{t}/m^{1/2}$ gradually diminishes and σ_{opt} rapidly increases as m/h^2 is increased. Material yield stress provides an upper limit in usable stress, and the minimum weight occurs for the structural index at which σ_{opt} is equal to the yield stress. Once the yield cutoff limitation is reached, it becomes necessary to modify the faceplate-to-web thickness ratio and the h/b_f ratio to provide sufficient section modulus for increased values of structural index. This is accomplished by placing the numerical value for yield stress into equation (8) and using the constraining relationship between geometrical proportions provided by equation (6). It is then necessary to compute the geometrical ratios t_f/t_c and h/b_f at each specific value of m/h^2 . In figure 40, constant-stress lines are presented for two cutoff stresses. An ideal elastic-plastic material was assumed, which is achieved by setting the plasticity reduction factor equal to unity and by considering the material to have perfectly linear elastic properties to the yield stress and a uniform stress equal to the yield stress in the plastic region. The procedure can be extended readily to account for inelasticity by generating a curve for plasticity reduction factor vs stress for the particular material under consideration. These calculations were programmed in Fortran IV for the ideal elastic-plastic case, and the curves shown in figure 40 are based on computer output data. The minimum weight occurs for a structural index slightly higher than that at which the optimum and yield stresses intersect, but this further weight reduction (less than 1 percent) was

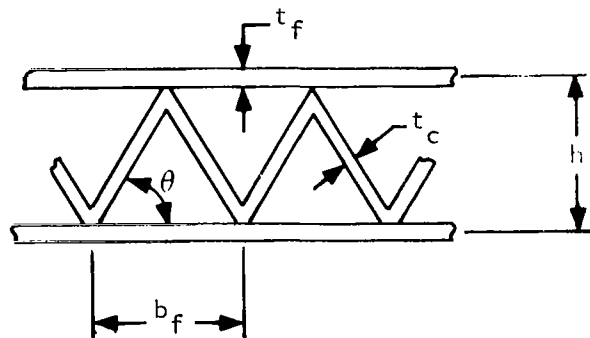
considered negligible. Consequently, minimum weight was taken to be at the value of structural index for which the optimum stress equalled the yield stress. The computation for a yield cutoff stress of 130,000 psi (896,000 kN/m²) shows that the minimum value of $\bar{t}/m^{1/2}$ is 0.001209 in./lb^{1/2} (1.455 x 10⁻⁵ m/N^{1/2}), and this occurs at a structural index value of 3367 psi (23,250 kN/m²). Curves are also shown on figure 40 for t_f/t_c (and therefore, from equation (6), h/b_f) vs m/h^2 .

Equation (12) can be modified by eliminating m/h^2 from equations (8) and (11) to obtain a relation of particular significance, and it will be used to great advantage in subsequent portions of this appendix. The minimum value of the weight function, $(\bar{t}/m^{1/2})_{\min}$, is defined as C_{p1} , which will be called the panel merit parameter. Therefore, the formula for C_{p1} is (using $\eta=1$)

$$C_{p1} = 2.78/(K_1 K_2)^{1/8} (E\sigma)^{1/4}, \text{ in./lb}^{1/2} (\text{m/N}^{1/2}) \quad (13)$$

This expression is dependent only on the buckling coefficients and material properties. In particular, for fixed buckling coefficients, various panel materials may be evaluated by calculating C_{p1} . To compare different panel materials, it is only necessary to multiply by material density, γ_{p1} , and evaluate $\gamma_{p1} C_{p1}$.

Triangular-web-core sandwich panel. - The derivation for the triangular-web-core sandwich panel closely follows that of the rectangular-web core, and the same assumptions are made. A typical element is shown below.



A-24533

The panel structural index and the weight parameter are the same as for the rectangular-web-core panel, $\bar{t}/m^{1/2}$ and m/h^2 , where \bar{t} is now given by

$$\bar{t} = 2t_f + t_c / \cos \theta$$

The weight function is given in terms of the structural index in the elastic range by

$$\bar{t}/m^{1/2} = \frac{1}{(K_2 E)^{1/3}} \frac{4\delta \cos \theta + 1/\cos \theta}{2\delta \cos \theta + 1/6 \cos \theta} \frac{1}{(\sin \theta)^{2/3} (m/h^2)^{1/6}}$$

In the constant stress range

$$\bar{t}/m^{1/2} = \frac{1}{(K_2 E \sigma)^{1/4}} \frac{(4\delta \cos \theta + 1/\cos \theta)}{(\sin \theta)^{1/2} (2\delta \cos \theta + 1/6 \cos \theta)^{1/2}}$$

In these equations

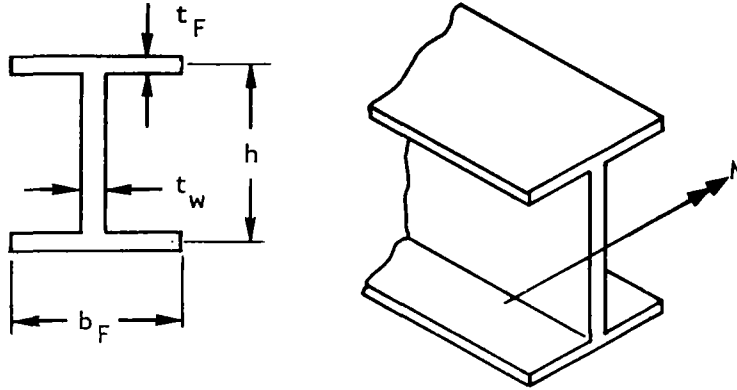
$$\delta = \sqrt{K_2/K_1} = (h/b_f)(t_f/t_c)(1/\sin \theta)$$

Comparison of triangular-web core with rectangular-web-core sandwich panels.- In all cases, the minimum weight occurs for a structural index slightly higher than the start of the constant-stress lines. The further weight reduction is quite negligible, and the following table shows the comparison for the structural index points at which $\sigma_{opt} =$ cutoff stress.

Panel web configuration	Cutoff stress = 100,000 psi (695 000 kN/M ²)		Cutoff stress = 130 000 psi (896 000 kN/m ²)	
	$(\bar{t}/m^{1/2})_{opt},$ in./lb ^{1/2} (m/N ^{1/2})	$(m/h^2)_{opt},$ psi (kN/m ²)	$(\bar{t}/m^{1/2})_{opt},$ in./lb ^{1/2} (m/N ^{1/2})	$(m/h^2)_{opt},$ psi (kN/m ²)
Rectangular-web-core panel	0.00128 (1.54x10 ⁻⁵)	2250 (15 500)	0.00121 (1.46x10 ⁻⁵)	3367 (23 250)
Triangular-web-core panel	0.00162 (1.95x10 ⁻⁵)	3115 (21 500)	0.00152 (1.83x10 ⁻⁵)	4610 (31 750)

It is seen that the triangular-web-core sandwich is approximately 25-percent heavier than the rectangular-web-core sandwich and that the former is somewhat more compact (i.e., higher m/h²). The rectangular-web-core sandwich was used for all the subsequent weight analyses because of its clearcut weight advantage.

I-Beam.- Before the potential benefits of combining beam backup structure with panels can be assessed, optimum beam weight must be determined. The following analysis was performed to provide a tool similar to the one developed for the panel structure. The approach taken for the panel, i.e., the development of an appropriate weight function vs structural index, leads to an expression that can be used to evaluate the best arrangement of beams and panels. The sketch below shows the beam cross section and the geometrical variables.



A-23659

The cross-sectional area, moment of inertia, and section modulus are

$$A = 2b_F t_F + h t_w$$

$$I = \frac{b_F t_F h^2}{2} + \frac{t_w h^3}{12}$$

$$Z = \frac{I}{h/2} = t_F b_F h + \frac{t_w h^2}{6}$$

Bending stress due to an applied moment, M , is $\sigma = M/Z$. This can be combined with the expression for section modulus and written in the form

$$\sigma = (M/h^3)(h/t_w)(h/b_F)/(t_F/t_w + \frac{1}{6} h/b_F) \quad (14)$$

The structural index for the beam is therefore M/h^3 . The buckling formulas for the flange and rectangular web are

$$(\sigma_{cc})_{\text{flange}} = \frac{K_4 E \eta^{1/2}}{(b_F/2t_F)^2} \quad (15)$$

$$(\sigma_{cc})_{\text{web}} = \frac{K_2 E \eta^{1/2}}{(h/t_w)^2}$$

The buckling coefficient, K_4 , for the flange is for a plate that is simply supported along one edge and free along the other edge. Substitution of (14) into (15) leads to the following equation for optimum stress in terms of the structural index, the flange buckling coefficient, and the dimensionless geometrical ratios (using $\eta = 1$ hereafter)

$$\sigma = \left(\frac{M}{h^3} \right)^{2/3} (K_2 E)^{1/3} \frac{(h/b_F)^{2/3}}{(t_F/t_w + \frac{1}{6} h/b_F)^{2/3}} \quad (16)$$

Equation (14) may be combined with the expression for cross-sectional area as follows

$$A = \left(\frac{M}{h^3} \right) \left(\frac{h^2}{b_F t_w} \right) \frac{(2 t_F/t_w + h/b_F) b_F t_w}{(t_F/t_w + \frac{1}{6} h/b_F) \sigma_{opt}}$$

which finally leads to

$$\left(\frac{A}{M^{2/3}} \right) = \left(\frac{M}{h^3} \right)^{1/3} \frac{(2 t_F/t_w + h/b_F)}{(t_F/t_w + \frac{1}{6} h/b_F)} \frac{1}{\sigma_{opt}} \quad (17)$$

The weight function therefore has the form $(A/M^{2/3})$. The weight parameter in terms of the structural index in the elastic range is then obtained by clearing σ_{opt} from equation (17) by using equation (16)

$$A/M^{2/3} = \frac{1}{(K_2 E)^{1/3}} \frac{(2 t_F/t_w + h/b_F)}{[t_F/t_w + (1/6)(h/b_F)]^{1/3}} \frac{1}{(h/b_F)^{2/3}} \frac{1}{(M/h^3)^{1/3}} \quad (18)$$

In the constant-stress range, (M/h^3) is eliminated from equation (17) by using equation (16)

$$A/M^{2/3} = \frac{1}{(K_2 E)^{1/6}} \frac{(2 t_F/t_w + h/b_F)}{[t_F/t_w + (1/6)(h/b_F)]^{2/3}} \frac{1}{(h/b_F)^{1/3}} \frac{1}{\sigma^{1/2}} \quad (19)$$

Equating the two equations for local buckling stress for the flange and web produces

$$\left(\frac{h}{b_F} \right) \left(\frac{t_F}{t_w} \right) = \sqrt{\frac{K_2}{4K_4}} = \delta \quad (20)$$

The minimum elastic line is obtained by using equation (18) with the minimum value of the expression involving the geometrical variables. This is accomplished by substituting for h/b_F from equation (20), differentiating the

expression with respect to t_F/t_w , setting this result equal to zero, and solving. The maximum occurs at $t_F/t_w = 0$, and the minimum weight appears to occur when the flange width and thickness are reduced to zero. This solution does not have physical significance, however, and a beam with insufficient flanges would be unsatisfactory on the basis of lateral instability. This elastic line for $A/M^{2/3}$ and the line for σ_{opt} are plotted vs (M/h^3) for an ideal elastic-plastic material in figure 41. A cutoff stress of 130 000 psi (896 000 kN/m²) occurs when $M/h^3 = 338$ psi (2330 kN/m²) at which point the weight function must follow a constant-stress line. Equations (16) and (19) are used and the minimum value of the geometrical variables is obtained for this portion of the curve. A considerable further weight reduction occurs beyond the cutoff stress transition, and the minimum value of 0.000254 in.^{4/3}/lb^{2/3} (0.70×10^{-6} m^{4/3}/N^{2/3}) is reached when $(M/h^3) = 1350$ psi (9310 kN/m²). Inspection of the 130 000 psi (896 000 kN/m²) constant-stress line shows that the beam weight function is extremely flat over a wide range of structural index values and that nonoptimum structural index values may be used with very little weight increase. As a result, the ratios of t_F/t_w and h/b_F , particularly the latter, may be adjusted if necessary to meet space restrictions.

The general minimum-weight expression can be conveniently reduced to the following form using the optimum geometric ratios in equation (19).

$$A/M^{2/3} = 2.62/(K_2 E)^{1/6} \sigma^{1/2}$$

The minimum value of the weight function, $(A/M^{2/3})_{min}$, is defined as C_{bm} , which will be called the beam merit parameter. The formula for C_{bm} is

$$C_{bm} = \frac{2.62}{(K_2 E)^{1/6} \sigma^{1/2}}, \text{ in.}^{4/3}/\text{lb}^{2/3} (\text{m}^{4/3}/\text{N}^{2/3}) \quad (21)$$

The beam merit parameter is analogous to the panel merit parameter derived previously in this section. It is dependent only on the material properties and the buckling coefficient. Since the buckling coefficient is unaffected by material choice, evaluation of C_{bm} for various materials provide a direct estimate of weight vs temperature.

Combined panel and I-beam optimization.- The following analysis was carried out to determine the optimum array of beam and panel proportions, and the comparative weight reduction, if any, if only a panel were used. This analysis makes use of the previous optimization analyses for the panel structure and the I-beam analysis.

The basic ground rule for this analysis is the assumption that continuous edgewise support is available for the panels or the panel-beam combination at a specified dimension, a , apart (see figure 42). If the panel only is employed, Case I, the strong direction of the panel will span the a dimension. When a combination of panel and beams is used, Case II, the beams will be used

to span the dimension. The beams will be the dimension \underline{c} apart. The panel strong direction will be utilized to span the beam spacings. Figure 42 illustrates these two arrangements. A final configuration shown in figure 43 investigated the possibility of spanning the dimension \underline{c} with additional beams at spacing \underline{d} . The panel strong direction would be parallel to the \underline{a} dimension. If all supports are assumed simple supports, the panel dimension \underline{b} does not influence panel weight per unit area for any of these configurations.

It has been previously shown that for a panel construction, the weight function parameter for an optimized structure may be expressed as C_{p1} , where C_{p1} depends upon panel type (rectangular-web-core, triangular-web-core, etc.), material elastic modulus, and material strength properties. Using the expression for bending moment for simple support conditions, the panel weight per unit area is

$$(Wt/unit\ area)_{p1} = \gamma_{p1} \bar{t} = \gamma_{p1} C_{p1} m^{1/2} = \frac{\gamma_{p1} C_{p1} p^{1/2} a}{\sqrt{8}}$$

Similarly for the beams

$$(Wt/unit\ area)_{bm} = \gamma_{bm} A/c = \gamma_{bm} \frac{C_{bm} M^{2/3}}{c} = \frac{\gamma_{bm} C_{bm} p^{2/3} a^{4/3} c^{-1/3}}{4}$$

The combined weight of panel and beam can be expressed as a function of a panel alone as follows

$$(Wt/unit\ area)_{total} = \frac{\gamma_{p1} C_{p1} p^{1/2} a}{\sqrt{8}} \beta \quad (22)$$

where

$$\beta = c/a + \frac{\gamma_{bm} C_{bm}}{\sqrt{2} \gamma_{p1} C_{p1}} p^{1/6} (c/a)^{-1/3}$$

Therefore, if β is less than unity, the panel and I-beam combination offers a potential weight reduction compared to the panel alone. The equation above may be minimized with respect to the ratio of beam spacing to beam span, (c/a) , to determine the optimum value of (c/a) . The resulting expression gives

$$\beta_{min} = 4(c/a)_{opt} = 4 \left(\frac{1}{3\sqrt{2}} \right)^{3/4} \left(\frac{\gamma_{bm} C_{bm}}{\gamma_{p1} C_{p1}} \right)^{3/4} p^{1/8} \quad (23)$$

Thus the minimum panel and beam combination may be expressed as a function of the $\gamma_{bm} C_{bm}$ and $\gamma_{p1} C_{p1}$ values. These terms will be denoted hereafter as the beam and panel merit parameters. The value of applied pressure, p , also

influences the weight saving potentials. Curves of β_{\min} vs p for several values of the ratio of beam weight parameter to panel weight parameter are shown in figure 44. Similar results were derived for the two-dimensional I-beam array. The curves presented in figure 45 indicate that the two-dimensional array is lighter for pressures less than 225 psi (1550 kN/m²), but, an extremely large number of secondary beams are needed. The relatively small savings in weight does not provide sufficient incentive to warrant the added complexity. The comparative weights for case I vs case II shown in figure 45 conclusively show that the panel and one-way-beam support system will be desirable over the entire pressure range considered in this program. This concept was therefore used exclusively in the panel designs determined during this study.

Computer programs.- Computer programs were written during the study program to obtain panel and beam weight calculations and to perform the panel optimization analysis for both rectangular-web-core and triangular-web-core panels. The programs were written in FORTRAN II for use on an IBM 7074 computer or FORTRAN IV to be used with the 7094 or System 360 IBM computer systems.

Panel and beam weight calculations: Figure 46 (see also figure 71, Appendix F) shows the logic diagram for the panel and I-beam design procedure. The figure also shows the required input data, the equations used to perform the calculation, and the output data. The symbols for the variables used in the program are listed in table 15. The input data consist of five cards; two of these are title cards, and the remaining three cards contain the required 16 inputs. A listing of the FORTRAN II source deck is provided in table 16. Sample computer output results are shown in table 17, and the input data printed on the output sheet provide a detailed record of the problem solved.

Rectangular-web-core optimization calculation: The computer program for the rectangular-web-core structural optimization was written for ideal elastic-plastic materials. All results were tabulated vs the structural index, m/h^2 (XMDH2 in program language), and the output printouts provide the numerical values for σ_{opt} (SIGØP), t_f/t_c (TFDTC), h/b_f (HDBF), $\bar{t}/m^{1/2}$ (TBDMR), and p (P). The FORTRAN IV source deck listing is provided in table 18 and a sample output is shown in table 19. The input data consists of two cards per problem (any number can be run at one time): the first is a title card, requiring "1" in column 1, and the second contains the seven inputs; initial m/h^2 value (VMDH2), increments of m/h^2 (DMDH2), K_2 (VK2), K_1 (VK1), E (E), σ_y (SIGY), and number of m/h^2 values (MDH2I).

Triangular-web-core optimization calculation: The FORTRAN IV source-deck listing for the triangular-web-core analysis is given in table 20. The input data list is identical to the input data for the rectangular-web-core panel, and the output data is the same except for the added variable, θ (THETA), the optimum angle between the web and faceplates.

Optimization Analysis For Combined Shear and Bending Loads and Minimum-Gage Restraints; Selection of Design Method

In order to achieve a minimum-panel-weight design to carry a specific bending moment and shear load associated with applied uniform external pressure, it is necessary to introduce the web/faceplate fixity interaction in addition to the four geometric variables, t_f , t_c , h , and b_f . As indicated in reference 2, the weight of multiweb sandwich panel structures can be reduced for a pure bending load if the edge-support interaction between the webs and faceplates is utilized. The weight reduction is achieved by adjusting the web spacing so that the faceplates provide partial edge fixity for the webs. This permits enough reduction in web thickness to compensate for the slight increase in faceplate thickness that is necessary to maintain the same section modulus; the net result is a slight reduction in panel weight. The weight reduction is obtained at the expense of a large decrease in shear capability of the panel. Conversely, this implies that a marked improvement in panel shear capability can be obtained with very little weight addition by increasing the web thickness. Minimum-gage constraints play an important role in determining the lightest practical panel configuration that can be constructed. Specific lower limits for total panel depth and for minimum metal thickness were used, but the methods can be applied equally well to different numerical limits. Application of the web/faceplate interaction combined with the effect of minimum-gage constraints leads to a unique minimum-weight design that will simultaneously provide the required bending and shear capability. The procedure involves lengthy computation. Several alternative design approaches, including the one discussed in appendix F, can be used to greatly reduce the computational effort. The resulting designs are somewhat heavier, but the differences in weight are inconsequential.

Panel shear capability for normal pressure loads.- The application of a uniform normal pressure to a panel, gives rise to both shear loads and bending moments. The results given above were developed for the pure bending case, but it is also possible to account for the shear loading. This is accomplished by deriving a curve of panel allowable pressure vs structural index. The maximum shear stress, τ , in the web is given by the equation

$$\tau = 1/2 pa/(t_c h/b_f)$$

This can be related, using equation (9), to the rectangular-web-core geometry in terms of the structural index and the direct stresses to obtain the following equation

$$P_{all} = \frac{0.5 (\tau/\sigma)^2 (2t_f/t_c + h/b_f)^2 (m/h^2)}{\left[t_f/t_c + (1/6)(h/b_f) \right]^2 \left[1 + 2(t_f/t_c)(h/b_f) \right]^2}$$

The appropriate ratio, τ/σ , will depend on whether web failure will be due to yielding or shear buckling. The critical shear yield stress to direct yield stress ratio, based upon the distortion energy theorem, is

$$\tau_y/\sigma_y = \sqrt{3}/3 = 0.577$$

The comparison of web shear buckling criticality is obtained from the ratio between the shear local buckling coefficient, K_3 , and the web buckling coefficient, K_2 , due to the maximum applied bending moment. This leads to a ratio relating K_3 to K_2

$$\tau_{cc}/\sigma_{cc} = K_3/K_2$$

For plates with fixed edges and a very large length-to-width ratio, $K_3 = 8.1$. The fixed-edge assumption appears to be reasonable because of the local reinforcement that will be present near the panel edges. It is necessary to ascertain which expression for τ/σ is valid. For designs in which the webs restrain the faceplates, K_2 may be so small that the critical ratio of shear buckling coefficient to direct stress buckling coefficient will exceed the yield stress ratio-- i.e., $K_3/K_2 \geq 0.577$. A crossover will occur such that

$$\tau/\sigma = K_3/K_2 \text{ for } 0 \leq \sigma \leq 0.577 \sigma_y / (K_3/K_2)$$

$$\tau/\sigma = \frac{0.577 \sigma_y}{\sigma} \text{ for } \sigma \geq 0.577 \sigma_y / (K_3/K_2)$$

Typical results are shown in figure 47 for the rectangular-web-core panel structure for several buckling constraints. Maximum pressure-load capability decreases as the value of δ is increased.

Optimum panel for bending and shear.- The web/faceplate fixity interaction, which determines the web and faceplate buckling coefficients, is then used to generate a family of curves for $\bar{t}/m^{1/2}$ vs m/h^2 (figure 48) and for pressure capability, p , vs m/h^2 (figure 47) for various values of δ . The required interaction curve between the buckling coefficients was obtained from reference 2. The notations used in reference 2 differ from those used in this program; the equivalent notation symbols and the interaction curve are shown in figure 49. As shown in figure 47, the panel design based on $\delta = 2.45$ (simply supported webs and faceplates) will carry a pressure loading up to 265 psi (1830 kN/m²). The optimum structural index would be 3367 psi (21 210 kN/m²), and the related value of the weight function would be $\bar{t}/m^{1/2} = 0.00121$ in./lb^{1/2} (1.46×10^{-5} m/N^{1/2}). If the pressure were 114 psi (791 kN/m²), a panel design based upon $\delta = 3.0$ would be acceptable, the optimum structural index would be reduced to 3084 psi (21 300 kN/m²), and the weight function would be reduced to 0.00116 in./lb^{1/2} (1.39×10^{-5} m/N^{1/2}). As a final example, a pressure loading of 640 psi (4420 kN/m²) would require the use of $\delta = 2.0$, the optimum structural index would be 3705 psi (25 600 kN/m²), and the weight function would increase to 0.00127 in./lb^{1/2} (1.52×10^{-5} m/N^{1/2}). Satisfying the combined effects of bending and shear loads in a panel loaded by normal pressures provides the minimum possible panel weight for those designs in which minimum-gage effects are not a factor.

Effect of minimum-gage. - The optimum panel metal thicknesses determined from the optimum structural design formulations may be very small when the applied bending moment and/or applied pressure is small. In these cases, the panel faceplates or webs can be less than the minimum fabricable size, and departure from the minimum-weight curve is necessary. Figure 50 shows the panel weight vs applied bending moment for a typical case. The dotted line is the optimum-panel-weight line. For an applied moment equal to or less than 740 in.-lb/in. (3300 N-m/m), the panel weight must exceed the optimum because in these instances the optimum facesheet would be less than the minimum gage choice of 0.010 in. (0.0254 cm). Furthermore, when the minimum fin thickness and height restrictions shown in the figure are used, the minimum possible panel weight is 0.90 lb/ft² (4.4 kg/m²). The weight curve consists of four portions coinciding with the number of constraints on the four panel geometric variables. The four subdivisions of the curve may be categorized as follows:

- Constant-weight design - All panel dimensions are minimum, and structural design consists of finding the proper beam spacing and design details.
- Variable-panel-height design - The only varying panel dimension is height--i.e., panel web thickness and panel facesheet thickness are fixed.
- Modified optimum panel design - The panel face sheet thickness is constant while both panel height and web thickness are variable. This actually makes use of the optimum design curves at structural index values above the true optimum design point, and a small weight increase occurs.
- Optimum panel design - The minimum-weight panel is obtained as a function of the loading with no restrictions.

The optimum design formulation may be used to satisfy combined bending moment and shear loads in the minimum-gage region. The following calculation sequence is used

- Select m/h^2
- Tabulate t_f/t_c and h/b_f
- Compute h and t_c
- Compute bending moment
- Obtain p
- Compute \bar{t}

This calculation was carried out, and typical results were plotted in figure 51. Actually, p vs m and \bar{t} vs m are plotted separately in this figure, and lines of constant pressure capability of 100 and 250 psi (689 and 1720 kN/m²), were

superimposed on the \bar{t} vs m curves. With figure 51, it is possible to obtain the lightest panel for a specific bending moment and pressure. Since the derivation of optimum beam spacing was determined without consideration of minimum gage, the spacing must be somewhat adjusted in the minimum-gage design region. This can be accomplished by using the constant-pressure line on the \bar{t} vs m curve and by scanning and computing both beam and panel weight as a function of beam spacing to determine the lightest design.

Comparison of four panel and beam design procedures.- Structural weights have been computed for four designs, some of which do not satisfy the minimum-gage restrictions or do not possess adequate panel shear capability. The most important comparison is between the weight obtained from the above procedure and that used for the baseline concepts evaluation and the tradeoff study. A sample calculation gave a combined panel and I-beam weight of 4.315 lb/ft² (21.07 kg/m²) compared to minimum panel and beam weights of 4.284 lb/ft² (20.91 kg/m²) from the method just described. This comparison shows that the simplicity of the procedure used for program evaluations justifies its use and that the panel and beam weight calculations obtained are a realistic appraisal of the design weight. The comparison was performed for a 24 by 24 in. (0.61 by 0.61 m) area under a uniform pressure of 100 psi (689 kN/m²). Panel and beam material properties and minimum-gage restrictions are shown in figure 50.

Pure bending design, simple support buckling coefficients: The panel and beam combination was sized based on the optimization technique for pure bending, disregarding panel minimum-gage restrictions and shear capability. The simple support buckling coefficients, $K_1 = 3.62$ and $K_2 = 21.7$, were used. The resulting facesheet thickness was 0.00763 in. (0.0194 cm), less than the 0.010-in. (0.0254-cm) minimum gage. The total weight per unit area was 4.276 lb/ft² (20.88 kg/m²).

Pure bending design, optimum buckling coefficients: The weight function shown in equation (12) is minimized when the product of K_1 and K_2 is maximized. This occurs when $K_1 = 3.46$ and $K_2 = 33.3$. The weight given above, for the pure bending case with no minimum-gage or shear considerations, is reduced to 4.224 lb/ft² (20.62 kg/m²).

Minimum possible weight for combined shear, bending, and minimum gage: The complete optimization technique satisfying all design constraints was used in curves such as those in figures 46, 47, and 50. This involved a detailed computation of panel and beam weight vs beam spacing including cross-plotted curves for \bar{t} vs m with a constant-pressure capability (figure 50). The resulting minimum possible panel and beam weight was 4.284 lb/ft² (20.91 kg/m²).

Program procedure for combined shear, bending, and minimum gages: The procedure used for the baseline concept evaluation and tradeoff study (see figures 46 and 71) consisted basically of (1) computing the weight parameter for the panel using simple support buckling conditions, (2) determining optimum beam spacing for pure bending, (3) calculating panel dimensions including minimum-gage restrictions, (4) checking panel shear capability and increasing the web thickness if necessary, and (5) computing beam dimensions and total panel and beam weight. The basic departure from the optimum design technique was the

method of satisfying shear capability. The panel and beam weight per unit area for the case considered was 4.315 lb/ft² (21.07 kg/m²).

Effect of Metal Temperature on Weight

The optimum structural design derivations outlined above provide a convenient tool for determining the relative merits of any panel or beam materials with respect to temperature. It is possible to express the weight parameter of the structure at the minimum-weight point as a function of material properties. By including material density, a direct comparison to any other material is possible. The minimum-weight combination of panel and beams vs temperature may then be determined. The analysis of material merits is one of the important benefits of the structural optimization technique.

Panel weight evaluation. - To evaluate the merits of various panel materials vs temperature, the product of material density, γ_{p1} , and structural index, $\bar{t}/m^{1/2}$, must be expressed as a function of material properties at the point of minimum panel weight. The product, $\gamma_{p1}(\bar{t}/m^{1/2})$, is called the panel weight parameter, and from equation (13) for $K_1 = 3.62$ and $K_2 = 21.7$,

$$\gamma_{p1} C_{p1} = \gamma_{p1} (\bar{t}/m^{1/2}) = 1.625 \gamma_{p1} / (E\sigma)^{1/4}$$

Figure 52 shows $\gamma_{p1} C_{p1}$ vs temperature for several candidate panel materials. The allowable stress used in this expression was the lesser of the material yield strength or the 100-hr rupture strength as determined from property data in references 3 through 9. The form of the panel weight parameter shows that its value is directly proportional to density and inversely proportional to a fractional power of both elastic modulus and yield strength. For this reason, the light alloys show to great advantage at low temperatures. The superalloys are clearly preferable at temperatures above 1000°F (811°K). The curves show that for temperatures above 1200°F (922°K) there is a very marked increase in superalloy panel weight corresponding to the transition from yield-strength-limited to creep-strength-limited designs.

Beam weight evaluation. - The similar expression used to evaluate candidate beam materials from equation (21) is given by

$$\gamma_{bm} C_{bm} = 1.565 \gamma_{bm} / E^{1/6} \sigma_y^{1/2}$$

The beam weight parameter is plotted as a function of temperature for several materials in figure 53. The curves clearly show that the lowest values of beam weight parameter would be obtained by using the titanium alloy at temperatures below 300°F (422°K). Over the temperature range from 400° to 800°F (478° to 700°K), the maraging steel alloy shows to best advantage. Above 900°F (756°K), high-nickel superalloys are preferable. The curves indicate that it would be advantageous to employ cooled beam structures if titanium or aluminum beams are used and that very little metal weight reduction can be obtained by

operating superalloy beams at 100°F (311°K) instead of 1100°F (867°K). This figure also shows the typical increase in superalloy beam weight due to the transition to creep-strength-limited designs for material temperatures above 1200°F (922°K).

Combined beam and panel weight. - Figure 54 shows the parameter $(\gamma_{pl} C_{pl})^{1/4} (\gamma_{bm} C_{bm})^{3/4}$ vs temperature for a minimum-weight panel and minimum-weight beams at that same temperature. This parameter measures the combined minimum weight of the panel and beams for varying temperatures at a constant pressure. The parameter was derived from the equations of total combined beam and panel weight (equations (22) and (23)).

$$\left(\frac{Wt}{\text{unit area}} \right)_{\text{total}} = 0.478 p^{5/8} a (\gamma_{pl} C_{pl})^{1/4} (\gamma_{bm} C_{bm})^{3/4}$$

The resulting curve for minimum combined panel and beam weight can be closely approximated by a straight line from the temperature range -360° to 1100°F (56° to 867°K). The potential total weight savings would be 38 percent for a reduction of panel and beam temperature from 1100° to 70°F (867° to 294°K). It should be noted that the curves of figure 54 are intended to indicate minimum possible weight and that some of the materials shown would be restricted in their use due to fabrication considerations or, in the case of titanium, hydrogen embrittlement. These type of considerations are discussed in Appendix G. Figure 54 also shows the value of the parameter $(\gamma_{bm} C_{bm} / \gamma_{pl} C_{pl})$ for minimum-weight combined beams and panels vs temperature. This parameter, which was discussed earlier in this section, indicates the merits of using a panel and beams relative to the merits of using a panel alone. A peak value of 0.25 in. ^{1/3} / lb ^{1/6} (0.06m ^{1/3} / N ^{1/6}) is reached at 300°F (422°K), and from figure 44, it can be noted that, for pressures of 370 psi (2550 kN/m²) or greater, the panel by itself would be more efficient from a weight standpoint compared to the beam and panel combination. Since the panel and beam structures are designed to a safety factor of 1.5 on load capability, an applied pressure of 250 psi (1720 kN/m²) would require that the structures be sized to carry an equivalent pressure of 375 psi (2590 kN/m²). Situations may arise, therefore, where the optimized panel and beam combination would theoretically weight as much or slightly more than the equivalent panel. Even in these cases, the versatility in design provided by using beams and panels makes this design approach more desirable.

Panel In-Plane Thermal Stresses

Thermal stresses in the plane of the panel resulting from various temperature profiles and nonlinearities in material properties have been considered. The main reason for determining these stresses is that in prime structure panels, the combined thermal and pressure-load stresses must not exceed the allowable material stress. The panel weight could greatly increase due to high thermal stresses because the applied pressure load that the panel can carry would be seriously reduced. The thermal stress analysis was performed

by a computer program that solves the problem for two-dimensional plate structures. The computed stresses are based on the assumption that the panel edges are not constrained from in-plane thermal expansion. Preliminary calculations showed that edgewise constraint would lead to excessive thermal stresses that must be avoided. Therefore, assuming no edge restraint, the coolant flow routing method is assumed to be the primary cause of temperature distributions which lead to thermal stresses.

Three different flow routing schemes (see Flow Routing Arrangements, appendix A) which result in the temperature distributions along the panel length shown in figure 55 were considered. In addition, thermal stresses due to two types of flow nonlinearities, shown in figure 56, were investigated. The nonlinear temperature rise (figure 56a) may result from nonuniform heating along the panel and the maldistribution normal to the flow direction (figure 56b) may result from nonuniform heating or variations in coolant flow rate across the width of the panel.

The results of the analysis, discussed in the subsections which follow, indicated that the only acceptable coolant routing scheme is one in which the coolant enters at one end and exits at the other to give a linear or nearly linear profile as shown in figure 55a. The stresses for this case were less than 5000 psi (34 500 kN/m²) maximum for any panel aspect ratio (length/width ratio), whereas for the range of aspect ratios considered reasonable for this program, the sawtooth and triangular temperature profiles produce stresses well in excess of 10000 psi (68 900 kN/m²). With the selection of the linear temperature profile, the magnitude of the thermal stresses was small enough to be ignored in the subsequent design of minimum-weight panel structures. However, the analysis of stresses due to nonlinearities indicated that severe variations from the linear profile must be avoided to insure that the above assumption is valid.

Stresses due to axial temperature profiles.- The axial temperature profiles in figure 55 are

- Linear temperature rise from one end to the other (straight-through single-pass coolant flow)
- Triangular temperature profile, which would occur if coolant were manifolded into both ends of the panel and then taken out at the middle
- Sawtooth profile, which would occur if flow length were one-half the panel length and if hot and cold manifolds were placed next to each other at the middle of the panel

For the preliminary comparison of the three profiles, the metal temperature differential was taken to be from -60°R (222°K) at the cold end rising to 1140°R (889°K) at the maximum temperature point. The panel was taken to be 40 in. (1.03 m) wide by 60 in. (1.52 m) long, with the coolant flow in the long direction. Temperature was assumed to be uniform across the width dimension of the panel.

The thermal stresses for the panel with the linear temperature profile were very low, those for the triangular profile were much higher (although possibly acceptable), and those for the sawtooth prohibitively high. For the latter profile the maximum stresses were in excess of 100 000 psi (689 000 kN/m²). Since thermal stresses of this magnitude would seriously reduce the applied loads that the prime structure could support, the sawtooth profile was not considered further.

Effect of panel aspect ratio on in-plane thermal stresses.- Thermal stresses were computed for the triangular temperature profile and linear temperature profiles as a function of panel aspect ratio. The range of aspect ratios studied was $0.5 \leq l/w \leq 5.0$. Nine different cases were solved for the triangular profile, and a summary of the results is shown in figure 57. The figure also shows the panel layout and temperature distribution. The results indicate maximum thermal stresses in excess of 40 000 psi (286 000 kN/m²) for all values of $l/w < 4.0$ ($w/l > 0.25$).

The three cases that were computed for the linear profile are summarized in figure 58. The results indicate that the maximum stress for any aspect ratio is 4500 psi (31 000 kN/m²). Comparison of these stresses with the results for a triangular temperature profile shows that the linear profile is definitely preferable. Panel stresses are much lower, and no restriction is placed on panel aspect ratio. Figure 59 shows the panel layout for one of the cases analyzed. The nodal point array, temperature distribution, and stress distribution are shown.

The temperature profile in figure 58 shows a constant temperature portion at the extreme temperatures which contributed to the maximum thermal stresses in the linear profile. This constant temperature region was a necessary input since the computer program assigned the same temperature to the boundary as that of the adjacent node point. In actual operation a similar constant temperature may result at the panel ends due to the header bars enclosing the heat exchanger, although the exact magnitude may differ from the cases analyzed. It is expected that the results shown in figure 58 represent a fairly severe case for the linear profile and the stresses shown would be conservative. A similar situation holds for the triangular profile in figure 57 (the dotted line shows the desired profile), however, the maximum thermal stresses do not occur at the end boundary regions in this case. The constant temperature region lowers the maximum stress slightly by the resulting reductions in total panel ΔT .

Nonlinear temperature profiles.- Analyses were performed to determine the effects of the lengthwise and widthwise temperature nonuniformities shown in figure 56 on the thermal stresses for panels with linear temperature profiles. The results indicated that a 200°F (111°K) nonuniformity would increase the maximum stress to about 10 000 psi (69 000 kN/m²), more than two times the stress for a comparable panel without the nonuniformity. It is therefore apparent that large temperature nonuniformities would significantly reduce the load carrying capacity of the prime panel and must be avoided.

For the purposes of the present study it was assumed that the temperature nonuniformities were small enough that the resulting thermal stresses could be neglected. This assumption was consistent with the uniform or nearly uniform heating and the uniform coolant flow conditions postulated for the study. In cases where larger temperature nonuniformities exist, the design procedures presented herein would have to be adjusted to account for the resulting thermal stresses.

Two-dimensional thermal stress derivation. - Two-dimensional problems of elasticity are solved by determining the stress function, ϕ , which satisfies the biharmonic equation for interior points with given forces or absence of forces at the boundaries. The stress-strain relationships are

$$\begin{aligned}\epsilon_x &= (1/E)(\sigma_x - \nu\sigma_y) + \alpha T & \gamma_{xy} &= \tau_{xy}/G \\ \epsilon_y &= (1/E)(\sigma_y - \nu\sigma_x) + \alpha T & G &= E/2(1 + \nu)\end{aligned}\quad (24)$$

To solve this problem, it is necessary to know the temperature distribution (i.e., the thermal expansion) throughout the structure from a given reference temperature, $(\alpha T)_i - (\alpha T)_{ref}$. The stress distribution within the structure must then satisfy the conditions of equilibrium and deformation compatibility throughout. The equilibrium equations are

$$\begin{aligned}\partial\sigma_x/\partial x + \partial\tau_{xy}/\partial y + X &= 0 \\ \partial\tau_{xy}/\partial x + \partial\sigma_y/\partial y + Y &= 0\end{aligned}\quad (25)$$

where X and Y are body forces. From the expressions for deformations, the compatibility condition is

$$\partial^2\gamma_{xy}/\partial x\partial y = \partial^2\epsilon_x/\partial y^2 + \partial^2\epsilon_y/\partial x^2\quad (26)$$

The stress function is defined such that

$$\sigma_x = \partial^2\phi/\partial x^2, \quad \sigma_y = \partial^2\phi/\partial y^2, \quad \tau_{xy} = -\partial^2\phi/\partial x\partial y\quad (27)$$

By differentiating the first of equations (25) with respect to x and the second with respect to y , and combining equations (24) with (26), the following result is obtained

$$\nabla^2(\sigma_x + \sigma_y) = -(1 + \nu) \operatorname{div} \bar{F} - \nabla^2(E\alpha T)/(1 - \nu)$$

where $\nabla^2 = \partial^2/\partial x^2 + \partial^2/\partial y^2$

$$\operatorname{div} \bar{F} = \partial X/\partial x + \partial Y/\partial y$$

Substituting in the stress function ϕ from (27)

$$\nabla^4 \phi = - (1 + \nu) \operatorname{div} \bar{F} - \nabla^2(E\alpha T)/(1 - \nu)$$

For constant forces, $\operatorname{div} \bar{F} = 0$, and this reduces to

$$\nabla^4 \phi = - \nabla^2(E\alpha T)/(1 - \nu) \quad (28)$$

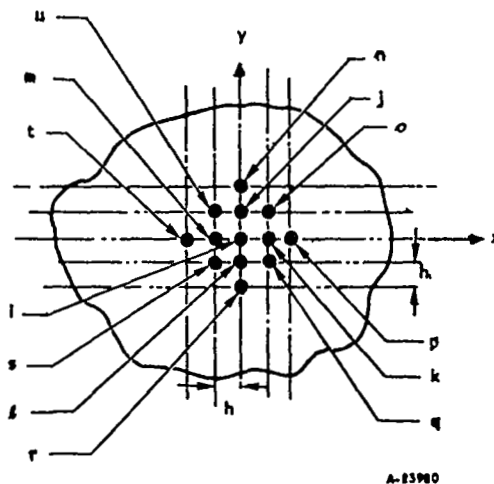
The solution is best obtained by finite difference methods. For $\Omega = [1/(1 - \nu)](E\alpha T)$, equation (28) may be written as

$$\nabla^4 \phi = - \nabla^2 \Omega \quad (29)$$

The finite difference form using a grid spacing, h , leads to the following differential operators

$$\nabla^4 \Big|_{\text{op}} = 1/h^4 \begin{bmatrix} & & 1 & & \\ & 2 & -8 & 2 & \\ 1 & -8 & 20 & -8 & 1 \\ & 2 & -8 & 2 & \\ & & 1 & & \end{bmatrix}, \quad \nabla^2 \Big|_{\text{op}} = 1/h^2 \begin{bmatrix} & 1 & \\ 1 & -4 & 1 \\ & 1 & \end{bmatrix} \quad (30)$$

The grid array notation is shown below.



For free edges, the boundary values are

$$(\phi)_b = 0, \quad (\partial\phi/\partial h)_b = 0$$

For each node point i , equation (30) may be used to express the stress function at i in terms of the stress function values at the neighboring points as follows

$$\begin{aligned} 1/h^4 [20\phi_i - 8(\phi_j + \phi_k + \phi_l + \phi_m) + 2(\phi_o + \phi_q + \phi_s + \phi_u) \\ + (\phi_n + \phi_p + \phi_r + \phi_t)] = -\nabla^2\Omega_i \end{aligned} \quad (31)$$

Note that equation (29) corresponds to a normally loaded plate with fixed edges from the following observed analogy

$$\nabla^4 w = q/D$$

where, at the boundary, $w = 0$, $\partial w/\partial h = 0$, and $-\nabla^2\Omega = q/D$

The solution of any specific thermal distribution is obtained by writing an equation as given by (31) for each node point, which gives the stress function ϕ_i at each node point in terms of the neighboring twelve node points.

Then, by applying the boundary conditions and writing a system of as many linear equations as there are node points, the stress function ϕ_i at each node point can be directly computed. Stresses may then be determined at each node point from equation (27) by converting these expressions into finite difference forms as follows

$$\sigma_x = \partial^2\phi_i/\partial x^2 \approx 1/h^2(\phi_k - 2\phi_i + \phi_m)$$

$$\sigma_y = \partial^2\phi_i/\partial y^2 \approx 1/h^2(\phi_j - 2\phi_i + \phi_l)$$

$$\tau_{xy} = -\partial^2\phi_i/\partial x\partial y \approx -1/4h^2(\phi_o + \phi_s - \phi_u - \phi_q)$$

Hot-Surface Thermal Fatigue Studies

When integral metallurgical bonding is used for attachment of the heat exchanger to the prime-load-carrying structure, the thermal expansion differential between the heated heat exchanger plate and the prime structure will be almost entirely accommodated by compressively loading the heated plate. In addition, compressive loading is produced on the heated sheet by the bending action of the prime structure under normal pressure. The heat exchanger surface will be forced to deform into the same contour as the prime structure. The compressive strains induced in the heated heat exchanger sheet (and to a lesser extent the fins) are of such magnitude that fatigue life calculations for the heat exchanger must be performed to determine if sufficient operating life is attained. To avoid excessive thermal fatigue calculations, the approach taken in the heat exchanger design was to establish a maximum allowable temperature differential between the hot face plate and the prime structure that would permit the fatigue life of the structure, using the more attractive candidate materials, to meet or exceed the required cycle life with a suitable margin of safety. Based on the analysis presented in the following paragraphs a maximum

allowable temperature differential of 400°R was established. This temperature permits the attainment of a cycle life of 300 cycles for the materials of interest with a factor of safety of 10 or greater. This factor appears reasonable in view of the uncertainties involved with the prediction of fatigue life for fabricated parts.

The analysis was based on the accumulated plastic strain approach for estimating fatigue life. The number of cycles to failure, N, is determined from the empirical relation discussed in references 10 and 11

$$N = (C/\epsilon_p)^2$$

where ϵ_p = the plastic strain

C = a ductility constant

The constant, C, was determined from the relation discussed in reference 12 which relates the fracture ductility, ϵ_f , to C by the equation

$$C = 0.8 \epsilon_f^{3/4}$$

where ϵ_f is related to the reduction in area, percent RA, of a standard ultimate tensile test by the equation

$$\epsilon_f = -\ln (100 - \%RA)/100$$

A difficulty lies in determining the influence of creep on cycles to failure. An upper bound on the effect of creep on plastic-stress range can be obtained by assuming that the hold time at elevated temperature is sufficiently long to allow total relaxation of the stress. This will increase the strain range per cycle, and it will reduce the number of cycles to failure. This is shown in figure 60 for an ideal elastic-plastic material.

Each cycle with creep was treated as two half-cycles, one with a plastic range of $(\epsilon_p)_{1-2}$ and the other half-cycle with a plastic range of $(\epsilon_p)_{4-5}$. The combined effect was handled by use of the following equation

$$N = \frac{2C^2}{(\epsilon_p)_{1-2}^2 + (\epsilon_p)_{4-5}^2}$$

For the purpose of the analysis it was assumed that all of the thermal strain due to the differential elongations between the hot face plate and the prime structure, and an additional mechanical strain of 0.00593 in./in. (cm/cm) were absorbed by the hot face plate. The latter strain is used to account for the effect of bowing of the structural panel under the external load and corresponds to 110 percent of the strain for Inconel 718 at its yeild point. It is also assumed that buckling of the outer sheet does not occur and that the

sheet is uniformly strained, i.e., there are no discontinuities in geometry leading to strain concentrations. Stresses on the outer sheet due to differences between internal hydrogen pressure and external air load were not considered because they are comparatively negligible.

Curves of cycles to failure vs temperature are shown in figure 61 for six possible materials with an Inconel 718 prime structure at 1140°F (889°K). From the figure it can be seen that the desired 300 cycle life with a factor of safety of 10 or greater can be expected with Waspaloy, Hastelloy X, Hastelloy C, and Inconel 625 if the temperature differential is limited to 400°F (220°K). The superior performance of these materials is primarily due to the superior high-temperature ductility properties of these materials at elevated temperatures, as shown in figure 62. Material property data used to generate figures 61 through 63 were obtained from references 13 through 19. Of the materials, Inconel 625 appears to be preferable because of its superior cycle life expectancy. It should be emphasized that the reduction-in-area data available at the present time, for the temperature ranges desired, are incomplete. In particular, it was necessary to use elongation data for Hastelloy X and Inconel 625 in the absence of reduction-in-area data. Therefore, figure 61 should be interpreted as a qualitative indication of the relative merits of the six materials. Figure 63 shows the fatigue strength of a Waspaloy heat exchanger sheet as a function of the Inconel 718 prime structure temperature. The curves show (1) the effects of temperature difference between the heat exchanger material and the prime structure on fatigue life and (2) the decrease in fatigue life of the heat exchanger with increased temperature difference.

Panel Flutter Considerations

During hypersonic cruise vehicle operations, airflow or combustion gas flow over the panel surface can cause flutter instability. The design approach taken in considering such flutter instability was, in general, to complete the entire panel design by the procedures outlined in appendix F and then check flutter susceptibility utilizing the results of a flutter analysis of orthotropic panels (reference 20). Where flutter sensitivity occurred, the designs were not modified since it was determined that overall panel weights, and hence the weight comparisons in this study, were not significantly affected when stability was achieved.

Since preliminary analysis had indicated that low-pressure load designs might be susceptible to flutter, several panel and beam arrays were investigated to determine if a preferred beam orientation relative to gas flow existed. The preliminary results did not indicate that a particular beam orientation would be advantageous. The selected orientation (see appendix D, Problem Area Identification) was to assume that gas flow was parallel to coolant flow and perpendicular to the beams (see figure 3 for example).

The concept evaluation and tradeoff study results were checked for both general flutter instability (entire structure in motion) and local flutter instability (panel sections between beams in motion). Panels were considered to be insensitive to flutter when the critical dynamic pressure parameter (reference 20) exceeded the calculated dynamic pressure parameter by a factor of 1.5

for an assumed minimum gas flow velocity of Mach 1.5 at a dynamic pressure of 2000 psf (96 kN/m²). The survey showed that the panel designs (tables 6 through 8 and 12 through 14) were not susceptible to local flutter and concepts 2 and 3 were not sensitive to general flutter. Some of the low pressure load designs for concept 1 were sensitive to general flutter, however, as discussed below, the weights are not appreciably affected when flutter strength is satisfied.

The survey showed that for 2-by 2-ft (0.61-by 0.61-m) panels, eight of the concept 1 tradeoff study designs (table 12) were sensitive to general flutter, seven for the 6.95 psi (48 kN/m²) design pressure load and one for 20 psi (138 kN/m²) pressure. These designs were susceptible for panel heights less than about 0.075 in. (0.191 cm). For 2- by 5-ft (0.61- by 1.52-m) concept 1 panels, all of the 6.95 psi (48 kN/m²) designs (tables 6 and 12) and one 50 psi (345 kN/m²) pressure load case (table 12) were flutter sensitive. The required panel heights to prevent flutter for these longer flow lengths was about 0.165 in. (0.419 cm) for 6.95 psi (48 kN/m²) and 0.145 in. (0.368 cm) for 50 psi (345 kN/m²).

The above reference to required minimum panel heights is based on increased panel height being the most efficient method of strengthening the panel array. Since the weight of the panel, beams, and clips is a weak function of concept 1 panel height (see figure 66), nominal weight increases will result from choosing non-optimum beam and panel combinations. For example, the 20R-0.025-0.003 (7.9R-0.064-0.0076) design for a 2- by 2-ft (0.61- by 0.61-m) panel with 50 Btu/sec-ft² (568 kN/m²), 1600°F (889°K) and 6.95 psi (48 kN/m²) in table 12 would have less than a three percent increase if the 20R-0.075-0.003 (7.9R-0.191-0.0076) fin were required. However, increased panel heights may not always be acceptable due to the associated increases in maximum panel surface temperature. In cases where maximum temperature limitations occur, several additional options are available to the designer such as decreasing coolant flow length (the critical dynamic pressure parameter increases), use of offset rather than plain fins (cross-section ΔT decreases) or changing to the concept 2 design. Weight increases would occur in any case and the proposed choice for improved flutter performance would depend on a detailed comparison of the various options.

APPENDIX F

DESIGN PROCEDURES AND SAMPLE CALCULATIONS

Detailed design procedures were developed for the major components in a panel. The procedure for low loading, both external pressure and heat flux, was significantly different from that for the higher loads.

Concept 1 Panel, Clips, and Beams

The design of the panel structures in the low-pressure-load, low-heat-flux region is primarily concerned with a single-layer sandwich panel on I-beam supports. Combining the heat exchanger and load-carrying functions into a single-layer sandwich panel leads to significantly different design considerations from the high-pressure, high-flux design case. The important considerations arising are:

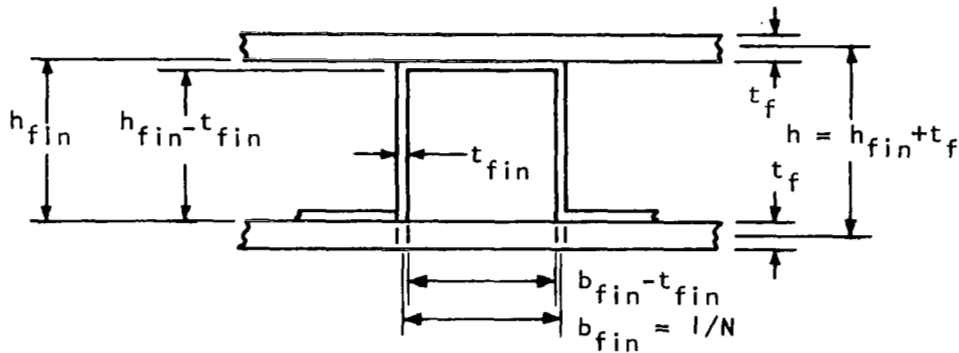
- Panel material properties used for normal pressure design are highly dependent on heat transfer design, primarily because the higher sheet temperature is strongly affected by fin height, fin thickness, fin spacing, and applied heat flux.
- The panel sheets and fins must be designed to withstand both coolant internal pressure stresses and normal pressure shear and bending stresses.
- The panel will be held flat by the beams, and temperature differences between the upper and lower sandwich sheets will produce thermal compressive stresses in the top sheet and tensile stresses in the lower sheet. This will load the panel structure in exactly the same way as the applied pressure bending loads.

The first step in the design approach is a heat transfer analysis on panel fin geometry. The heat transfer analytical results are then used to establish beam spacing, beam dimensions, and attachment clip weight. This leads to the identification of the specific design with the lightest combined weight of the panel, beams, and attachment clips. The material selections were a Waspaloy panel and Inconel 718 beams and attachment clips. The Waspaloy sandwich panel must be designed to provide for (a) the containment of the hydrogen coolant and (b) the concurrent application of bending and shear loads due to normal pressure. The following assumptions were used:

- Panels and beams are simply supported
- In-plane thermal stress in the sandwich panel due to in-plane thermal gradients is negligibly small
- Design safety factor is 1.5 on applied load

- Minimum gage limitations are not violated
- Temperature difference across beams is zero
- I-beam design temperature is the coolant outlet temperature. An exception occurs for coolant outlet temperatures higher than 1600°R (889°K), where the beam nearest to the hot end is designed for coolant outlet temperature, and the other beams are designed based on material properties at 1600°R (889°K).
- The panel span between beams is checked for flutter sensitivity
- The panel and beam array is not flutter sensitive

A typical square-cornered plate-fin construction used in this study is shown below.



The equation for effective metal thickness is

$$\bar{t} = t_{fin} + \left(\frac{h_{fin} - t_{fin}}{b_{fin}} \right) t_{fin} + 2t_f \quad (32)$$

In addition, the section modulus properties must be computed to calculate the required beam spacings. Referring to the above sketch showing the square-cornered plate-fin geometry, the structural height is defined as

$$h = h_{fin} + t_f$$

For plain fins, full credit is taken for the strength contribution of the fins. The cross-sectional amount of inertia per unit width is

$$I = \frac{t_f h^2}{2} + \frac{t_{fin}(h_{fin} - t_{fin})^2}{4} + \frac{t_{fin}(h_{fin} - t_{fin})^3}{12 b_{fin}}$$

The section modulus per unit width is

$$z = \frac{I}{h/2} = t_f h + \frac{1}{2} t_{fin} (h_{fin} - t_{fin}) \left(\frac{h_{fin} - t_{fin}}{h} \right) + \frac{1}{6} \frac{t_{fin}}{b_{fin}} (h_{fin} - t_{fin})^2 \left(\frac{h_{fin} - t_{fin}}{h} \right)$$

For offset fins, the fin material is assumed to carry the shear loads from normal pressure, but due to the discontinuity in the fin geometry introduced by the offsets, the assumption is made that the fin material does not contribute to bending strength. The section modulus then becomes simply

$$z = t_f h$$

Heat transfer analysis.- The heat transfer analysis employs the procedures described in reference 1. A typical set of curves of fin ΔT vs fin height is shown in figure 64. The sum of coolant outlet temperature and fin ΔT provides the maximum hot-surface metal temperature for obtaining the allowable stresses and panel thermal stresses. In the design procedure, similar curves were obtained for fin spacings up to 40 fins/in. (15.8 fins/cm). Coolant pressure drop was not a critical problem. Total pressure drop for the manifolds and panel flow length was found not to exceed 50 psi (345 kN/m²), and fin containment for all concept 1 designs was based on an internal pressure of 300 psi (2070 kN/m²).

Structural analysis for coolant pressure containment.- It was determined that stresses due to coolant pressures were not an important design consideration in the low-flux concept 1 panels. For higher heat fluxes, these stresses may very well become critical, in which case the problem can usually be resolved by increasing the fin metal thickness or decreasing the fin spacing. Therefore, the low-load, low-flux design procedure does not formally include coolant containment design, although adequate strength was verified. The allowable fin stress for pressure containment, as indicated in other sections of this report, is determined from the lower value of the yield stress or the rupture stress for the 100-hr required life, where a safety factor of 1.5 is used to obtain the allowable stress. Applicable Waspaloy material properties are shown in figure 65. The fin tensile capability was then computed from the formula

$$p_{all} = 0.5 \sigma_{all} / (b_{fin}/t_{fin} - 1) \quad (33)$$

The 0.5 coefficient in this formula is a typical ratio of actual strength to theoretical strength based on test results of typical fin configurations.

The fin spacing and maximum face sheet temperature data are used to establish required face sheet thickness. In all designs, 0.010-in. (0.0254-cm) minimum gauge facesheets were satisfactory. The facesheet bending stress is given by the formula

$$\sigma = 0.5 p (b_{fin} - t_{fin})^2 / t_f^2 \quad (34)$$

Pressure containment bending stresses are so low that they were assumed not to subtract from the bending capability of the sandwich panel.

Structural analysis for external pressure loads.- The required beam spacing for each panel configuration is determined solely from the heat transfer analysis and panel bending strength for normal pressures. Therefore, beam spacing, c_{all} , is determined from the equation

$$c_{all} = (8\sigma_{all} z/p)^{1/2}$$

where z is the section modulus per unit width of the panel. The thermal stress due to temperature difference across the fin height will induce thermal stresses in the sandwich panel equal to $E \alpha \Delta T / 2 (1 - \nu)$. Actually the thermal stresses vary because the panel is held flat by the restraint at the discrete beam points rather than by a pure bending moment. The allowable design stress for bending loads was taken from the more conservative of

$$\sigma_{all} = \left| \sigma_y - E \alpha \Delta T / 2 (1 - \nu) \right| / 1.5$$

or

$$\sigma_{all} = \sigma_{100 \text{ hr stress rupture}}^{1/1.5}$$

The above stress criterion is based upon the assumption that the thermal stress will be rapidly alleviated if creep occurs, and thus thermal stress effects will not materially alter the creep-rupture life of the panel. A further assumption implied here is that low-cycle-fatigue failure is not a critical design factor because the yield stress will not be exceeded.

Minimum combined weight.- The allowable beam spacing for a given panel geometry is used to calculate beam and attachment clip weight (see below) and hence the combined weight of the three components. Figure 66 shows curves of the panel, beam, and attachment clip weights in addition to a summation of these weights plotted against fin height. The fin height that produces the minimum total weight can then be selected. It can be readily observed that the attachment weight is not small, and that it has a significant effect on the minimum weight points. It can be further noted that the curve for total weight sum vs fin height shows a relatively small weight change over the entire range of fin heights. Although the minimum weight point is not sharply defined in this figure, the error in the estimate of minimum weight will be small.

The calculation of total panel weight requires the addition of braze-alloy weight. It has been established that a typical single-layered-sandwich construction will require approximately 0.089 lb/ft² (0.438 kg/m²) of braze alloy. This weight was added directly to the panel weight for face plates and fins.

The analysis for minimum weight involves the investigation of a large number of fin height, thickness, and spacing combinations. The estimate of beam weight can be greatly facilitated for all of these different cases once the beam weight at one spacing is known. Beam weight is proportional to spacing raised to the one-third power, and this permits use of the relation

$$\text{Beam weight} = \text{Weight}_{\text{ref. beam}} \left(\frac{c_{\text{ref.}}}{c} \right)^{1/3}$$

Additional data in table 21 show that there is virtually no difference in combined weight between designs that use offset fins and designs that use plain fins of the same spacing and height. Since plain fins offered a slight weight advantage and lower fabrication costs, they were selected as the primary fin configuration for concept 1 panels. This choice was made to reduce the computation effort for the tradeoff analysis (all concept 1 panels in the tradeoff study use plain fins), and it should not be construed as a hard and fast selection. Detailed investigation would be needed to establish the optimum choice between plain and offset fins at other heat fluxes. The offset fins might be superior for moderately higher heat fluxes or for higher coolant outlet temperatures due to their lower cross section ΔT , and this could extend the range of applicability of the concept 1 panels. Since the fin weights are very similar, the panel weights used for concept 1 designs are realistic even if the fin preference eventually changes.

Concepts 2 and 3 Prime Structural Panel and Beams

In concepts 2 and 3, the panels consist of a composite two-layered-sandwich construction in which a heat transfer surface is metallurgically joined to a structural web-core, multiweb panel. In the high-pressure-load region, the structural weight of the prime panels and the I-beams is highly dependent on the metal temperature. As a result, it is advantageous to separate the heat exchanger and structural functions so that the pressure-carrying structure is not penalized by the necessarily higher metal temperatures in the heat exchanger. The design procedure calls for the prime structural panel and I-beam designs to be performed independently of the heat exchanger design. Interaction due to the attached heat exchanger design, such as in-plane stresses due to the heat exchanger temperature distribution and heat exchanger fluid-containment pressure stresses, are small enough to be ignored in the calculation; this is true even though one of the prime panel face sheets is common to the heat exchanger and prime structure.

The design procedure for optimizing the prime panel structure and the I-beams is shown in figure 67. The required input variables in the figures reflect the results of optimization analyses in appendix E. The only heat transfer parameter used is the coolant outlet temperature which determines the prime

panel and beam design metal temperature. The safety factor must be used as a multiplier on applied load because the various beam and panel members are designed on the basis of compressive buckling, and in some designs, the optimum stress may be different from the material yield strength. Since postbuckling behavior, whether elastic or inelastic, has not been considered in the design procedures, the safety factor on load automatically ensures at least the same factor on yield stress.

The output results of the analysis are panel and beam weights and detailed dimensions. The calculation procedure was programmed in FORTRAN II for an IBM 7074 computer. The diagram in figure 67 illustrates the various panel design ranges. The numerical values given on this flow chart are based upon Inconel 718 material properties at 1600⁰R (889⁰K).

Concepts 2 and 3 Heat Exchanger Optimization

The design procedures for concepts 2 and 3 determine the minimum-weight heat exchanger, particularly for high-heat-flux applications. The interaction between heat transfer analysis and stress analysis is considered, excluding the effects of the prime-load-carrying structure. Design curves have been developed that provide a complete picture of the workable designs, including the minimum-weight point.

The following assumptions were made to limit the range of variables, to impose practical considerations on the fabricability of the heat transfer plate-fin surfaces, and to separate the heat exchanger and prime structure design

- The number of fins per unit panel width was restricted to not less than 20 fins/in. (7.88 fins/cm) to ensure that pressure-bending stresses in the top surface sheet and the common prime-structural-panel faceplate would not be excessive. The compact fin spacing would also reduce any possibility that the hot surface sheet would buckle from the compressive in-plane loading.
- The maximum temperature difference across the heat exchanger would be equal to or less than 400⁰R (222⁰K) in accordance with the low-cycle-fatigue analysis.

The fin spacing and metal thickness combinations used were the following:

Fins/in. (cm)	Fin thickness		
	0.003 in. (0.0076 cm)	0.004 in. (0.0102 cm)	0.006 in. (0.0152 cm)
20 (7.9)	X	X	X
30 (11.8)	X	X	-
40 (15.8)	X	-	-

X Analyzed
 - Not analyzed

The heat exchanger fin analysis requires that the following variables be specified:

- Coolant inlet and outlet temperatures and outlet pressure
- Heat exchanger material and dimensions
- Panel dimensions (flow length and flow width)
- Applied heat flux
- Hot-gas recovery temperature

With a complete set of numerical values for these variables and appropriate fin performance data, the fluid pressure drop, ΔP , and temperature difference across the heat exchanger, ΔT , can be computed. Derivations of the appropriate formulas and analysis approach are given in reference 1. The primary result of the calculation method is the determination of lightest fin configuration that satisfies inlet and outlet hydrogen pressure and temperature conditions as well as adequacy for pressure containment strength. In the systematic calculations, fin height was treated as the independent variable, and a fin height range from 0.025 in. (0.064 cm) to 0.100 in. (0.254 cm) was scanned at increments of 0.025 in. (0.064 cm). Separate curves were then plotted for hot-surface temperature and required inlet hydrogen pressure vs fin height for each combination of fin spacing and flow length at each of the two heat fluxes. In all cases, the hot-surface face sheet thickness was taken to be 0.010 in. (0.025 cm). The temperature difference through the face sheet was computed to be 53°R (29°K) for the heat flux of 250 Btu/sec-ft² (2840 kW/m²) and 105°R (58°K) for the heat flux of 500 Btu/sec-ft² (5680 kW/m²). The effective average temperature of the facesheet was taken as surface metal hot-side temperature minus one-third of the difference through the thickness.

The next step in the heat exchanger design was the calculation of fin rupture pressure vs fin height for all of the design configurations. The maximum fin temperature was used to determine allowable fin stress. The allowable design stress for Hastelloy X fins vs metal temperature is shown in figure 68. The allowable stress is based upon the lower value of the shorttime yield stress or the 100-hr rupture stress at design temperature, and a safety factor of 1.5 is used in the governing design criterion. Fin allowable pressure is computed from equation (33).

Curves of maximum metal temperature, required inlet hydrogen pressure, and fin allowable pressure may be plotted against fin heights as shown in figure 69. The assumed inlet pressure limitation of 1000 psi (6890 kN/m²) precludes the use of fin heights less than 0.026 in. (0.066 cm), whereas the upper limit of 2000°R (1110°K) effective metal temperature restricts the maximum fin height to 0.046 in. (0.117 cm). Therefore, for this particular design problem, there is a rather narrow bandwidth of usable fin heights.

Fin weight will be minimized by selecting the combination of minimum fin thickness and height that does not exceed the specified inlet pressure and

outlet temperature conditions. Consideration of fin strength for pressure containment provides the final necessary restriction. The fins will be designed for the combination of inlet pressure and outlet temperature, and this introduces an element of conservatism into the design. This conservatism is well justified because a rupture of the heat exchanger surface would lead to a loss of coolant as well as a loss of local cooling capability and would involve a very strong possibility of loss of the vehicle. The fin allowable pressure curve intersects the inlet hydrogen pressure curve in figure 69 at two points. For the bandwidth between these two points, the fin strength is always at least sufficient to contain the hydrogen pressure.

The usable bandwidth based on inlet pressure and outlet temperature will not necessarily overlap the bandwidth based on pressure containment; if it does not overlap, a valid design will not exist. If there is an overlap, the lowest common point represents the lowest possible fin height and, therefore, the lowest possible fin weight. The existence of an overlapping bandwidth indicates that further weight reduction may be achieved by reducing fin thickness or by increasing fin spacing. The easiest design approach is to retain the same fin spacing and reduce fin thickness. This will shift the fin allowable pressure curve downward until the two intersection points merge into a single tangent point. This would represent the thinnest possible fin at the fixed number of fins/in. for pressure containment.

Figure 70 presents a plot of fin effective thicknesses vs fins per unit width for a single fin thickness, at a particular heat flux and flow length, but with variable fin heights. The upper and lower limits of permissible fin height are affected by allowable metal temperature, inlet hydrogen pressure, fin containment strength, and minimum fabricable fin height. The effects of these various parameters are clearly brought out by figure 70. The shaded area in figure 70 represents the complete envelope of acceptable fin designs for the prescribed fin thickness, heat load and design constraints of this study.

Manifold Design

The typical manifolding arrangement used for weight analysis is shown in figure 71. The choice of the rectangular manifolding as the reference design configuration was based on the design layout studies, appendix D, and on the fluid flow analysis described in reference 1. A fundamental assumption in the manifold design was that internal baffling or orificing would be employed to achieve zero flow maldistribution at the flow rate design point. This assumption implies that the overall manifold pressure drop will be equal to the maximum pressure drop flow path. Thus all other flow paths would require flow restrictions to raise their pressure drops to the maximum value. The large number of dimensional variables involved in the manifold design required that additional guidelines and definitions be established to calculate consistent manifold pressure drops and weights for the varied problem statements that would arise. The most important points related to the weight and pressure drop analysis are:

- One or more manifold inlet ports may be used. The heat exchanger width associated with each inlet port will be the total panel width divided by the number of ports. This permits specification of manifold flow in terms of a parameter involving heat flux and the heat exchanger length-to-width ratio.
- The manifold port diameter was sized to provide a free flow area equal to the heat exchanger width multiplied by a height dimension of 0.10 in. (0.25 cm). The piping pressure drop will be a small percentage of the heat exchanger pressure drop in all cases.
- Developed manifold length was taken to be 1.5 in. (3.8 cm) plus one port diameter. This dimension was based upon the design layout studies, and it allows for accommodation of the port, the seals, and the routing of pipe lines.
- Manifold pressure containment was obtained by the use of plain rectangular fins between the manifold facesheets with a fixed fin spacing of 10 fins/in. (3.94 fins/cm). Fin thickness was determined for pressures of 300 psi (2070 kN/m²) to 1400 psi (9650 kN/m²) at coolant temperature.
- The manifold material selected was Hastelloy X.
- Manifold minimum thicknesses were the same as for the heat exchanger.
- Manifold height dimensions (fin height) were restricted to the range from 0.025 in. (0.064 cm) minimum up to 0.25 in. (0.64 cm) maximum.
- Inlet manifold height was 0.025 in. (0.064 cm) for concept 1 and 0.05 in. (0.13 cm) for concepts 2 and 3.

Within the constraints established by these restrictions, a negligible pressure drop occurred through the inlet manifold. This was due to the high fluid density at the inlet arising from the combination of high inlet pressure and low hydrogen temperature. The fin height on the outlet manifold was adjusted to satisfy a maximum pressure drop of 45 psi (310 kN/m²) for concepts 2 and 3 and 5 psi (35 kN/m²) for concept 1 at the design coolant temperature and a manifold outlet fluid pressure of 250 psi (1720 kN/m²). The required fin height was computed with the aid of the curve for manifold fin pressure drop vs the parameter (q/A) (l/w) shown in figure 72. Each curve was generated for a fixed fin height; the formula for computing required fin height is (from reference 1)

$$h = h_{\text{ref.}} \left(\frac{0.6\Delta p_c}{\Delta p_a - 0.4\Delta p_c} \right)^{1/2}$$

where Δp_a = pressure drop allotted to outlet manifold

Δp_c = total manifold fin pressure drop from figure 72

Pressure containment stresses determined the required facesheet and fin thicknesses. Figure 68 is applicable because material choice and allowable stresses were the same as for the heat exchanger. Required fin and facesheet thickness were determined from equations (33) and (34). The total manifold effective thickness was computed from equation (32). Allowing for a manifold developed length dimension of 1.5 in. (3.8 cm) plus port diameter, the expression for manifold weight is

$$\begin{aligned}\text{Manifold weight} &= \gamma (1.50 + D_{\text{port}}) (\bar{t}) (\text{width}), \text{ lb} \\ &= \gamma (3.81 + D_{\text{port}}) (\bar{t}) (\text{width}), \text{ kg}\end{aligned}$$

Total manifold weight per unit area is

$$\text{Manifold weight/unit area} = (Wt_{\text{inlet}} + Wt_{\text{outlet}}) / \text{panel area}$$

Although this approach for manifold design has not been carried to the degree of optimization employed for the prime panels, I-beams, and heat exchangers, it does provide representative manifold weights. It does not in any way affect the choice of lightest panel weight for a particular pressure load and heat flux. Furthermore, it provides the designer or analyst with a sound reference starting point for obtaining an optimum design.

Piping

Piping weights were estimated assuming that the manifolding arrangement requires lengths of hot outlet piping equal to panel length. No contribution due to inlet piping weight was considered. The following additional assumptions were used

- (a) Number of outlet pipes equals number of outlet manifold ports
- (b) Pipe material is Inconel 718
- (c) Pipe diameter equals outlet port diameter

It was determined that an assumed wall thickness of 0.030 in. (0.076 cm) would be satisfactory in all cases.

Seal Design

The joints between adjacent panel edges require an adequate sealing arrangement that will withstand high heat loads and normal pressure loads. A weight estimate of the sealing mechanism is required to obtain the weight contribution per unit panel area. A sliding type of seal was envisioned as the most practical design concept. The panel dimensions will be sized to an initial gap which closes as the panels are heated thus precluding direct exposure of the seal strips to high heating rates. Good thermal contact between the seals and the panels is assumed to sustain the seals at local panel temperature.

The local panel temperature was used to establish allowable material stress, and the seal was then sized to withstand the applied normal pressure. Figure 73 is a sketch of the seal and the region of normal pressure loading. The total seal width and the portion of the seal width under pressure were determined from the layout studies. For all superalloy panels, these dimensions were 1.3 in. (3.3 cm) and 1.0 in. (2.5 cm), respectively. For the concept 3 designs, the pressure seal is between the aluminum prime structural panels, having lower thermal movements than the superalloy panels; the total width and pressure width were taken to be 1.0 in. (2.5 cm) and 0.8 in. (2.0 cm), respectively. The seal material was assumed to be Hastelloy X for the concept 1 and 2 panel designs and 6061-T6 aluminum for the concept 3 panel. The seal thickness was then based upon satisfying the allowable stress by treating the loaded portion as a simply supported span under uniform pressure. The seal rings provide the actual pressure-tight joint, and by virtue of their geometry, they make the condition of simple edge support realistic. The maximum beam bending stress is given by the formula:

$$\sigma = m/z = \frac{3}{4} \frac{pa^2}{t^2}$$

A safety factor of 1.5 was used to compute the allowable stress, and therefore the design stresses vs temperature plotted in figure 72 are applicable for Hastelloy X seals. The seals were assumed to be at room temperature or local gas temperature, whichever was higher. The required thickness is:

$$t_{\text{required}} = \left(\frac{3}{4} \frac{p}{\sigma_{\text{all}}} \right)^{1/2} (a)$$

The seal weight is the product of cross-sectional area, length, and material density. The seal weight per unit area is then one-half of the total seal weight along the four panel edges (each seal forms a common joint between adjacent panels) divided by panel area.

Attachment Clip Design

Attachment clips have been designed for joining the panels to the I-beam supports. The function of the attachments is transmission of the panel loads to the beams. These loads are primarily due to the externally applied uniform normal pressure and the thermal loads caused by the bowing tendency of the heat exchanger surface, which has a temperature gradient across its height. The clips, shown in figure 74, are designed to minimize stresses due to temperature differences between the panel and the beam. The attachment is brazed directly to the panel, and the attachment material contacts the panel between the bolts to increase the conduction path length to the attachment material farthest from the panel. It would be desirable to place the attachments intermittently along the panel to reduce the thermal stresses. However, the applied pressure must be transferred by the panel webs (or fins) in compression, and intermittent attachments would lead to increases in the panel web (fin) thickness. Since a brief investigation showed that continuous support gives the

lightest weight for the panel and attachment combination, a continuous clip was used. Slotted bolt holes are used to permit differential expansion between the panel attachment and the beams to minimize thermal stresses.

A 0.010-in. (0.0254 cm) attachment wall thickness was determined to be satisfactory in all cases, with the following assumptions:

- Attachment clip developed width is 2 in. (5 cm) plus the beam flange width, b_f
- Bolt weight is 25 percent of attachment weight

The clip weight per unit area for a material density of 0.30 lb/in³ (8300 kg/m³) is then given by the equation:

$$Wt/unit\ area = (0.54/c) (2.0 + b_f) \text{ lb/ft}^2 \text{ (U. S. customary units)}$$

$$Wt/unit\ area = (2.63/c) (5.1 + b_f) \text{ kg/m}^2 \text{ (S.I. units)}$$

where c = beam spacing, in. (cm)

b_f = beam flange width, in. (cm)

Concept 3 Shingle Support Panel

The regeneratively cooled shingle consists of a heat exchanger top-surface sheet made of Hastelloy X, Hastelloy X fins, and a sandwich support panel fabricated from Inconel 718. The support panel provides support for the regeneratively cooled shingle; it will keep the shingle flat and prevent flutter instability. To prevent the application of large pressure differentials to the shingle surface, the shingle will not be sealed around the edges. The shingle structure has been sized to carry a normal pressure force of 2000 psf (96 kN/m²) and an equal dynamic pressure. The amount of thermal bowing deflection that would be caused by the temperature difference between the hot surface of the heat exchanger and the Inconel 718 sandwich panel was calculated. The thermal deflections would be excessive for an unsupported span of 24 in. (0.61 m). For this reason, spacer beams are provided 6 in. (0.152 m) apart to hold the panel flat. The support panel is then sized to carry the combined bending moments due to applied normal pressure and thermal stresses.

Spacer Beam Design for Concept 3

The concept 3 panel design requires that spacer beams be used to mount the cooled shingles to the underside prime panel structure. These spacer beams will be made from Inconel 718, and they will not transmit or be exposed to high structural loads. The spacers serve the twofold function of holding the shingle relatively flat and of ensuring against local flutter instability of the shingle spans between the spacer beams. A spacer separation of 6 in. (15.24 cm) was assumed for all concept 3 designs. The spacer beam was assumed to be an I-beam of the following dimensions:

Flange width = 0.25 in. (0.64 cm)

Flange thickness = 0.030 in. (0.076 cm)

Web height = 1.0 in. (2.5 cm)

Web thickness = 0.020 in. (0.051 cm)

Beam weight/unit area = 0.30 lb/ft² (1.47 kg/m²)

The spacer beam will be exposed to shingle temperature on the upper flange and prime panel metal temperature on the lower flange. If a solid web were used, the beam would tend to bow, and a sizable bowing deflection would take place. On the other hand, constraint against bowing would produce very high loads on the beams, panels, and attachment clips. One solution would be the application of an insulation layer on the contacting surfaces of both flanges, but this introduces the requirement to select and apply a workable insulator. A more reasonable approach would be the use of a corrugated web attached to the flange at discrete points only. An improved solution is shown in figure 75. The web consists of several small plate elements that provide flexibility along the lengthwise beam axis. A short length of web at the center of the beam is oriented along the the beam axis to provide flange-to-flange rigidity in the beam axis. The flanges will then be somewhat free to grow relative to each other and still maintain the proper load paths and rigidity characteristics to support the shingles. Segmenting the beams will then prevent thermal stresses from limiting the distance over which the beam can provide support.

Sample Calculation for Concept 1

A sample calculation is provided for concept 1 to illustrate the principal calculations outlined in the preceding design procedure. Table 22 provides a summary of the results for this calculation using a 7 psi (48 kN/m²) applied normal pressure and a 10 Btu/sec-ft² (114 kW/m²) heat flux.

Panel, beams, and attachment clip weight.- Curves such as those shown in figure 64 together with the selected coolant outlet temperature of 1600^oR (889^oK) were used to obtain panel design temperatures. The resulting metal temperatures, thermal stresses, and design stresses are shown in table 23 for two fin spacings using plain fins. Table 23 also gives the weight summary for each fin height from which the configuration for minimum weight presented in table 22 was selected.

Coolant containment strength.- Pressure containment strength must be verified for both the fins and the faceplates. The fins and faceplates were checked to contain 300 psi (2070 kN/m²) at the outlet-end hot-surface metal temperature. Fin tensile stress is obtained from equation (33)

$$\sigma_{fin} = p \left[(b_{fin}/t_{fin}) - 1 \right] / 0.5 = 9400 \text{ psi (64 700 kN/m}^2)$$

Faceplate bending stress is computed from equation (34)

$$\sigma = 0.5 p (b_{fin} - t_{fin})^2 / t_f^2 = 3310 \text{ psi (22 800 kN/m}^2\text{)}$$

These stresses are not critical.

Manifold design.- The following data inputs are used to investigate the manifold design:

- (a) Coolant inlet pressure, 300 psi (2070 kN/m²)
- (b) Outlet manifold design temperature = 1600°F (889°K)
- (c) Manifold flow parameter, (q/A)(l/w) = 10 Btu/sec-ft² (114 kN/m²)
- (d) Single outlet port, with diameter = 1.75 in. (4.44 cm)

By following the analysis procedure indicated in the section, Manifold Design, it was determined that a pressure drop limitation of 5 psi (35 kN/m²) is satisfied with a fin height of 0.023 in. (0.058 cm) in the outlet manifold. This is less than the minimum gage fin height. The fin height for the outlet manifold, as well as for the inlet manifold, should be 0.025 in. (0.064 cm).

The next step is the verification of pressure containment strength for 10 fins/in. (3.94 fins/cm) and 0.003 in. (0.008 cm) fin thickness. For a Hastelloy X manifold material at 1600°R (889°K), the allowable stress is 27 000 psi (186 000 kN/m²). Tensile stress and bending stress for the faceplates are computed using the same formulas as above for the sandwich panel

$$\sigma_{fin} = p [(b_{fin} / t_{fin}) - 1] / 0.5 = 5820 \text{ psi (40 200 kN/m}^2\text{)}$$

$$\sigma = 0.5 p (b_{fin} - t_{fin})^2 / t_f^2 = 14 100 \text{ psi (97 200 kN/m}^2\text{)}$$

These stresses are well within the allowable design value, and the weight calculations will be based upon the minimum gages. The effective metal thickness is

$$\bar{t} = t_{fin} + \left(\frac{h_{fin} - t_{fin}}{b_{fin}} \right) t_{fin} + 2t_f = 0.0247 \text{ in. (0.0602 cm)}$$

The rectangular manifold runs the full width of the panel, 2 ft (0.61 m), and its developed length is the port diameter of 1.75 in. (4.44 cm) plus 1.5 in. (3.81 cm), or a total of 3.25 in. (8.25 cm). Hence, the weight of each manifold for a metal density of 0.3 lb/in.³ (8300 kg/m³) is

$$\text{Weight/manifold} = (0.3)(0.0247)(24)(3.25) = 0.556 \text{ lb (0.251 kg)}$$

Therefore, for panel dimensions of 2 ft by 2 ft (0.61 m by 0.61 m), the weight per unit area is

$$\text{Weight/unit area} = 0.14 \text{ lb/ft}^2 \text{ (0.68 kg/m}^2\text{)}$$

The piping weight has been assigned as part of the manifold weight. A minimum pipe thickness of 0.030 in. (0.076 cm) has been assumed for the piping, and this easily satisfies the pressure containment strength. This leads to a pipe weight of 0.595 lb/ft (0.886 kg/m), and for a 2-ft (0.61-m) panel width, the pipe weight per unit area is 0.30 lb/ft² (1.45 kg/m²).

The total weight for the inlet manifold, outlet manifold, and piping is

$$\text{Weight/unit area} = 2 (0.14) + 0.30 = 0.58 \text{ lb/ft}^2 \text{ (2.83 kg/m}^2\text{)}$$

Seal design.- Hastelloy X seal required thickness is calculated for temperatures of 1600^oR (889^oK) at the hot end, 850^oR (472^oK) on the sides, and room temperature on the inlet end. Using the appropriate material allowable strengths for each section under an applied pressure of 7 psi (48 kN/m²) with a safety factor of 1.5, the weight per unit area for a 2-ft (0.61-m) square panel is 0.06 lb/ft² (0.29 kg/m²).

Sample Calculation for Concept 2

The design loads are 100 psi (689 kW/m²) for normal pressure and 250 Btu/sec-ft² (2840 kW/m²) for heat flux. A summary of component weights, material selections, and detailed dimensions is provided in table 24.

Structural panel and I-beam design.- The dimensions and weights for the primary panel and the I-beam were obtained from the computer program. The results of this computation are listed in table 24. The optimum beam spacing is 4.704 in. (0.120 m); this is denoted as panel optimum span.

Heat exchanger design.- The basic inputs for the Hastelloy X heat exchanger using offset fins are given in table 24. A wide variety of fin heights, spacings, and metal thicknesses were analyzed. The minimum possible fin weight occurred for a fin design with 21 fins/in. (8.27 fins/cm) and a metal thickness of 0.003 in. (0.0076 cm). The selected fin spacing of 20 fins/in. (7.9 fins/cm) produces a very small weight change. The weight shown in table 24 includes the allowance of 0.09 lb/ft² (0.44 kg/m²) for brazing alloy.

Manifold design.- The manifold design procedure used for this panel was virtually identical to that used for the concept 1 design. The inputs that are different are:

- (a) Coolant inlet pressure = 1000 psi (6890 kN/m²)
- (b) One or more manifold ports may be used over the panel width
(A single port was found to suffice)
- (c) Manifold flow parameter = 250 Btu/sec-ft² (2840 kW/m²)
- (d) Minimum manifold height = 0.050 in. (0.127 cm)

(e) Maximum manifold height = 0.250 in. (0.635 cm)

(f) Allowable pressure drop for outlet manifold = 15 psi (310 kN/m²)

The calculated outlet manifold height was 0.142 in. (0.361 cm) for a manifold with a single inlet port. For a metal temperature of 1600°R (889°K), required fin thickness is computed as follows

$$t_{fin} = p b_{fin} / (0.5\sigma_{all} + p)$$

$$t_{fin} = (1000)(0.100) / [(0.5)(27\,000 + 1000)] = 0.007 \text{ in. (0.018 cm)}$$

The required faceplate thickness is

$$t_f = \left(p / 2\sigma_{all} \right)^{1/2} (b_{fin} - t_{fin}) = \left[\frac{1000}{(2)(27\,000)} \right]^{1/2} (0.097) \\ = 0.013 \text{ in. (0.033 cm)}$$

The outlet manifold effective thickness is 0.044 in. (0.112 cm). Total developed length of the manifold is 3.25 in. (8.25 cm). The weight per unit area based upon a 2-ft by 2-ft (0.61-m by 0.61-m) panel is

$$\text{Weight/unit area} = (0.3)(3.25)(24)(0.044) / (2)(2) = 0.26 \text{ lb/ft}^2 (1.27 \text{ kg/m}^2)$$

Pressure drop for the inlet manifold is negligible, and the minimum fin height of 0.050 in. (0.127 cm) is used. The design of the inlet manifold is based upon room-temperature properties of Hastelloy X. The computed metal thickness, using the same formulas as for the outlet manifold is

$$t_{fin} = 0.0055 \text{ in. (0.014 cm)}$$

$$t_f = 0.012 \text{ in. (0.031 cm)}$$

Inlet manifold weight per unit area is

$$\text{Weight/unit area} = 0.19 \text{ lb/ft}^2 (0.93 \text{ kg/m}^2)$$

The piping diameter is 1.75 in. (4.45 cm), and the minimum wall thickness of 0.030 in. (0.076 cm) is adequate for containment of 1000 psi (6890 kN/m²) at 1600°R (889°K). Piping weight is the same as for the concept 1 design, 0.30 lb/ft² (1.46 kg/m²).

Attachment clip design. - Following the procedure given above, the clip weight for the 1.216 in. (3.09 cm) beam flange width and 4.704 in. (11.9 cm) beam spacing given in table 24 is

$$\text{Weight/unit area} = (0.54/4.704)(2.0 + 1.216) = 0.37 \text{ lb/ft}^2 (1.80 \text{ kg/m}^2)$$

Seal design.- The seal thickness is based upon the applied normal pressure of 100 psi (689 kN/m²). The weight of the seal per unit area was found to be

$$\text{Weight/unit area} = 0.23 \text{ lb/ft}^2 (1.12 \text{ kg/m}^2)$$

Sample Calculation for Concept 3

The design loads are 250 psi (1720 kN/m²) for normal pressure and 500 Btu/sec-ft² (5680 kW/m²) for heat flux. The resulting weights, material selections, and detailed dimensions are presented in table 25.

Prime structural panel and I-beam design.- The optimum material choices were aluminum alloy 6061-T6 for the prime structural panel and titanium 5Al-2.5 Sn for the I-beams. The computed detailed dimensions and weight results are shown in table 25.

Heat exchanger designs.- Two heat exchanger plate-fin surfaces are used with the concept 3 panel design. The heat exchanger for the regeneratively cooled shingle will absorb most of the heat load and will operate at elevated temperature. This heat exchanger will be made from Hastelloy X, and the design procedure for the heat exchanger is virtually identical with that used for the concept 2 design. An aluminum plate-fin heat exchanger surface will be brazed to the aluminum prime structural panel; its major function is to protect the prime panel and titanium beams from bypass heat leakage around and through the shingles. The aluminum heat exchanger is essentially a minimum-gage design. For the purposes of analysis, it was assumed that 10 percent of the applied heat load was absorbed by the aluminum heat exchanger, and that the coolant-flow routing path was a series connection through the aluminum heat exchanger and then through the Hastelloy X exchanger.

Hastelloy X heat exchanger: The inlet temperature into the Hastelloy X heat exchanger is 250°R (139°K). Other inputs used to establish this design are listed in table 25. The results of the heat transfer analysis and fin strength calculations showed that minimum permissible fin height is 0.037 in. (0.094 cm), with 40 fins/in. (15.76 fins/cm), and that required fin thickness is 0.003 in. (0.0076 cm). Pressure containment capability of the fins and the faceplate was found to be satisfactory. The weight of heat exchanger, including the hot-surface sheet, the fins, and an allowance of 0.09 lb/ft² (0.44 kg/m²) for brazing alloy is

$$\text{Weight/unit area} = 0.85 \text{ lb/ft}^2 (4.15 \text{ kg/m}^2)$$

Aluminum heat exchanger: The heat exchanger weight and dimensional details are presented in table 25. The weight estimate includes an allowance of 0.03 lb/ft² (0.152 kg/m²) for the brazing alloy. The fin height of 0.050 in. (0.127 cm) was selected; this produces a negligible pressure drop--less than 5 psi (34.5 kN/m²)--through the heat exchanger. A fin spacing of 20 fins/in. (7.88 fins/cm) and a fin minimum-gage thickness of 0.004 in. (0.0102 cm) were used, as was a minimum-gage faceplate thickness of 0.016 in. (0.041 cm). The fin tensile stresses and faceplate bending stresses were verified for pressure containment and found to be satisfactory.

Manifold design.- The manifolding for concept 3 includes Hastelloy X manifolds for the shingle and aluminum manifolds for the prime panel heat exchanger. The piping is constructed from Inconel 718 for the shingle and from aluminum for the prime panel. An itemized discussion of these components is presented below.

Hastelloy X inlet manifold: The minimum fin height of 0.050 in. (0.127 cm) and a fin spacing of 0.100 (0.254 cm) were used. The required metal thicknesses for the fins and sideplates are the same as for concept 2. The developed length of the manifold can be reduced because seals are not required. A dimension of 2.25 in. (5.71 cm) was used instead of 3.25 in. (8.25 cm). The weight per unit area for a 2-ft by 2-ft (0.61-m by 0.61-m) panel is

$$\text{Weight/unit area} = \frac{(2.25)}{(3.25)} (0.14) = 0.1 \text{ lb/ft}^2 (0.49 \text{ kg/m}^2)$$

Hastelloy X outlet manifold: The outlet manifold was sized for an allowable pressure drop of 45 psi (310 kN/m²). For the required flow rate, it was determined that two outlet ports would be needed. Hence, the manifold flow parameter is 1000 Btu/sec-ft² (11 350 kW/m²). The required manifold fin height is 0.193 in. (0.49 cm). The metal thicknesses of the fin and sideplates are the same as those needed for concept 2 because hydrogen pressure and metal temperature are the same. The required port diameter is 1.25 in. (3.17 cm), and the developed length of the outlet manifold is the port diameter plus 0.5 in. (1.27 cm), or 1.75 in. (4.44 cm). The outlet manifold weight per unit area is

$$\text{Weight/unit area} = 0.15 \text{ lb/ft}^2 (0.73 \text{ kg/m}^2)$$

Inconel 718 piping: Two pipes 1.25 in. (3.17 cm) in. diameter and with a wall thickness of 0.030 in. (0.076 cm) are required. The piping weight per unit area is 0.43 lb/ft² (2.10 kg/m²).

Aluminum manifolds: The aluminum inlet and outlet manifolds operate below room temperature. Since the pressure drop is negligible through these manifolds and the aluminum heat exchanger, the containment pressures will be the same, and required metal thicknesses will be identical. A 1.0-in. (2.54-cm) port diameter was used, and the developed length dimension of the manifold was therefore taken to be 2.5 in. (6.35 cm). The total weight per unit area for the two manifolds is 0.12 lb/ft² (0.59 kg/m²).

Aluminum piping: A single aluminum pipe 1.0 in. (2.54 cm) in diameter is used with a wall thickness of 0.030 in. (0.076 cm). Containment strength is satisfactory for an internal pressure of 1000 psi (6890 kN/m²), and the weight per unit area is 0.06 lb/ft² (0.30 kg/m²).

Total weight of manifolds and pipes: The combined weight of the manifolds and piping for both heat exchangers is

$$\text{Weight/unit area} = 0.10 + 0.15 + 0.43 + 0.12 + 0.06 = 0.86 \text{ lb/ft}^2 (4.20 \text{ kg/m}^2)$$

Attachment clip design.- There are three sets of attachment clips in the concept 3 design compared with one set for concepts 1 and 2. The additional two sets provide for attachment of the regeneratively cooled shingle to the upper flanges of the spacer beams and for attachment of the aluminum panel to the lower flange of the spacer beams. The attachment clips for the joint between the shingles and the spacer beams are Inconel 718. The remaining two sets are aluminum alloy 6061-T6.

Cooled shingle-to-spacer beam attachment clips: The spacer beams will be placed 6.0 in. (0.152 m) apart; the spacer beam flange width is 0.250 in. (0.64 cm). The weight per unit area for these attachment clips is

$$\text{Weight/unit area} = (0.54/6.0)(2.0 + 0.25) = 0.20 \text{ lb/ft}^2 (0.98 \text{ kg/m}^2)$$

Spacer beam-to-aluminum panel attachment clips: These clips may be computed directly from the above value since all dimensions are identical. The density ratio of aluminum to Inconel 718 is used to give a weight of 0.07 lb/ft² (0.33 kg/m²).

Prime structural panel-to-I-beam attachment clips: The I-beam spacing is 5.185 in. (0.132), and the computed beam flange width is 1.469 in. (3.73 cm). The weight per unit area is

$$\text{Weight/unit area} = (0.1/0.3)(0.54/5.185)(2.0 + 1.469) = 0.12 \text{ lb/ft}^2 (0.59 \text{ kg/m}^2)$$

Total weight of attachment clips: The combined weight for the three sets of attachment clips is

$$\text{Weight/unit area} = 0.20 + 0.07 + 0.12 = 0.39 \text{ lb/ft}^2 (1.91 \text{ kg/m}^2)$$

Seal design.- Seals will be required for the prime structural panel only. The aluminum panel will operate at less than room temperature so the seal design will be based upon the room-temperature yield stress of 41 000 psi (282 000 kN/m²). The seal thickness required to carry 250 psi (1720 kN/m²) with a safety factor of 1.5 is 0.067 in. (0.17 cm). The seal weight per unit area for a 2-by 2-ft (0.61-by 0.61-m) panel is

$$\text{Weight/unit area} = (0.1)(1.0) (48) (0.067)/(2) (2) = 0.08 \text{ lb/ft}^2 (0.39 \text{ kg/m}^2)$$

Inconel 718 support panel.- This single-layer panel will be sized for a normal pressure of 2000 psf (96 kN/m²). Thermal stresses must be computed to determine the amount by which these stresses reduce the load capability. It is assumed that the Hastelloy X hot-surface sheet and the two Inconel 718 faceplates are the minimum-gauge thickness of 0.010 in. (0.0254 cm). It is further assumed that the shingle will be held perfectly flat by the spacer beams, that the difference in temperature between the Inconel 718 sandwich and the hot surface approaches 400°F (222°K), and that the Hastelloy X faceplate reaches a yield stress of 36 000 psi (248 000 kN/m²). Since the cross-section metal area of the Inconel 718 faceplates is twice the Hastelloy X area, the thermal stress induced in the Inconel 718 panel is 18 000 psi (124 000 kN/m²). This thermal stress will be deducted from the Inconel 718 yield stress of 130 000 psi

(896 000 kN/m²) at 1140°F (889°K), which leaves an allowable stress of 112 000 psi (772 000 kN/m²) to carry bending loads. The design bending moment due to the assumed normal pressure at a 6.0-in. (0.152-m) beam spacing (including the safety factor of 1.5) is

$$m = 1/8 pc^2 = (1.5)(2000)(6)^2/(8)(144) = 94 \text{ in.-lb/in. (418 N-m/m)}$$

This is a relatively low bending moment, and it falls in the panel design range for which the minimum metal gages apply for the webs and faceplates, and only the web height may be variable. The desired section modulus is obtained with a web height of 0.086 in. (0.216 m); the weight per unit area is 0.91 lb/ft² (4.44 kg/m²).

Inconel 718 spacer beams. - The spacer beam dimensions were given above. The weight per unit area was calculated to be 0.30 lb/ft² (1.47 kg/m²).

APPENDIX G

MATERIAL SELECTIONS

The selection of appropriate materials for the component elements of the design concepts is one of the most important aspects of the panel design. The materials chosen in this study were the result of different analysis stages of the program, ranging from the design layout studies and structural analysis to the heat transfer and manifold analysis. The choices of operating metal temperatures, nature and magnitude of applied stresses, fabricability of the optimum design configurations, and the general requirement for low panel weights were directly related to the material selections. The maximum metal temperature selection is further affected by the desire to (1) extract the maximum heat sink capacity from the hydrogen fuel, (2) hold the differential between maximum metal temperature and coolant bulk temperature to a minimum, and (3) avoid oxidation of the exposed hot surface. Resistance to oxidation at elevated metal surface temperatures is an important design requirement. Since protective coatings with an extended life of 100 hr or more are not available for refractory metals, refractory alloys were not considered further for this study. It was concluded that superalloys should be used only at temperature levels that do not introduce serious oxidation difficulties.

Inconel 718 was found to be the most suitable material for the prime panel structure in the composite-layer design of concept 2 and for I-beams. Hastelloy X or Inconel 625 are the best materials for the heat exchanger and fins, and Waspaloy is preferred for the single-layered sandwich panel used in concept 1. For the concept 3 design, it has been determined that the heat protected shingles should be made from Inconel 718 and Hastelloy X, the load-bearing panel structures from an aluminum alloy, and the I-beams from a titanium alloy. The materials and operating temperatures of each of the design concepts are discussed below.

Concept 2 Materials and Operating Temperatures

The material properties of the metallurgically joined heat exchanger (either fins or tubes) have an important influence on the panel design. In particular, the desirability of conserving coolant dictates that the hydrogen coolant be operated at the highest possible outlet temperature. Since the heat exchanger hot surface will be at an even higher temperature than will the outlet coolant, the selection of heat exchanger material is an important limiting factor on the choice of the outlet coolant temperature. The strength and oxidation properties of the material chosen impose a temperature limitation of approximately 2000°R (1110°K) for the heat exchanger. The high compressive loadings along with hydrogen pressure containment capability for the heat exchanger fins and hot surface sheet demand a material with good ductility and strength properties over the entire temperature range. Another important consideration is the need to form the material into a compact array of offset fins. Hastelloy X satisfies all these requirements. It has good strength at 2000°R (1110°K) and adequate low-cycle-fatigue performance over the operating range. It is a proven material in terms of formability and brazeability. Limited data

on material properties indicate that Inconel 625 offers improved performance, but experience with the material is less extensive than with Hastelloy X. Although Waspaloy also indicates good fatigue performance, it is much more difficult to form into fins, and its involved heat treatment detracts from its applicability in the composite layer panels. For the same reasons, Hastelloy X also was chosen for the manifold and seal material.

The selection of prime panel material is based largely upon material strength properties, although fabricability is an important consideration. Since the prime panels and beams constitute approximately 70 percent of the total weight, the requirement for high outlet coolant temperature, which will be virtually identical with the maximum prime structure temperature, must be balanced against increased structural weight. The panel and I-beam analyses demonstrated that Inconel 718 was the best material choice. Waspaloy and Rene 41 were close contenders from a weight standpoint, but they were eliminated because of their increased fabrication difficulties, including the need for more involved heat treatment. The prime panel design temperature of 1600°R (889°K) for the baseline concept evaluation was selected as an effective compromise between the conflicting demands of coolant needs and structural weight. It also is very close to the crossover point between short-time yield stress and the 100-hr creep-rupture stress. Temperature differences between the prime panel temperature and the heat exchanger hot-sheet temperature roughly coincide with the allowable temperature differences based upon thermal low-cycle-fatigue life. The material choices for the heat exchanger and the prime panel, therefore, appear to be compatible for their respective maximum allowable temperatures, and the limitation on maximum allowable ΔT imposed by the thermal fatigue considerations.

The beam materials evaluation also showed that Inconel 718 yielded the lowest weight for temperatures between about 900 to 1200°F (500 to 666°K) and that beam weight was relatively insensitive to temperatures up to 1600°F (889°K). Since the beam material contributes most of the total panel weight, there is a strong incentive to operate below the transition temperature between short-time and creep properties. Inconel 718 also was selected for the manifold piping.

Concept 1 Materials and Operating Temperatures

There are several important differences between the single-layered sandwich panel used in concept 1 and the concept 2 structural concept. The single-layered panel is held flat by the I-beams and the difference in temperature between the upper and lower sheets of the sandwich produces compressive thermal stress in the upper sheet and tensile stress in the lower sheet. The thermal stress and the bending stress due to external load are additive; therefore, the pressure load capability of the panel must be reduced to accommodate the thermal stress. The allowable temperatures across the panel thickness dimension must therefore be reduced from the 400° to 600°R (222° to 333°K) range used with the panels of concept 2. Reduced differential temperatures, which are a natural by-product of lower heat fluxes, confer the benefit that the maximum top-side temperature will be much closer to coolant outlet temperature;

this permits a higher outlet hydrogen temperature for the same maximum allowable metal temperature. It was determined that a difference of 100°R (56°K) would be reasonable.

A review of comparative material properties in the range from 1600°R (889°K) to 1900°R (1060°K) indicated that Waspaloy was the most suitable metal. For this design concept, in which the single-layered sandwich performs the structural and heat exchanger functions, the stresses due to the combined thermal and pressure loads were required to be less than the yield strength of the material (as was the case for the prime panel of concept 2). In addition, the possible use of metal at temperatures above 1600°R (889°K) means that creep deformations cannot be ignored. The yield and creep strength of Waspaloy in the desired temperature range were definitely superior to those of other superalloys. The remaining components, such as manifolds, seals, and I-beams, retained the same material choices as used for concept 2.

Concept 3 Materials and Operating Temperatures

The regeneratively cooled shingle portion of the concept 3 configuration (shown in figure 5) is very similar to the composite panel used with concept 2. The heat exchanger top sheet and fins were Hastelloy X, the manifolding was Hastelloy X, and the structural sandwich backup layer was Inconel 718. The spacer beams and the hot pipes were specified to be Inconel 718.

The normal pressure forces will be reacted by the primary load-carrying structure that is located below the shingles. This will consist of a sandwich panel construction with a protective surface heat exchanger similar to concept 2. The heat exchanger will protect the underlying prime panel structure and I-beam array from heat input due to bypass hot-gas leakage and conduction through the spacer beams. Since the coolant will be ducted through the secondary heat exchanger prior to use in the shingles, the secondary heat exchanger will be held to a low temperature. The prime panel structure and I-beams will also operate at this low temperature, which was estimated to be approximately 250°R (139°K), based upon a 10-percent heat leak around the shingle. The panel material analysis showed that aluminum alloy 6061-T6 was the optimum choice at the operating temperature of the prime panels. Aluminum 6061-T6 is preferred to other, somewhat stronger, aluminum alloys such as 2024-T6 or 7075-T6 because of its superior ductility, weldability, and brazeability. The metallurgically bonded heat exchanger top sheet, the fins, and the associated manifolding and seals were assumed to be made from aluminum 6061-T6 also. The beam material analysis showed that titanium 5Al-2.5 Sn yields the lightest I-beam structure at a 250°R (139°K) operating temperature. This particular titanium alloy was selected over others because of its relative ease of heat treatment, its ductility, its notched tensile properties at cryogenic temperature, and its comparative ease of welding.

REFERENCES

1. Walters, Fliegler M.; and Buchmann, Oscar A.: Heat Transfer and Fluid Flow Analysis of Hydrogen Cooled Panels and Manifold Systems. NASA CR-66925, July 1970.
2. Semonian, Joseph W.; and Anderson, Roger A.: An Analysis of the Stability and Ultimate Bending Strength of Multiweb Beams with Formed-Channel Webs. NACA TN 3232, 1954.
3. Sessler, J. G.; and Weiss, V., ed: Aerospace Structural Metals Handbook. Fourth Revision, Syracuse University Press, 1967.
4. Anon: Metallic Materials and Elements for Aerospace Vehicle Structures (MIL-HDBK-5A). Department of Defense, February 8, 1966.
5. Durham, T. F.; McClintock, R. M.; and Reed, R. P.: Cryogenic Materials Data Handbook. U.S. Department of Commerce, National Bureau of Standards, March 15, 1961.
6. Anon: Lescalloy 718 Vac-Arc Property Data. Latrobe Steel Company, August 1962.
7. Anon: High Temperature Metals. Rept. HTM300, Universal-Cyclops Steel Corporation, January 1959.
8. Anon: 18 Percent Nickel Maraging Steels. Rept. A-373, The International Nickel Company, March 30, 1965.
9. Anon: High Temperature, High Strength, Nickel Base Alloys. Revised, The International Nickel Company, 1964.
10. Coffin, L. F., Jr.: Thermal Stress and Thermal Stress Fatigue. Special Summer Program, Massachusetts Institute of Technology, June 1968.
11. Tavernelli, T. F.; and Coffin, L. F., Jr.: Experimental Support for a Generalized Equation Predicting Low-Cycle Fatigue. Journal of Basic Engineering, December 1963.
12. Manson, S. S.; and Hirschberg, M. H.: Fatigue Behavior in Strain Cycling in the Low and Intermediate-Cycle Range. Proceedings of the 10th Sagamore Army Materials Research Conference, Syracuse University Press, 1964.
13. Anon: Haynes Alloy No. 25. Rept. F-30, 041-C, Haynes Stellite Company, June 1962.
14. Anon: Comparative Properties of Haynes High-Temperature Alloys. Rept. F-30, 134, Haynes Stellite Company, October 1960.
15. Slunder, C. J.: Short-Time Tensile Properties of the Co-20Cr-15W-10Ni Cobalt-Base Alloy (L-605). Memorandum 179, Defense Metals Information Center, September 27, 1963.

16. Anon: Engineering Properties of Inconel Alloy 625. Rept. T-42, International Nickel Company, August 1966.
17. Anon: Inconel 718 Age-Hardenable Nickel-Chromium Alloy. Data Reports, The International Nickel Company, September 1960 and May 1961.
18. Anon: Hastelloy Alloy X. Rept. F-30, 037D, Union Carbide Corporation, Stellite Division, October 1964.
19. Anon: Hastelloy Alloy C. Rept. F-30, 041-C, Haynes Stellite Company, September 1960.
20. Bohon, Herman L.; and Anderson, Melvin S.: The Role of Boundary Conditions on Flutter of Orthotropic Panels. AIAA J. Vol. 4, No. 7, July 1966, pp. 1241-1248.

TABLE 1
BASIC PANEL CONFIGURATIONS

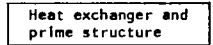
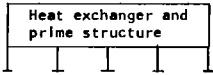
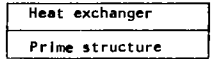
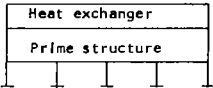
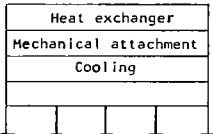
Configuration		Status		Comments
Description	Schematic	Applicability	Program	
Heat exchanger and prime structure combined		Limited	Not retained	Heavier than panel supported with I-beams
Heat exchanger and prime structure combined, additionally supported by I-beams		Limited	Retained	Configuration most useful at low flux and low normal pressures. Load-carrying ability affected by cross-section ΔT .
Heat exchanger bonded to prime structure		Broad problem range	Not retained	Heavier than panel supported with I-beams for normal pressures less than 375 psi (2680 kN/m ²)
Heat exchanger bonded to prime structure, additionally supported by I-beams		Broad problem range	Retained	Configuration most useful for normal pressures > 7 psi (48 kN/m ²). Heat exchanger cross section ΔT does not materially affect panel load-carrying ability. Prime structure limited by H ₂ bulk outlet temperature.
Heat exchanger mechanically attached to prime structure, additionally supported by I-beams (regeneratively cooled shingle)		Limited	Retained	Configuration most useful at high flux, high normal pressures. Prime structure uncoupled from H ₂ bulk outlet temperature, but some secondary cooling with or without insulation is needed between heat exchanger and prime structure.

TABLE 2
DETAILED STRUCTURAL CONFIGURATIONS

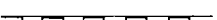






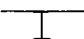
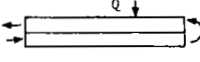
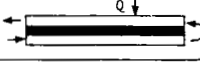
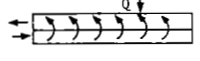
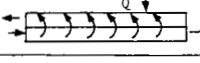
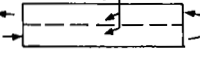
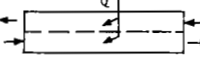
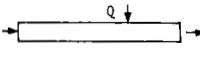
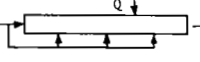
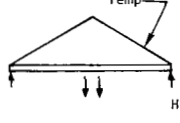
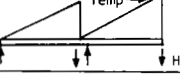
Configuration		Status		Comments
Description	Schematic	Applicability	Program	
Heat exchanger and prime structure combined		Limited	Retained	Rectangular- and triangular-fin-cores both suitable. Triangular core not retained.
Rectangular sandwich core				
Tubular sandwich core		None	Not retained	Offers good method for H ₂ pressure containment.
Prime structure				
Plain plate		Limited	Not retained	Both plain and stiffened plate require weight penalties over sandwich configurations.
Stiffened plate				
Sandwich, rectangular-web-core		Broad problem range	Retained	Rectangular-web-core retained for evaluation, triangular-web-core not retained. Hexcel cores not considered.
Support structure (I-beams)		Broad problem range	Retained	Use of I-beams allows mechanical attachment to prime structure to accommodate prime structure thermal expansion. No others considered.

TABLE 3
PANEL FLOW ARRANGEMENTS

Configuration		Status		Comments
Description	Schematic	Applicability	Program	
Flow folded in depth dimension of heat exchanger		Limited	Not retained	Benefits limited to low heat flux and by cross-section ΔT ; heavier than in-plane folding configuration; results in short flow lengths.
Simple fold				
Simple fold with insulation between folds		None	Not retained	Causes greater coolant penalty than above.
Fold with injection		Limited	Not retained	Injection slots too narrow to be generally useful. For both configurations, manufacturing and coolant flow control present serious problems.
Fold with injection and excess cold H_2		Limited	Not retained	
Counterflow in adjacent flow paths in width dimension of heat exchanger		Limited	Retained	Lowest coolant penalty at low flux and lowest cross-section ΔT . Disadvantages of in-plane temperature gradient normal to flow, complex manifolding. Rejected at high flux because of short flow lengths.
Folded flow				
Independent flow streams				
Nonfolded flow		Broad problem range	Retained	Simplest configuration
Single pass (straight-through flow)				
Multiple flow rates in heat exchanger plane (parallel flow)		Limited	Not retained	Sawtooth temperature profile produced high thermal stresses; complex manifolding and controls required.
Manifolding connections, flow lengths less than panel length		Limited	Not Retained	In-plane thermal stresses limit range of useful aspect ratio. Eliminates one hot seal, reduces number of hot manifolds
Similar temperature fluids adjacent				
Dissimilar temperature fluids adjacent		None	Not retained	In-plane thermal stresses prohibit use for most applications.

NOTE: Restriction of 600°F (333°K) maximum cross-section ΔT from top sheet to prime structure placed on all flow route comparisons.

TABLE 4
HEAT EXCHANGER GEOMETRIC CONFIGURATIONS

Configuration	Status		Comment
	Applicability	Program	
Surface uninterrupted in flow-length dimension	Broad problem range	Retained	Generally suitable
Plain rectangular		Not retained	Lower performance than plain rectangular
Plain triangular		Retained	Best H ₂ pressure containment
Surface interrupted in flow-length dimension	Broad problem range	Retained	Provides high heat transfer coefficient; triangular offset not considered
Rectangular offset		Not retained	No performance gain over rectangular offset
Wavy		Not retained	Best surface for minimum cross-section ΔT at given pressure drop
Pin fins	Limited	Retained	Always provides a means for reducing coolant flow requirements. Most advantageous at low adiabatic wall temperature
External insulation (adjacent to hot gas)		Retained	Reduces cross-section ΔT with some pressure drop penalty
Composite fins (high conductivity cladding)	Limited	Retained	

TABLE 5
SUMMARY OF CONCEPTS RETAINED FOR CONCEPTS EVALUATION

Concept	Panel configuration	Structural configuration	Heat exchanger configuration	Flow arrangement
1	Combined heat exchanger and prime structure additionally supported	Rectangular-fin-core, I-beam support	Rectangular fins	Nonfolded 'single pass'
1a	Same as 1	Same as 1	Same as 1	Flow folded in width dimension of heat exchanger
2	Heat exchanger bonded to prime structure additionally supported	Rectangular-web-core, I-beam support	Rectangular fins	Nonfolded 'single pass'
2a	Same as 2	Same as 2	Same as 2	Flow folded in width dimension of heat exchanger
2b	Same as 2	Same as 2	Rectangular fins, external insulation	Nonfolded (single pass)
2c	Same as 2	Same as 2	Tubular	Same as 2b
3	Heat exchanger mechanically attached to prime structure (regeneratively cooled shingle)	Rectangular-web-core, I-beam support, heat exchanger support structure	Rectangular fins plus secondary cooling between heat exchanger and prime structure	Unfolded single pass, plus secondary coolant circuit

TABLE 6

SUMMARY TABLE FOR LOW LOAD-HEAT FLUX DESIGN POINT I: CONCEPT EVALUATION

a. - U.S. CUSTOMARY UNITS

Concept	Length, ft	Recovery temperature, °R	Fin geometry fins/in.; height, in.; thickness, in.	Heat exchanger weight, lb/ft ²	Prime panel weight, lb/ft ²	Beam weight, lb/ft ²	Manifold weight, lb/ft ²	Seal weight, lb/ft ²	Total weight, lb/ft ²	Coolant rate, lb/sec-ft ²
1	2	Infinite	20R-0.075-0.003	1.28	--	0.48	0.58	0.07	2.41	0.00169
	3	Infinite	20R- .075- .003	1.28	--	.48	.49	.06	2.31	.00169
	5	Infinite	20R- .075- .003	1.28	--	.48	.42	.05	2.23	.00169
	2	5000	15R- .075- .003	1.23	--	.48	.60	.07	2.38	.00146
1a	2	5000	14R-0.075-0.003	1.22	--	0.50	0.60	0.07	2.39	0.00135
2	2	Infinite	15R-0.025-0.003	0.70	0.90	0.44	0.58	0.06	2.68	0.00187

b. - SI UNITS

Concept	Length, m	Recovery temperature, °K	Fin geometry fins/cm; height, cm; thickness, cm	Heat exchanger weight, kg/m ²	Prime panel weight, kg/m ²	Beam weight, kg/m ²	Manifold weight, kg/m ²	Seal weight, kg/m ²	Total weight, kg/m ²	Coolant rate, kg/s-m ²
1	0.61	Infinite	7.9R-0.191-0.0076	6.25	--	2.34	2.83	0.34	11.76	0.00825
	.91	Infinite	7.9R- .191- .0076	6.25	--	2.34	2.39	.29	11.27	.00825
	1.52	Infinite	7.9R- .191- .0076	6.25	--	2.34	2.05	.24	10.88	.00825
	.61	2780	5.9R- .191- .0076	6.00	--	2.34	2.93	.34	11.61	.00713
1a	0.61	2780	5.5R-0.191-0.0076	5.95	--	2.44	2.93	0.34	11.66	0.00659
2	0.61	Infinite	5.9R-0.064-0.0076	3.42	4.40	2.15	2.83	0.29	13.09	0.00825

TABLE 7

SUMMARY TABLE FOR INTERMEDIATE LOAD-HEAT FLUX DESIGN POINT 2,
CONCEPT EVALUATION

a. - U.S. CUSTOMARY UNITS

Concept	Length, ft	Recovery temperature, °R	Fin geometry fins/in.; height, in.; thickness, in.	Fin k, Btu/ft-hr-°R	Heat exchanger weight, lb/ft ²	Prime panel weight, lb/ft ²	Beam weight, lb/ft ²	Manifold weight, lb/ft ²	Seal weight, lb/ft ²	Total weight, lb/ft ²	Coolant rate, lb/sec-ft ²
2	2	Infinite	20R-0.027-0.003	10	0.72	1.13	3.19	0.75	0.24	6.03	0.0468
	3	Infinite	30R- .031- .003	10	.78	1.13	3.19	.63	.20	5.93	.0468
	2	Infinite	20R- .027- .006	100	.93	1.13	3.19	.75	.24	6.24	.0468
	2	5000	20R- .050- .004	10	.86	1.13	3.19	.65	.24	6.07	.0395
2a	2	5000	20R-0.050-0.004	10	0.86	1.13	3.19	0.70	0.24	6.12	0.0375
2b	2	5000	20R-0.050-0.004	10	1.63**	1.13	3.19	0.60	0.24	6.79	0.0328
2c	2	Infinite	0.050 OD by 0.010 thickness	10	1.17	1.13	3.19	0.80	0.24	6.53	0.0468 to .0556
3	2	Infinite	20R-0.028-0.003*	10	1.10	1.59	1.97	0.80	0.06	5.52	0.0468
	3	Infinite	30R- .032- .003*	10	1.15	1.59	1.97	.68	.05	5.44	.0468

* Fin geometry of primary heat exchanger

** Includes insulation weight

b. - SI UNITS

Concept	Length, m	Recovery temperature, °K	Fin geometry fins/cm; height, cm; thickness, cm	Fin k, W/m-°K	Heat exchanger weight, kg/m ²	Prime panel weight, kg/m ²	Beam weight, kg/m ²	Manifold weight, kg/m ²	Seal weight, kg/m ²	Total weight, kg/m ²	Coolant rate, kg/s-m ²
2	0.61	Infinite	7.9R-0.069-0.0076	17.3	3.52	5.52	15.60	3.66	1.17	29.47	0.228
	.91	Infinite	11.8R- .079- .0076	17.3	3.81	5.52	15.60	3.08	.98	28.99	.228
	.61	Infinite	7.9R- .069- .0152	173	4.54	5.52	15.60	3.66	1.17	30.49	.228
	.61	2780	7.9R- .127- .0102	17.3	4.20	5.52	15.60	3.88	1.17	29.67	.193
2a	0.61	2780	7.9R-0.127-0.0102	17.3	4.20	5.52	15.60	3.42	1.17	29.91	0.183
2b	0.61	2780	7.9R-0.127-0.0102	17.3	7.96**	5.52	15.60	3.93	1.17	33.18	0.160
2c	0.61	Infinite	0.127 OD by 0.0254 thickness	17.3	5.71	5.52	15.60	3.91	1.17	31.91	0.229 to .272
3	0.61	Infinite	7.9R-0.071-0.0076*	17.3	5.37	7.77	9.62	3.91	0.29	26.96	0.228
	.91	Infinite	11.8R- .081- .0076*	17.3	5.61	7.77	9.62	3.32	.24	26.56	.228

* Fin geometry of primary heat exchanger

** Includes insulation weight

TABLE 8

SUMMARY TABLE FOR HIGH LOAD-HEAT FLUX DESIGN POINT, CONCEPT EVALUATION

a. - U. S. CUSTOMARY UNITS

Concept	Length, ft	Recovery temperature, °R	Fin geometry fins/in.; height, in; thickness, in.	Fin k, Btu/ft-hr-°R	Heat exchanger weight, lb/ft ²	Prime panel weight, lb/ft ²	Beam weight, lb/ft ²	Manifold weight, lb/ft ²	Seal weight, lb/ft ²	Total weight, lb/ft ²	Coolant rate, lb/sec-ft ²
2	2	Infinite	40R-0.035-0.003	10	0.84	1.77	5.83	0.86	0.38	9.68	0.0935
	3	Infinite	30R- .062- .004	10	1.02	1.77	5.83	.83	.32	9.77	.0935
	2	Infinite	30R- .038- .006	100	1.08	1.77	5.83	.86	.38	9.92	.0935
	2	5000	20R- .050- .006	10	1.01	1.77	5.83	.75	.38	9.74	.0758
2a	2	5000	20R-0.062-0.006	10	1.08	1.77	5.83	0.80	0.38	9.86	0.0745
2b	2	5000	20R-0.050-0.006	10	1.72**	1.77	5.83	0.70	0.38	10.40	0.0630
2c	2	Infinite	0.05 OD by 0.010 thickness	10	1.17	1.77	5.83	0.92	0.38	10.07	0.0935 to .111
3	2	Infinite	40R-0.037-0.003*	10	1.22	2.31	3.14	0.92	0.08	7.67	0.0935
	3	Infinite	30R- .067- .004*	10	1.41	2.31	3.14	.89	.07	7.82	.0935

* Fin geometry of prime heat exchanger

** Includes Insulation weight

b. - SI UNITS

Concept	Length, ft	Recovery temperature, °K	Fin geometry fins/cm; height, cm; thickness, cm	Fin k, W/m-°K	Heat exchanger weight, kg/m ²	Prime panel weight, kg/m ²	Beam weight, kg/m ²	Manifold weight, kg/m ²	Seal weight, kg/m ²	Total weight, kg/m ²	Coolant rate, kg/s-m ²
2	0.61	Infinite	15.8R-0.089-0.0076	17.3	4.11	8.65	28.50	4.20	1.86	47.32	0.456
	.91	Infinite	11.8R- .158- .0102	17.3	4.98	8.65	28.50	4.05	1.56	47.74	.456
	.61	Infinite	11.8R- .097- .0152	173	5.28	8.65	28.50	4.20	1.86	48.49	.456
	.61	2780	7.9R- .127- .0152	17.3	4.93	8.65	28.50	3.66	1.86	47.60	.371
2a	0.61	2780	7.9R-0.158-0.0152	17.3	5.28	8.65	28.50	3.91	1.86	48.20	0.364
2b	0.61	2780	7.9R-0.127-0.0152	17.3	8.40**	8.65	28.50	3.42	1.86	50.83	0.308
2c	0.61	Infinite	0.127 OD by 0.0254 thickness	17.3	5.72	8.65	28.50	4.50	1.86	49.23	0.456 to .543
3	0.61	Infinite	15.8R-0.094-0.0076*	17.3	5.96	11.30	15.35	4.50	0.39	37.50	0.456
	.91	Infinite	11.8R- .170- .0102*	17.3	6.89	11.30	15.35	4.35	.34	38.23	.456

*Fin geometry of primary heat exchanger

** Includes insulation weight

TABLE 9
COOLANT EFFICIENCY FACTOR

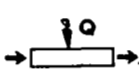


q/A		T _R		Efficiency factor, $\frac{T_R - 2000^{\circ}\text{R}(1110^{\circ}\text{K})}{T_R - T_{\text{WH,AVE}}}$		
						
Btu/sec-ft ²	kW/m ²	^o R	^o K	Single pass	In-depth folding	In-width folding
10	114	7000	3890	0.83	0.89	0.94
		3000	1670	0.47	0.69	0.64
250	2840	7000	3890	0.89	0.86	0.89
500	5680	7000	3890	0.86	0.86	0.88

TABLE 10
HEAT EXCHANGER MANUFACTURING AND HANDLING LIMITATIONS

Component	Governing condition	Affected parameter	Limitation
Heat transfer fin	Erosion of parent metal by braze filler alloy	Fin thickness	Minimum thickness: Superalloy: 0.003 in. (0.0076 cm) Aluminum: 0.004 in. (0.0102 cm)
	Collapse of fins due to braze fixture loads	Fin height, fin density, fin thickness	Minimum collapsing load of 5 psi (35 kN/m ²) at 2100°F (1420°K ^o) for superalloys
	Forming tools and material properties	Fin density and thickness	40 to 10 fins/in. (15.8 to 3.9 fins/cm), 0.003 to 0.010 in. (0.0076 to 0.0254 cm) fin thicknesses
Heat exchanger surface sheet	Handling, particle damage, fabrication	Thickness	Minimum thickness: Superalloy: 0.010 in. (0.0254 cm) Aluminum: 0.016 in. (0.0406 cm)
Coolant manifold pipes	Handling	Wall thickness	Minimum thickness: 0.030 in. (0.076 cm)

TABLE II
DESIGN INPUTS

Inputs	Concept 1	Concept 2	Concept 3 (a)
Material choices			
Heat exchanger	Waspaloy	Hastelloy X	Hastelloy X
Prime panel	Waspaloy	Inconel 718	Inconel 718
Beams	Inconel 718	Inconel 718	Inconel 718
Coolant conditions			
Hydrogen pressures, psi (kN/m ²)			
Inlet to manifold (maximum)	500 (3450)	1000 (6890)	1000 (6890)
Outlet from manifold (minimum)	250 (1720)	250 (1720)	250 (1720)
Hydrogen bulk temperature, °R (°K)			
Inlet	100 (56)	100 (56)	100 (56)
Outlet	1760 (978)	1600 (889)	1600 (889)
Metal temperatures, °F (°K)			
Heat exchanger surface temperature			
Inlet (reference only)	200 (111)	500 (278)	500 (278)
Outlet	1860 (1030)	2000 (1110)	2000 (1110)
Beam maximum temperature	1600 (889)	1600 (889)	1600 (889)
Panel size, ft (m)			
Width	2 (0.61)	2 (0.61)	2 (0.61)
Length	2, 3, and 5 (0.61, 0.91, and 1.52)	2 and 3 (0.61 and 0.91)	2 and 3 (0.61 and 0.91)
Stress-rupture life, hr			
	100	100	100
Fatigue life			
Thermal fatigue temperature differential across heat exchanger height, °R (°K)	Not a factor	400 to 600 (222 to 333)	400 to 600 (222 to 333)
Cycles to failure	Not a factor	300	300

(a) Inputs below generally refer to the cooled shingle portion; the cooled pressure-carrying structure has an aluminum composite panel and titanium beams operating at a maximum temperature of 250°R (139°K).

TABLE 12

MINIMUM WEIGHT CONCEPT I PANEL WEIGHTS FOR SELECTED HEATING,
LOADING, AND COOLANT OUTLET TEMPERATURE CONDITIONS
a.-U.S. CUSTOMARY UNITS

Length, ft	Fin k, Btu/hr- ft ² -°R	p, psi	T, CO °R	q/A, Btu/sec- ft ²	Fin geometry			P _{Cl} , psia	T _{DHW} , °F	T _{DHW} -T _{CO} , ΔT, °F	Panel wt., lb/ft ²	Beam wt., lb/ft ²	Clip wt., lb/ft ²	Manifold wt., lb/ft ²	Seal wt., lb/ft ²	Total wt., lb/ft ²	Hydrogen rate, lb/sec- ft ²
					N, fins/in.	h _{fin} , in.	t _{fin} , in.										
2	10	6.95	1400	10	20R -	0.075 -	0.003	300.1	1058	118	1.27	0.46	0.18	0.58	0.06	2.55	0.002175
2	10	6.95	1600	10	20R -	.075 -	.003	300.1	1250	110	1.27	.46	.18	.58	.06	2.55	.00187
2	10	6.95	1760	10	20R -	.075 -	.003	300.1	1404	104	1.27	.50	.22	.58	.07	2.64	.00169
2	10	6.95	1900	10	20R -	.075 -	.003	300.1	1540	100	1.27	.55	.28	.60	.07	2.77	.00157
2	10	6.95	1400	25	20R -	.075 -	.003	300.2	1210	270	1.27	.48	.20	.59	.06	2.60	.00544
2	10	6.95	1600	25	20R -	.050 -	.003	300.4	1358	218	1.20	.52	.25	.59	.06	2.62	.00468
2	10	6.95	1760	25	20R -	.075 -	.003	300.2	1544 ⁽¹⁾	244	1.27	.57	.32	.59	.07	2.82	.004225
2	10	6.95	1900	25	30R -	.075 -	.003	300.3	1598 ⁽¹⁾	158	1.36	.57	.32	.64	.07	2.96	.00391
2	10	6.95	1400	50	20R -	.050 -	.003	300.9	1329	389	1.20	.53	.26	.69	.06	2.74	.010875
2	10	6.95	1600	50	20R -	.025 -	.003	304.8	1390	250	1.14	.59	.35	.69	.06	2.83	.00935
2	10	6.95	1760	50	40R -	.050 -	.003	301.9	1505	205	1.33	.57	.32	.69	.07	2.98	.00845
2	10	6.95	1900	50	40R -	.050 -	.003	301.9	1639 ⁽¹⁾	199	1.33	.63	.42	.72	.07	3.17	.007825
2	10	6.95	1600	100	20R -	.025 -	.003	321.4	1425	285	1.14	.61	.38	.70	.06	2.89	.0187
2	10	20	1400	10	20R -	0.100 -	0.003	300.0	1068	128	1.33	1.06	0.28	0.58	0.10	3.35	0.002175
2	10	20	1600	10	20R -	.125 -	.003	300.0	1266	126	1.39	1.02	.25	.58	.10	3.34	.00187
2	10	20	1760	10	20R -	.100 -	.003	300.0	1412	112	1.33	1.14	.33	.58	.11	3.49	.00169
2	10	20	1900	10	20R -	.125 -	.003	300.0	1553 ⁽¹⁾	113	1.39	1.21	.40	.60	.12	3.72	.00157
2	10	20	1600	25	20R -	.100 -	.003	300.1	1420	280	1.33	1.15	.34	.59	.10	3.51	.00468
2	10	20	1600	50	30R -	.075 -	.003	300.6	1456	316	1.36	1.24	.42	.69	.10	3.81	.00935
2	10	20	1600	100	40R -	.025 -	.003	331.2	1380	240	1.20	1.42	.58	.70	.10	4.00	.0187
2	10	50	1400	10	20R -	0.150 -	0.003	300.0	1080	140	1.46	2.14	0.38	0.58	0.16	4.72	0.002175
2	10	50	1600	10	20R -	.150 -	.003	300.0	1272	132	1.46	2.13	.38	.58	.16	4.71	.00187
2	10	50	1760	10	20R -	.150 -	.003	300.0	1423	123	1.46	2.29	.48	.58	.17	4.98	.00169
2	10	50	1900	10	20R -	.150 -	.003	300.0	1557 ⁽¹⁾	117	1.46	2.52	.57	.60	.19	5.34	.00157
2	10	50	1400	25	20R -	.150 -	.003	300.1	1270	330	1.46	2.23	.42	.59	.16	4.86	.00544
2	10	50	1600	25	30R -	.125 -	.003	300.1	1330	190	1.56	2.24	.43	.59	.16	4.98	.00468
2	10	50	1760	25	30R -	.150 -	.003	300.1	1486	186	1.65	2.38	.52	.59	.17	5.31	.004225
2	10	50	1900	25	40R -	.150 -	.003	300.2	1566 ⁽¹⁾	126	1.84	2.51	.59	.64	.19	5.77	.00391
2	10	50	1400	50	30R -	.150 -	.003	300.2	1333	393	1.65	2.24	.44	.69	.16	5.18	.010875
2	10	50	1600	50	40R -	.150 -	.003	300.4	1405	265	1.84	2.24	.43	.69	.16	5.36	.00935
2	10	50	1760	50	40R -	.150 -	.003	300.4	1555 ⁽¹⁾	255	1.84	2.49	.59	.69	.17	5.78	.00845
2	10	50	1900	50	40R -	.150 -	.003	300.4	1686 ⁽¹⁾	246	1.84	2.80	.81	.72	.19	6.36	.007825
2	10	50	1600	100	40R -	.075 -	.003	302.1	1560 ⁽¹⁾	420	1.46	2.85	.86	.70	.16	6.03	.0187
2	10	100	1400	10	20R -	0.150 -	0.003	300.0	1080	140	1.46	3.81	0.56	0.58	0.23	6.64	0.002175
2	10	100	1600	10	20R -	.150 -	.003	300.0	1272	132	1.46	3.79	.56	.58	.23	6.62	.00187
2	10	100	1760	10	30R -	.150 -	.003	300.0	1376	76	1.65	3.93	.58	.58	.24	6.98	.00169
2	10	100	1900	10	30R -	.150 -	.003	300.0	1512	72	1.65	4.32	.81	.60	.26	7.64	.00157
2	10	100	1400	25	30R -	.150 -	.003	300.1	1150	210	1.65	3.82	.57	.59	.23	6.86	.00544
2	10	100	1600	25	40R -	.150 -	.003	310.2	1280	140	1.84	3.74	.54	.59	.23	6.94	.00468
2	10	100	1760	25	40R -	.150 -	.003	300.2	1431	131	1.84	4.05	.67	.59	.24	7.36	.004225
2	10	100	1900	25	40R -	.150 -	.003	300.2	1566 ⁽¹⁾	126	1.84	4.46	.88	.64	.26	8.08	.00391
2	10	100	1400	50	40R -	.150 -	.003	300.4	1222	282	1.84	3.82	.59	.69	.23	7.17	.010875
2	10	100	1600	50	40R -	.150 -	.003	300.4	1405	265	1.84	3.98	.64	.69	.23	7.38	.00935
2	10	100	1760	50	40R -	.150 -	.003	300.4	1555 ⁽¹⁾	255	1.84	4.44	.86	.69	.24	8.07	.00845
2	10	100	1900	50	40R -	.150 -	.003	300.4	1686 ⁽¹⁾	246	1.84	5.01	1.19	.72	.26	9.02	.007825
2	10	100	1600	100	40R -	.075 -	.003	302.1	1560 ⁽¹⁾	420	1.46	5.08	1.27	.70	.23	8.74	.0187

TABLE 12. Continued

MINIMUM WEIGHT CONCEPT I PANEL WEIGHTS FOR SELECTED HEATING,
LOADING, AND COOLANT OUTLET TEMPERATURE CONDITIONS

a.- U.S. CUSTOMARY UNITS

Length, ft	Fin k, Btu/hr- ft-°R	P, psi	T CO °R	q/A, Btu/sec- ft ²	Fin geometry			PCI, psia	T _{DHW} °F	T _{DHW} -T _{CO} ΔT, °F	Panel wt, lb/ft ²	Beam wt, lb/ft ²	Clip wt, lb/ft ²	Manifold wt, lb/ft ²	Seal wt, lb/ft ²	Total wt, lb/ft ²	Hydrogen rate, lb/sec- ft ²
					N, fins/in.	h _{fin} in.	t _{fin} in.										
5	10	6.95	1400	10	20R -	0.050	0.003	300.9	1032	92	1.20	0.48	0.21	0.42	0.04	2.35	0.002175
5	10	6.95	1600	10	20R -	.075	.003	300.4	1242	102	1.27	.46	.18	.42	.04	2.37	.00187
5	10	6.95	1760	10	20R -	.075	.003	300.4	1398	98	1.27	.50	.22	.42	.04	2.45	.00169
5	10	6.95	1900	10	20R -	.075	.003	300.4	1534	94	1.27	.55	.28	.43	.05	2.58	.00157
5	10	6.95	1600	25	20R -	.050	.003	302.7	1320	180	1.20	.51	.23	.53	.04	2.51	.00468
5	10	6.95	1600	50	20R -	.035	.003	331.2	1295	155	1.16	.53	.26	.61	.04	2.60	.00955
5	10	6.95	1600	100	20R -	.050	.003	344.5	1355	215	1.20	.52	.24	.62	.04	2.62	.0187
5	10	50	1400	10	20R -	0.150	0.003	300.1	1074	134	1.46	2.13	0.37	0.42	0.11	4.49	0.002175
5	10	50	1600	10	20R -	.150	.003	300.1	1269	129	1.46	2.13	.38	.42	.11	4.50	.00187
5	10	50	1900	10	20R -	.150	.003	300.1	1559 ⁽¹⁾	119	1.46	2.54	.61	.43	.12	5.15	.00157
5	10	50	1400	25	20R -	.150	.003	300.3	1228	288	1.46	2.20	.41	.53	.11	4.71	.00544
5	10	50	1600	25	30R -	.150	.003	300.7	1322	182	1.65	2.14	.39	.53	.11	4.82	.00468
5	10	50	1900	25	40R -	.150	.003	301.1	1562 ⁽¹⁾	122	1.84	2.50	.60	.55	.12	5.61	.00391
5	10	50	1400	50	20R -	.150	.003	300.9	1421	481	1.46	2.32	.48	.61	.11	4.98	.010875
5	10	50	1600	50	40R -	.100	.003	304.2	1350	210	1.59	2.35	.49	.61	.11	5.15	.00935
5	10	50	1900	50	40R -	.150	.003	302.3	1666 ⁽¹⁾	226	1.84	2.75	.78	.62	.12	6.11	.007825
5	10	100	1400	10	20R -	0.150	0.003	300.1	1074	134	1.46	3.78	0.56	0.42	0.15	6.37	0.002175
5	10	100	1600	10	20R -	.150	.003	300.1	1269	129	1.46	3.78	.56	.42	.16	6.38	.00187
5	10	100	1900	10	40R -	.150	.003	300.4	1491	51	1.84	4.12	.75	.43	.17	7.31	.00157
5	10	100	1400	25	20R -	.150	.003	300.3	1228	288	1.46	3.92	.61	.53	.15	6.67	.00468
5	10	100	1600	25	30R -	.150	.003	300.7	1322	182	1.65	3.82	.57	.53	.16	6.73	.00391
5	10	100	1900	25	40R -	.150	.003	301.1	1562 ⁽¹⁾	122	1.84	4.46	.88	.55	.17	7.90	.00391
5	10	100	1400	50	30R -	.150	.003	301.4	1272	332	1.65	3.93	.62	.61	.15	6.96	.010875
5	10	100	1600	50	40R -	.150	.003	302.4	1379	239	1.84	3.92	.62	.61	.16	7.15	.00935
5	10	100	1900	50	40R -	.150	.003	302.3	1666 ⁽¹⁾	226	1.84	4.90	1.15	.62	.17	8.68	.007825
2	100	6.95	1600	10	20R -	0.075	0.006	300.1	1201	61	1.26	0.46	0.18	0.58	0.06	2.54	0.00187
2	100	6.95	1600	100	20R -	.025	.006	336.6	1308	168	1.33	.58	.34	.70	.06	3.01	.0187
5	100	6.95	1600	10	20R -	.050	.006	301.2	1193	53	1.46	.48	.21	.42	.04	2.61	.00187
5	100	6.95	1600	100	20R -	.050	.006	359.6	1277	137	1.46	.50	.22	.62	.04	2.84	.0187
2	100	20	1600	10	20R -	.125	.006	300.0	1202	62	1.88	1.01	.24	.58	.10	3.81	.00187
2	100	50	1600	10	20R -	.150	.006	300.0	1203	63	2.01	2.10	.37	.58	.16	5.22	.00187
2	100	100	1600	10	20R -	.150	.006	300.0	1203	63	2.01	3.74	.54	.58	.23	7.10	.00187
2	100	100	1600	100	40R -	.100	.006	302.0	1339	137	2.23	4.13	.75	.70	.23	8.02	.0187

- NOTES: (1) Maximum surface temperature exceeds stated 2000°R (1540°F) maximum allowable. The concept I design procedure was based on a maximum fin height of 0.150 in. for fabrication reasons, permitting surface temperatures to exceed 2000°R.
(2) Infinite recovery temperature
(3) Two-foot panel width

TABLE 12. Continued

MINIMUM WEIGHT CONCEPT I PANEL WEIGHTS FOR SELECTED HEATING,
LOADING, AND COOLANT OUTLET TEMPERATURE CONDITIONS

b.- SI UNITS

Length, cm	Fin k, W/m ² °K	P, kN/m ²	T _o , °K	q/A, kW/m ²	Fin geometry			P _{CI} , kN/m ²	T _{DHW} , °K	T _{DHW} -T _{CO} , °C	Panel wt., kg/m ²	Beam wt., kg/m ²	Clip wt., kg/m ²	Manifold wt., kg/m ²	Seal wt., kg/m ²	Total wt., kg/m ²	Hydrogen rate, kg/s-m ²
					N _s fins/cm	h _{fin} , cm	t _{fin} , cm										
0.61	17.3	48	778	114	7.9R	-0.191	-0.0076	2069	844	66	6.20	2.24	0.88	2.83	0.29	12.4	0.0106
.61	17.3	48	889	114	7.9R	-.191	-.0076	2069	950	61	6.20	2.24	.88	2.83	.29	12.4	.00912
.61	17.3	48	889	114	7.9R	-.191	-.0076	2069	1036	58	6.20	2.44	1.07	2.83	.34	12.9	.00824
.61	17.3	48	1060	114	7.9R	-.191	-.0076	2069	1112	56	6.20	2.68	1.37	2.93	.34	13.5	.00766
.61	17.3	48	778	284	7.9R	-.191	-.0076	2070	928	150	6.20	2.34	.97	2.88	.29	12.7	.0266
.61	17.3	48	889	284	7.9R	-.127	-.0076	2071	1010	121	5.87	2.54	1.22	2.88	.29	12.8	.0228
.61	17.3	48	978	284	7.9R	-.191	-.0076	2070	1113 ⁽¹⁾	135	6.20	2.78	1.56	2.88	.34	13.8	.0206
.61	17.3	48	1060	284	11.8R	-.191	-.0076	2070	1144 ⁽¹⁾	80	6.64	2.78	1.56	3.13	.34	14.5	.0191
.61	17.3	48	778	568	7.9R	-.127	-.0076	2074	994	216	5.86	2.59	1.27	3.37	.29	13.4	.0532
.61	17.3	48	889	568	7.9R	-.064	-.0076	2101	1028	139	5.56	2.88	1.71	3.37	.29	13.8	.0456
.61	17.3	48	978	568	15.8R	-.127	-.0076	2081	1092	114	6.49	2.78	1.56	3.37	.34	14.5	.0412
.61	17.3	48	1060	568	15.8R	-.127	-.0076	2081	1167 ⁽¹⁾	111	6.49	3.08	2.05	3.52	.34	15.5	.0384
.61	17.3	48	889	1140	7.8R	-.064	-.0076	2216	1047	158	5.56	2.98	1.85	3.42	.29	14.1	.0912
0.61	17.3	138	778	114	7.9R	-0.254	-0.0076	2068	849	71	6.49	5.17	1.37	2.83	0.49	16.4	0.0106
.61	17.3	138	889	114	7.9R	-.318	-.0076	2068	959	70	6.78	4.98	1.22	2.83	.49	16.3	.00912
.61	17.3	138	978	114	7.9R	-.254	-.0076	2068	1040	62	6.49	5.56	1.61	2.83	.54	17.0	.00824
.61	17.3	138	1060	114	7.9R	-.318	-.0076	2068	1119 ⁽¹⁾	63	6.78	5.90	1.95	2.93	.59	18.2	.00766
.61	17.3	138	889	284	7.9R	-.254	-.0076	2069	1045	156	6.49	5.61	1.66	2.88	.49	17.1	.0228
.61	17.3	138	889	568	11.8R	-.191	-.0076	2072	1065	176	6.64	6.05	2.05	3.37	.49	18.6	.0456
.61	17.3	138	889	1140	15.8R	-.064	-.0076	2283	1022	133	5.86	6.93	2.83	3.42	.49	19.5	.0912
0.61	17.3	345	778	114	7.9R	-0.381	-0.0076	2068	856	78	7.13	10.44	1.86	2.83	0.78	23.0	0.0106
.61	17.3	345	889	114	7.9R	-.381	-.0076	2068	962	73	7.13	10.39	1.86	2.83	.78	23.0	.00912
.61	17.3	345	978	114	7.9R	-.381	-.0076	2068	1046	68	7.13	11.19	2.34	2.83	.83	24.3	.00824
.61	17.3	345	1060	114	7.9R	-.381	-.0076	2068	1121 ⁽¹⁾	65	7.13	12.30	2.78	2.92	.93	26.1	.00766
.61	17.3	345	778	284	7.9R	-.381	-.0076	2069	961	183	7.13	10.89	2.05	2.88	.78	23.7	.0266
.61	17.3	345	889	284	11.8R	-.318	-.0076	2069	995	106	7.61	10.94	2.10	2.88	.78	24.3	.0228
.61	17.3	345	978	284	11.8R	-.381	-.0076	2069	1081	103	8.06	11.62	2.54	2.88	.83	25.9	.0206
.61	17.3	345	1060	284	15.8R	-.381	-.0076	2070	1126 ⁽¹⁾	70	8.98	12.26	2.88	3.13	.93	28.2	.0191
.61	17.3	345	778	568	11.8R	-.381	-.0076	2070	996	118	8.06	10.94	2.15	3.37	.78	25.3	.0532
.61	17.3	345	889	568	15.8R	-.381	-.0076	2071	1036	147	8.98	10.94	2.10	3.37	.78	26.2	.0456
.61	17.3	345	978	568	15.8R	-.381	-.0076	2071	1120 ⁽¹⁾	142	8.98	12.16	2.88	3.37	.83	28.2	.0412
.61	17.3	345	1060	568	15.8R	-.381	-.0076	2071	1193 ⁽¹⁾	137	8.98	13.67	3.96	3.52	.93	31.1	.0384
.61	17.3	345	889	1140	15.8R	-.191	-.0076	2083	1123 ⁽¹⁾	234	7.12	13.91	4.20	3.42	.78	29.4	.0912
0.61	17.3	689	778	114	7.9R	-0.381	-0.0076	2068	856	78	7.13	18.60	2.74	2.83	1.12	32.4	0.0106
.61	17.3	689	889	114	7.9R	-.381	-.0076	2068	962	73	7.13	18.50	2.74	2.83	1.12	32.3	.00912
.61	17.3	689	978	114	11.8R	-.381	-.0076	2068	1020	42	8.06	19.20	2.83	2.83	1.17	34.1	.00824
.61	17.3	689	1060	114	11.8R	-.381	-.0076	2068	1096	40	8.06	21.05	3.95	2.93	1.27	37.3	.00766
.61	17.3	689	778	284	11.8R	-.381	-.0076	2069	895	117	8.06	18.65	2.78	2.88	1.12	33.5	.0266
.61	17.3	689	889	284	15.8R	-.381	-.0076	2070	967	78	8.98	18.25	2.64	2.88	1.12	33.9	.0228
.61	17.3	689	978	284	15.8R	-.381	-.0076	2070	1051	73	8.98	19.78	3.27	2.88	1.17	36.1	.0206
.61	17.3	689	1060	284	15.8R	-.381	-.0076	2070	1126 ⁽¹⁾	70	8.98	21.78	4.30	3.13	1.27	39.3	.0191
.61	17.3	689	778	568	15.8R	-.381	-.0076	2071	935	157	8.98	18.65	2.88	3.37	1.12	35.0	.0532
.61	17.3	689	889	568	15.8R	-.381	-.0076	2071	1036	147	8.98	19.42	3.12	3.37	1.12	36.0	.0456
.61	17.3	689	978	568	15.8R	-.381	-.0076	2071	1120 ⁽¹⁾	142	8.98	21.68	4.20	3.37	1.17	39.4	.0412
.61	17.3	689	1060	568	15.8R	-.381	-.0076	2071	1193 ⁽¹⁾	137	8.98	24.46	5.81	3.52	1.27	44.0	.0384
.61	17.3	689	889	1140	15.8R	-.191	-.0076	2083	1123 ⁽¹⁾	234	7.13	24.80	6.20	3.42	1.12	42.7	.0912

TABLE 12. Concluded

MINIMUM WEIGHT CONCEPT I PANEL WEIGHTS FOR SELECTED HEATING,
LOADING, AND COOLANT OUTLET TEMPERATURE CONDITIONS

b.- SI UNITS

Length, cm	Fin k, W/m ² °K	P, kN/m ²	T _o , °K	q/A ₂ , kW/m ²	Fin geometry			p _{CI} , kN/m ²	T _{DMW} , °K	T _{DMW} -T _{CO} , ΔT, °F	Panel wt, kg/m ²	Beam wt, kg/m ²	Clip wt, kg/m ²	Manifold wt, kg/m ²	Seal wt, kg/m ²	Total wt, kg/m ²	Hydrogen rate, kg/s-m ²
					N, fins/cm	h _{fin} , cm	t _{fin} , cm										
1.52	17.3	48	778	114	7.9R	-0.127	-0.0076	2074	829	51	5.86	2.34	1.02	2.05	0.20	11.5	0.0106
1.52	17.3	48	889	114	7.9R	-.191	-.0076	2071	946	57	6.20	2.24	.88	2.05	.20	11.6	.00912
1.52	17.3	48	978	114	7.9R	-.191	-.0076	2071	1022	54	6.20	2.44	1.07	2.05	.20	12.0	.00824
1.52	17.3	48	1060	114	7.9R	-.191	-.0076	2071	1108	52	6.20	2.68	1.37	2.10	.24	12.6	.00766
1.52	17.3	48	889	284	7.9R	-.127	-.0076	2087	989	100	5.86	2.49	1.12	2.59	.20	12.3	.0228
1.52	17.3	48	889	568	7.9R	-.089	-.0076	2283	975	86	5.65	2.59	1.27	2.98	.20	12.7	.0456
1.52	17.3	48	889	1140	7.9R	-.127	-.0076	2375	1008	119	5.86	2.54	1.17	3.03	.20	12.8	.0912
1.52	17.3	345	778	114	7.9R	-0.381	-0.0076	2069	853	75	7.13	10.40	1.81	2.05	0.54	21.9	0.0106
1.52	17.3	345	889	114	7.9R	-.381	-.0076	2069	961	72	7.13	10.40	1.86	2.05	.54	22.0	.00912
1.52	17.3	345	1060	114	7.9R	-.381	-.0076	2069	1122 ⁽¹⁾	66	7.13	12.40	2.98	2.10	.58	25.2	.00766
1.52	17.3	345	778	284	7.9R	-.381	-.0076	2070	938	160	7.13	10.74	2.00	2.59	.54	23.0	.0266
1.52	17.3	345	889	284	11.8R	-.381	-.0076	2073	990	101	8.06	10.45	1.90	2.59	.54	23.5	.0228
1.52	17.3	345	1060	284	15.8R	-.381	-.0076	2076	1124 ⁽¹⁾	68	8.98	12.21	2.93	2.69	.58	27.4	.0191
1.52	17.3	345	778	568	7.9R	-.381	-.0076	2074	1045	267	7.13	11.33	2.34	2.98	.54	24.3	.0532
1.52	17.3	345	889	568	15.8R	-.254	-.0076	2097	1006 ⁽¹⁾	117	7.76	11.48	2.39	2.98	.54	25.2	.0456
1.52	16.3	345	1060	568	15.8R	-.381	-.0076	2084	1181 ⁽¹⁾	125	8.98	13.43	3.81	3.03	.58	29.8	.0389
1.52	17.3	689	778	114	7.9R	-0.381	-0.0076	2069	853	75	7.13	18.46	2.73	2.05	0.73	31.1	0.0106
1.52	17.3	689	889	114	7.9R	-.381	-.0076	2069	961	72	7.13	18.46	2.73	2.05	.78	31.1	.00912
1.52	17.3	689	1060	114	15.8R	-.381	-.0076	2071	1084	28	8.98	20.12	3.66	2.10	.83	35.7	.00766
1.52	17.3	689	778	284	7.9R	-.381	-.0076	2070	938	160	7.13	19.14	2.98	2.59	.73	32.6	.0266
1.52	17.3	689	889	284	11.8R	-.381	-.0076	2073	990	101	8.06	18.65	2.78	2.59	.78	32.9	.0228
1.52	17.3	689	1060	284	15.8R	-.381	-.0076	2076	1124 ⁽¹⁾	68	8.98	21.78	4.30	2.69	.83	38.6	.0191
1.52	17.3	689	778	568	11.8R	-.381	-.0076	2078	962	184	8.06	19.19	3.03	2.98	.73	34.0	.0532
1.52	17.3	689	889	568	15.8R	-.381	-.0076	2085	1022 ⁽¹⁾	133	8.98	19.14	3.03	2.98	.78	34.9	.0456
1.52	17.3	689	1060	568	15.8R	-.381	-.0076	2084	1182 ⁽¹⁾	126	8.98	23.93	5.62	3.03	.83	42.4	.0384
0.61	173	48	889	114	7.9R	-0.191	-0.0152	2069	923	34	6.15	2.24	0.88	2.83	0.29	12.4	0.00912
.61	173	48	889	1140	7.9R	-.064	-.0152	2321	982	93	6.49	2.83	1.66	3.42	.29	14.7	.00912
1.52	173	48	889	114	7.9R	-.127	-.0152	2076	918	29	7.13	2.34	1.02	2.05	.20	12.7	.00912
1.52	173	48	889	1140	7.9R	-.127	-.0152	2479	965	76	7.13	2.44	1.07	3.03	.20	13.9	.00912
.61	173	138	889	114	7.9R	-.318	-.0152	2068	923	34	9.17	4.93	1.17	2.83	.49	18.6	.00912
.61	173	345	889	114	7.9R	-.381	-.0152	2068	924	35	9.80	10.25	1.81	2.83	.78	25.5	.00912
.61	173	689	889	114	7.9R	-.381	-.0152	2068	924	35	9.80	18.25	2.64	2.83	1.12	34.6	.00912
.61	173	689	889	1140	15.8R	-.254	-.0152	2082	999	110	10.89	20.17	3.56	3.42	1.12	39.2	.00912

NOTES: (1) Maximum surface temperature exceeds stated 1110°K maximum allowable. The concept I design procedure was based on a maximum fin height of 0.381 cm for fabrication reasons, permitting surface temperatures to exceed 1110°K

(2) Infinite recovery temperature

(3) 0.61-m panel width

TABLE 13. Continued

MINIMUM WEIGHT CONCEPT 2 PANEL WEIGHTS FOR SELECTED HEATING,
LOADING, AND COOLANT OUTLET TEMPERATURE CONDITIONS

PART I INFINITE RECOVERY TEMPERATURE

a.- U.S. CUSTOMARY UNITS

Panel length, ft	Panel width, ft	Fin k, Btu hr-ft ⁻² -°R	T _{CO} , °R	q/A, Btu/sec-ft ²	p, psi	Fin geometry			P _{Cl} , psia	T _{DHW} , °F	T _{DHW} -T _{CO} , ΔT, °F	Heat exchanger wt, lb/ft ²	Prime panel wt, lb/ft ²	Beam wt, lb/ft ²	Clip wt, lb/ft ²	Manifold wt, lb/ft ²	Seal wt, lb/ft ²	Total wt, lb/ft ²	Hydrogen rate, lb/sec-ft ²		
						N, fins/in.	h _{fin} , in.	t _{fin} , in.													
5	2	10	1400	10	6.95	20R0	-	0.025	-	0.003	328	963	23	0.72	0.93	0.38	0.11	0.42	0.04	2.60	0.002175
5	2	10	1600	10	6.95	20R0	-	.025	-	.003	326	1163	23	.72	.93	.39	.12	.42	.04	2.62	.00187
5	2	10	1900	10	6.95	20R0	-	.025	-	.003	325	1463	23	.72	.94	.63	.23	.43	.05	3.00	.00157
5	2	10	1400	25	6.95	20R0	-	.025	-	.003	420	976	36	.72	.93	.38	.11	.53	.04	2.71	.00544
5	2	10	1600	25	6.95	20R0	-	.025	-	.003	406	1177	37	.72	.93	.39	.12	.53	.04	2.73	.00468
5	2	10	1900	25	6.95	30R0	-	.025	-	.003	423	1473	33	.75	.94	.63	.23	.55	.05	3.15	.00391
5	2	10	1400	50	6.95	20R0	-	.025	-	.003	639	991	51	.72	.93	.38	.11	.61	.04	2.79	.010875
5	2	10	1600	50	6.95	20R0	-	.025	-	.003	599	1193	53	.72	.93	.39	.12	.61	.04	2.81	.00935
5	2	10	1900	50	6.95	30R0	-	.031	-	.003	727	1483	43	.77	.94	.63	.23	.62	.05	3.24	.007825
5	2	10	1400	10	50	20R0	-	0.025	-	0.003	328	963	23	0.72	0.95	1.94	0.34	0.42	0.11	4.48	0.002175
5	2	10	1600	10	50	20R0	-	.025	-	.003	326	1163	23	.72	.95	2.07	.37	.42	.11	4.64	.00187
5	2	10	1900	10	50	20R0	-	.025	-	.003	325	1463	23	.72	1.17	2.59	.48	.43	.12	5.51	.00157
5	2	10	1400	25	50	20R0	-	.025	-	.003	420	976	36	.72	.95	1.94	.34	.53	.11	4.59	.00544
5	2	10	1600	25	50	20R0	-	.025	-	.003	406	1177	37	.72	.95	2.07	.37	.53	.11	4.75	.00468
5	2	10	1900	25	50	30R0	-	.025	-	.003	423	1473	33	.75	1.17	2.59	.48	.55	.12	5.66	.00391
5	2	10	1400	50	50	20R0	-	.025	-	.003	639	991	51	.72	.95	1.94	.34	.61	.11	4.67	.010875
5	2	10	1600	50	50	20R0	-	.025	-	.003	599	1193	53	.72	.95	2.07	.37	.61	.11	4.83	.00935
5	2	10	1900	50	50	30R0	-	.031	-	.003	727	1483	43	.77	1.17	2.59	.48	.62	.12	5.75	.007825
5	2	10	1400	10	100	20R0	-	0.025	-	0.003	328	963	23	0.72	1.03	3.10	0.37	0.42	0.15	5.84	0.002175
5	2	10	1600	10	100	20R0	-	.025	-	.003	326	1163	23	.72	1.11	3.19	.37	.42	.16	5.97	.00187
5	2	10	1900	10	100	20R0	-	.025	-	.003	325	1463	23	.72	1.55	4.06	.48	.43	.17	7.41	.00157
5	2	10	1400	25	100	20R0	-	.025	-	.003	420	976	36	.72	1.08	3.10	.37	.53	.15	5.95	.00544
5	2	10	1600	25	100	20R0	-	.025	-	.003	406	1177	37	.72	1.11	3.19	.37	.53	.16	6.08	.00468
5	2	10	1900	25	100	30R0	-	.025	-	.003	423	1473	33	.75	1.55	4.06	.48	.55	.17	7.56	.00391
5	2	10	1400	50	100	20R0	-	.025	-	.003	639	991	51	.72	1.08	3.10	.37	.61	.15	6.03	.010875
5	2	10	1600	50	100	20R0	-	.025	-	.003	599	1193	53	.72	1.11	3.19	.37	.61	.16	6.16	.00935
5	2	10	1900	50	100	30R0	-	.031	-	.003	727	1483	43	.77	1.55	4.06	.48	.62	.17	7.65	.007825
2	2	100	1600	10	6.95	20R0	-	0.025	-	0.003	305	1163	23	0.91	0.93	0.39	0.12	0.58	0.06	2.99	0.00187
2	2	100	1600	250	6.95	20R0	-	.027	-	.003	800	1275	135	.93	.93	.39	.12	.75	.06	3.18	.0468
2	2	100	1600	10	50	20R0	-	.025	-	.003	305	1163	23	.91	.95	2.07	.37	.58	.16	5.04	.00187
2	2	100	1600	250	50	20R0	-	.027	-	.003	800	1275	135	.93	.95	2.07	.37	.75	.16	5.23	.0468
2	2	100	1600	10	100	20R0	-	.025	-	.003	305	1163	23	.91	1.11	3.19	.37	.58	.23	6.39	.00187
2	2	100	1600	250	100	20R0	-	.027	-	.003	800	1275	135	.93	1.11	3.19	.37	.75	.23	6.58	.0468

NOTES: (1) Maximum design inlet pressure is 700 psia; except as noted, all designs were based on a maximum inlet pressure of 1000 psia.
(2) Maximum design inlet pressure is 1400 psia.

TABLE 13. Continued

MINIMUM WEIGHT CONCEPT 2 PANEL WEIGHTS FOR SELECTED HEATING,
LOADING, AND COOLANT OUTLET TEMPERATURE CONDITIONS

PART I INFINITE RECOVERY TEMPERATURE

b.- SI UNITS

Panel length, m	Panel width, m	Fin k, W/m ² °K	T _{CO} , °K	q/A, kW/m ²	P _i , kN/m ²	Fin geometry			P _{CI} , kN/m ²	T _{DMU} , °K	T _{DMU} -T _{CO} , ΔT, °K	Heat exchanger wt, kg/m ²	Prime panel wt, kg/m ²	Beam wt, kg/m ²	Clip wt, kg/m ²	Manifold wt, kg/m ²	Seal wt, kg/m ²	Total wt, kg/m ²	Hydrogen rate, kg/s-m ²
						N _f , fins/cm	h _{fin} , cm	t _{fin} , cm											
1.52	0.61	17.3	778	114	48	7.9R0	-0.064	-0.0076	2260	791	13	3.52	4.54	1.86	0.54	2.05	0.20	12.7	0.0106
1.52	.61	17.3	889	114	48	7.9R0	-.064	-.0076	2250	902	13	3.52	4.54	1.91	.59	2.05	.20	12.8	.00912
1.52	.61	17.3	1060	114	48	7.9R0	-.064	-.0076	2240	1069	13	3.52	4.59	3.08	.73	2.10	.24	13.3	.00766
1.52	.61	17.3	778	284	48	7.9R0	-.064	-.0076	2900	798	20	3.52	4.54	1.86	.54	2.59	.54	13.6	.0266
1.52	.61	17.3	889	284	48	7.9R0	-.064	-.0076	2800	910	21	3.52	4.54	1.91	.59	2.59	.54	13.7	.0228
1.52	.61	17.3	1060	284	49	11.8R0	-.064	-.0076	2920	1074	18	3.66	4.59	3.08	.73	2.78	.59	14.4	.0191
1.52	.61	17.3	778	568	48	7.9R0	-.064	-.0076	4410	806	28	3.52	4.54	1.86	.54	2.98	.73	14.2	.0532
1.52	.61	17.3	889	568	48	7.9R0	-.064	-.0076	4130	918	29	3.52	4.54	1.91	.59	2.98	.78	14.3	.0456
1.52	.61	17.3	1060	568	48	11.8R0	-.079	-.0076	5010	1080	24	3.76	4.59	2.08	.73	3.03	.83	14.8	.0384
1.52	0.61	17.3	778	114	345	7.9R0	-0.064	-0.0076	2260	791	13	3.52	4.64	9.47	1.66	2.05	0.20	21.5	0.0106
1.52	.61	17.3	889	114	345	7.9R0	-.064	-.0076	2250	902	13	3.52	4.64	10.10	1.81	2.05	.20	22.3	.00912
1.52	.61	17.3	1060	114	345	7.9R0	-.064	-.0076	2240	1069	13	3.52	5.72	12.65	2.35	2.10	.24	26.6	.00766
1.52	.61	17.3	778	284	345	7.9R0	-.064	-.0076	2900	798	20	3.52	4.64	9.47	1.66	2.59	.54	22.4	.0266
1.52	.61	17.3	889	284	345	7.9R0	-.064	-.0076	2800	910	21	3.52	4.64	10.10	1.81	2.59	.54	23.2	.0228
1.52	.61	17.3	1060	284	345	11.8R0	-.064	-.0076	2920	1074	18	3.66	5.72	12.65	2.35	2.78	.59	27.8	.0191
1.52	.61	17.3	778	568	345	7.9R0	-.064	-.0076	4410	806	28	3.52	4.64	9.47	1.66	2.98	.73	23.0	.0532
1.52	.61	17.3	889	568	345	7.9R0	-.064	-.0076	4130	918	29	3.52	4.64	10.12	1.81	2.98	.78	23.9	.0456
1.52	.61	17.3	1060	568	345	11.8R0	-.079	-.0076	5010	1080	24	3.76	5.72	12.65	2.35	3.03	.83	28.3	.0384
1.52	0.61	17.3	778	114	689	7.9R0	-0.064	-0.0076	2260	791	13	3.52	5.27	15.15	1.81	2.05	0.20	28.0	0.0106
1.52	.61	17.3	889	114	689	7.9R0	-.064	-.0076	2250	902	13	3.52	5.42	15.60	1.81	2.05	.20	28.6	.00912
1.52	.61	17.3	1060	114	689	7.9R0	-.064	-.0076	2240	1069	13	3.52	7.57	19.80	2.35	2.10	.24	35.6	.00766
1.52	.61	17.3	778	284	689	7.9R0	-.064	-.0076	2900	798	20	3.52	5.27	15.15	1.81	2.59	.54	28.9	.0266
1.52	.61	17.3	889	284	689	7.9R0	-.064	-.0076	2800	910	21	3.52	5.42	15.60	1.81	2.59	.54	29.5	.0228
1.52	.61	17.3	1060	284	689	11.8R0	-.064	-.0076	2920	1074	13	3.66	7.57	19.80	2.35	2.78	.59	36.8	.0191
1.52	.61	17.3	778	568	689	7.9R0	-.064	-.0076	4410	806	28	3.52	5.27	15.15	1.81	2.98	.73	29.5	.0532
1.52	.61	17.3	889	568	689	7.9R0	-.064	-.0076	4130	918	29	3.52	5.42	15.58	1.81	2.98	.78	30.1	.0456
1.52	.61	17.3	1060	568	689	11.8R0	-.079	-.0076	5010	1080	24	3.76	7.57	19.80	2.35	3.03	.83	37.2	.0384
0.61	0.61	173	889	114	48	7.9R0	-0.064	-0.0152	2100	902	13	4.44	4.54	1.91	0.59	2.83	0.29	14.6	0.00912
.61	.61	173	889	2840	48	7.9R0	-.069	-.0152	5510	964	75	4.54	4.54	1.91	.59	3.67	.29	15.5	.228
.61	.61	173	889	114	345	7.9R0	-.064	-.0152	2100	902	13	4.44	4.64	10.10	1.81	2.83	.78	24.6	.00912
.61	.61	173	889	2840	345	7.9R0	-.069	-.0152	5510	964	75	4.54	4.64	10.10	1.81	3.67	.78	25.5	.228
.61	.61	173	889	114	689	7.9R0	-.064	-.0152	2100	902	13	4.44	5.42	10.60	1.81	2.83	1.12	31.2	.00912
.61	.61	173	889	2840	689	7.9R0	-.069	-.0152	5510	964	75	4.54	5.42	15.60	1.81	3.67	1.12	32.2	.228

NOTES: (1) Maximum design inlet pressure is 4820 kN/m², all designs except as noted were based on a maximum inlet pressure of 6890 kN/m²
(2) Maximum design inlet pressure is 9650 kN/m²

TABLE 13. Continued
 MINIMUM WEIGHT CONCEPT 2 PANEL WEIGHTS FOR SELECTED HEATING,
 LOADING, AND COOLANT OUTLET TEMPERATURE CONDITIONS

PART II 5000°R RECOVERY TEMPERATURE

a. - U.S. CUSTOMARY UNITS

Panel length, ft	Panel width, ft	Fin k, Btu hr-ft ⁻² -°R	T _{CO} , °R	q/A, Btu/sec-ft ²	p, psi	Fin geometry			PCI, psia	T _{DMW} , °F	T _{DMW} -T _{CO} , =ΔT, °F	Heat exchanger wt, lb/ft ²	Prime panel wt, lb/ft ²	Beam wt, lb/ft ²	Clip wt, lb/ft ²	Manifold wt, lb/ft ²	Seal wt, lb/ft ²	Total wt, lb/ft ²	Hydrogen rate, lb/sec-ft ²
						N, fins/in.	h _{fin} , in.	t _{fin} , in.											
2	2	10	1400	10	6.95	20R0	0.025	0.003	303	961	21	0.717	0.93	0.38	0.11	0.58	0.06	2.78	0.00198
2	2	10	1400	10	6.95	20R0	0.050	0.003	300	975	35	.782	.93	.38	.11	.58	.06	2.85	.00198
2	2	10	1400	10	6.95	20R0	0.075	0.003	300	984	44	.847	.93	.38	.11	.58	.06	2.92	.00198
2	2	10	1600	10	6.95	20R0	0.025	0.003	302	1159	19	.717	.93	.39	.12	.58	.06	2.80	.00167
2	2	10	1600	10	6.95	20R0	0.050	0.003	300	1172	32	.782	.93	.39	.12	.58	.06	2.87	.00167
2	2	10	1600	10	6.95	20R0	0.075	0.003	300	1182	42	.847	.93	.39	.12	.58	.06	2.94	.00167
2	2	10	1760	10	6.95	20R0	0.025	0.003	302	1318	18	.717	.91	.49	.15	.58	.07	2.92	.00148
2	2	10	1760	10	6.95	20R0	0.050	0.003	300	1330	30	.782	.91	.49	.15	.58	.07	2.99	.00148
2	2	10	1760	10	6.95	20R0	0.075	0.003	300	1339	39	.847	.91	.49	.15	.58	.07	3.06	.00148
2	2	10	1900	10	6.95	20R0	0.025	0.003	302	1457	17	.717	.94	.63	.23	.60	.07	3.19	.00134
2	2	10	1900	10	6.95	20R0	0.050	0.003	300	1469	29	.782	.94	.63	.23	.60	.07	3.26	.00134
2	2	10	1900	10	6.95	20R0	0.075	0.003	300	1477	37	.847	.94	.63	.23	.60	.07	3.33	.00134
2	2	10	1400	100	6.95	20R0	0.025	0.003	385	1024	84	0.717	0.93	0.38	0.11	0.69	0.06	2.89	0.0195
2	2	10	1400	100	6.95	20R0	0.050	0.003	314	1082	142	.782	.93	.38	.11	.69	.06	2.96	.0190
2	2	10	1400	100	6.95	20R0	0.075	0.003	305	1123	183	.847	.93	.38	.11	.69	.06	3.03	.0187
2	2	10	1600	100	6.95	20R0	0.025	0.003	377	1222	82	.717	.93	.39	.12	.70	.06	2.92	.0165
2	2	10	1600	100	6.95	20R0	0.050	0.003	312	1279	139	.782	.93	.39	.12	.70	.06	2.99	.01605
2	2	10	1600	100	6.95	20R0	0.075	0.003	305	1320	180	.847	.93	.39	.12	.70	.06	3.06	.0158
2	2	10	1760	100	6.95	20R0	0.025	0.003	370	1380	80	.717	.91	.49	.15	.73	.07	3.07	.0146
2	2	10	1760	100	6.95	20R0	0.050	0.003	311	1436	136	.782	.91	.49	.15	.73	.07	3.14	.01425
2	2	10	1760	100	6.95	20R0	0.075	0.003	304	1477	177	.847	.91	.49	.15	.73	.07	3.21	.0140
2	2	10	1900	100	6.95	30R0	0.025	0.003	383	1509	69	.750	.94	.63	.23	.85	.07	3.47	.01315
2	2	10	1900	100	6.95	30R0	0.050	0.003	316	1550 ⁽³⁾	110	.868	.94	.63	.23	.85	.07	3.59	.0129
2	2	10	1900	100	6.95	30R0	0.075	0.003	305	1580 ⁽³⁾	140	.987	.94	.63	.23	.85	.07	3.71	.01275
2	2	10	1400	250	6.95	20R0	0.025	0.003	620	1080	140	0.717	0.93	0.38	0.11	0.74	0.06	2.94	0.0479
2	2	10	1400	250	6.95	20R0	0.050	0.003	370	1160	220	.782	.93	.38	.11	.74	.06	3.01	.04675
2	2	10	1400	250	6.95	20R0	0.075	0.003	320	1230	290	.847	.93	.38	.11	.74	.06	3.08	.04515
2	2	10	1600	250	6.95	20R0	0.025	0.003	590	1280	140	.717	.93	.39	.12	.75	.06	2.97	.04025
2	2	10	1600	250	6.95	20R0	0.050	0.003	360	1360	220	.782	.93	.39	.12	.75	.06	3.04	.03905
2	2	10	1600	250	6.95	20R0	0.075	0.003	620	1400	260	.847	.93	.39	.12	.75	.06	3.11	.038
2	2	10	1760	250	6.95	30R0	0.025	0.003	620	1325	125	.750	.91	.49	.15	.78	.07	3.15	.03605
2	2	10	1760	250	6.95	30R0	0.050	0.003	370	1490	190	.868	.91	.49	.15	.78	.07	3.27	.0354
2	2	10	1760	250	6.95	30R0	0.075	0.003	325	1535	235	.987	.91	.49	.15	.78	.07	3.39	.0345
2	2	10	1900	250	6.95	40R0	0.029	0.003	580	1555 ⁽³⁾	115	.782	.94	.63	.23	.90	.07	3.55	.0329
2	2	10	1900	250	6.95	40R0	0.050	0.003	380	1595 ⁽³⁾	155	.912	.94	.63	.23	.90	.07	3.68	.0322
2	2	10	1900	250	6.95	40R0	0.075	0.003	360	1660 ⁽³⁾	220	1.042	.94	.63	.23	.90	.07	3.81	.0315
2	2	10	1400		50							0.95	1.94	0.34		0.16			
2	2	10	1600		50							.95	2.07	.37		.16			
2	2	10	1760		50							1.00	2.26	.41		.17			
2	2	10	1900		50							1.17	2.59	.48		.19			
2	2	10	1400		100							1.08	3.10	.37		.23			
2	2	10	1600		100							1.11	3.19	.37		.23			
2	2	10	1760		100							1.18	3.51	.41		.24			
2	2	10	1900		100							1.55	4.06	.48		.26			

NOTES: (3) Maximum surface temperature exceeds stated 2000°R maximum allowable.

(4) 5000°R recovery temperature cases with varying fin height have not been repeated for 50 and 100 psi, because the heat exchanger and manifold designs and the coolant rate are not affected by external pressure. The associated panel, beam, clip and seal weights for 50 and 100 psi are listed at the bottom of the table.

TABLE 15

LIST OF VARIABLES

a. INPUT

A	~ Beam span, a
P	~ Uniform normal pressure, p
BK1	~ Facesheet buckling coefficient, K_1
BK2	~ Web bending buckling coefficient, K_2
BK3	~ Web shear buckling coefficient, K_3
BK4	~ Flange buckling coefficient, K_4
SAFACT	~ Safety factor on load
TCMIN	~ Minimum panel fin thickness, t_{cmin}
TFMIN	~ Minimum panel facesheet thickness, t_{fmin}
HMIN	~ Minimum panel height, h_{min}
STRPL	~ Panel allowable stress, σ_{pl}
EMØDPL	~ Panel elastic modulus, E_{pl}
DENSPL	~ Panel material density, γ_{pl}
STRBM	~ Beam allowable stress, σ_{bm}
EMØDBM	~ Beam elastic modulus, E_{bm}
DENSBM	~ Beam material density, γ_{bm}

b. OUTPUT

HPL	~ Panel height, h
BFPL	~ Panel fin spacing, b_f
TCPL	~ Panel fin thickness, t_c
TFPL	~ Panel facesheet thickness, t_f
HBM	~ Beam height, h
BFBM	~ Beam flange total width, b_F
TWBM	~ Beam web thickness, t_w
TFBM	~ Beam flange thickness, t_F
WTPL	~ Panel weight
WTBM	~ Beam weight
C	~ Optimum beam spacing
CAL	~ Adjusted beam spacing

TABLE 16

PANEL AND I-BEAM WEIGHT CALCULATION, SOURCE-DECK LISTING

```

*      JOB      X0660      C. RICHARD

*F      COMP
C      INPUT
      DIMENSION TITLF1(15),TITLF2(15)
1001  FORMAT(11,15A5)
1002  FORMAT(15A5)
1003  FORMAT(3F10.5)
1004  FORMAT(6F10.5)
1005  FORMAT(7F10.5)
107  READ INPUT TAPE 41,1001,IJ,TITLF1
      IT(IJ-1)100,101,100
101  READ INPUT TAPE 41,1002,TITLF2
      READ INPUT TAPE 41,1003,P,SAFACT,A
      READ INPUT TAPE 41,1004,STRPL,EMODPL,DFNSPL,STRBM,FMODBM,DENSBM
      READ INPUT TAPE 41,1005,TCMIN,TFMIN,HMIN,BK1,BK2,BK3,BK4
      CAL=0.
1  CBM=.242/(((BK2*FMODBM)**.16667)*(STRBM**.5))
2  CPL=.28005/(((BK1*BK2)**.125)*((100.*STRPL*EMODPL)**.25))
      PMOD=SAFACT*P
3  C=.338*((DENSBM*CBM)/(DFNSPL*CPL)**.75)*A*(PMOD**.125)
4  PLMOM=.125*PMOD*C*C
5  AFP1=((BK1*EMODPL)/STRPL)**.5*1000.*TFMIN
6  TPL=TFMIN/(.9799*((BK2/BK1)**.25))
7  HPL=1000.*TCPL*((BK2*EMODPL)/STRPL)**.5)
8  PLMOM1=STRPL*((TFMIN*HPL)+((TCPL*HPL*HPL)/(6.*AFP1)))
9  HPL=1000.*TCMIN*((BK2*EMODPL)/STRPL)**.5)
10  PLMOM2=STRPL*((TFMIN*HPL)+((TCMIN*HPL*HPL)/(6.*AFP1)))
11  PLMOM3=STRPL*((TFMIN*HMIN)+((TCMIN*HMIN*HMIN)/(6.*AFP1)))
      K=0
      IF(PLMOM - PLMOM1) 40, 12, 12
12  THRTPL=.8799*((BK2/BK1)**.25)
13  SIRTPL=((BK2/BK1)**.5)/THRTPL
14  HPL=((PLMOM*((BK2*FMODPL)**.5))/((STRPL**1.5)*(THRTPL+SIRTPL/6.))
      )**.5)*31.60
15  TCPL=HPL*((STRPL/(BK2*FMODPL)**.5)*.001
16  TFPL=THRTPL*TCPL
      BFPL=HPL/SIRTPL
17  WTPL=144.*DENSPL*(2.*TFPL+(HPL*TCPL)/BFPL)
      GO TO 105
40  IF(PLMOM - PLMOM2) 41, 18, 18
18  TFPL=TFMIN
      A2=(6.*TFMIN*EMODPL*((BK1*BK2)**.5))/(.000001*STRPL)
      B2=A2*TFMIN
      B3=(A2*PLMOM)/STRPL
      HSTART=B2**.5
      DO 300 I = 1,50
      IF(I - 1) 301, 301, 302
302  IF(I - 50) 303, 304, 304
304  K=1
303  HSTART=HPL
3031  ENUM=HSTART**3.+B2*HSTART-B3
      DEN=3.*HSTART*HSTART+B2
      FEN=HSTART-ENUM/FDEN
      DIFX=HPL-HSTART
      IF(DIFX) 306, 306, 307
307  IF(DIFX - .0001) 308, 308, 300
306  IF(DIFX + .0001) 300, 300, 308
308  GO TO 19
300  CONTINUE
19  TCPL=HPL*((STRPL/(BK2*FMODPL)**.5)*.001
20  WTPL=144.*DENSPL*(2.*TFMIN+(HPL*TCPL)/BFPL)
      GO TO 105
41  IF(PLMOM - PLMOM3) 23, 21, 21
21  TFPL=TFMIN
      A3=TCMIN/(6.*AFP1)
      A4=TFMIN
      A5=-PLMOM/STRPL
      HPL=(-A4+((A4*A4-4.*A3*A5)**.5))/(2.*A3)
22  WTPL=144.*DENSPL*((2.*TFMIN)+(HPL*TCMIN)/BFPL)
      TCPL=TCMIN
      GO TO 105
23  WTPL=144.*DENSPL*((2.*TFMIN)+(HMIN*TCMIN)/BFPL)
24  CAL=((8.*STRPL*(TFMIN*HMIN+(TCMIN*HMIN*HMIN)/(6.*AFP1))))/PMOD**.5
      HPL=HMIN
      TFPL=TFMIN
      TCPL=TCMIN
      CI=CAL
      GO TO 25
105  CI=C
25  TCRQPL=(1.34*PMOD*CI*BFPL)/(HPL*STRPL)
      IF(TCRQPL - TCPL) 29, 29, 26
26  TCRQPL=(.893*PMOD*CI*BFPL)/(HPL*STRPL)
27  TAUPL=BK3*EMODPL*(TCRQPL/HPL)*(TCRQPL/HPL)*100000.
      TAUYP1=.577*STRPL
      IF(TAUPL-TAUYP1) 28, 114, 114

```

TABLE 16. Concluded

PANEL AND I-BEAM WEIGHT CALCULATION, SOURCE-DECK LISTING

```

114 TCPL=TCROPL
    IF(TCPL - TCMIN) 28, 28, 115
    GO TO 115
28 TCPL ((.0617*PMOD*C1*BFPL*HPL/FMODPI)**.3333)*.01
    IF(TCPL - TCMIN)116,116,115
116 TCPL TCMIN
115 WTPL=144.*DENSPL*(2.*TFPL+(HPL*TCPL)/BFPL)
29 BMMDM=.175*PMOD*C1*A*A
30 THRTBM=.4996*((BK2/BK4)**.25)
31 G?=.66667
32 HRM=((BMMDM*((BK2*FMODRM)**.5))/(G2*(STRBM**1.5)))**.3333)*10.
33 TWBM HRM*(STRBM/(BK2*FMODRM)**.5)*.001
34 TFBM=TWBM*THRTBM
35 RFBM=2.*TFBM*((BK4*EMODBM)/STRBM)**.5)*1000.
36 WTBM((144.*DENSBM*(2.*TFBM*RFBM+HBM*TWBM))/C1
2001 FORMAT(1H1,26HPANFI AND BEAM CALCULATION/)
2002 FORMAT(15A5)
2003 FORMAT(15A5//)
2004 FORMAT(34H APPLIED NORMAL PRESSURE, PSI = ,F10.2)
2005 FORMAT(34H SAFETY FACTOR ON LOAD = ,F10.2//)
2006 FORMAT(29H BEAM SPAN, IN = ,F10.3)
2007 FORMAT(29H PANEL OPTIMUM SPAN, IN = ,F10.3)
2008 FORMAT(29H PANEL ADJUSTED SPAN, IN = ,F10.3//)
2009 FORMAT(38H FACE SHEET BUCKLING COEFFICIENT = ,F10.2)
2010 FORMAT(38H WEB BENDING BUCKLING COEFFICIENT = ,F10.2)
2011 FORMAT(38H WEB SHEAR BUCKLING COEFFICIENT = ,F10.2)
2012 FORMAT(38H FLANGE BUCKLING COEFFICIENT = ,F10.3//)
2013 FORMAT(44H MINIMUM PANEL FIN THICKNESS, IN = ,F10.5)
2014 FORMAT(44H MINIMUM PANEL FACE SHEET THICKNESS, IN = ,F10.5)
2015 FORMAT(44H MINIMUM PANEL HEIGHT, IN = ,F10.5//)
2016 FORMAT(42X,16HPANEL BEAMS)
2017 FORMAT(39H ALLOWABLE STRESS, PSI = ,F10.2,2X,F10.2)
2018 FORMAT(39H ELASTIC MODULUS, PSI(MILLIONS) = ,F10.2,2X,F10.2)
2019 FORMAT(39H MATERIAL DENSITY, POUNDS/CUBIC IN = ,F10.3,2X,F10.3//)
1////)
2020 FORMAT(37H PANEL WEIGHT, POUNDS/SQUARE FT = ,F10.3)
2021 FORMAT(37H BEAM WEIGHT, POUNDS/SQUARE FT = ,F10.3//)
2022 FORMAT(21H STRUCTURE DIMENSIONS//)
2023 FORMAT(6H PANEL/)
2024 FORMAT(30H HEIGHT, IN = ,F10.5)
2025 FORMAT(30H FIN SPACING, IN = ,F10.5)
2026 FORMAT(30H FACE SHEET THICKNESS, IN = ,F10.5)
2027 FORMAT(30H FIN THICKNESS, IN = ,F10.5//)
2028 FORMAT(6H BEAMS/)
2029 FORMAT(26H HEIGHT, IN = ,F10.5)
2030 FORMAT(26H FLANGE WIDTH, IN = ,F10.5)
2031 FORMAT(26H FLANGE THICKNESS, IN = ,F10.5)
2032 FORMAT(26H WEB THICKNESS, IN = ,F10.5//)
2033 FORMAT(24H SO ITERATIONS COMPLETED)
WRITE OUTPUT TAPE 42,2001
WRITE OUTPUT TAPE 42,2002,TITLE1
WRITE OUTPUT TAPE 42,2003,TITLE2
WRITE OUTPUT TAPE 42,2004,P
WRITE OUTPUT TAPE 42,2005,SAFACT
WRITE OUTPUT TAPE 42,2006,A
WRITE OUTPUT TAPE 42,2007,C
WRITE OUTPUT TAPE 42,2008,CAL
WRITE OUTPUT TAPE 42,2009,BK1
WRITE OUTPUT TAPE 42,2010,BK2
WRITE OUTPUT TAPE 42,2011,BK3
WRITE OUTPUT TAPE 42,2012,BK4
WRITE OUTPUT TAPE 42,2013,TCMIN
WRITE OUTPUT TAPE 42,2014,TFMIN
WRITE OUTPUT TAPE 42,2015,HMIN
WRITE OUTPUT TAPE 42,2016
WRITE OUTPUT TAPE 42,2017,STRPL,STRBM
WRITE OUTPUT TAPE 42,2018,FMODPL,FMODRM
WRITE OUTPUT TAPE 42,2019,DENSPL,DENSBM
WRITE OUTPUT TAPE 42,2020,WTPL
WRITE OUTPUT TAPE 42,2021,WTBM
WRITE OUTPUT TAPE 42,2022
WRITE OUTPUT TAPE 42,2023
WRITE OUTPUT TAPE 42,2024,HPL
WRITE OUTPUT TAPE 42,2025,BFPL
WRITE OUTPUT TAPE 42,2026,TFPL
WRITE OUTPUT TAPE 42,2027,TCPL
WRITE OUTPUT TAPE 42,2028
WRITE OUTPUT TAPE 42,2029,HRM
WRITE OUTPUT TAPE 42,2030,RFBM
WRITE OUTPUT TAPE 42,2031,TFBM
WRITE OUTPUT TAPE 42,2032,TWBM
IF(K - 1) 111, 112, 112
112 WRITE OUTPUT TAPE 42,2033
111 GO TO 102
100 CALL EXIT
END

```

TABLE 17
SAMPLE CALCULATION - PANEL AND I-BEAM WEIGHTS

PANEL AND BEAM CALCULATION			
CONCEPT 3			
INCO BEAMS, PANEL AT 1140F			
APPLIED NORMAL PRESSURE, PSI	=	100.00	
SAFETY FACTOR ON LOAD	=	1.50	
BEAM SPAN, IN	=	24.000	
PANEL OPTIMUM SPAN, IN	=	4.704	
PANEL ADJUSTED SPAN, IN	=	0.000	
FACE SHEET BUCKLING COEFFICIENT	=	3.62	
WEB BENDING BUCKLING COEFFICIENT	=	21.70	
WEB SHEAR BUCKLING COEFFICIENT	=	8.10	
FLANGE BUCKLING COEFFICIENT	=	0.385	
MINIMUM PANEL FIN THICKNESS, IN	=	0.00300	
MINIMUM PANEL FACE SHEET THICKNESS, IN	=	0.01000	
MINIMUM PANEL HEIGHT, IN	=	0.07500	
		PANEL	BEAMS
ALLOWABLE STRESS, PSI	=	130000.00	130000.00
ELASTIC MODULUS, PSI (MILLIONS)	=	24.00	24.00
MATERIAL DENSITY, POUNDS/CUBIC IN	=	0.297	0.297

PANEL WEIGHT, POUNDS/SQUARE FT	=	1.106
BEAM WEIGHT, POUNDS/SQUARE FT	=	3.194

STRUCTURE DIMENSIONS

NOTE:

PANEL		
HEIGHT, IN	=	0.29339
FIN SPACING, IN	=	0.25052
FACE SHEET THICKNESS, IN	=	0.01000
FIN THICKNESS, IN	=	0.00516

1 psi = 6.89 kN/m²
 1 in. = 2.54 cm
 1 lb/in³ = 0.0277 kg/cm³
 1 lb/ft² = 4.88 kg/m²
 1140°F = 889°K

BEAMS

HEIGHT, IN	=	3.33560
FLANGE WIDTH, IN	=	1.21640
FLANGE THICKNESS, IN	=	0.07214
WEB THICKNESS, IN	=	0.05270

TABLE 18

RECTANGULAR-WEB-CORE PANEL OPTIMIZATION SOURCE-DECK LISTING

```

C      WFB CORE SANDWICH PLATE OPTIMIZATION - BEAM THEORY
C      IDEAL ELASTIC-PLASTIC ANALYSIS(ETA=1),K3=8.1
C      ANALYSIS BY W.G.FLIEDER AND C.E.RICHARD
1001  FORMAT(I1,19A4)
1002  FORMAT(6F10.4,I10)
      102  READ(5,1001)IJ
          IF(IJ-1)100,101,100
      101  READ(5,1002)VMDH2,DMDH2,VK2,VK1,E,SIGY,MDH2I
1003  FORMAT(1H1,14X,36HWEB CORE SANDWICH PLATE OPTIMIZATION///)
1004  FORMAT(20H YFLD,STRESS PSI = ,F7.0,8X,8HE,PSI = ,F9.0)
1005  FORMAT(6H K1 = ,F5.2,5X,5HK2 = ,F5.2,5X,6HK3=8.1//)
1006  FORMAT(1X,10HSTRESS,PSI,3X,3HETA,3X,8HM/H2,PSI,3X,5HTF/TC,5X,4HH/B
      1F,2X,14HTB/MR,IN/LB1/2,2X,9HPRESS,PSI/)
1007  FORMAT(2X,F7.0,3X,F6.4,3X,F7.2,3X,F6.4,3X,F6.4,3X,F9.7,6X,F8.2)
      WRITE(6,1003)
      WRITE(6,1004) SIGY,E
      WRITE(6,1005)VK1,VK2
      WRITE(6,1006)
      FTA=1.
      DELTA=SQRT(VK2/VK1)
      TFDTC=SQRT(DELTA*.774292)
      HDBF=DELTA/TFDTC
      F2=TFDTC+HDBF/6.
      DO 50 I=1,MDH2I
      XI=I
      XMDH2=VMDH2+(XI-1.)*DMDH2
      SIGOP=ETA**.1666667*(XMDH2*XMDH2*VK2*E/(F2*F2))**.333333
      IF(SIGOP-SIGY)10,10,30
10     TEM1=2.*TFDTC+HDBF
      TFM2=2.*TFDTC/HDBF+1.
      TBDMR=TEM1/(VK2*VK2*ETA*F2*F2*XMDH2*E*E)**.16666667
      GO TO 70
30     A=XMDH2*SQRT(VK2*E)*ETA**.1666667/SIGY**1.5
      TFDTC=.5*(A+SQRT(A*A-.666667*DELTA))
      HDBF=DELTA/TFDTC
      F2=TFDTC+HDBF/6.
      TEM1=2.*TFDTC+HDBF
      TEM2=2.*TFDTC/HDBF+1.
      SIGOP=SIGY
      TBDMR=TEM1*SQRT(XMDH2)/(F2*SIGOP)
70     IF(SIGOP-.0713*SIGY*VK2)71,71,75
71     TAUSIG=8.1/VK2
72     P=0.5*TAUSIG*TAUSIG*TEM1*TEM1*XMDH2/(F2*F2*TEM2*TFM2)
      GO TO 90
75     TAUSIG=0.577*SIGY/SIGOP
      GO TO 72
90     WRITE(6,1007)SIGOP,ETA,XMDH2,TFDTC,HDBF,TBDMR,P
50     CONTINUE
      GO TO 102
100    STOP
      END

```

TABLE 19

TYPICAL COMPUTER OUTPUT

WEB CORE SANDWICH PLATE OPTIMIZATION

YIELD STRESS, PSI = 130000. E, PSI = 25000000.
 K1 = 3.62 K2 = 21.70 K3=8.1

STRESS, PSI	ETA	M/H2, PSI	TF/TC	H/BF	TB/MR, IN/LB1/2	PRESS, PSI
22964.	1.0000	250.00	1.3769	1.7782	0.0018648	19.67
36453.	1.0000	500.00	1.3769	1.7782	0.0016614	39.34
47767.	1.0000	750.00	1.3769	1.7782	0.0015528	59.01
57866.	1.0000	1000.00	1.3769	1.7782	0.0014801	78.68
67147.	1.0000	1250.00	1.3769	1.7782	0.0014261	98.35
75826.	1.0000	1500.00	1.3769	1.7782	0.0013834	118.02
84033.	1.0000	1750.00	1.3769	1.7782	0.0013483	137.69
91856.	1.0000	2000.00	1.3769	1.7782	0.0013186	157.37
99360.	1.0000	2250.00	1.3769	1.7782	0.0012930	177.04
106590.	1.0000	2500.00	1.3769	1.7782	0.0012705	196.71
113583.	1.0000	2750.00	1.3769	1.7782	0.0012505	216.38
120366.	1.0000	3000.00	1.3769	1.7782	0.0012325	236.05
126963.	1.0000	3250.00	1.3769	1.7782	0.0012161	255.72
130000.	1.0000	3500.00	1.4597	1.6774	0.0012028	226.79
130000.	1.0000	3750.00	1.6100	1.5207	0.0011984	173.99
130000.	1.0000	4000.00	1.7552	1.3949	0.0012006	137.24
130000.	1.0000	4250.00	1.8968	1.2908	0.0012073	110.61
130000.	1.0000	4500.00	2.0357	1.2027	0.0012171	90.69
130000.	1.0000	4750.00	2.1725	1.1270	0.0012291	75.44
130000.	1.0000	5000.00	2.3078	1.0609	0.0012427	63.51
130000.	1.0000	5250.00	2.4417	1.0027	0.0012575	54.03
130000.	1.0000	5500.00	2.5746	0.9510	0.0012733	46.39
130000.	1.0000	5750.00	2.7065	0.9046	0.0012897	40.15
130000.	1.0000	6000.00	2.8377	0.8628	0.0013066	35.00

Notes (1) 1 psi = 6.89 kN/m²

(2) 1 in./lb^{1/2} = 0.0012 m/N^{1/2}

TABLE 20

TRIANGULAR-WEB-CORE PANEL OPTIMIZATION SOURCE-DECK LISTING

```

C   TRIANGULAR CORE SANDWICH PLATE OPTIMIZATION - BEAM THEORY
C   IDEAL ELASTIC-PLASTIC ANALYSIS(ETA=1),K3=8.1
C   ANALYSIS BY W.G.FLIEDER
1001 FORMAT(11,19A4)
1002 FORMAT(6F10.4,110)
102  READ(5,1001)IJ
     IF(IJ-1)100,101,100
101  READ(5,1002)VMDH2,DMDH2,VK2,VK1,E,SIGY,MDH2I
1003 FORMAT(11H1,10X,43HTRIANGULAR CORE SANDWICH PLATE OPTIMIZATION///)
1004 FOKMAT(20H YIELD STRESS,PSI = ,F7.0,8X,8HE,PSI = ,F9.0)
1005 FORMAT(6H K1 = ,F5.2,5X,5HK2 = ,F5.2,5X,6HK3=8.1//)
1006 FORMAT(11H STRESS,PSI,3X,3HETA,3X,8HM/H2,PSI,3X,5HTF/TC,5X,4HH/BF,
12X,14HTB/MR,IN/LBL/2,2X,9HPRESS,PSI,3X,9HTHETA,DEG/)
1007 FORMAT(F9.0,3X,F6.4,3X,F7.2,3X,F6.4,3X,F6.4,3X,F9.7,6X,F8.2,4X,F5.
11)
     WRITE(6,1003)
     WRITE(6,1004)SIGY,E
     WRITE(6,1005)VK1,VK2
     WRITE(6,1006)
     ETA=1.
     DELTA=SQRT(VK2/VK1)
     TM1=32.*DELTA+48.*DELTA*DELTA
     TM2=2.-16.*DELTA
     COSTH=SQRT((-TM2+SQRT(TM2*TM2+4.*TM1))/(2.*TM1))
     SINTH=SQRT(1.-COSTH*CCOSTH)
     THETA=ARSIN(SINTH)*180./3.1415926
     TFUTC=2.*DELTA*COSTH
     HDBF=SINTH*DELTA/TFUTC
     F2=2.*DELTA*COSTH+1./(6.*COSTH)
     UD 50 I=1,MDH2I
     XI=1
     XMDH2=VMDH2+(XI-1.)*DMDH2
     SIGOP=ETA**.16666667*(XMDH2*SINTH/F2)**.6666667*(VK2*E)**.3333333
     IF(SIGOP-SIGY)10,10,30
10  TEM1=4.*DELTA*COSTH+1./COSTH
     TBDMR=TEM1/((ETA*XMDH2)**.16667*(VK2*E*F2)**.33333*SINTH**.66666)
     GO TO 70
30  SIGOP=SIGY
     A=ETA**.3333333*XMDH2*(VK2*E/(SIGY*SIGY*SIGY))**.5
     A1=144.*DELTA*DELTA+36.*A*A
     A2=24.*DELTA-36.*A*A
     IF(A2)31,35,35
35  WRITE(6,32)
32  FORMAT(2CX,29HQUADRATIC ROOTS ARE IMAGINARY)
     GO TO 102
31  IF(A2*A2-4.*A1)35,33,33
33  COSTH=SQRT((-A2+SQRT(A2*A2-4.*A1))/(2.*A1))
     F2=2.*DELTA*COSTH+1./(6.*COSTH)
     TEM1=4.*DELTA*COSTH+1./COSTH
     TBDMR=SQRT(XMDH2)*TEM1/(F2*SIGY)
     TFUTC=2.*DELTA*COSTH
     HDBF=SQRT(1.-COSTH*COSTH)*DELTA/TFUTC
     THETA=ARCOS(COSTH)*180./3.1415926
70  IF(SIGOP-.0713*SIGY*VK2)71,71,75
71  TAUSIG=8.1/VK2
72  P=.5*TAUSIG*TAUSIG*TEM1*TEM1*XMDH2/(F2*F2*(2.*TFUTC*COSTH+1.))**.2.)
     GO TO 90
75  TAUSIG=.577*SIGY/SIGOP
     GO TO 72
90  WRITE(6,1007) SIGOP,ETA,XMDH2,TFUTC,HDBF,TBDMR,P,THETA
50  CONTINUE
     GO TO 102
100  STOP
     END

```

TABLE 21

- a. BEAM AND PANEL WEIGHTS VERSUS FIN CONFIGURATION, U. S. UNITS
 (Heat flux = 10 Btu/sec-ft²; pressure loading = 7 psi;
 combined weight given in lb/ft²)

Fin height, in.	0.003 in. fin thickness				0.004 in. fin thickness			
	15 fins/in.		20 fins/in.		15 fins/in.		20 fins/in.	
	Plain fin	Offset fin	Plain fin	Offset fin	Plain fin	Offset fin	Plain fin	Offset fin
0.050	1.62	1.62	1.64	1.64	1.67	1.68	1.73	1.74
.075	1.64	1.64	1.67	1.67	1.71	1.72	1.78	1.79
.100	1.67	1.67	1.71	1.71	1.75	1.76	1.85	1.86
.125	1.70	1.70	1.76	1.76	1.80	1.81	1.91	1.92
.150	1.74	1.74	1.81	1.81	1.85	1.86	1.98	1.99

- b. BEAM AND PANEL WEIGHTS VERSUS FIN CONFIGURATION, SI UNITS
 (Heat flux = 114 kW/m²; pressure loading = 48 kN/m²;
 combined weight given in kg/m²)

Fin height, in.	0.0076 cm fin thickness				0.0102 cm fin thickness			
	5.91 fins/cm		7.88 fins/cm		5.91 fins/cm		7.88 fins/cm	
	Plain fin	Offset fin	Plain fin	Offset fin	Plain fin	Offset fin	Plain fin	Offset fin
0.127cm	7.81	7.81	8.02	8.02	8.16	8.20	8.45	8.50
.191cm	8.02	8.02	8.16	8.16	8.35	8.40	8.69	8.74
.254cm	8.16	8.16	8.35	8.35	8.55	8.59	9.04	9.08
.318cm	8.30	8.30	8.59	8.59	8.79	8.84	9.33	9.38
.381cm	8.50	8.50	8.84	8.84	9.04	9.08	9.67	9.72

TABLE 22

GEOMETRIC PROPORTIONS AND MATERIALS OF
STRUCTURAL ELEMENTS AND WEIGHT SUMMARY FOR
CONCEPT I FOR THE FOLLOWING CONDITIONS

$l = 2 \text{ ft (0.61 m)}$

$w = 2 \text{ ft (0.61 m)}$

Coolant = hydrogen

Coolant inlet pressure = 300 psi (2070 kN/m²)

Coolant outlet temperature = 1600°R (889°K)

Normal pressure = 6.95 psi (48 kN/m²)

Uniform heat flux = 10 Btu/sec-ft² (114 kW/m²)

Fin conductivity = 10 Btu/ft-hr-°R (17.3 W/m-°K)

Waspaloy panel	Inconel 718 beams		Inconel 718 attachment clips
$h_{fin} = 0.075 \text{ in. (0.191 cm)}$	$h = 1.46 \text{ in. (3.70 cm)}$		Developed length = 2.605 in. (6.61 cm)
$b_{fin} = 0.050 \text{ in. (0.127 cm)}$	$b_F = 0.605 \text{ in. (1.54 cm)}$		$t = 0.010 \text{ in. (0.0254 cm)}$
$t_F = 0.010 \text{ in. (0.0254 cm)}$	$t_F = 0.035 \text{ in. (0.0879 cm)}$		Beam spacing = 7.77 in. (0.198 m)
$t_{fin} = 0.003 \text{ in. (0.0076 cm)}$	$t_w = 0.027 \text{ in. (0.0675 cm)}$		
$Wt = 1.27 \text{ lb/ft}^2 \text{ (6.20 kg/m}^2\text{)}$	$Wt = 0.46 \text{ lb/ft}^2 \text{ (2.24 kg/m}^2\text{)}$		$Wt = 0.18 \text{ lb/ft}^2 \text{ (0.88 kg/m}^2\text{)}$
Manifolding			Hastelloy X seal
Hastelloy X inlet	Hastelloy X outlet	Inconel 718 piping	Average thickness = 0.0130 in. (0.033 cm) Width = 1.30 in. (3.3 cm)
$l = 3.25 \text{ in. (8.15 cm)}$	$l = 3.25 \text{ in. (8.15 cm)}$	$t = 0.030 \text{ in. (0.076 cm)}$	
$h_{fin} = 0.025 \text{ in. (0.063 cm)}$	$h_{fin} = 0.025 \text{ in. (0.063 cm)}$	Diam = 1.75 in. (4.44 cm)	
$b_{fin} = 0.100 \text{ in. (0.0076 cm)}$	$b_{fin} = 0.100 \text{ in. (0.0254 cm)}$		
$t_{fin} = 0.003 \text{ in. (0.0076 cm)}$	$t_{fin} = 0.003 \text{ in. (0.0076 cm)}$		
$t_F = 0.010 \text{ in. (0.0254 cm)}$	$t_F = 0.010 \text{ in. (0.0254 cm)}$		
$Wt = 0.14 \text{ lb/ft}^2 \text{ (0.68 kg/m}^2\text{)}$	$Wt = 0.14 \text{ lb/ft}^2 \text{ (0.60 kg/m}^2\text{)}$	$Wt = 0.30 \text{ lb/ft}^2 \text{ (1.45 kg/m}^2\text{)}$	
Total manifold wt = 0.58 lb/ft ² (2.83 kg/m ²)			$Wt = 0.06 \text{ lb/ft}^2 \text{ (0.29 kg/m}^2\text{)}$

Total weight = 2.55 lb/ft² (12.45 kg/m²)

Coolant flow rate = 0.00187 lb/sec-ft² (0.00915 kg/s-m²)

TABLE 23
CONCEPT I DETAILED WEIGHT SUMMARY

a. Fin geometry; 20 fins/in (7.88 fins/cm) and 0.003 in. (0.0076 cm) thickness

h_{fin}		ΔT		$T_{maximum}$		$E\alpha\Delta T/2$		σ_y		$\sigma_{100\text{ hr}}$		σ_{all}		c_{all}		Beam weight		Clip weight		Panel weight		Total weight	
in.	cm	$^{\circ}F$	$^{\circ}K$	$^{\circ}F$	$^{\circ}K$	ksi	kN/m ²	ksi	kN/m ²	ksi	kN/m ²	ksi	kN/m ²	in.	m	lb/ft ²	kg/m ²	lb/ft ²	kg/m ²	lb/ft ²	kg/m ²	lb/ft ²	kg/m ²
0.025	0.064	70	39	1210	928	6.5	45 x 10 ³	100	689 x 10 ³	> σ_y	> σ_y	93.5	644 x 10 ³	4.60	0.117	0.553	2.70	0.294	1.44	1.048	5.12	1.895	9.26
.050	.127	96	53	1236	942	9.5	65	100	689	> σ_y	> σ_y	90.5	624	6.40	.163	.496	2.42	.216	1.05	1.112	5.43	1.824	8.90
.075	.191	110	61	1250	950	11.0	76	100	689	98.0	675 x 10 ³	89.0	613	7.77	.197	.464	2.27	.180	.88	1.176	5.74	1.820	8.89
.100	.254	119	66	1259	955	12.0	83	100	689	94.0	647	88.0	606	9.01	.229	.442	2.16	.157	.77	1.240	6.05	1.839	8.98
.125	.318	126	70	1266	959	12.3	85	100	689	93.0	641	87.7	604	10.19	.259	.424	2.07	.141	.69	1.304	6.37	1.869	9.13
.150	.381	132	73	1272	962	12.5	86	100	689	92.0	634	87.5	603	11.18	.284	.410	2.00	.129	.63	1.369	6.68	1.908	9.31

b. Fin geometry; 30 fins/in. (11.81 fins/cm) and 0.003 in. (0.0076 cm) thickness

h_{fin}		ΔT		$T_{maximum}$		$E\alpha\Delta T/2$		σ_y		$\sigma_{100\text{ hr}}$		σ_{all}		c_{all}		Beam weight		Clip weight		Panel weight		Total weight	
in.	cm	$^{\circ}F$	$^{\circ}K$	$^{\circ}F$	$^{\circ}K$	ksi	kN/m ²	ksi	kN/m ²	ksi	kN/m ²	ksi	kN/m ²	in.	m	lb/ft ²	kg/m ²	lb/ft ²	kg/m ²	lb/ft ²	kg/m ²	lb/ft ²	kg/m ²
0.025	0.064	56	31	1196	920	5.2	36 x 10 ³	100	689 x 10 ³	> σ_y	> σ_y	94.8	653 x 10 ³	4.65	0.118	0.550	2.69	0.290	1.42	1.080	5.27	1.920	9.38
.050	.127	66	37	1206	926	6.1	42	100	689	93.9	647	93.9	647	6.51	.165	.493	2.41	.207	1.01	1.176	5.74	1.876	9.16
.075	.191	73	40	1213	929	6.8	47	100	689	93.2	642	93.2	642	8.04	.204	.460	2.25	.168	.82	1.272	6.21	1.900	9.28
.100	.254	76	42	1216	931	7.0	48	100	689	93.0	641	93.0	641	9.42	.239	.435	2.12	.152	.74	1.369	6.68	1.956	9.54
.125	.318	79	44	1219	933	7.3	50	100	689	92.7	639	92.7	639	10.68	.271	.417	2.04	.134	.65	1.465	7.15	2.016	9.84
.150	.381	81	45	1221	934	7.5	52	100	689	92.5	637	92.5	637	11.84	.301	.403	1.97	.121	.59	1.561	7.62	2.085	10.18

Note:

- $T_{maximum} = \Delta T + T_{HO}$
- $c_{all} = (8Z_p \sigma_{all}/p)^{1/2}$
- $Z_p =$ Panel section modulus
- $\sigma_{all} = \left[\frac{\sigma_{100\text{ hr}}/1.5}{[\sigma_y - E\alpha\Delta T/2(1-u)]/1.5} \right]_{min}$
- Beam weight = $0.46 (8/c_{all})^{1/3}$, lb/ft²
= $2.25 (0.203/c_{all})^{1/3}$, kg/m²
- Material data from Figure E-2

TABLE 24

GEOMETRIC PROPORTIONS AND MATERIALS OF
STRUCTURAL ELEMENTS AND WEIGHT SUMMARY FOR
CONCEPT 2 FOR THE FOLLOWING CONDITIONS

$l = 2 \text{ ft (0.61 m)}$

$w = 2 \text{ ft (0.61 m)}$

Coolant = hydrogen

Coolant inlet pressure = 630 psi (4340 kN/m²)

Coolant outlet temperature = 1600°R (889°K)

Normal pressure = 100 psi (689 kN/m²)

Uniform heat flux = 250 Btu/sec-ft² (2840 kW/m²)

Fin conductivity = 10 Btu/ft-hr-°R (17.3 W/m-°K)

Hastelloy X heat exchanger	Inconel 718 prime panel	Inconel 718 beams		
$h_{fin} = 0.027 \text{ in. (0.0687 cm)}$	$h = 0.293 \text{ in. (0.745 cm)}$	$h = 3.335 \text{ in. (8.48 cm)}$		
$b_{fin} = 0.050 \text{ in. (0.127 cm)}$	$b_f = 0.258 \text{ in. (0.656 cm)}$	$b_f = 1.216 \text{ in. (3.09 cm)}$		
$t_f = 0.010 \text{ in. (0.0254 cm)}$	$t_f = 0.010 \text{ in. (0.0254 cm)}$	$t_f = 0.072 \text{ in. (0.0183 cm)}$		
$t_{fin} = 0.003 \text{ in. (0.0076 cm)}$	$t_c = 0.0052 \text{ in. (0.0132 cm)}$	$t_w = 0.053 \text{ in. (0.0135 cm)}$		
$Wt = 0.72 \text{ lb/ft}^2 (3.51 \text{ kg/m}^2)$	$Wt = 1.11 \text{ lb/ft}^2 (5.42 \text{ kg/m}^2)$	$Wt = 3.19 \text{ lb/ft}^2 (15.6 \text{ kg/m}^2)$		
Manifolding			Seals	Attachment clips
Hastelloy X inlet	Hastelloy X outlet	Inconel 718 piping		
$h_{fin} = 0.050 \text{ in. (0.127 cm)}$	$h_{fin} = 0.142 \text{ in. (0.361 cm)}$	Diameter = 1.75 in. (4.4 cm)	Width = 1.30 in. (3.3 cm)	Developed width = 3.26 in. (8.18 cm)
$b_{fin} = 0.100 \text{ in. (0.254 cm)}$	$b_{fin} = 0.100 \text{ in. (0.254 cm)}$	Thickness = 0.030 in. (0.076 cm)	Average thickness = 0.049 in. (0.124 cm)	Thickness = 0.010 in. (0.0254 cm)
$t_f = 0.012 \text{ in. (0.0305 cm)}$	$t_f = 0.0135 \text{ in. (0.0343 cm)}$			Beam spacing = 4.704 in. (0.120 m)
$l = 3.25 \text{ in. (8.25 cm)}$	$l = 3.25 \text{ in. (8.25 cm)}$			
$Wt = 0.19 \text{ lb/ft}^2 (0.93 \text{ kg/m}^2)$	$Wt = 0.26 \text{ lb/ft}^2 (1.27 \text{ kg/m}^2)$	$Wt = 0.30 \text{ lb/ft}^2 (1.46 \text{ kg/m}^2)$		
Total manifolding wt = 0.75 lb/ft ² (3.66 kg/m ²)			$Wt = 0.23 \text{ lb/ft}^2 (1.12 \text{ kg/m}^2)$	$Wt = 0.37 \text{ lb/ft}^2 (1.80 \text{ kg/m}^2)$

Total weight = 6.37 lb/ft² (31.1 kg/m²)

Coolant flow rate = 0.0468 lb/ft²-sec (0.228 kg/s-m²)

TABLE 25
GEOMETRIC PROPORTIONS AND MATERIALS OF
STRUCTURAL ELEMENTS AND WEIGHT SUMMARY FOR
CONCEPT 3 FOR THE FOLLOWING CONDITIONS

ℓ = 2 ft (0.61 m)
w = 2 ft (0.61 m)
Coolant = hydrogen
Coolant inlet pressure = 1000 psi (6890 kN/m²)

Coolant outlet temperature = 1600°R (889°K)
Normal pressure = 250 psi (1720 kN/m²)
Uniform heat flux = 500 Btu/sec-ft² (5680 kW/m²)
Fin conductivity = 10 Btu/ft-hr-°R (17.3 W/m-°K)

Hastelloy X heat exchanger		Inconel 718 support panel		Inconel 718 beams					
h_{fin} = 0.037 in. (0.094 cm)		h = 0.085 in. (0.216 cm)		h = 1.00 in. (2.54 cm)					
b_{fin} = 0.025 in. (0.063 cm)		b_f = 0.258 in. (0.66 cm)		b_f = 0.25 in. (0.64 cm)					
t_f = 0.010 in. (0.0254 cm)		t_f = 0.010 in. (0.0254 cm)		t_f = 0.030 in. (0.076 cm)					
t_{fin} = 0.005 in. (0.0076 cm)		t_c = 0.003 in. (0.0076 cm)		t_w = 0.020 in. (0.051 cm)					
Wt = 0.85 lb/ft ² (4.15 kg/m ²)		Wt = 0.91 lb/ft ² (4.44 kg/m ²)		Wt = 0.30 lb/ft ² (1.46 kg/m ²)					
Aluminum 6061-T6 heat exchanger		Aluminum 6061-T6 panel		Titanium 5A1-2.5Sn beams					
h_{fin} = 0.050 in. (0.127 cm)		h = 1.172 in. (3.0 cm)		h = 4.027 in. (10.2 cm)					
b_{fin} = 0.050 in. (0.127 cm)		b_f = 0.659 in. (1.67 cm)		b_f = 1.469 in. (3.72 cm)					
t_f = 0.016 in. (0.0406 cm)		t_f = 0.022 in. (0.056 cm)		t_f = 0.114 in. (0.29 cm)					
t_{fin} = 0.004 in. (0.0102 cm)		t_c = 0.024 in. (0.061 cm)		t_w = 0.084 in. (0.21 cm)					
Wt = 0.37 lb/ft ² (1.80 kg/m ²)		Wt = 1.21 lb/ft ² (5.92 kg/m ²)		Wt = 3.01 lb/ft ² (14.7 kg/m ²)					
Manifolding									
Hastelloy X inlet		Hastelloy X outlet		Inconel 718 piping		Aluminum 6061 inlet and outlet		Aluminum piping	
ℓ = 2.25 in. (5.7 cm)		ℓ = 1.75 in. (4.4 cm)		Diameter = 1.25 in. (3.18 cm)		ℓ = 2.50 in. (6.25 cm)		Diameter = 1.0 in. (2.54 cm)	
h_{fin} = 0.050 in. (0.127 cm)		h_{fin} = 0.193 in. (0.49 cm)		Thickness = 0.030 in. (0.076 cm)		h_{fin} = 0.050 in. (0.127 cm)		Thickness = 0.020 in. (0.076 cm)	
b_{fin} = 0.100 in. (0.254 cm)		b_{fin} = 0.100 in. (0.254 cm)		Number of pipes = 2		b_{fin} = 0.050 in. (0.127 cm)		Number of pipes = 1	
t_f = 0.012 in. (0.0305 cm)		t_f = 0.0135 in. (0.0343 cm)				t_{fin} = 0.004 in. (0.0102 cm)			
t_{fin} = 0.0055 in. (0.014 cm)		t_{fin} = 0.007 in. (0.0178 cm)				t_f = 0.016 in. (0.0406 cm)			
Wt = 0.10 lb/ft ² (0.49 kg/m ²)		Wt = 0.15 lb/ft ² (0.73 kg/m ²)		Wt = 0.43 lb/ft ² (2.10 kg/m ²)		Wt = 0.12 lb/ft ² (0.59 kg/m ²)		Wt = 0.06 lb/ft ² (0.29 kg/m ²)	
Total manifold wt = 0.86 lb/ft ² (4.20 kg/m ²)									
Attachments								Aluminum seals	
Inconel 718		Aluminum		Aluminum					
Beam spacing = 6.0 in. (0.152 cm)		Beam spacing = 6.0 in. (0.152 cm)		Beam spacing = 5.19 in. (0.132 cm)		Average thickness = 0.067 in. (0.17 cm)			
Flange width = 0.25 in. (0.63 cm)		Flange width = 0.25 in. (0.63 cm)		Flange width = 1.47 in. (3.74 cm)		Width = 0.80 in. (2.03 cm)			
Wt = 0.20 lb/ft ² (0.98 kg/m ²)		Wt = 0.07 lb/ft ² (0.33 kg/m ²)		Wt = 0.12 lb/ft ² (0.59 kg/m ²)		Wt = 0.08 lb/ft ² (0.39 kg/m ²)			
Total attachment wt = 0.39 lb/ft ² (1.91 kg/m ²)									

Total weight = 7.98 lb/ft² (39 kg/m²)

Coolant flow rate = 0.0935 lb/sec-ft² (0.456 kg/s-m²)

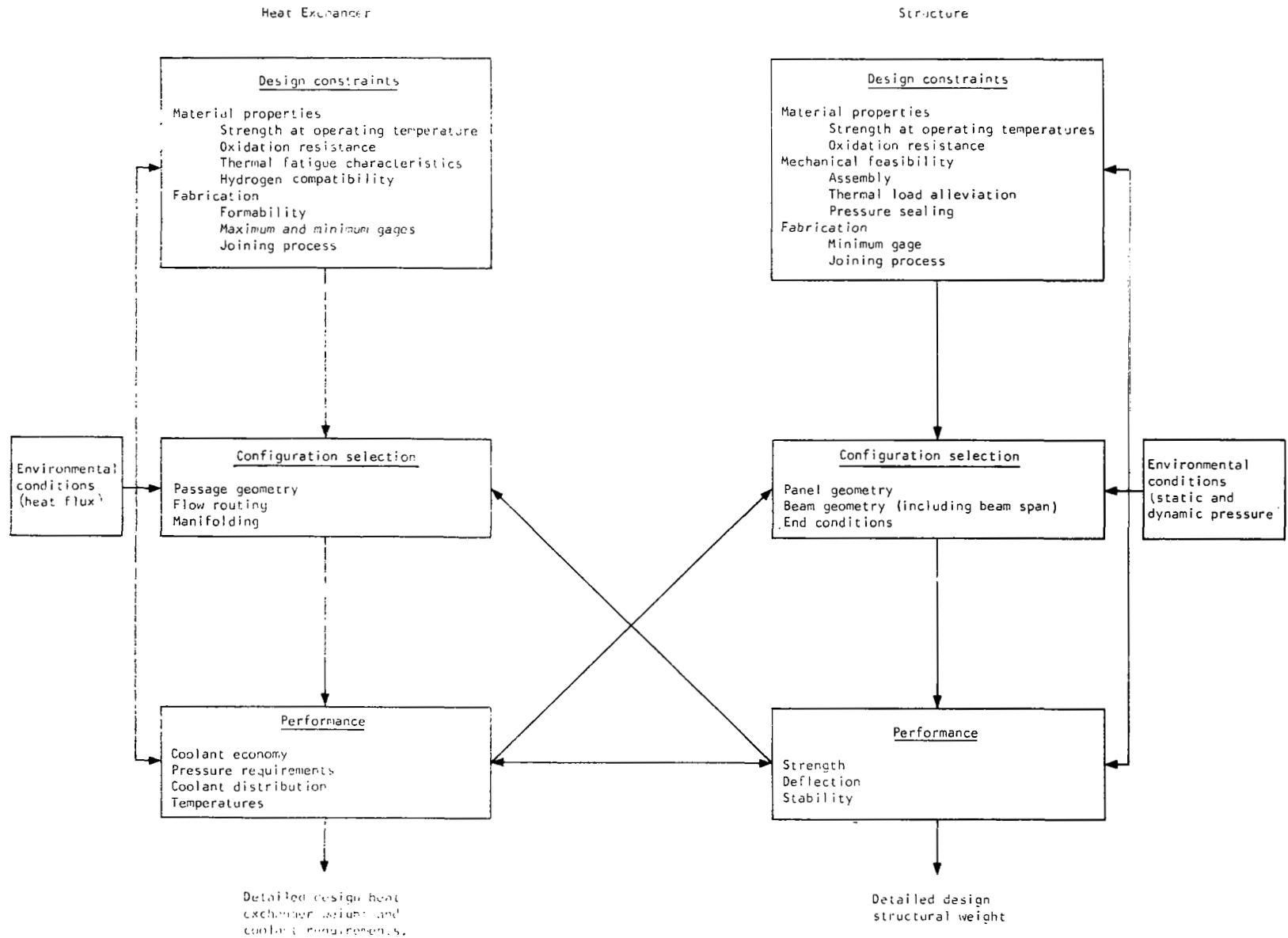


Figure 1. Panel Design Considerations

- ⊕ Baseline design points
- | | | | |
|--|-----------|---|---------------------|
| <div style="border: 1px solid black; width: 20px; height: 10px; background: repeating-linear-gradient(45deg, transparent, transparent 2px, black 2px, black 4px);"></div> | Concept 1 | } | Tradeoff boundaries |
| <div style="border: 1px solid black; width: 20px; height: 10px; background: repeating-linear-gradient(-45deg, transparent, transparent 2px, black 2px, black 4px);"></div> | Concept 2 | | |
| <div style="border: 1px solid black; width: 20px; height: 10px; background: repeating-linear-gradient(45deg, transparent, transparent 2px, black 2px, black 4px);"></div> | Concept 3 | | |

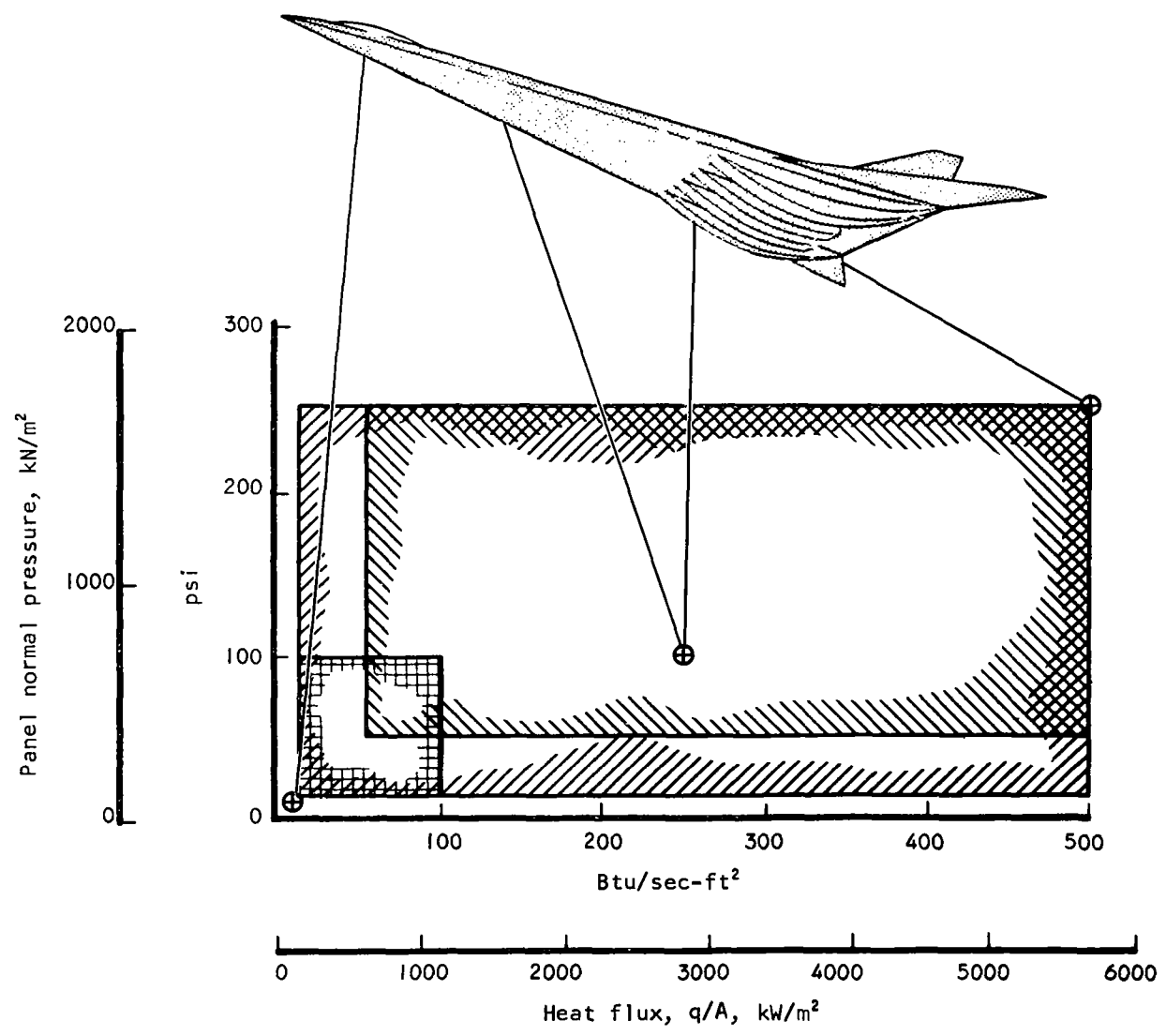
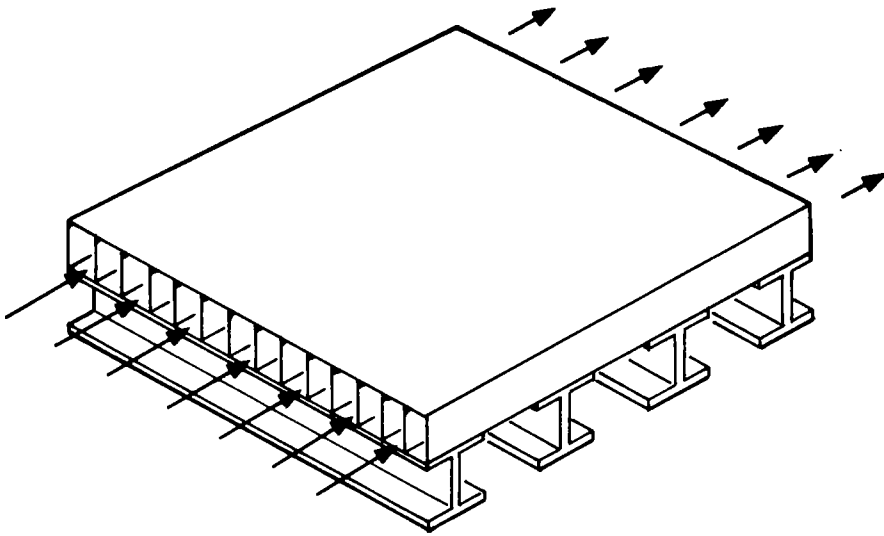
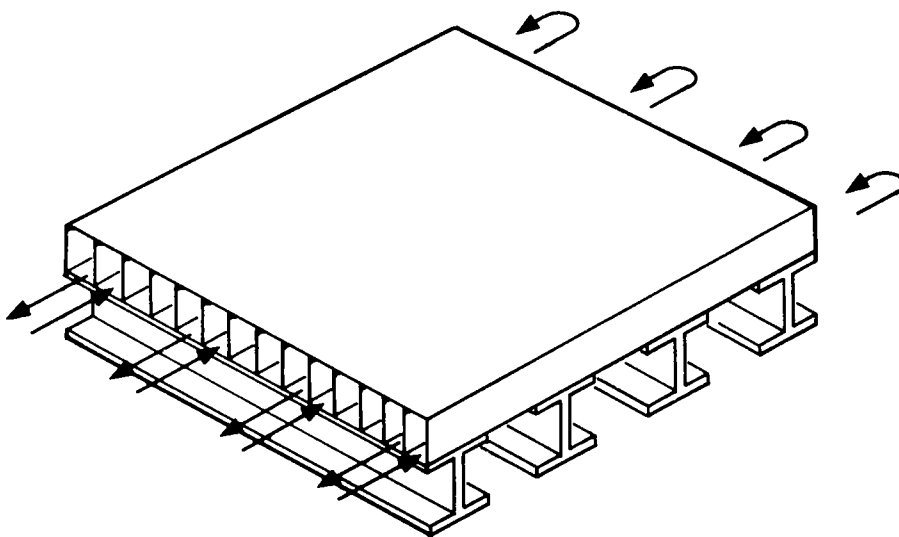


Figure 2. Baseline Design Points and Tradeoff Boundaries for the Regeneratively Cooled Panel Conceptual Design Study

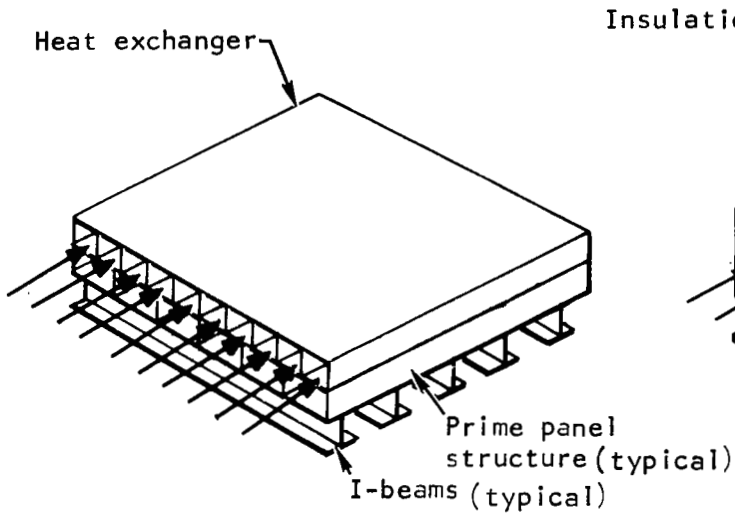


Concept 1.- Rectangular single-pass flow

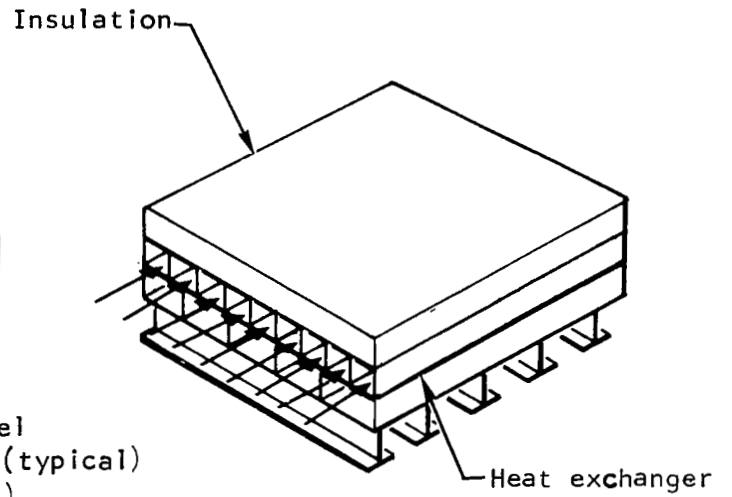


Concept 1a.- Rectangular flow folded-in-width

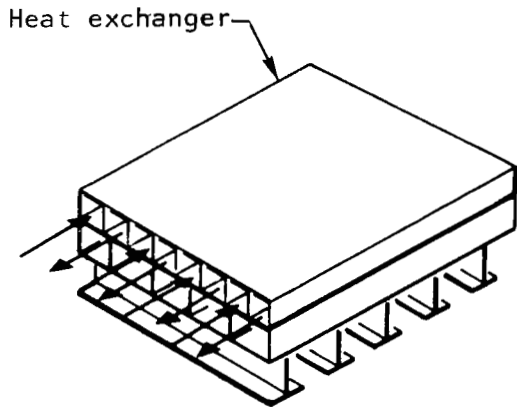
Figure 3. Concept 1. - Integral



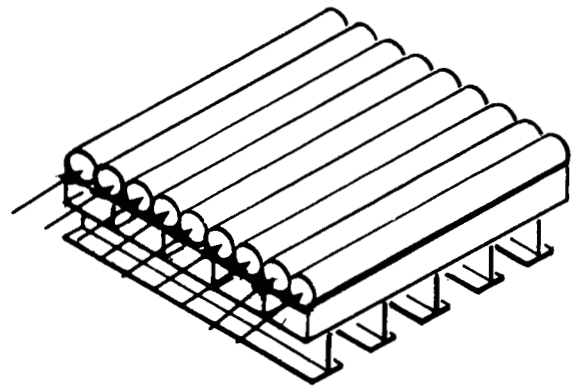
Concept 2. Rectangular single-pass flow



Concept 2b. Rectangular with insulation



Concept 2a. Rectangular folded-in-width



Concept 2c. Tubular single-pass

Figure 4. Concept 2. - Bonded

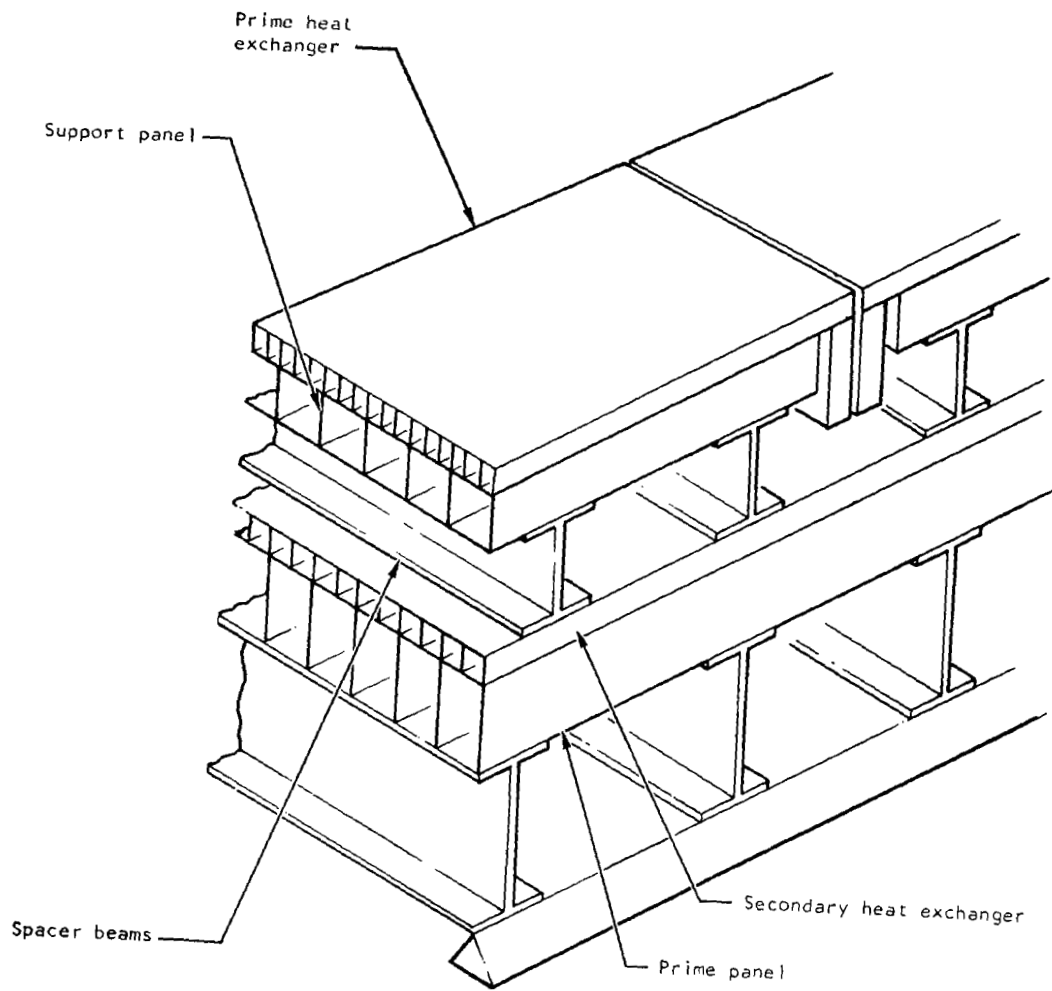


Figure 5. Concept 3.-Nonintegral

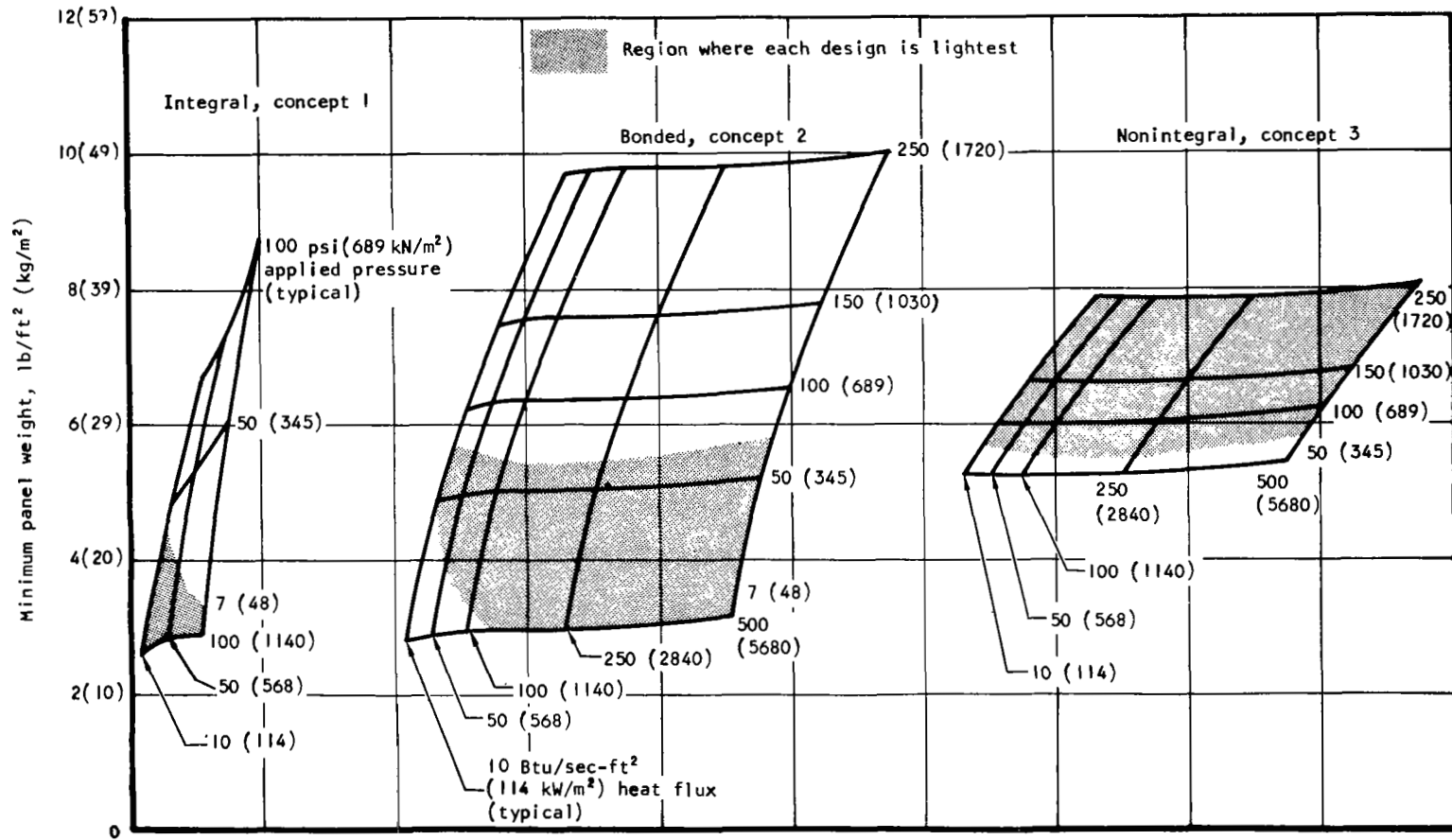


Figure 6. Variation of Minimum Panel Weight with Pressure and Heat Flux for Three Conceptual Designs. Hydrogen Outlet Temperature = 1600°R (889°K); Recovery Temperature = ∞; 2-ft by 2-ft (0.61-m by 0.61-m) Panels

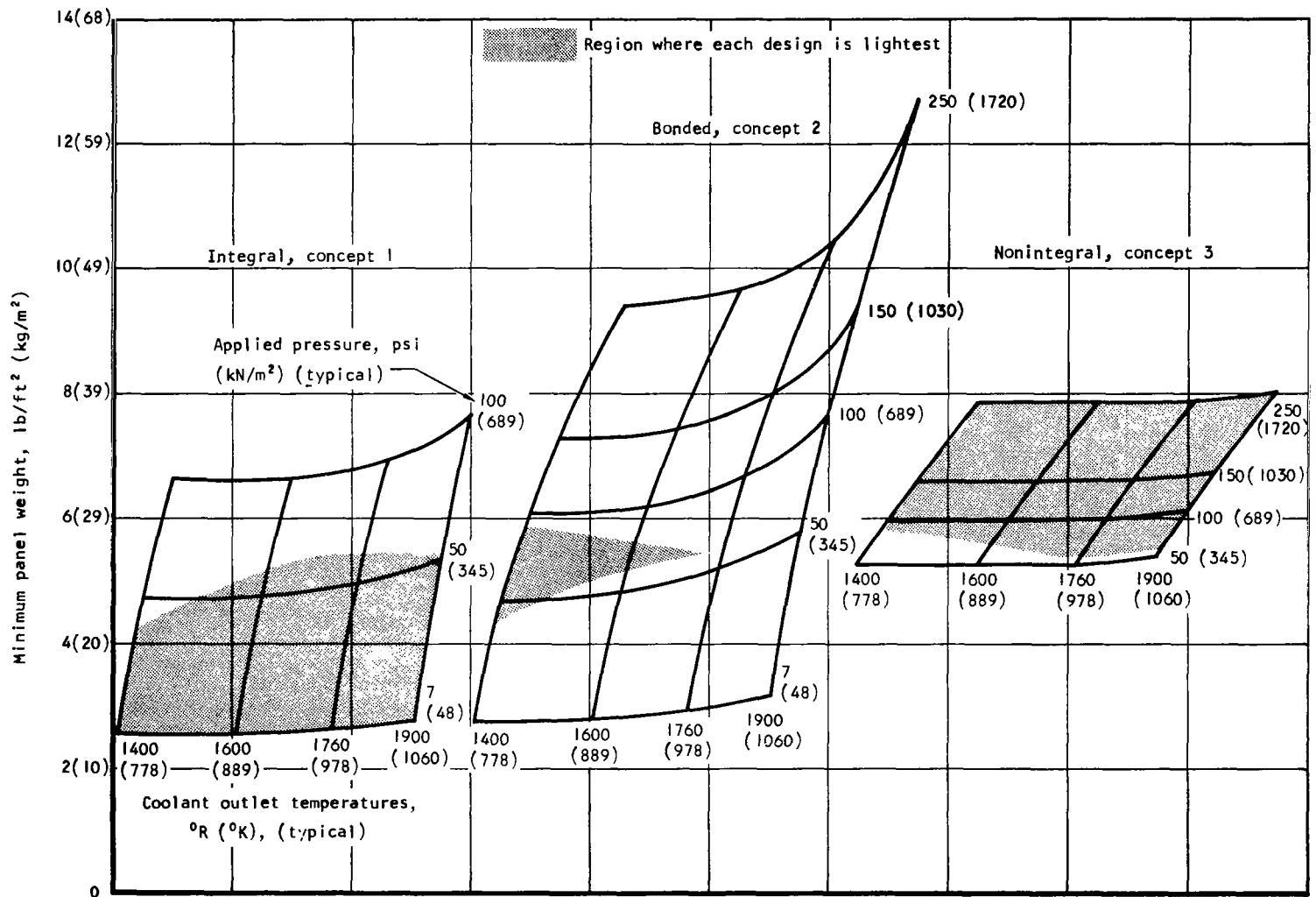


Figure 7. Variation of Minimum Panel Weight with Pressure and Coolant Outlet Temperature for Three Conceptual Designs. Heat Flux = 10 Btu/sec-ft² (114 kW/m²); Recovery Temperature = ∞; 2-ft by 2-ft (0.61-m by 0.61-m) Panels

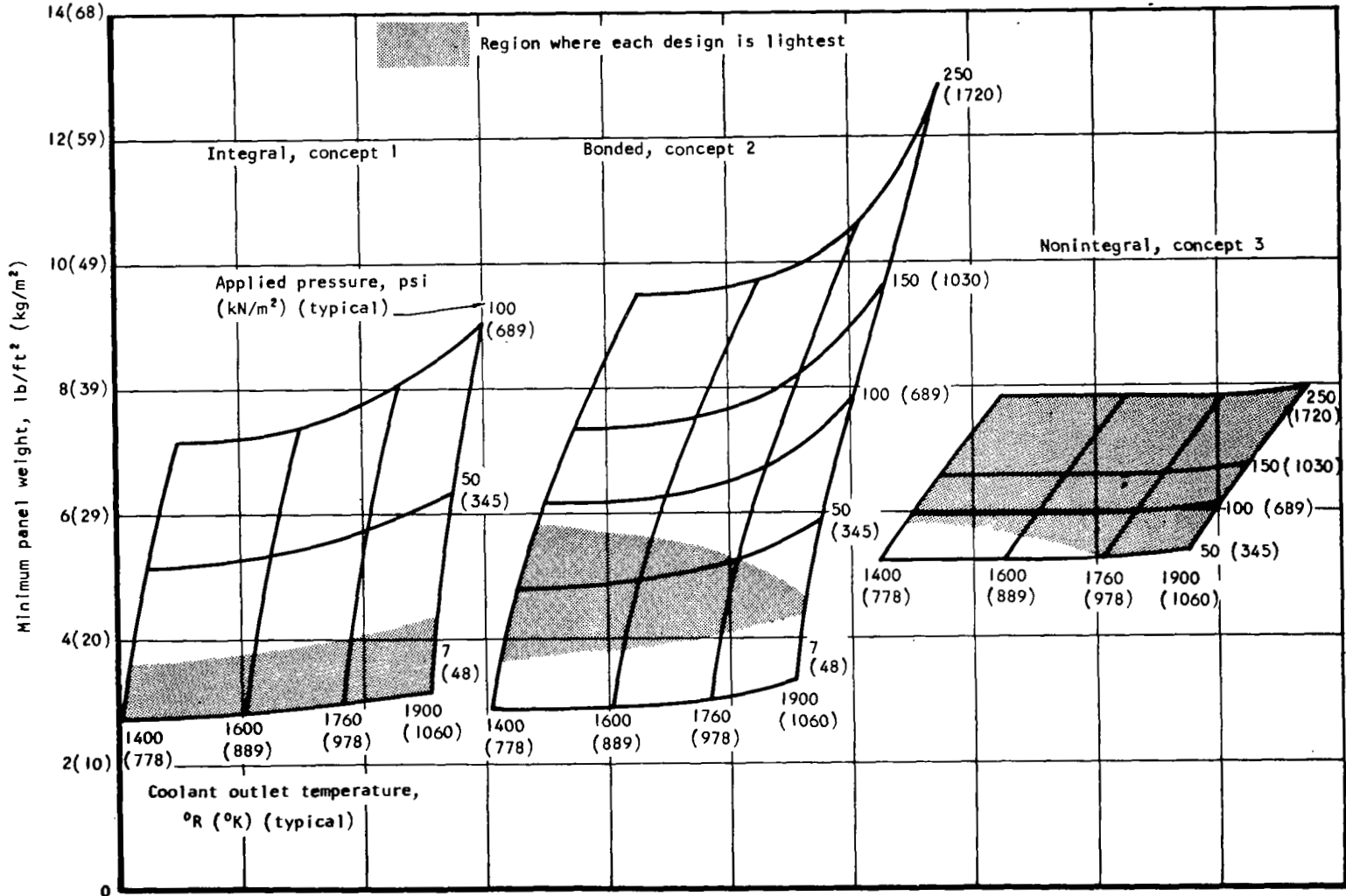


Figure 8. Variation of Minimum Panel Weight with Pressure and Coolant Outlet Temperature for Three Conceptual Designs. Heat Flux = 50 Btu/sec-ft² (568 kW/m²); Recovery Temperature = ∞; 2-ft by 2-ft (0.61-m by 0.61-m) Panels

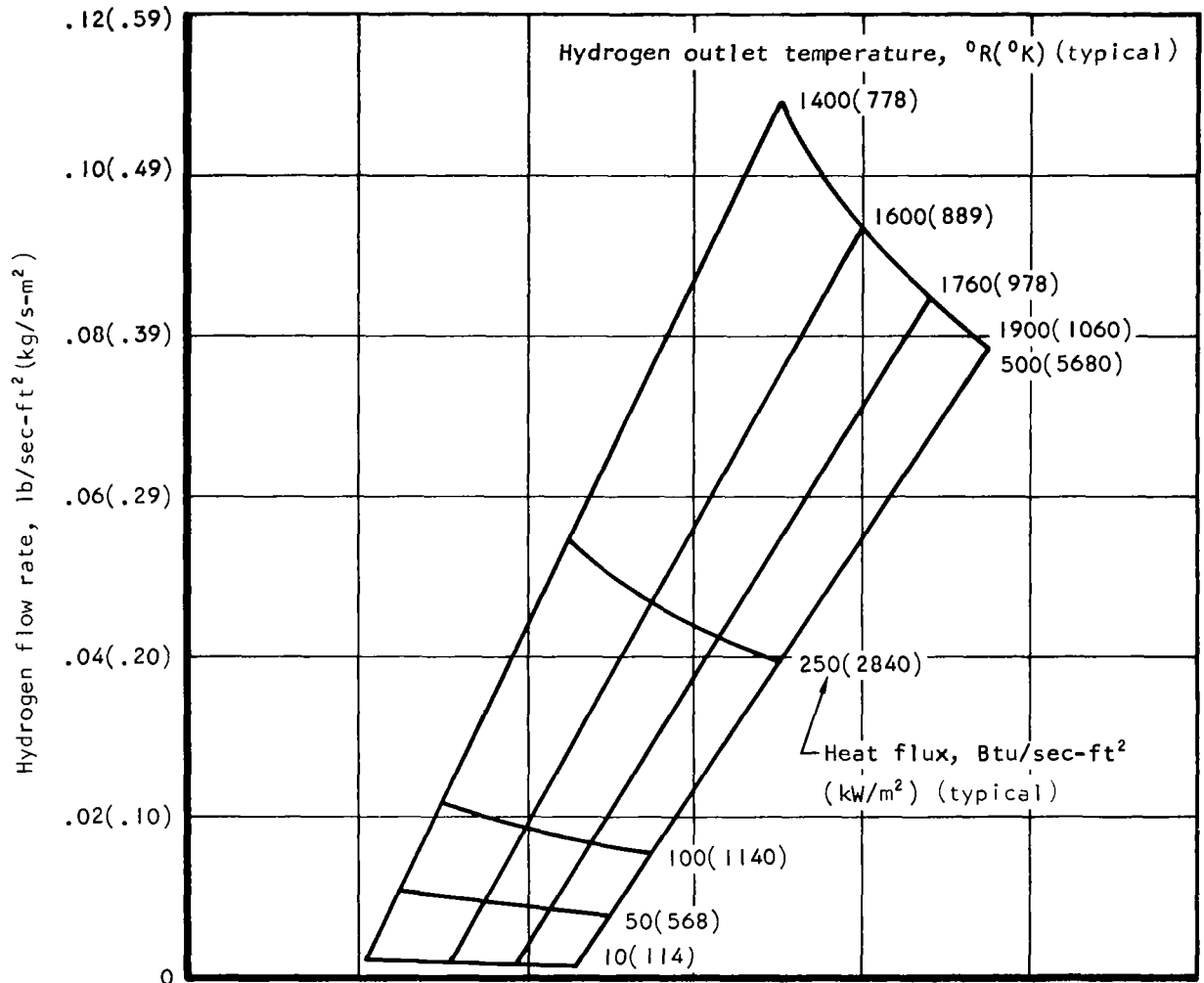
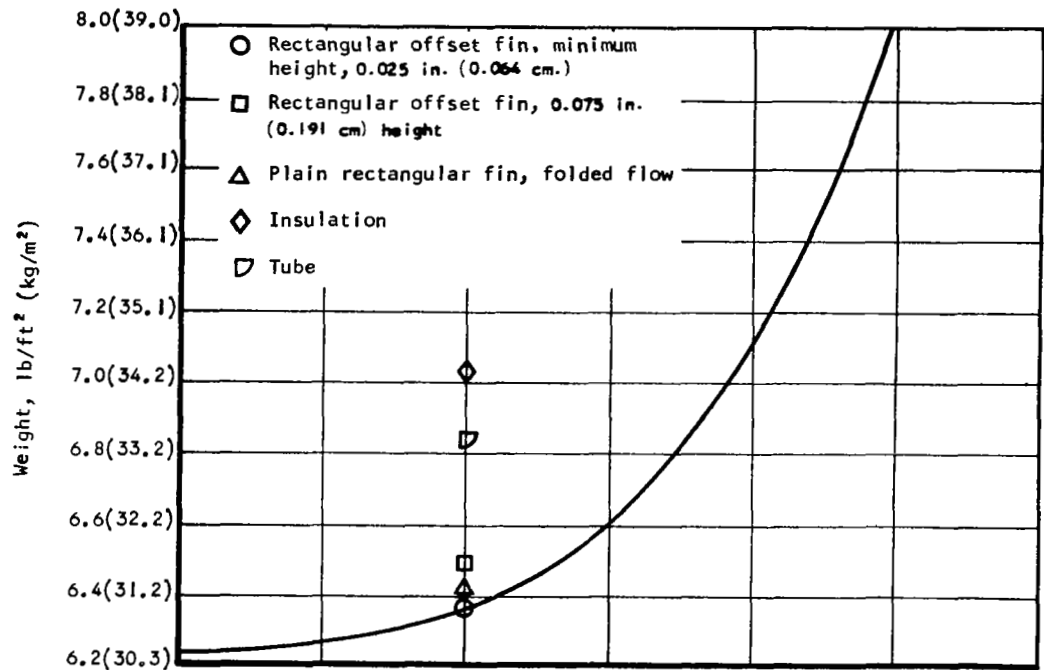
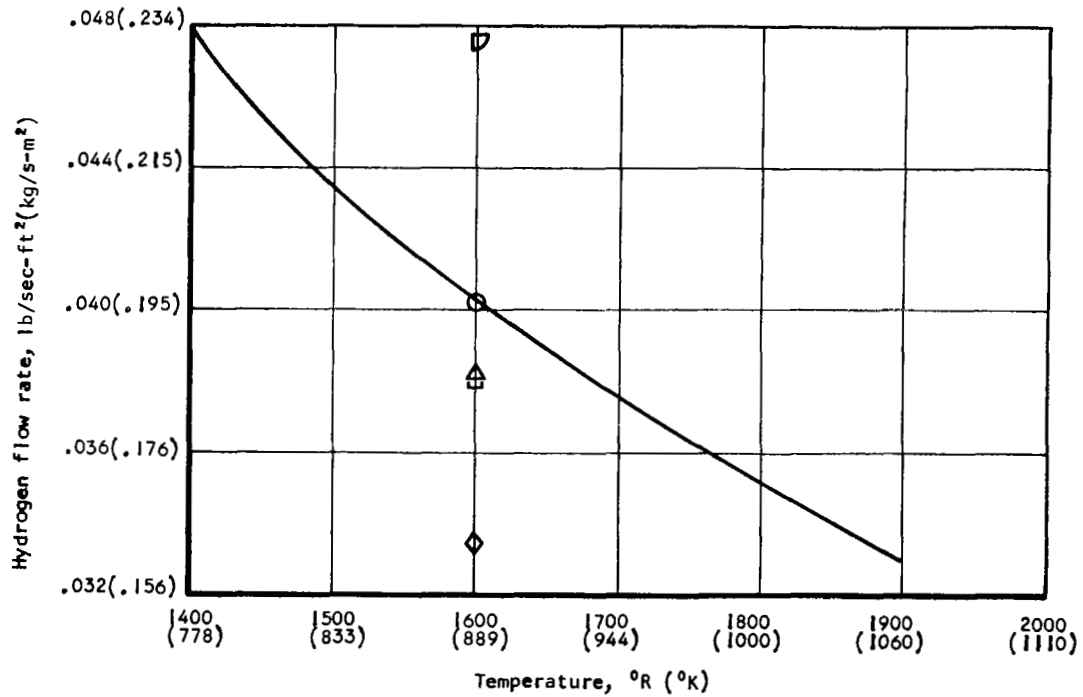


Figure 9. Variation of Hydrogen Flow Rate with Heat Flux and Coolant Outlet Temperature for an Infinite Recovery Temperature

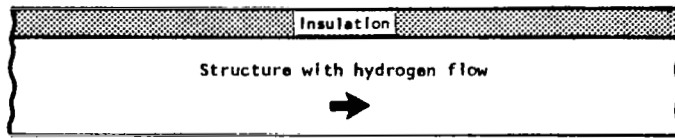


a. Configuration weight vs outlet temperature

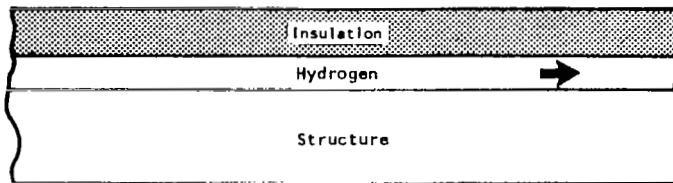


b. Hydrogen flow rate vs outlet temperature

Figure 10. Configuration Weight and Coolant Flow Rate for Various Bonded Concepts. External Pressure Loading = 100 psi (689 kN/m²), Nominal Heat Flux = 250 Btu/sec-ft² (2840 kW/m²); Recovery Temperature = 5000°R (2780°K), 2-ft by 2-ft (.61-m by .61-m) Panel.

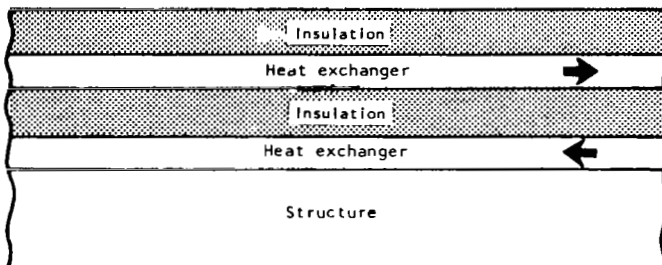


a. Single-layer combined structure and hydrogen passages

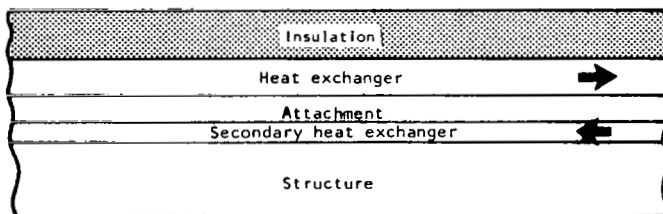


b. Metallurgically bonded thermal protection

Protective Superalloy or Coated Refractory Alloy Sheet

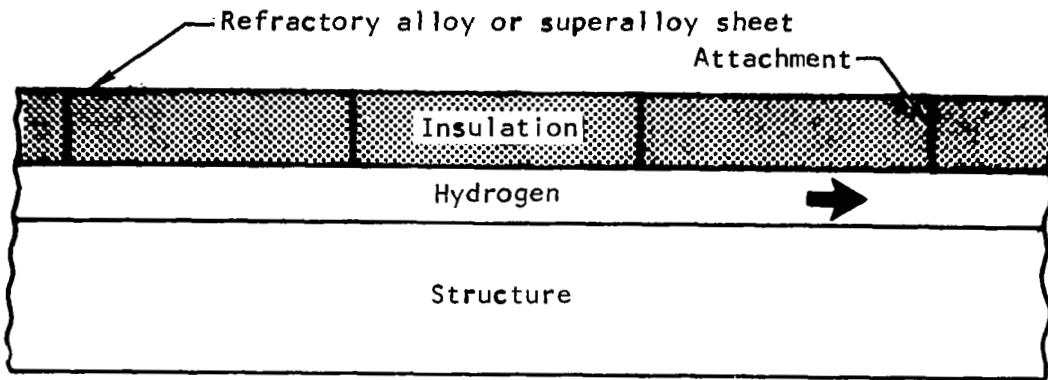


c. Multilayered insulation and heat exchanger (2 layers shown)

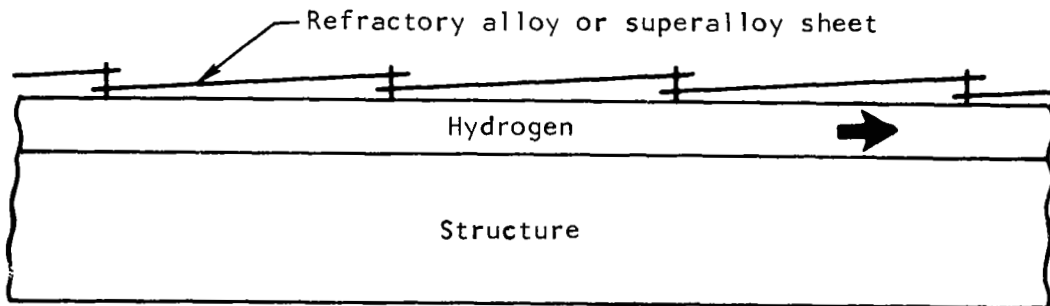


d. Mechanically attached thermal protection with secondary heat exchanger metallurgically bonded to prime structure

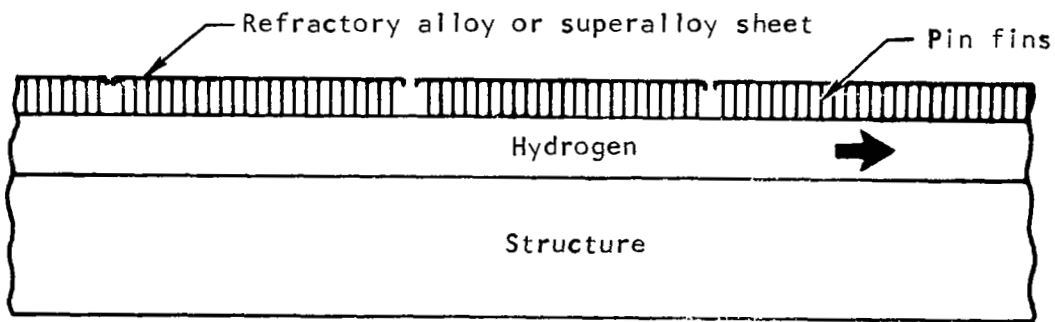
Figure 11. Composite Panel Elements



a. Sheet metal covered insulation

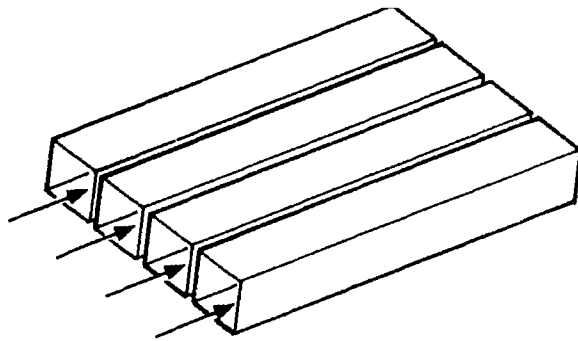


b. Sheet metal shingle array

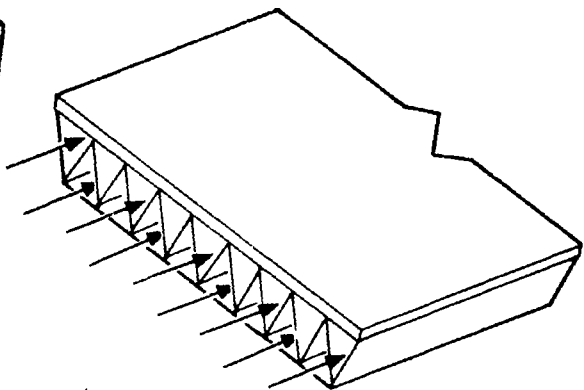


c. Pin-fin insulation

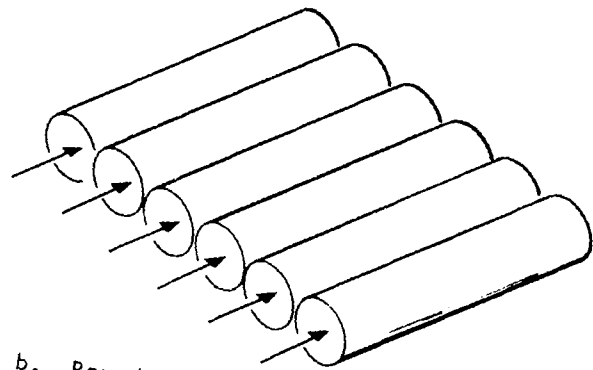
Figure 12. Insulation



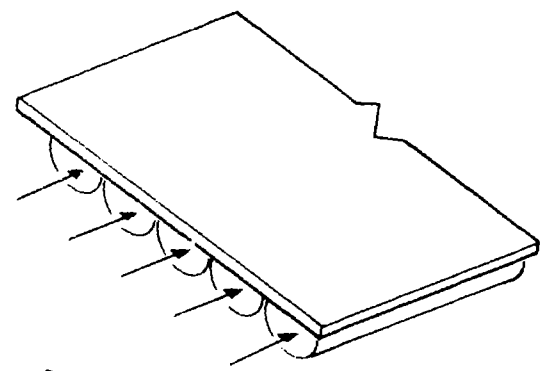
a. Rectangular tubes



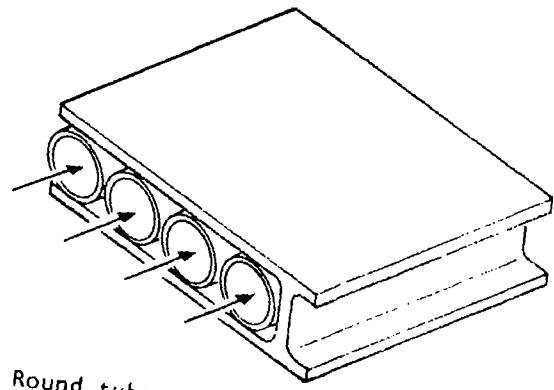
d. Triangular fin



b. Round tubes

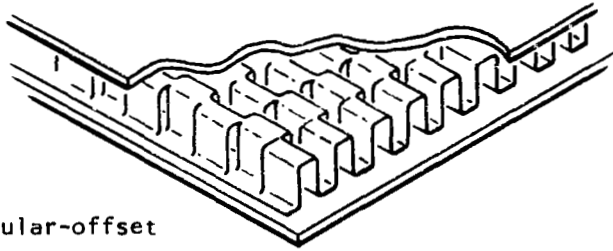


e. Semicircular fin

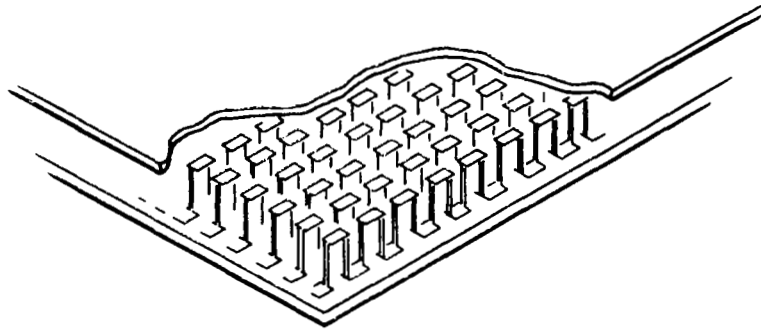


c. Round tubes with face sheets

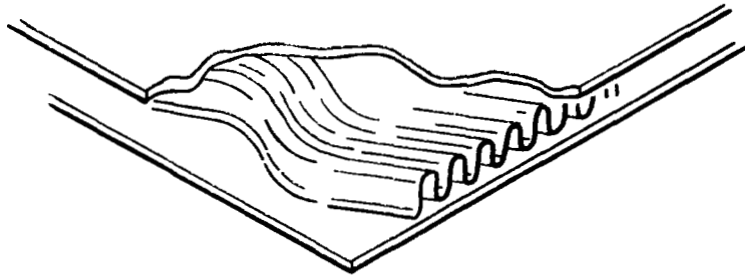
Figure 13. Heat Exchanger Geometries



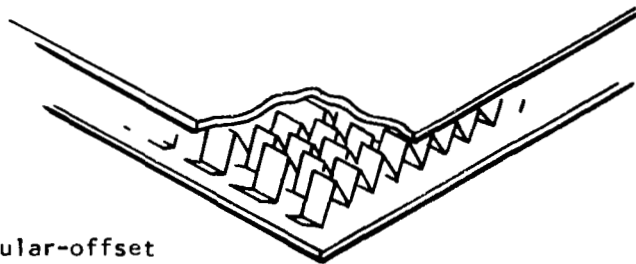
a. Rectangular-offset



b. Pin

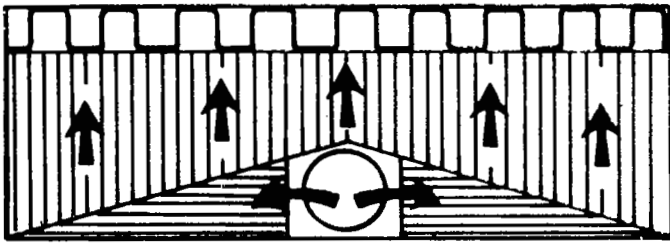


c. Wavy

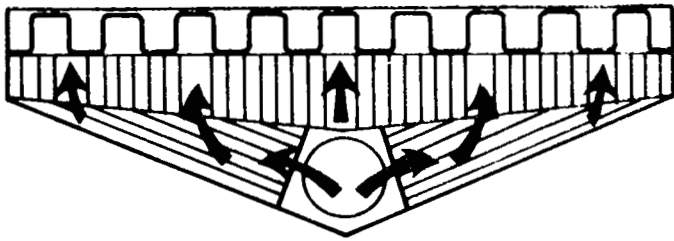
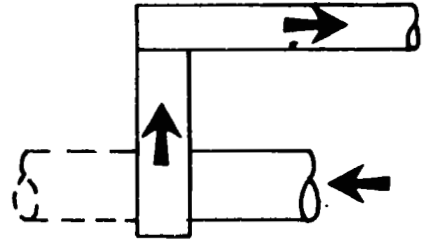


d. Triangular-offset

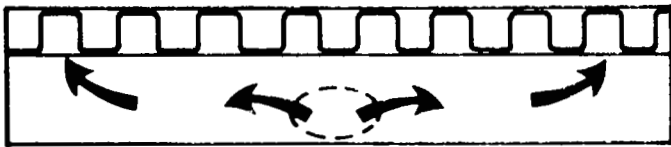
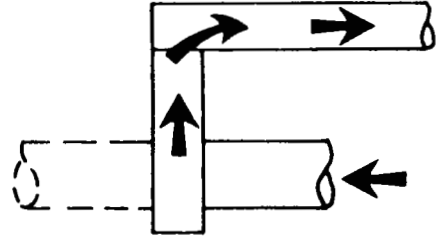
Figure 14. Fin Geometries for Increasing Hydrogen Thermal Conductance



a. Flat rectangular



b. Flat tapered



c. Semicylindrical

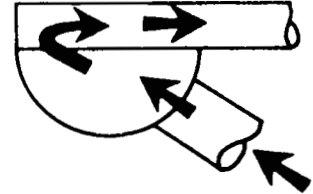
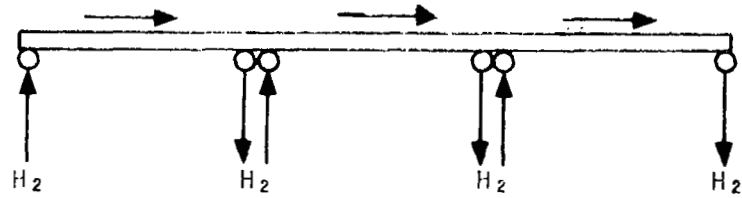
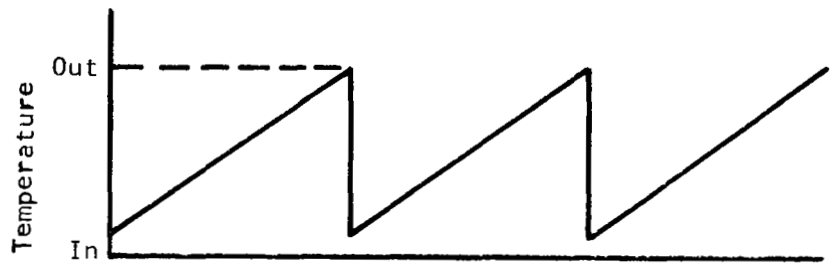
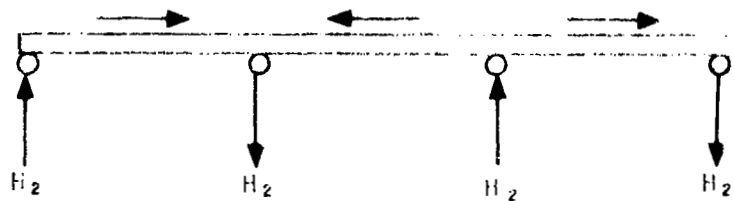
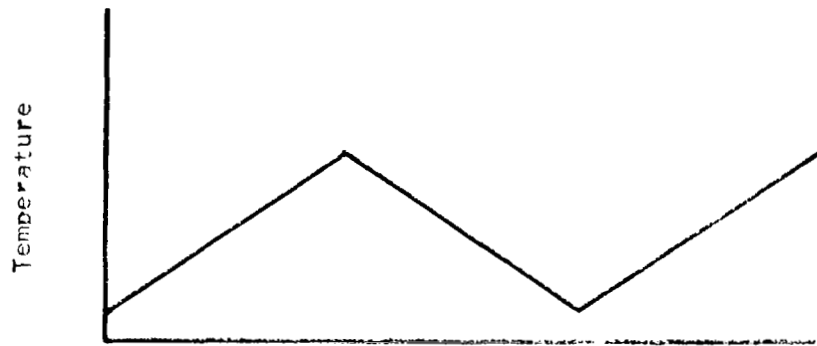


Figure 15. Manifold Configurations

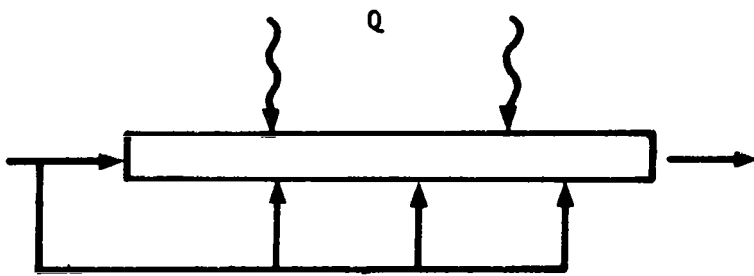


a. Adjacent inlet and outlet manifolds

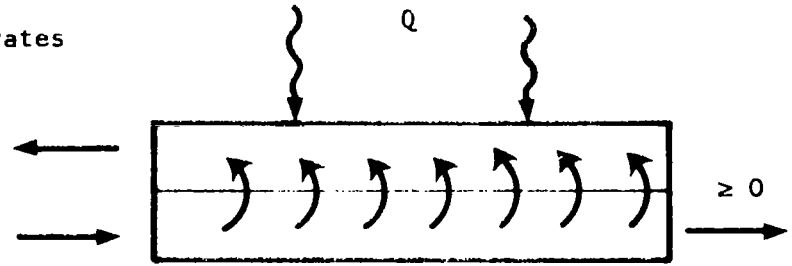


b. Common inlet and outlets

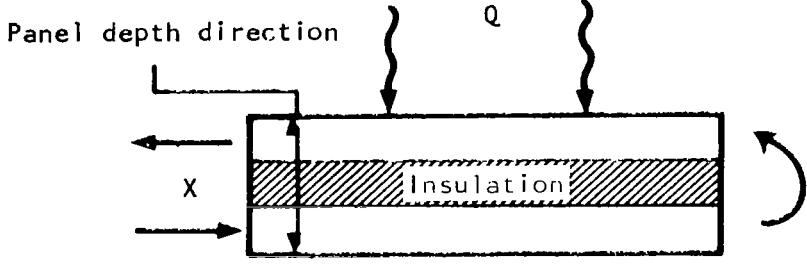
Figure 16. Multiple Manifold Flow Arrangements



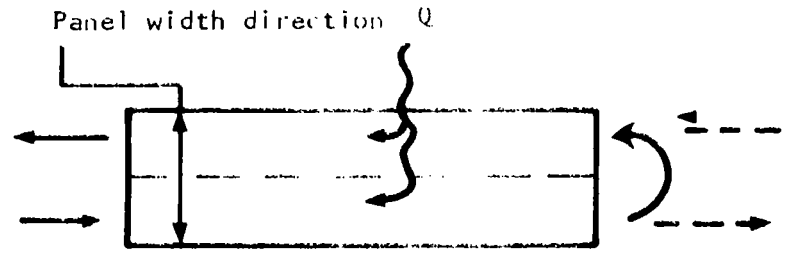
a. Multiple flow rates



c. Fold with injection

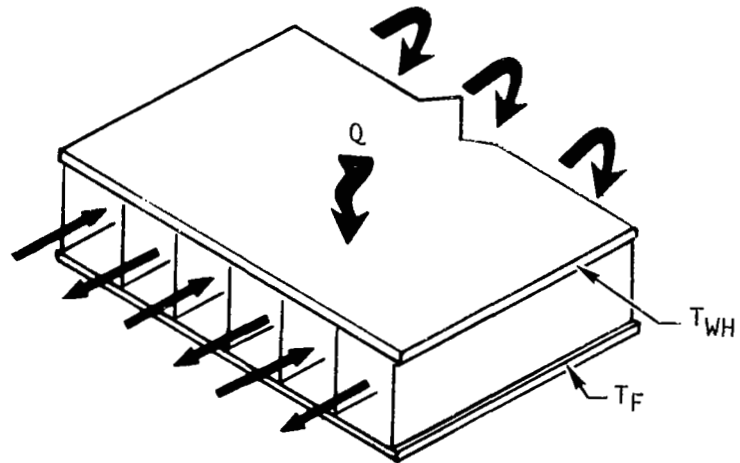


b. Folded in depth



d. Counterflow in adjacent passages

Figure 17. Flow Routing Concepts for Increased Cooling Efficiency



Folded-in-width flow

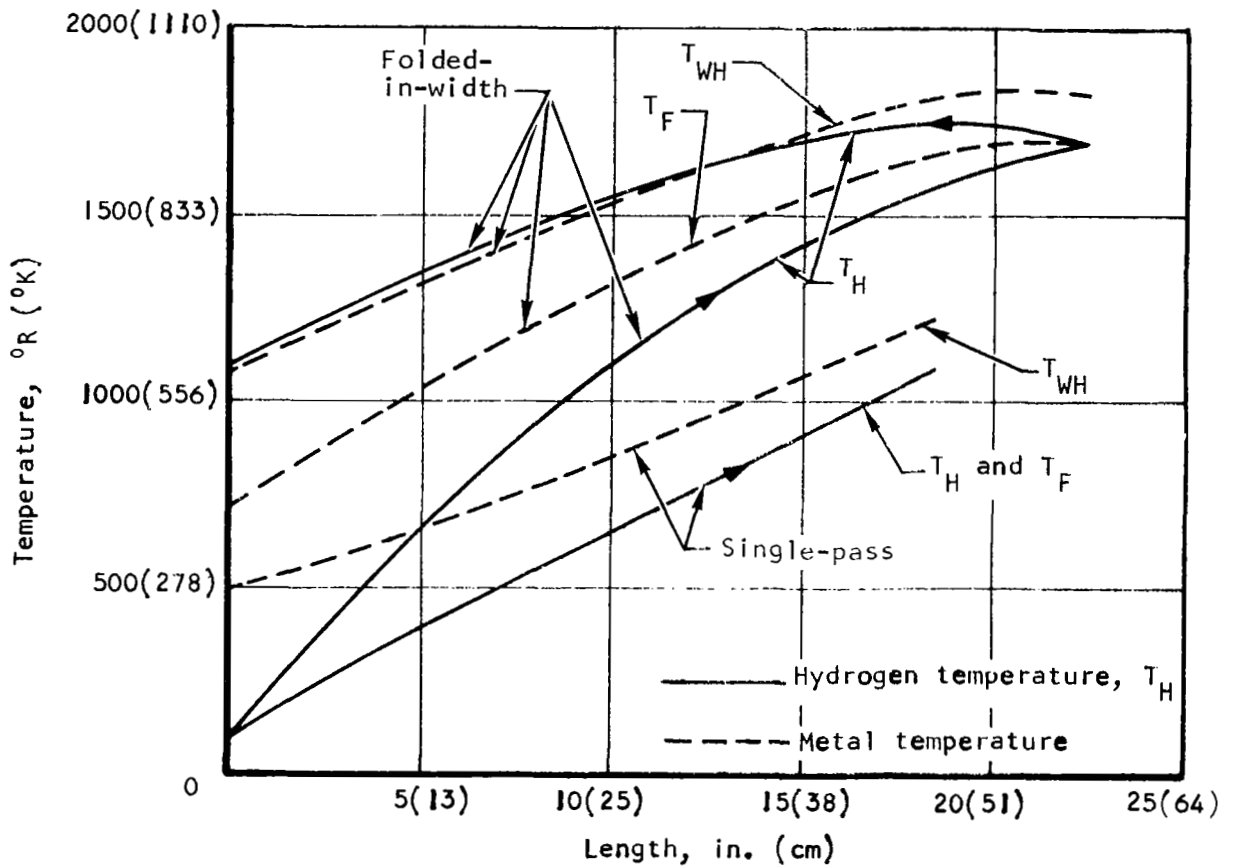


Figure 18. Coolant Flow Routing Comparison for Equal Coolant Inlet and Outlet Temperature
 $[T_R = 3000^{\circ}\text{R} (1670^{\circ}\text{K}), \text{Nominal Heat Flux} = 10 \text{ Btu/sec-ft}^2 (114 \text{ kW/m}^2)]$

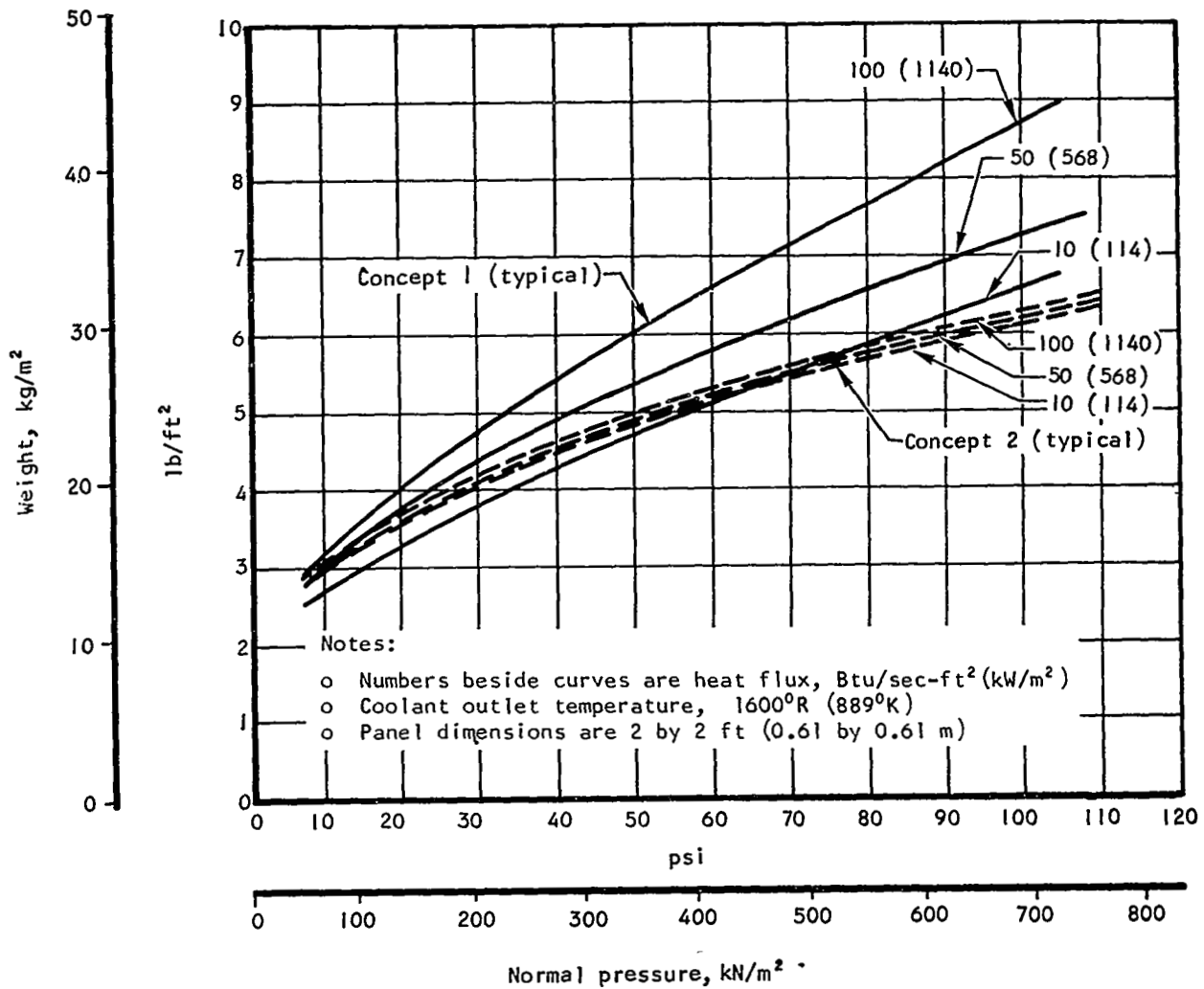


Figure 19. Concepts 1 and 2 Weights vs Applied Normal Pressure

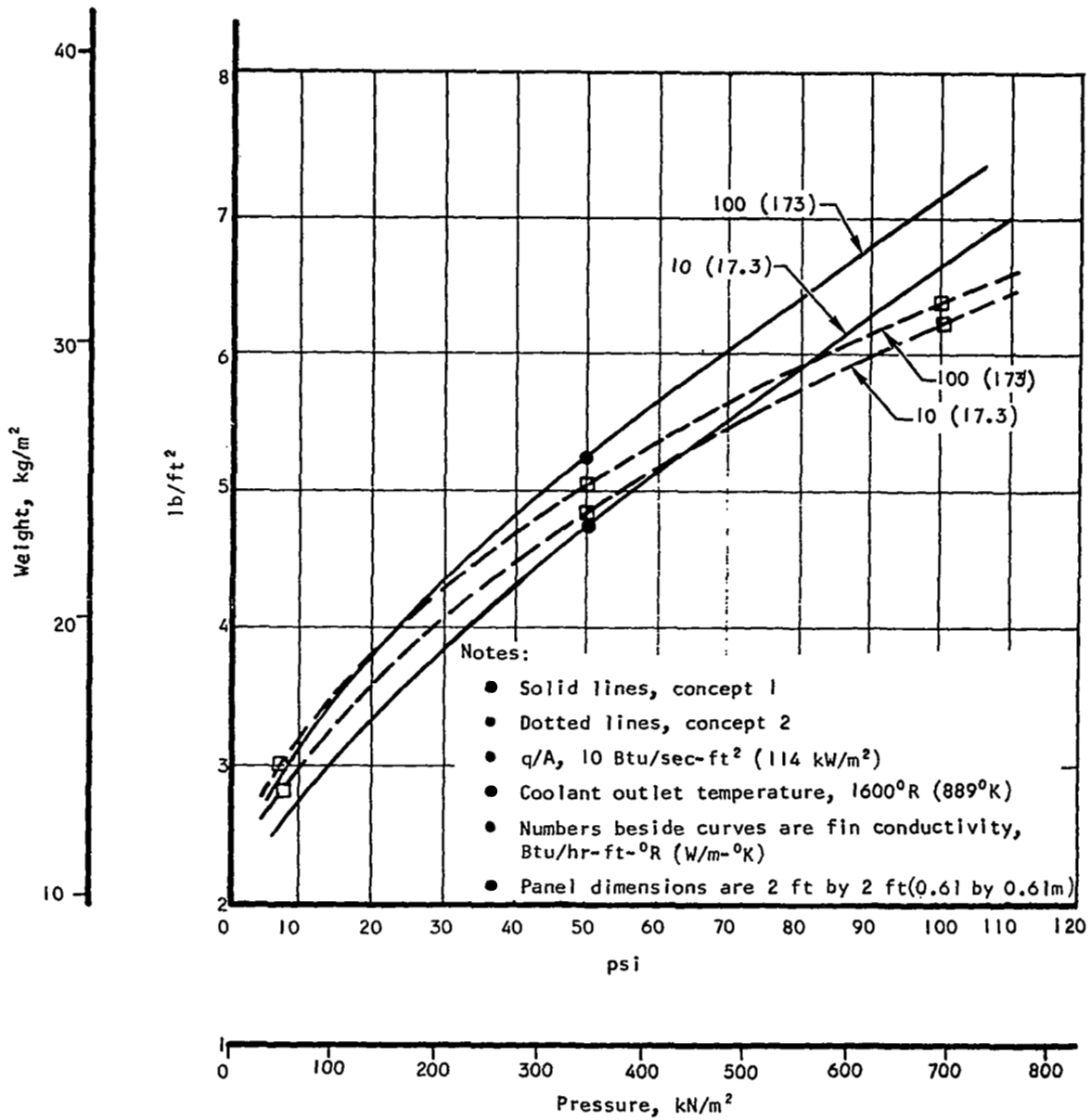


Figure 20. Concepts 1 and 2 Weight vs Applied Normal Pressure for Two Fin Conductivities

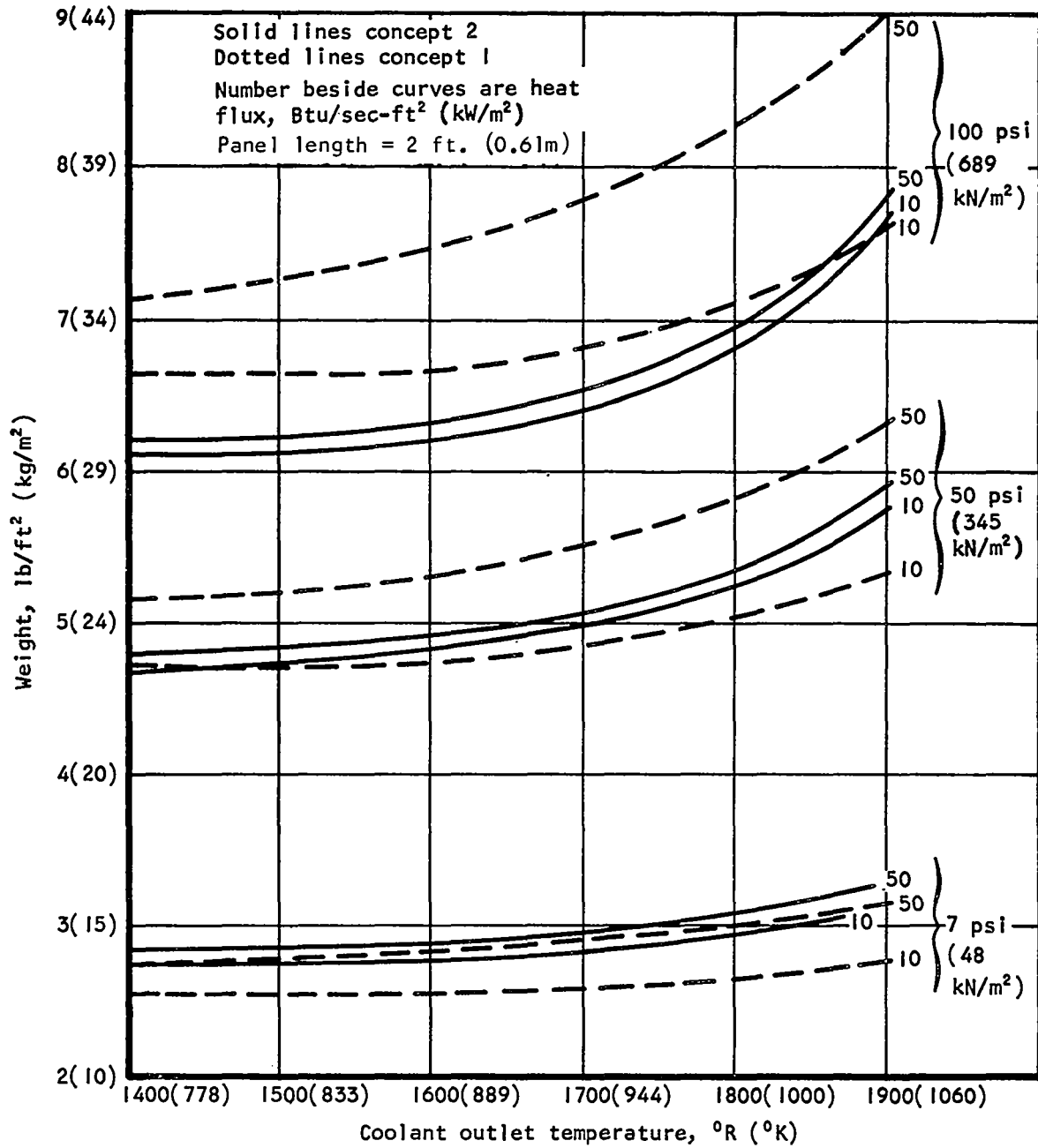


Figure 21. Concepts 1 and 2 Weights vs Coolant Outlet Temperature

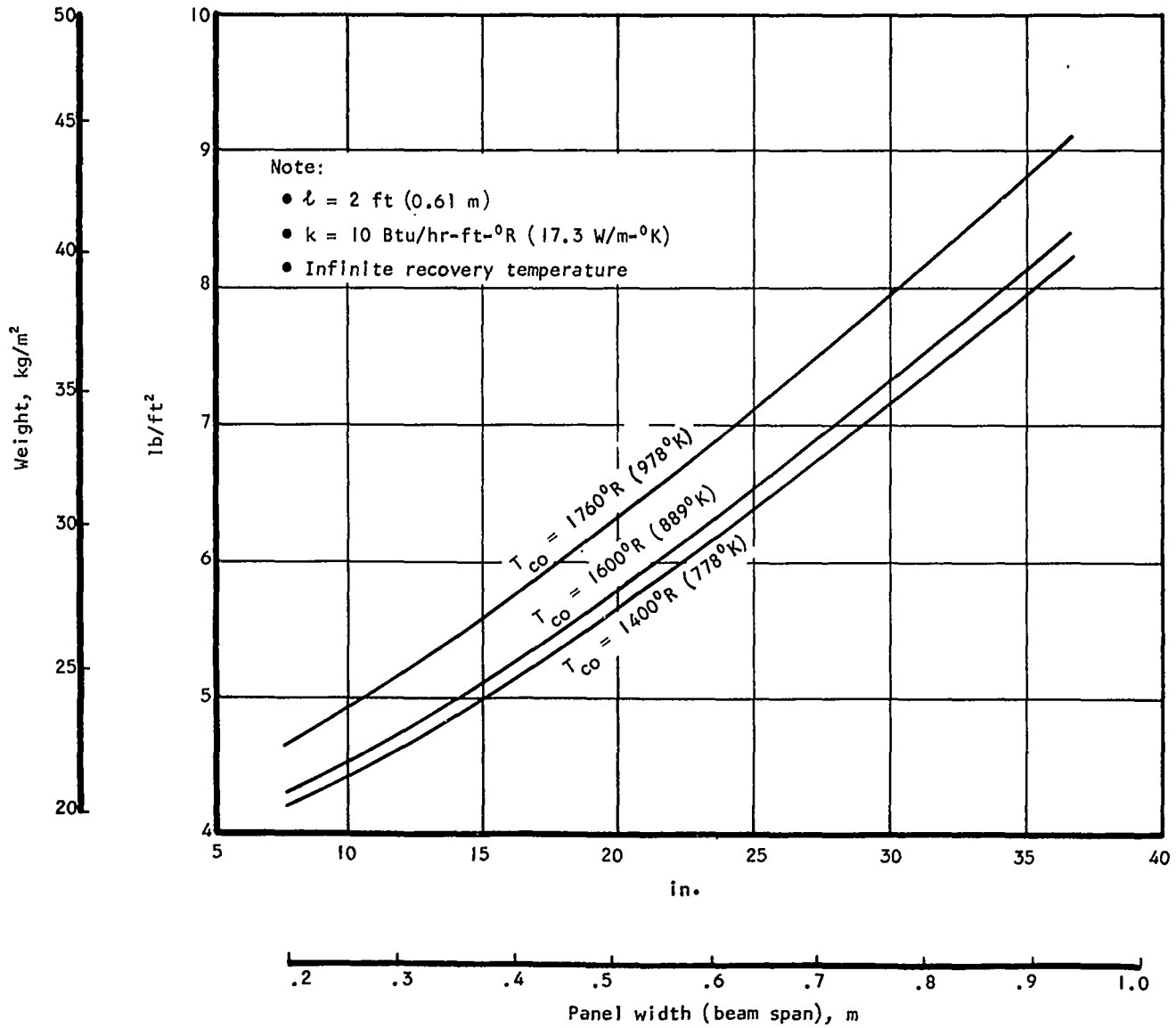


Figure 22. Concept 2 Weight vs Beam Span for Three Coolant Outlet Temperatures and Loading Conditions of 250 Btu/sec-ft² (2840 kW/m²) Heat Flux and 100 psi (689 kN/m²) Pressure

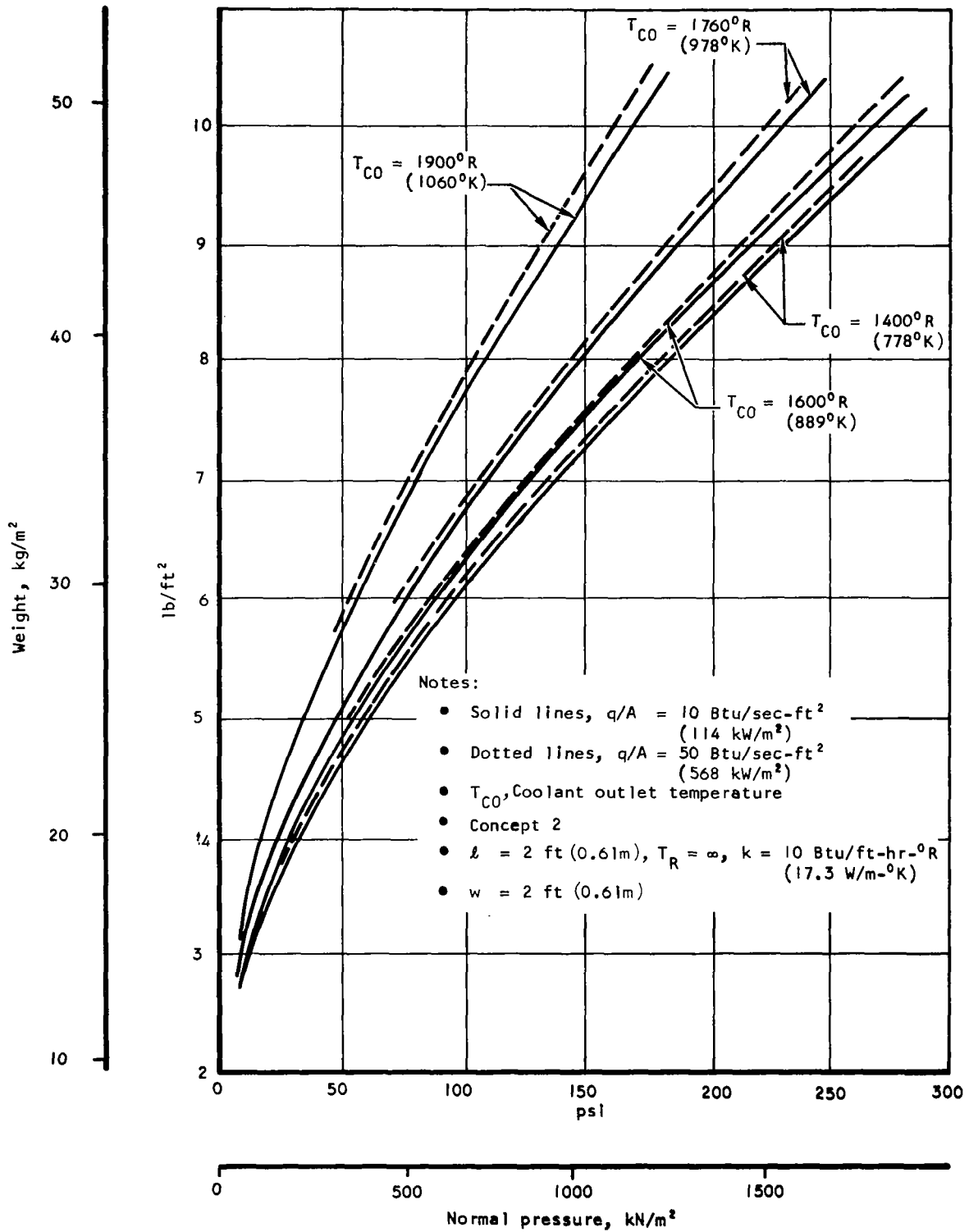


Figure 23. Concept 2 Weight vs Pressure

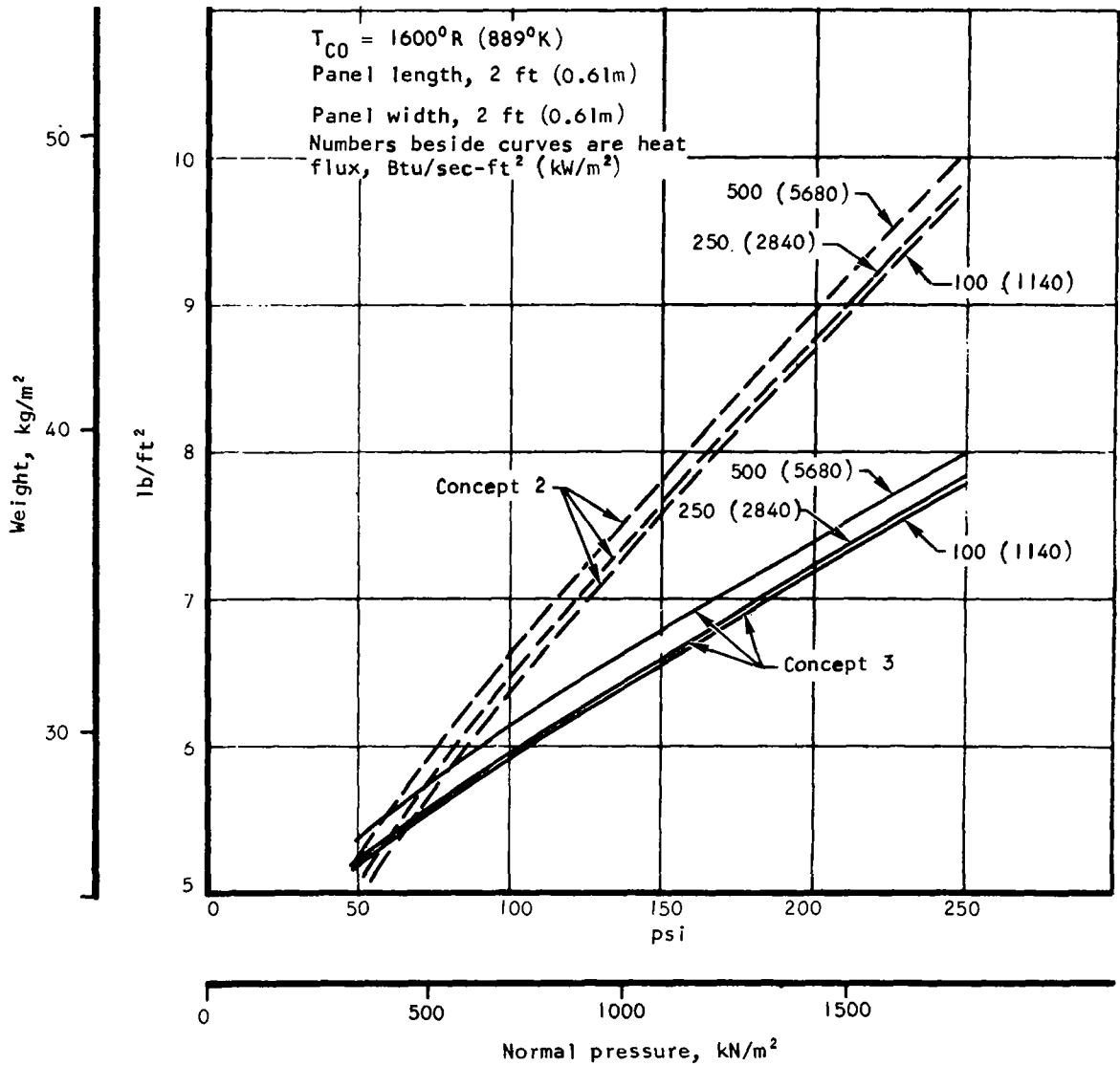


Figure 24. Comparison of Concepts 2 and 3 Weights vs Pressure

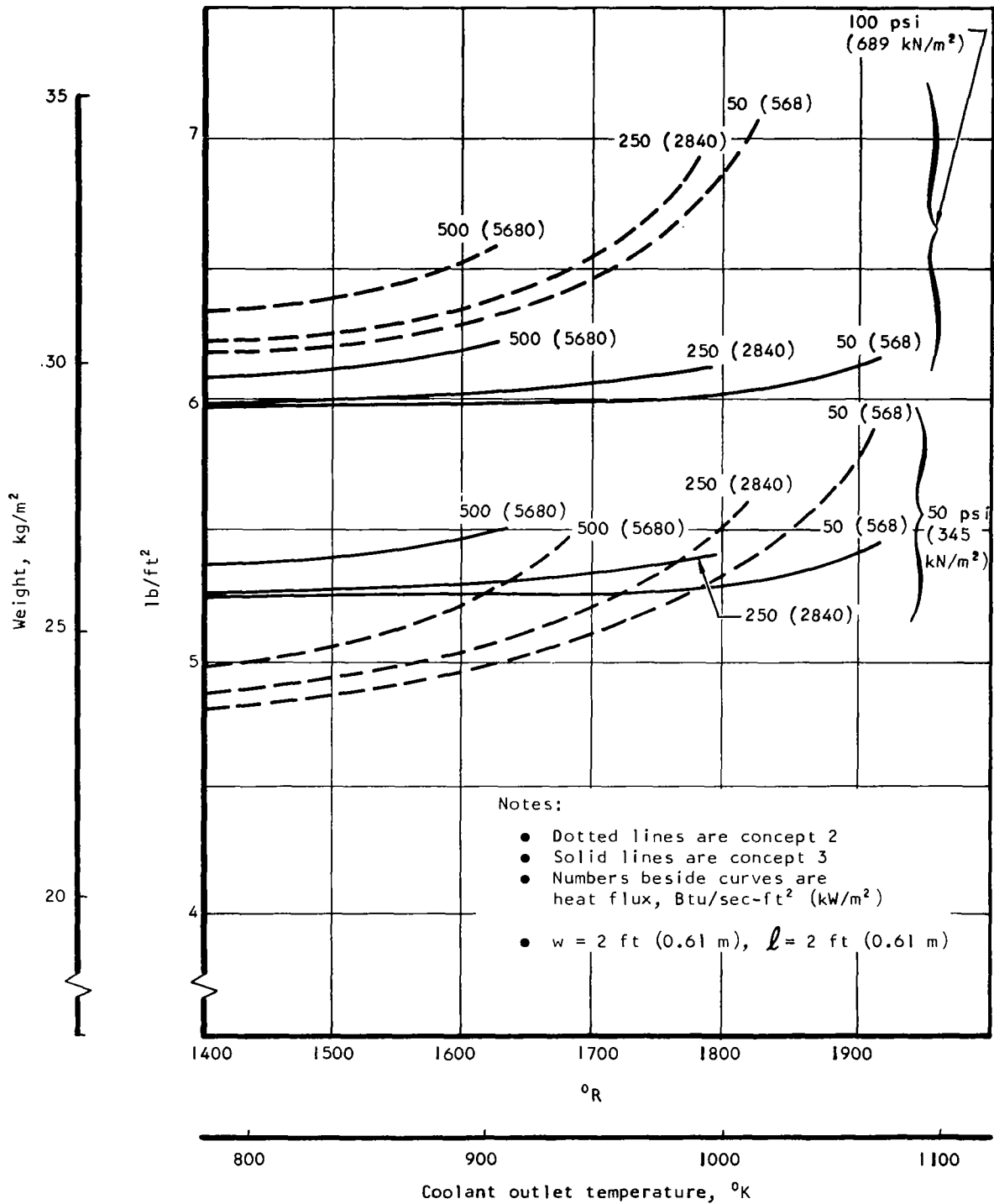


Figure 25. Concepts 2 and 3 Weight vs Coolant Outlet Temperature

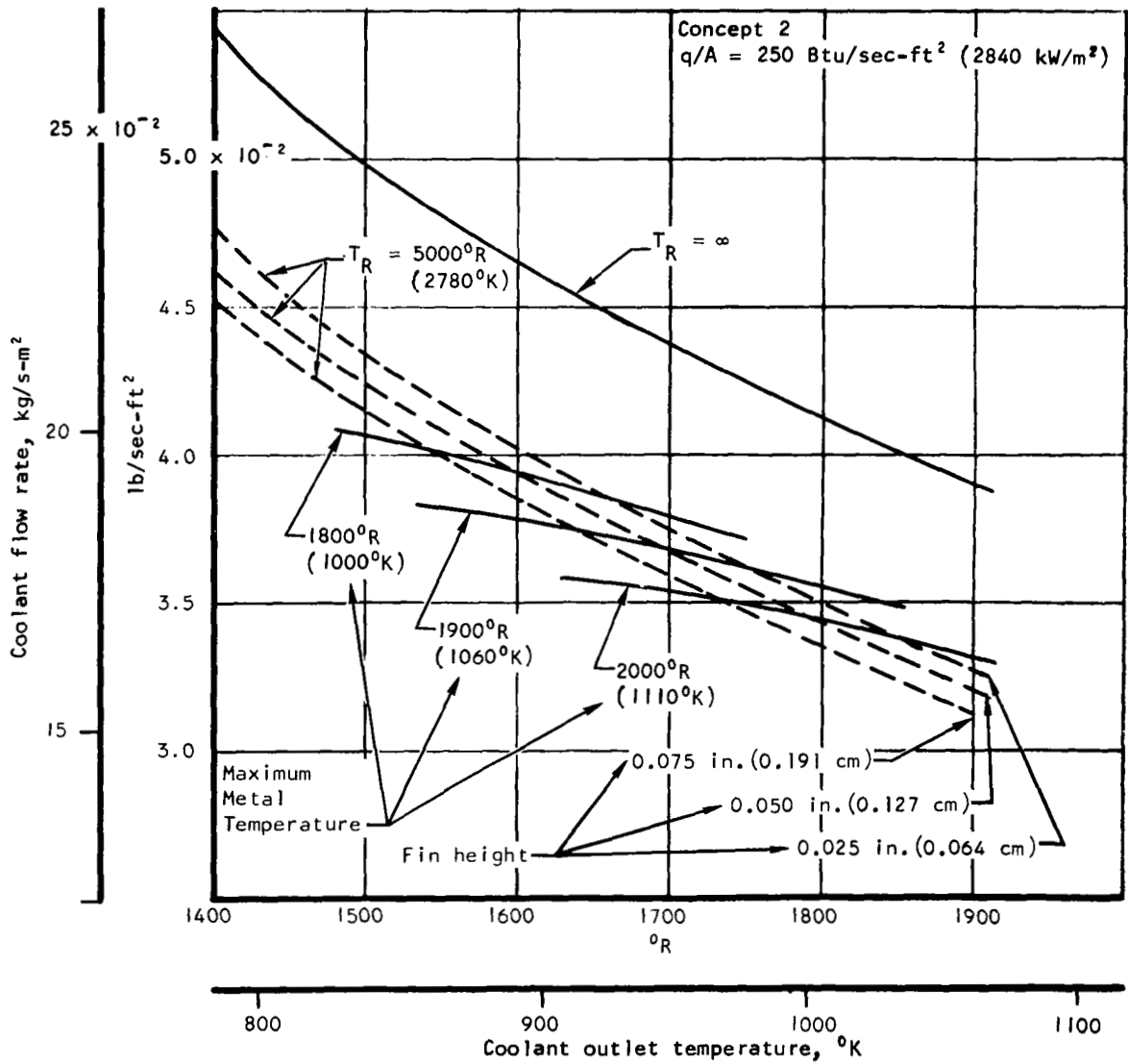


Figure 26. Concept 2 Coolant Flow Rate vs Coolant Outlet Temperature at 250 Btu/sec-ft² (2840 kW/m²)

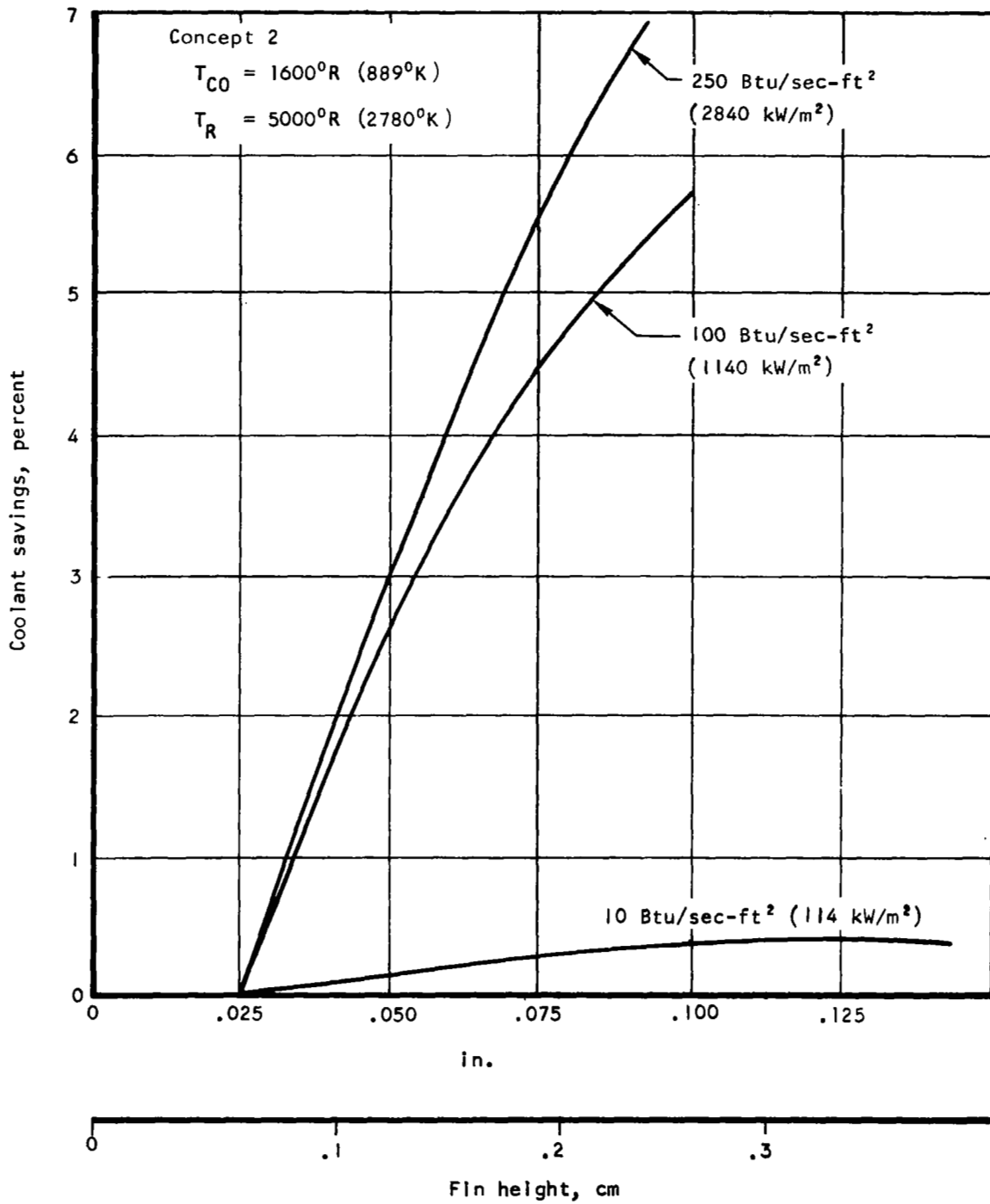


Figure 27. Concept 2 Coolant Savings vs Heat Exchanger Fin Height

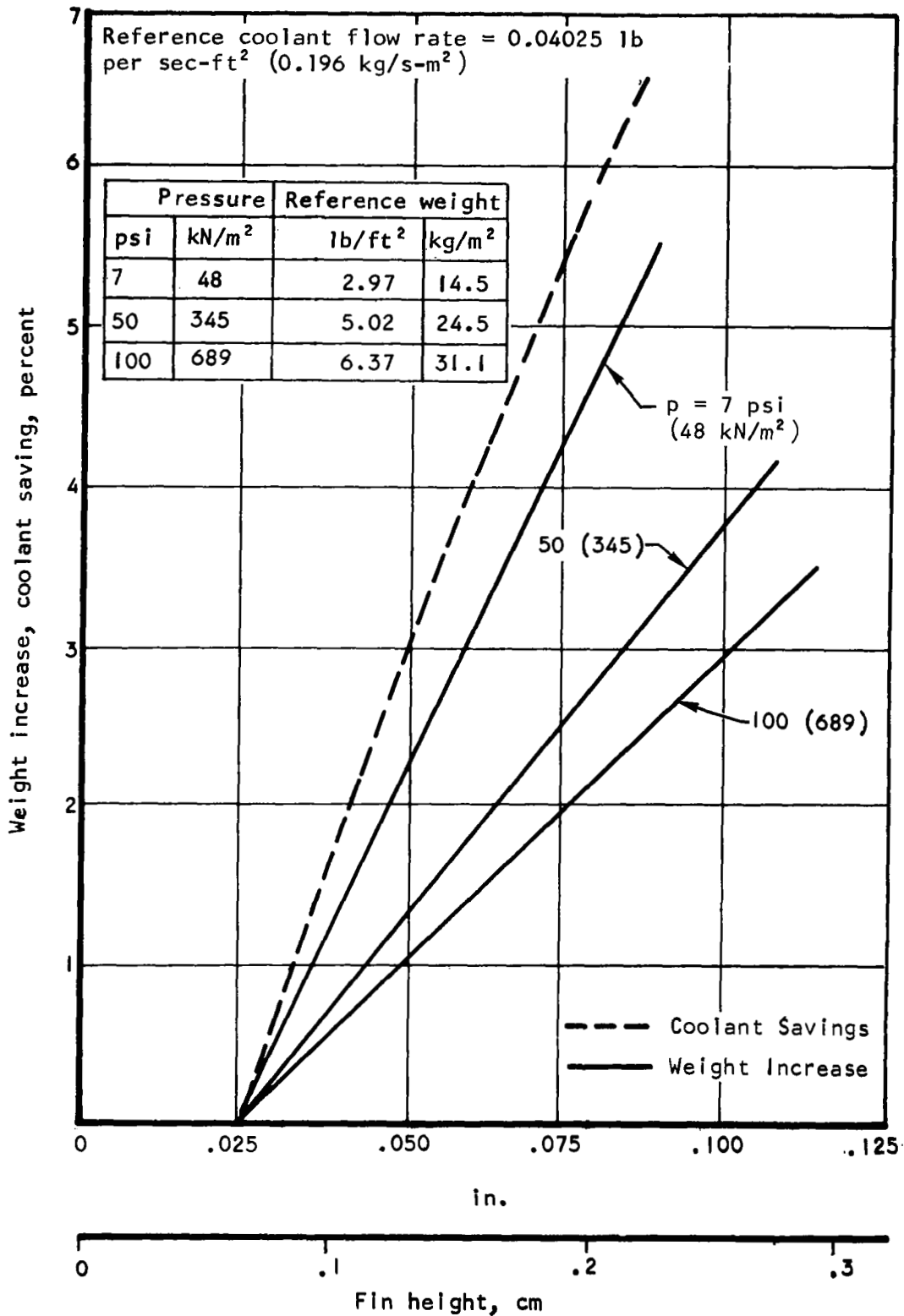


Figure 28. Coolant Saving and Weight Increase Relative to a Concept 2 Minimum Weight Structure as a Function of Fin Height, $T_{CO} = 1600^{\circ}R$ ($889^{\circ}K$), $q/A = 250$ Btu/sec-ft² (2840 kW/m²) $T_R = 5000^{\circ}R$ ($2780^{\circ}K$)

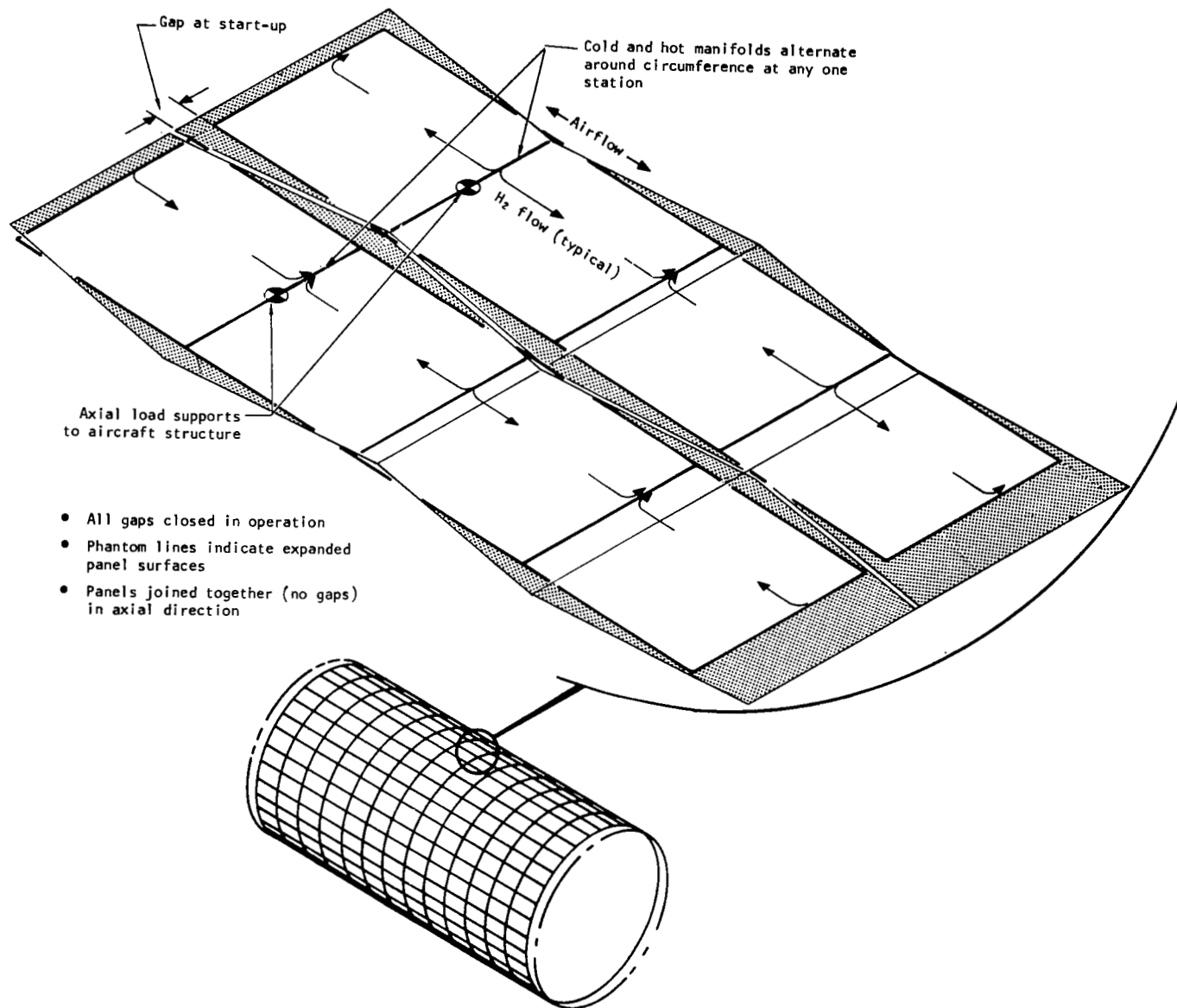


Figure 29. Configuration 1, Longitudinal Rows of Panels

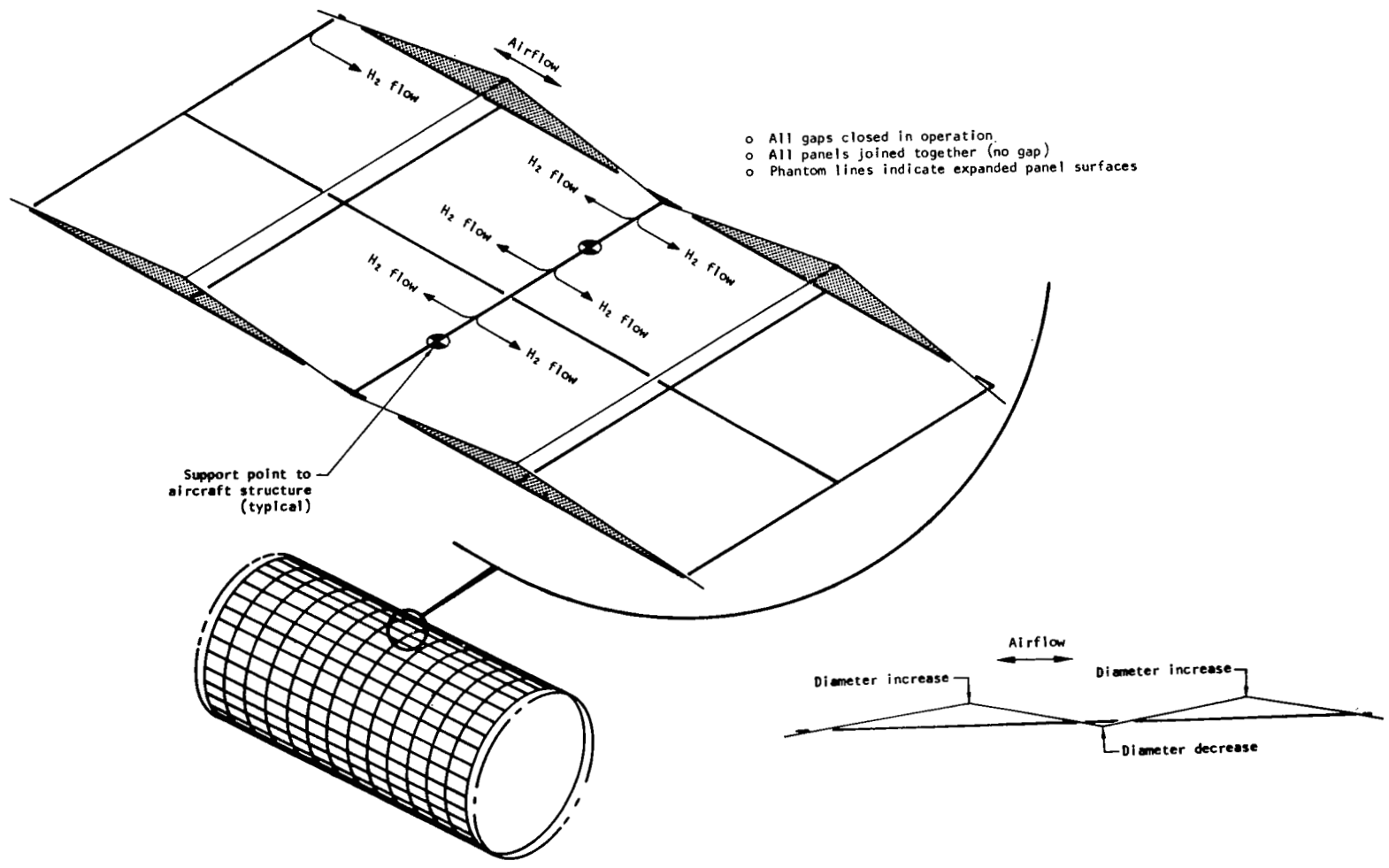


Figure 30. Configuration 2, Free Radial Expansion of Joined Panels

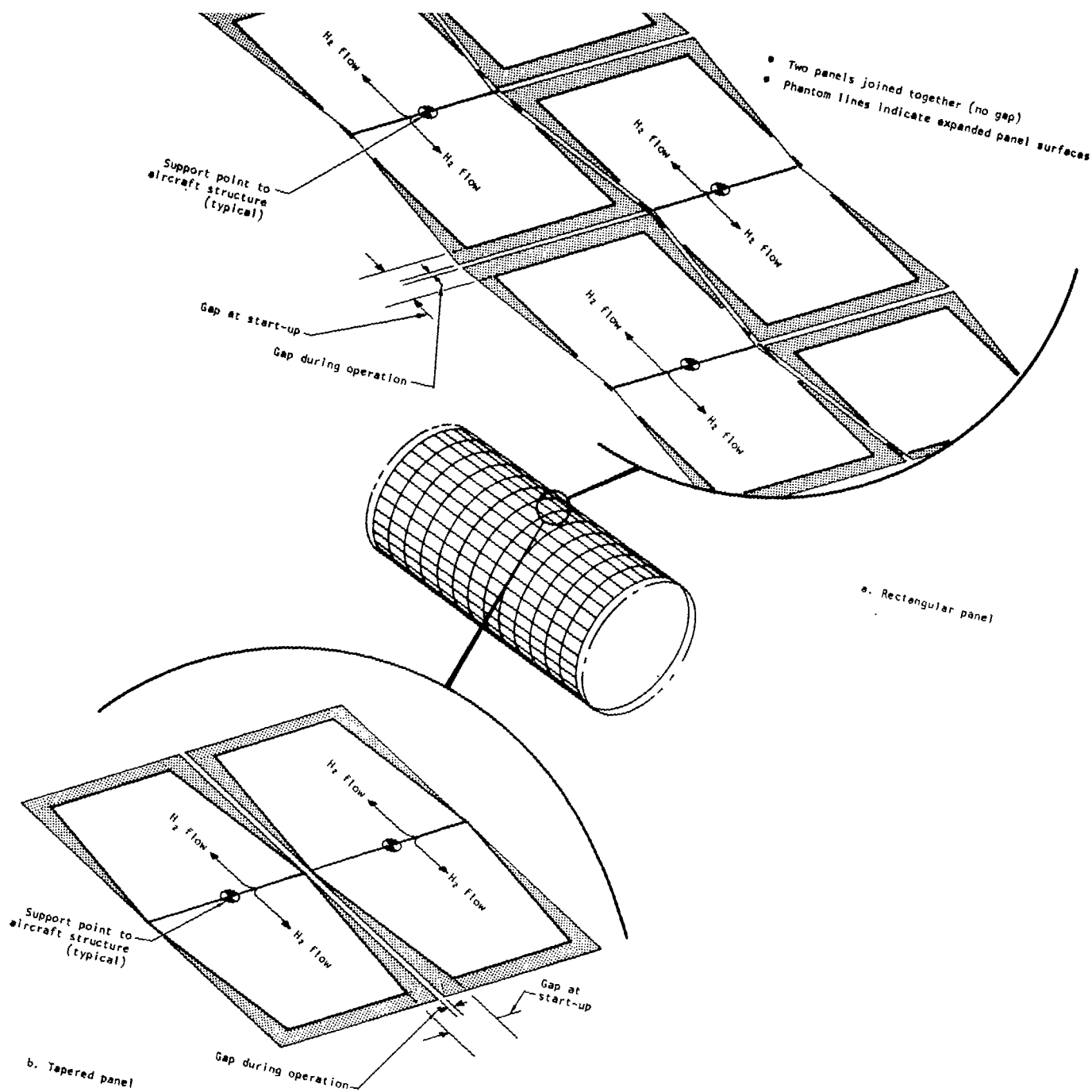


Figure 31. Configuration 3, Pairs of Panels Joined at the Inlet Edge

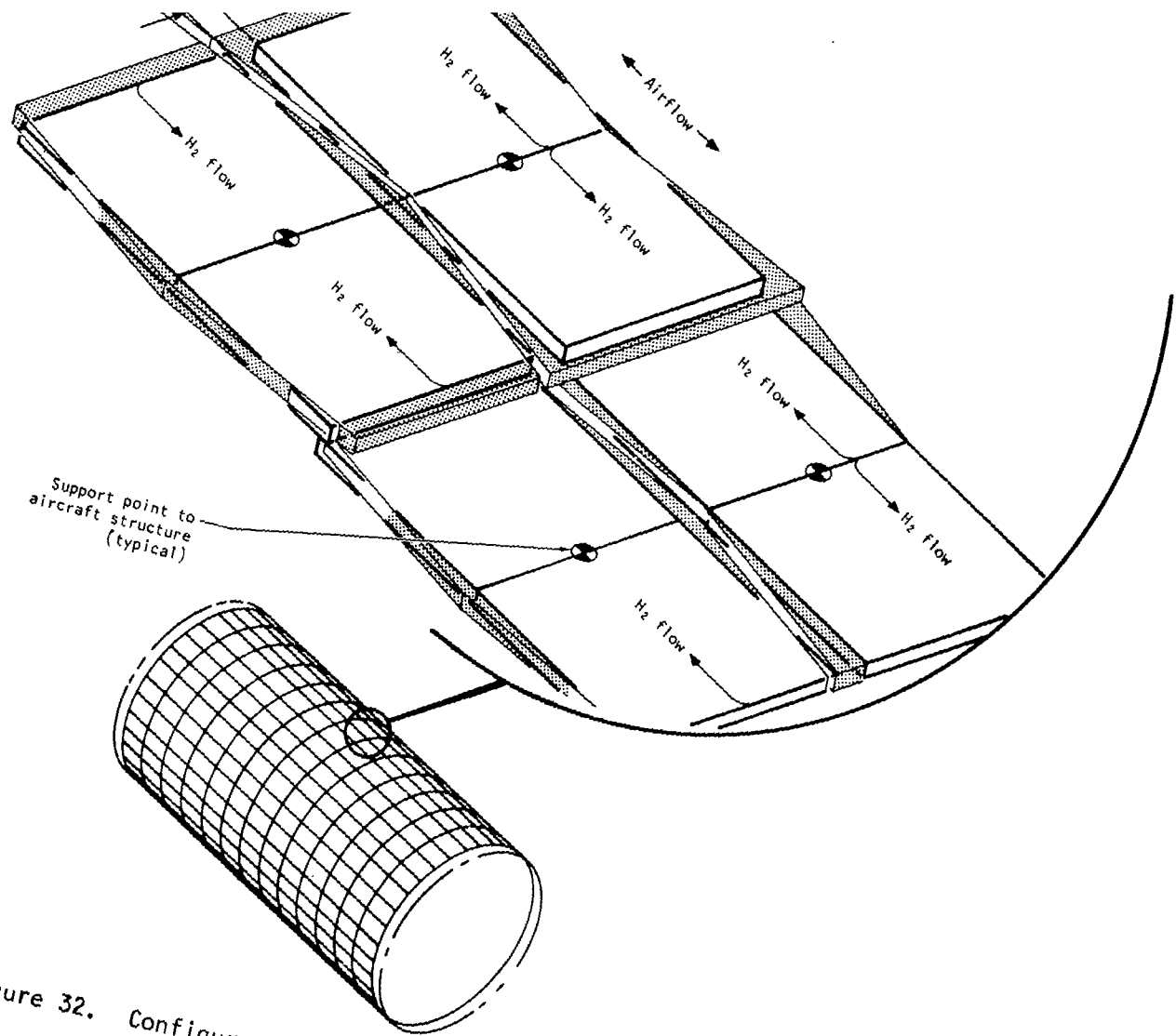


Figure 32. Configuration 4, Pairs of Overlapping Panels

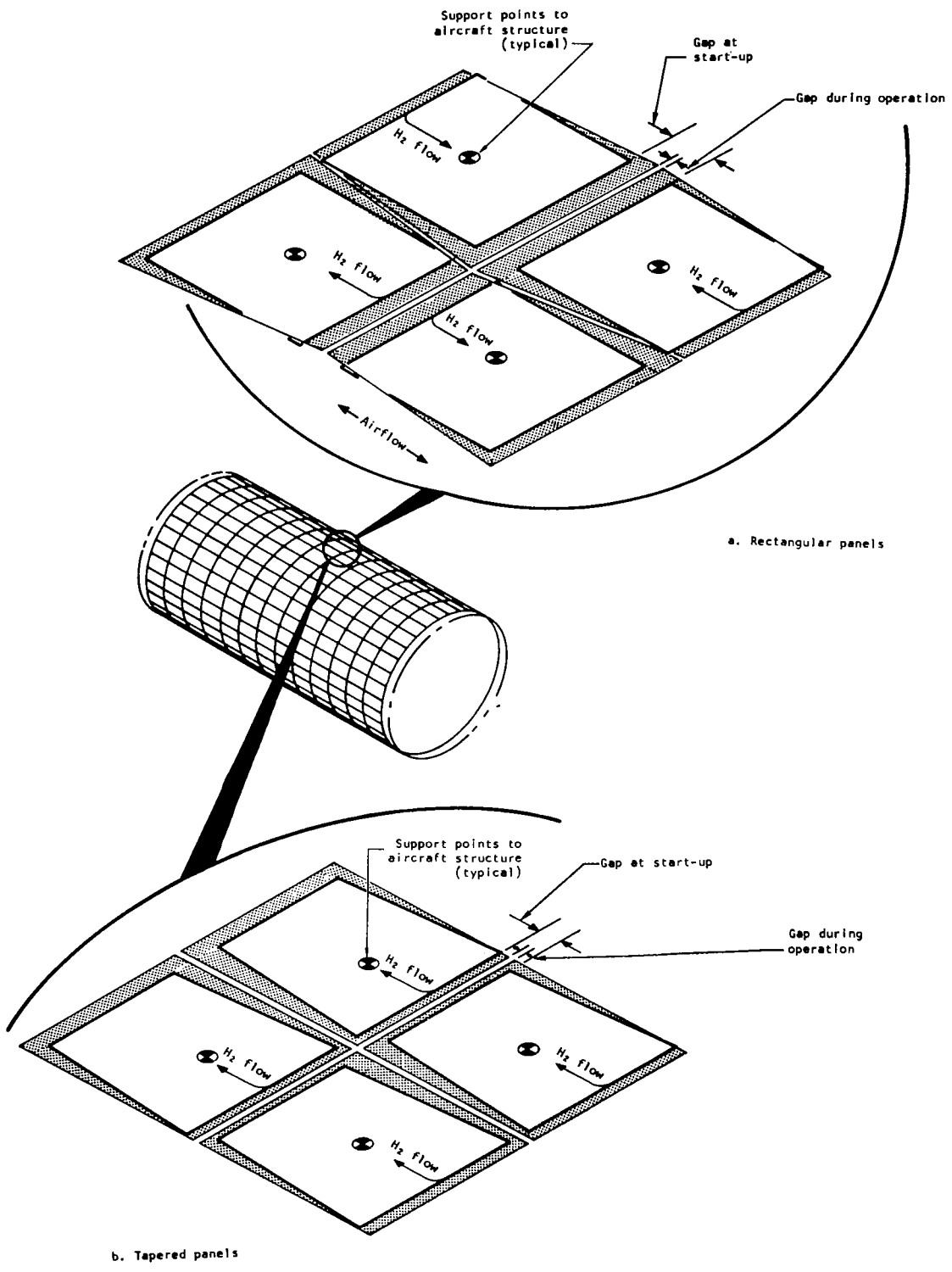


Figure 33. Configuration 5, Single Panels

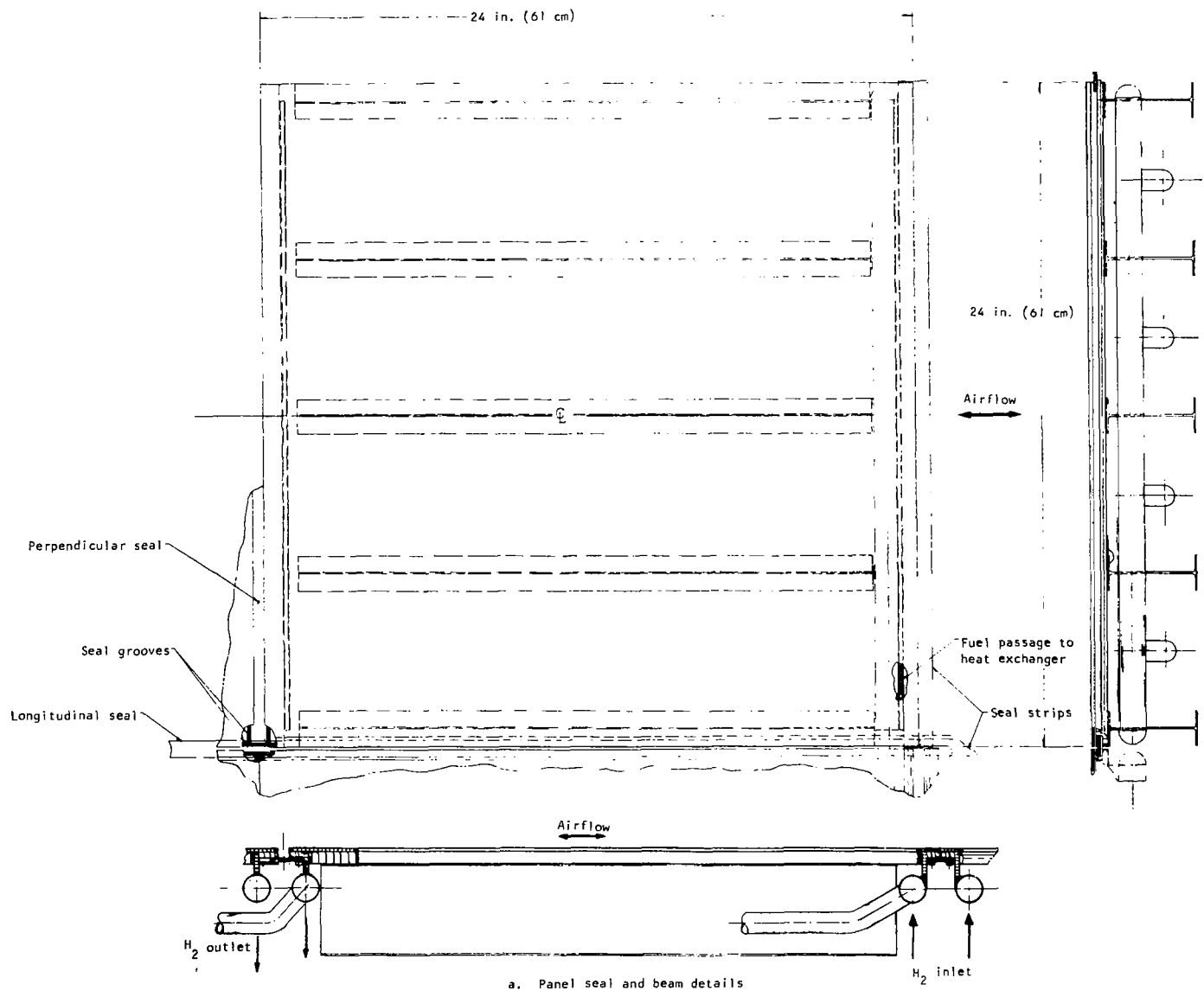


Figure 34. Configuration 3a

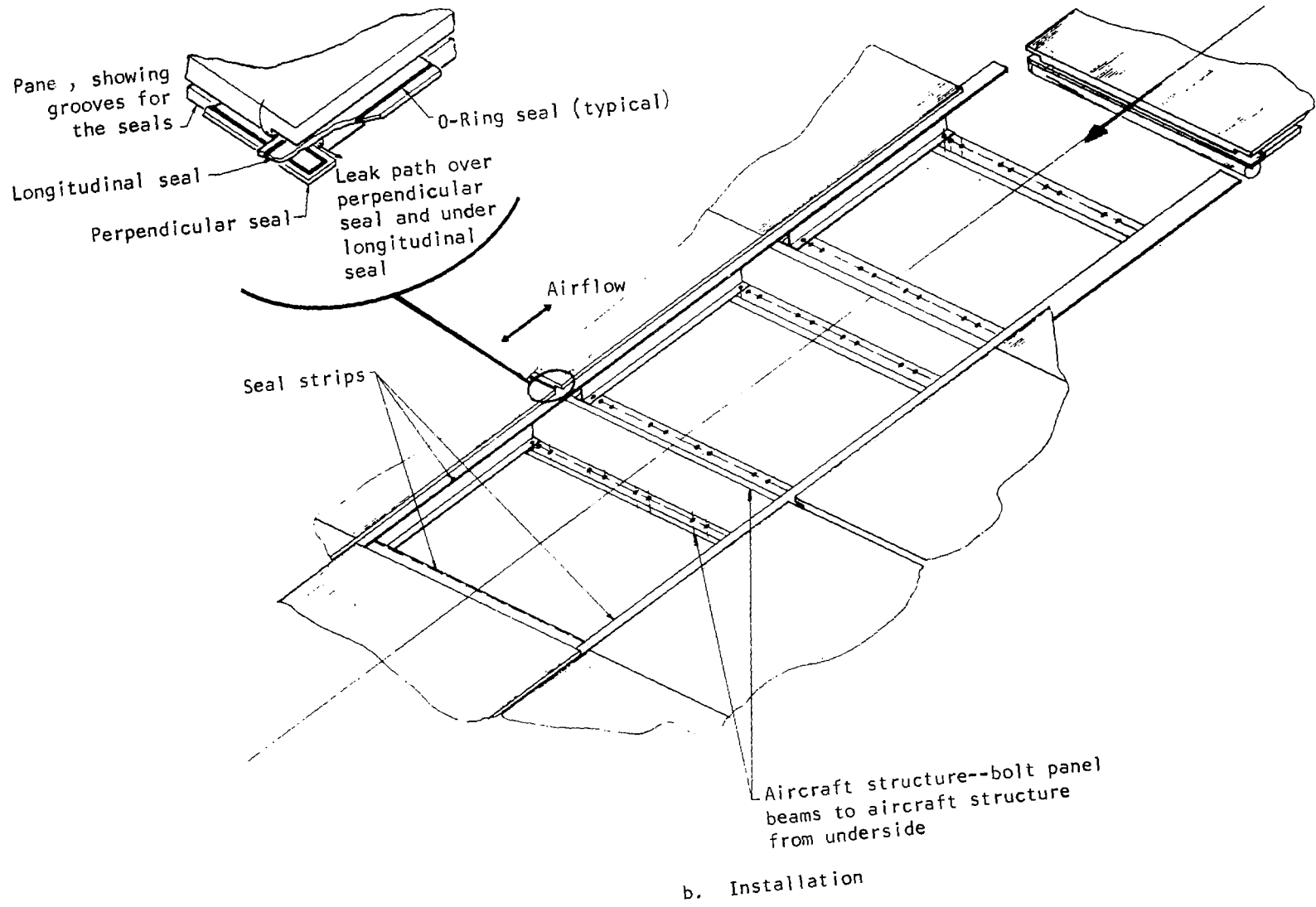
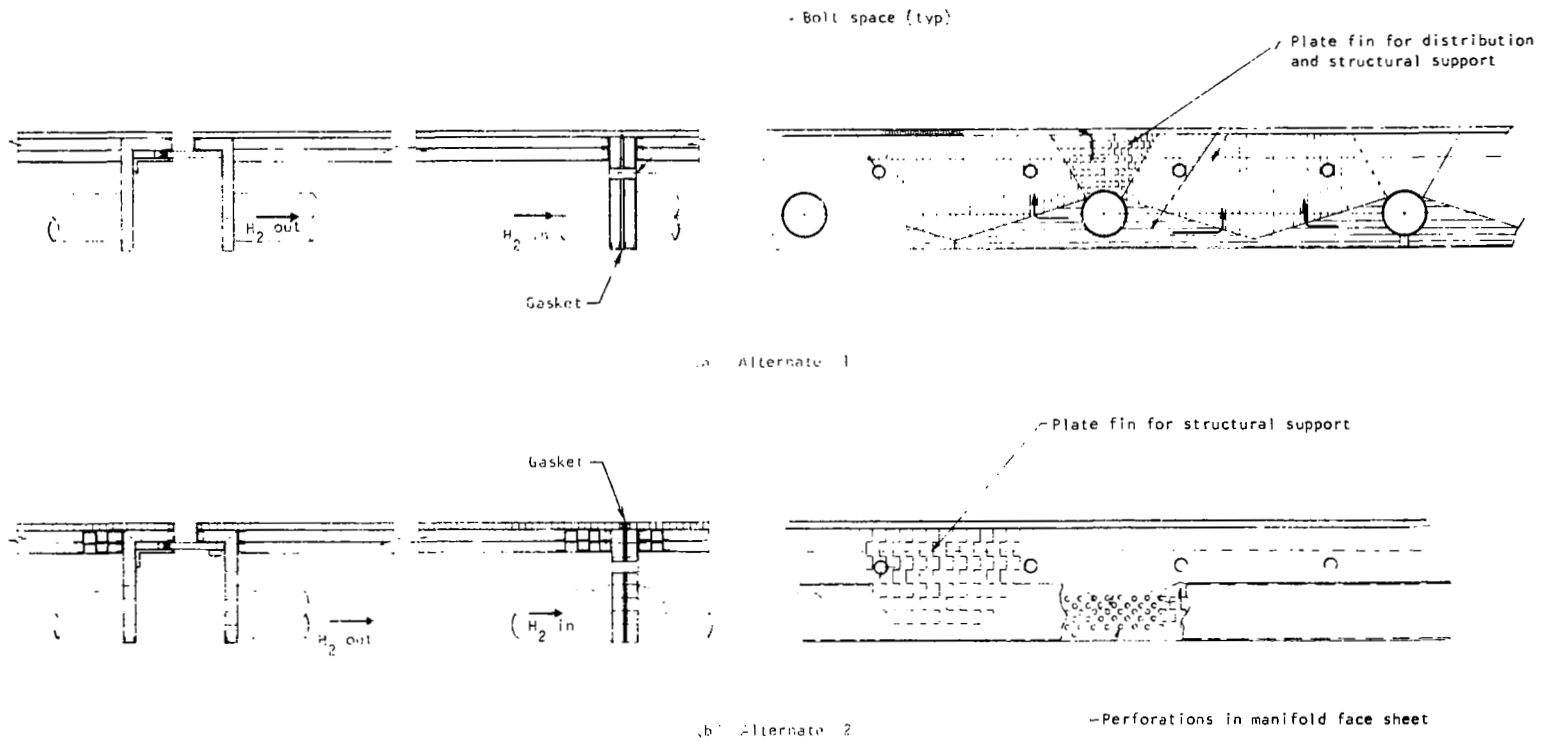


Figure 34. Concluded



Note: Bear back-up structure not shown

Figure 35. Configuration 3a, Alternate Manifolding Arrangements

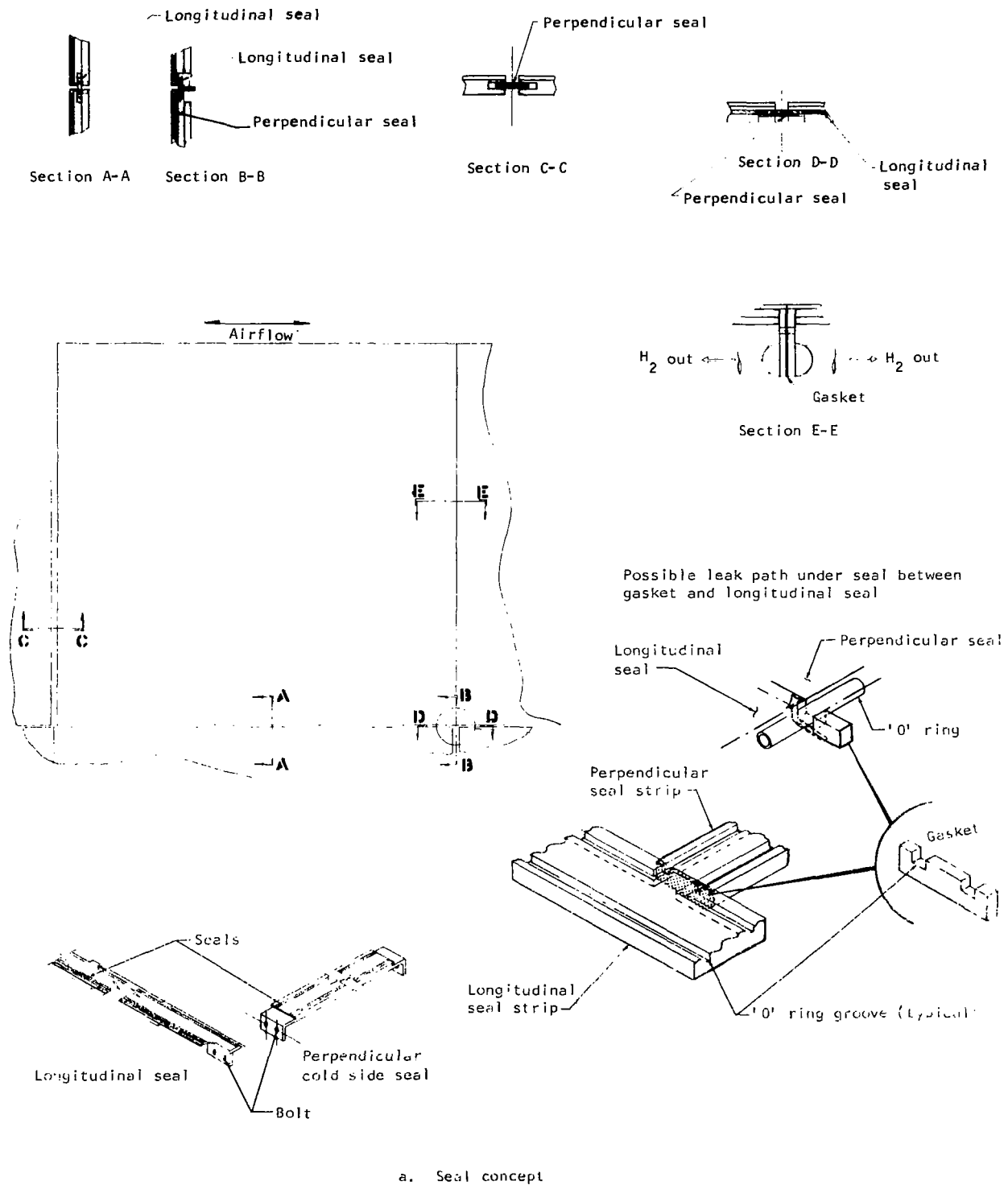
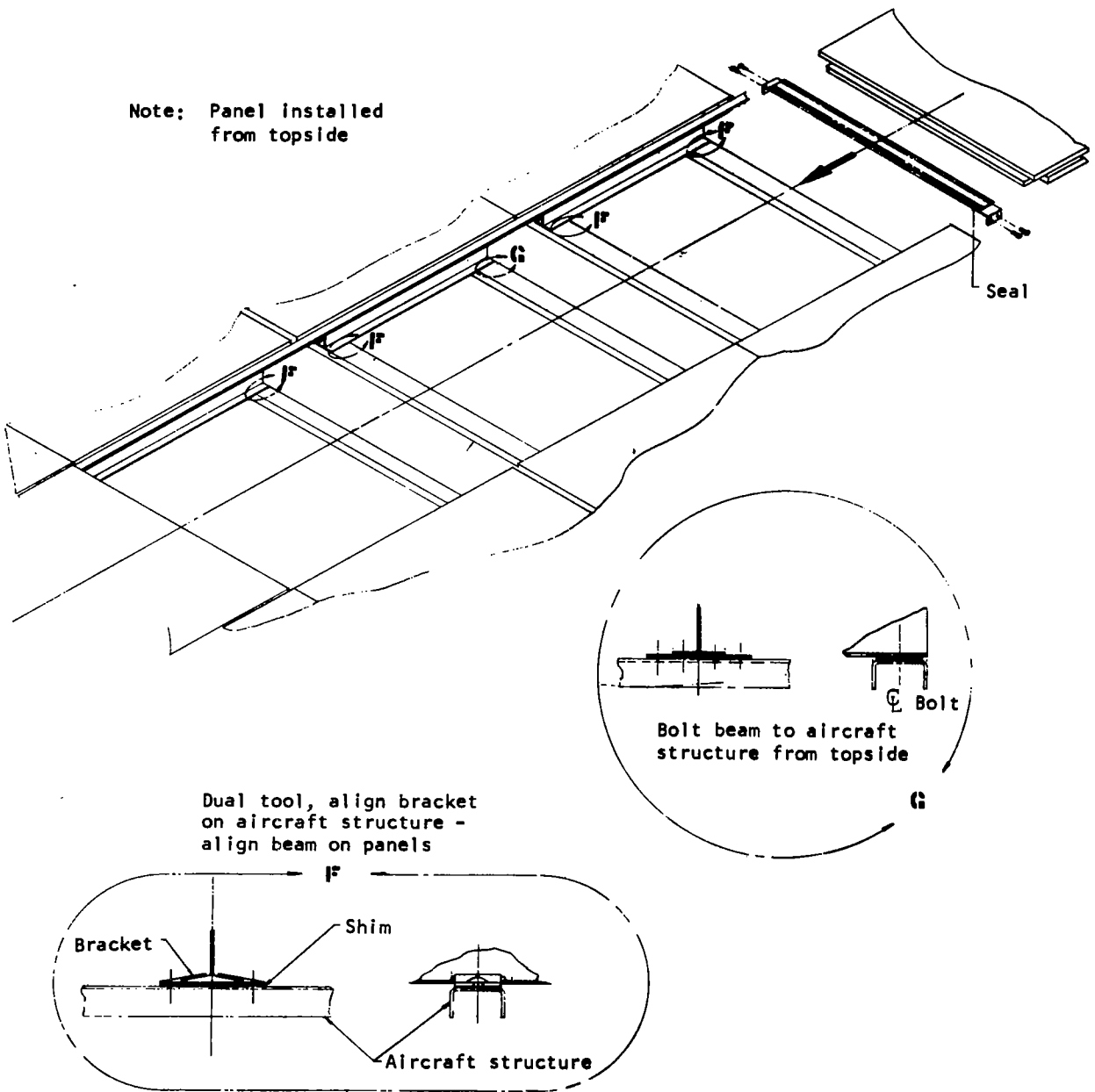


Figure 36. Configuration 3a, Alternate Sealing and Installation Concept



b. Installation

Figure 36. Concluded

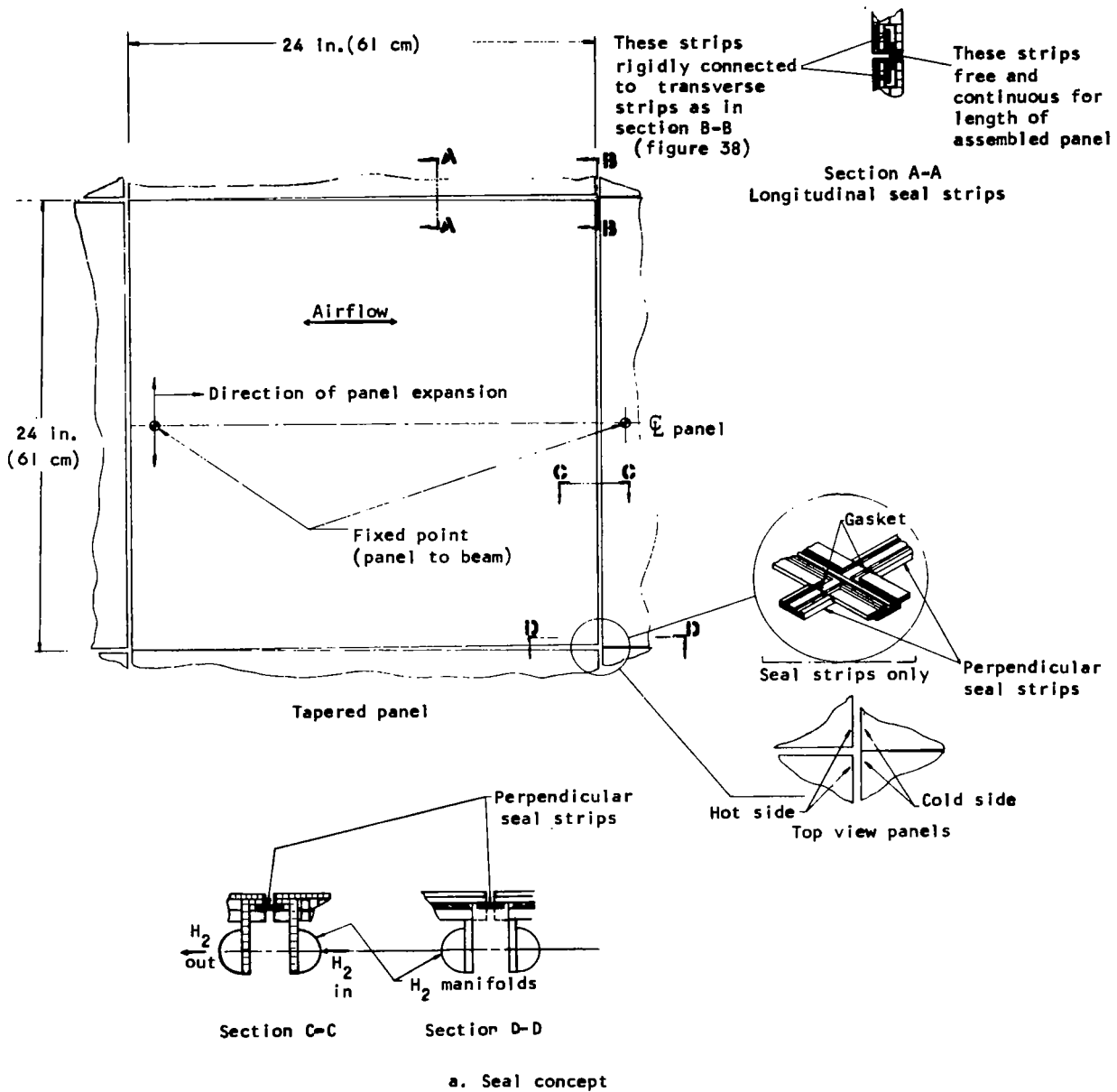
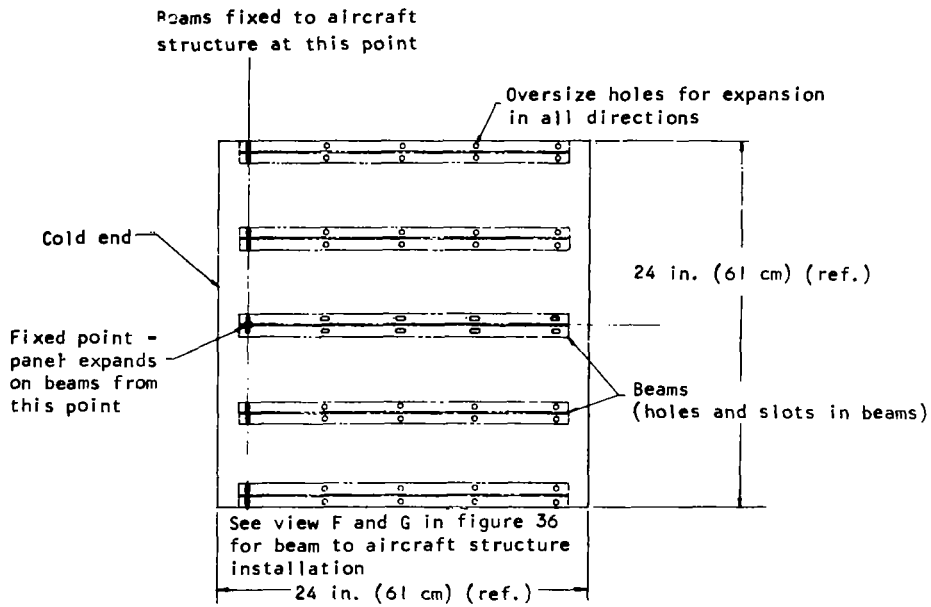
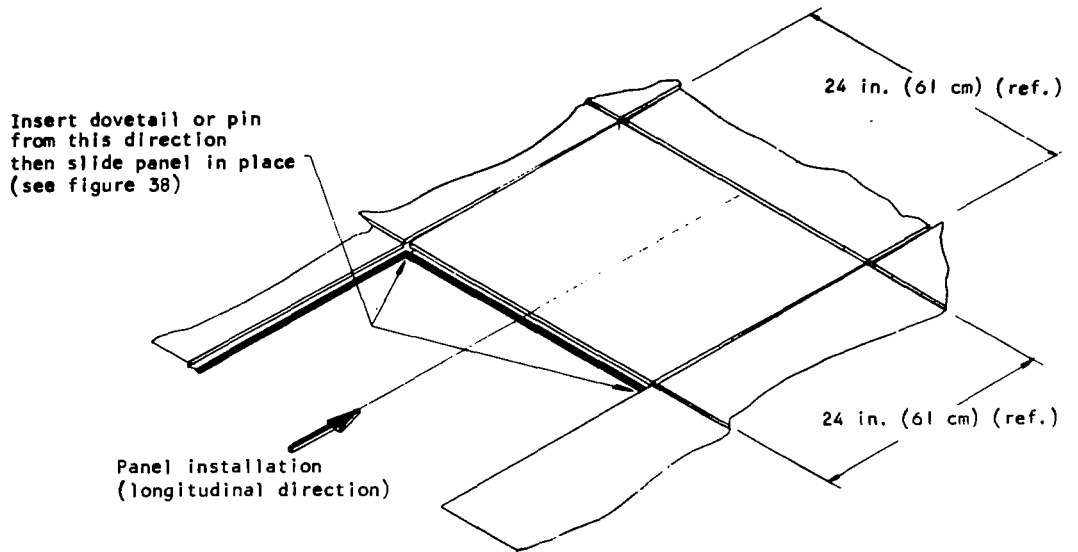
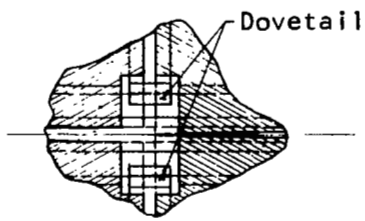
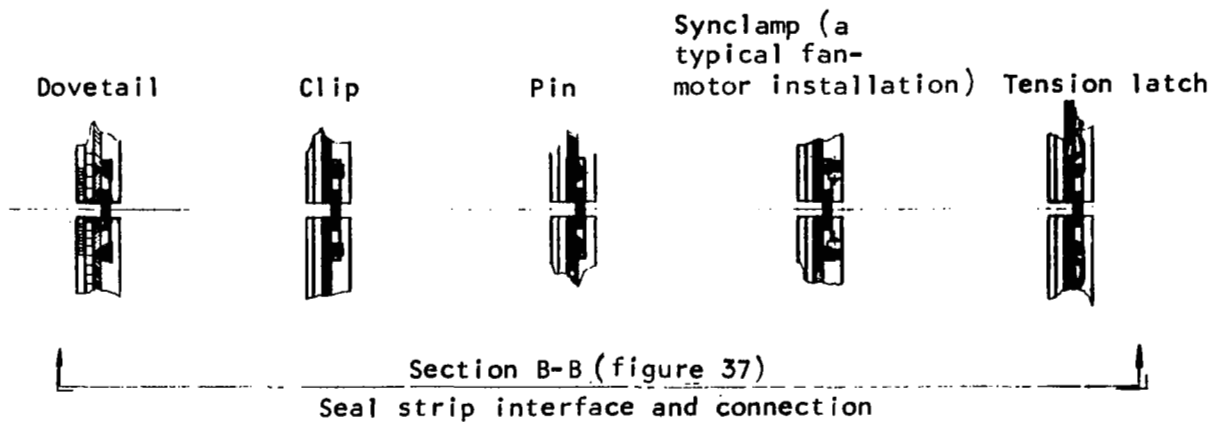


Figure 37. Configuration 5b, Single Panel Layout

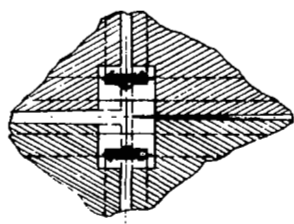


b. Installation

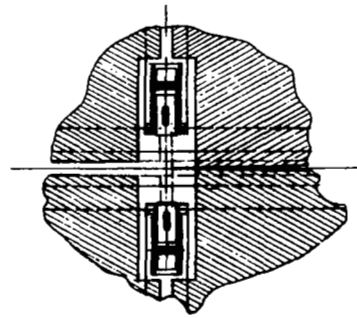
Figure 37. Concluded



Bottom view dovetail, shaded area is panel underside, manifolds omitted for clarity (in all bottom views of Section B-B)



Bottom view, pin



Bottom view, tension latch

Figure 38. Configuration 5b, Seal Connections

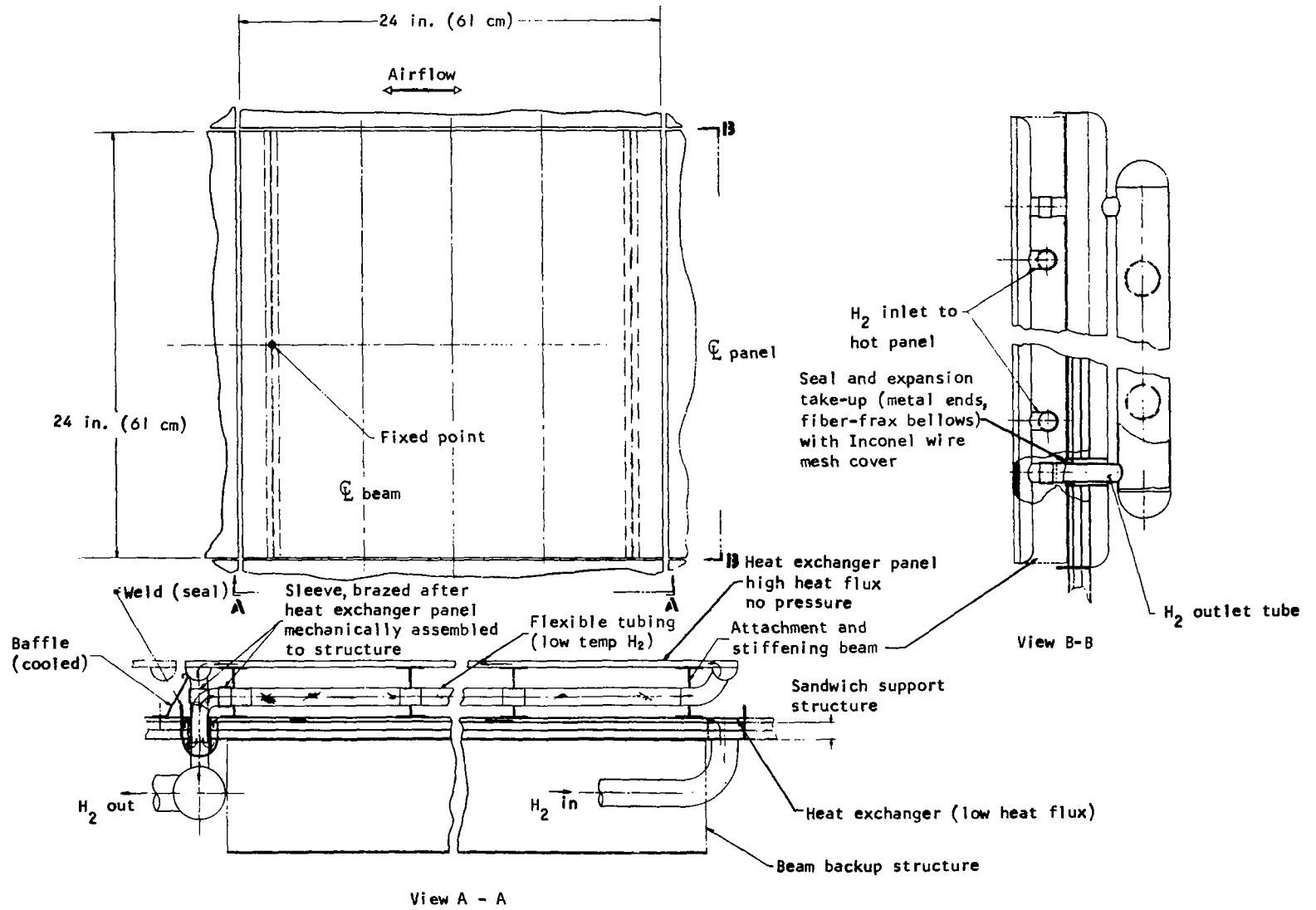


Figure 39. Concept 3 Panel Layout

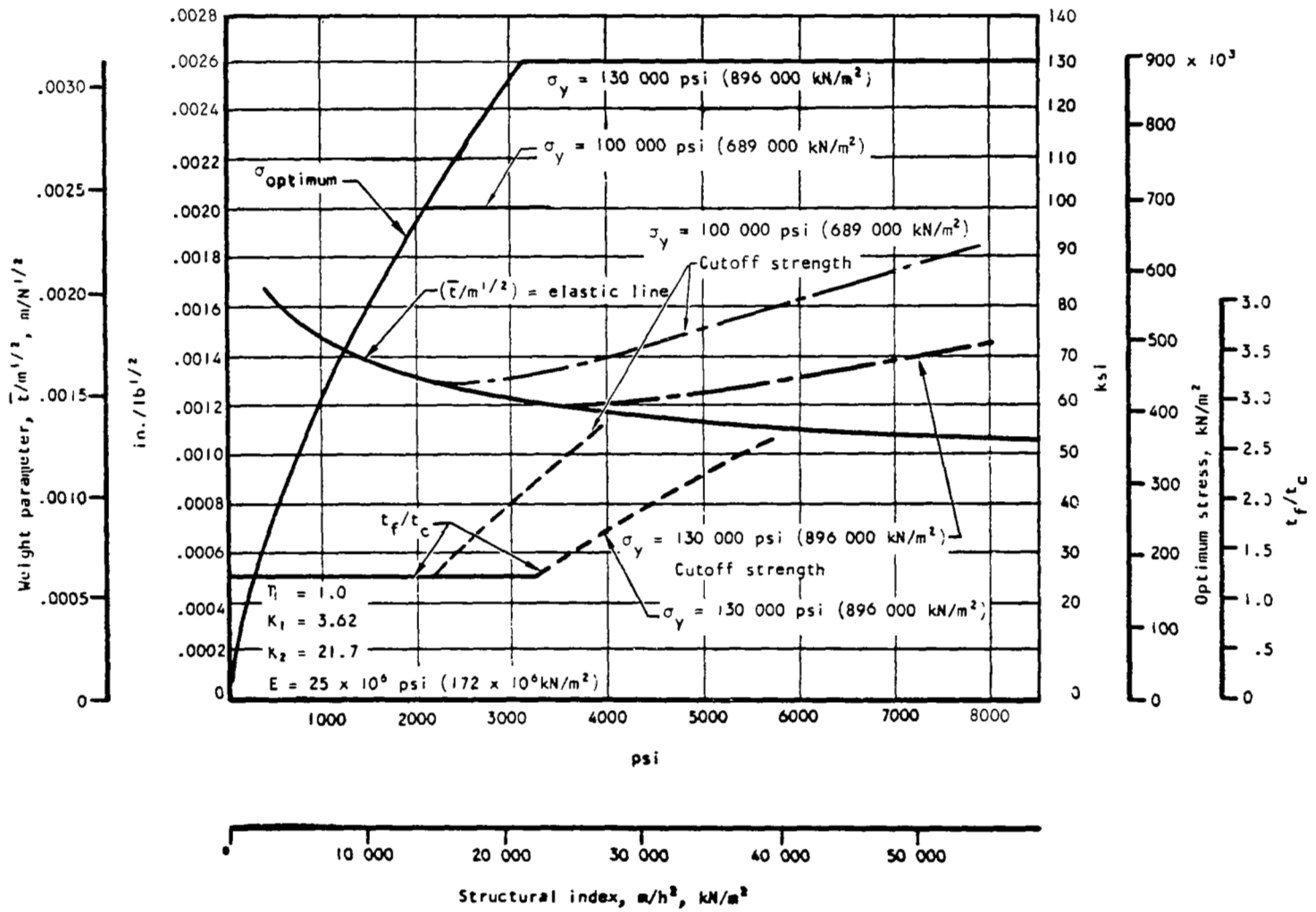


Figure 40. Rectangular-Web-Core Sandwich Plate Parameters vs Structural Index

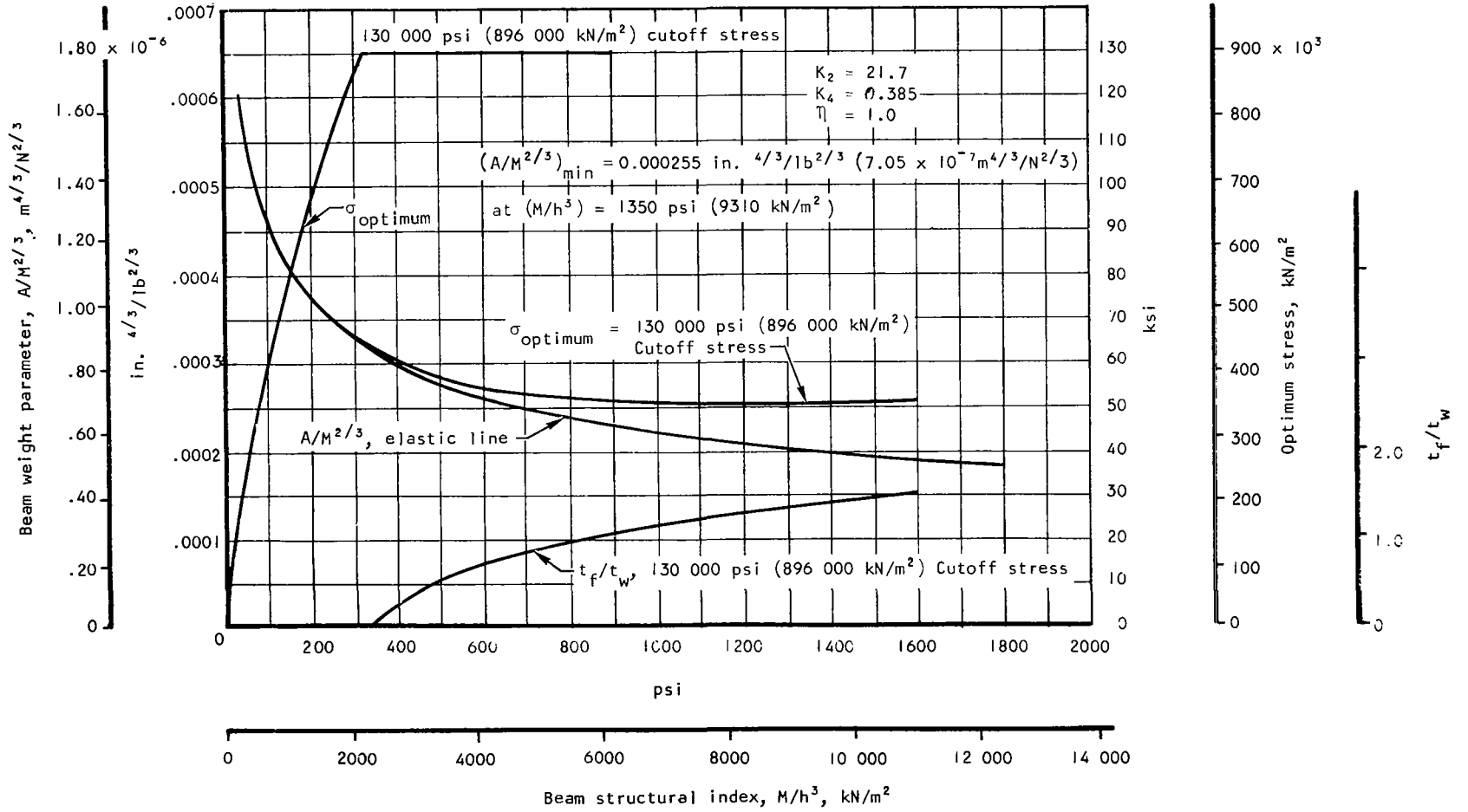
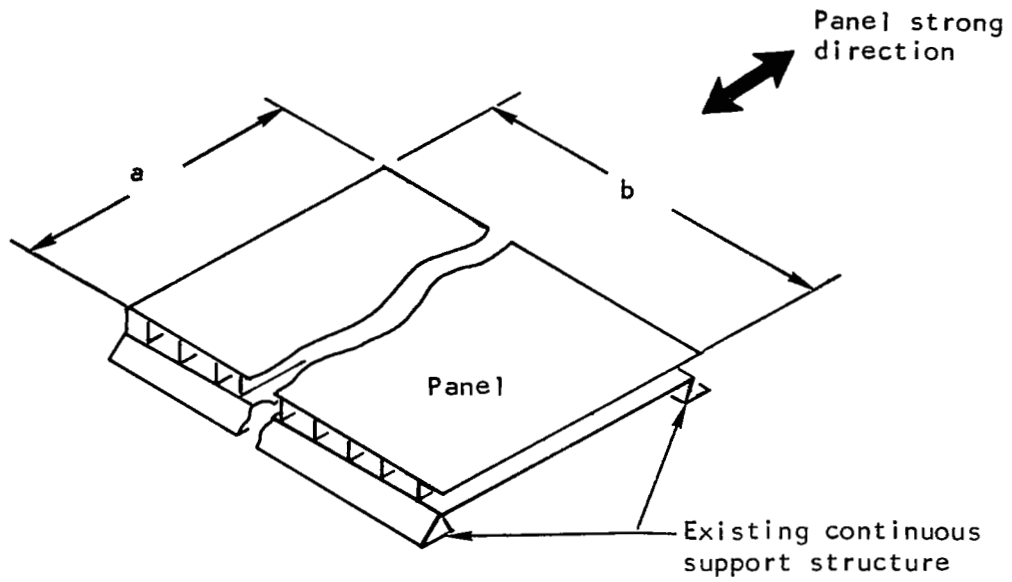
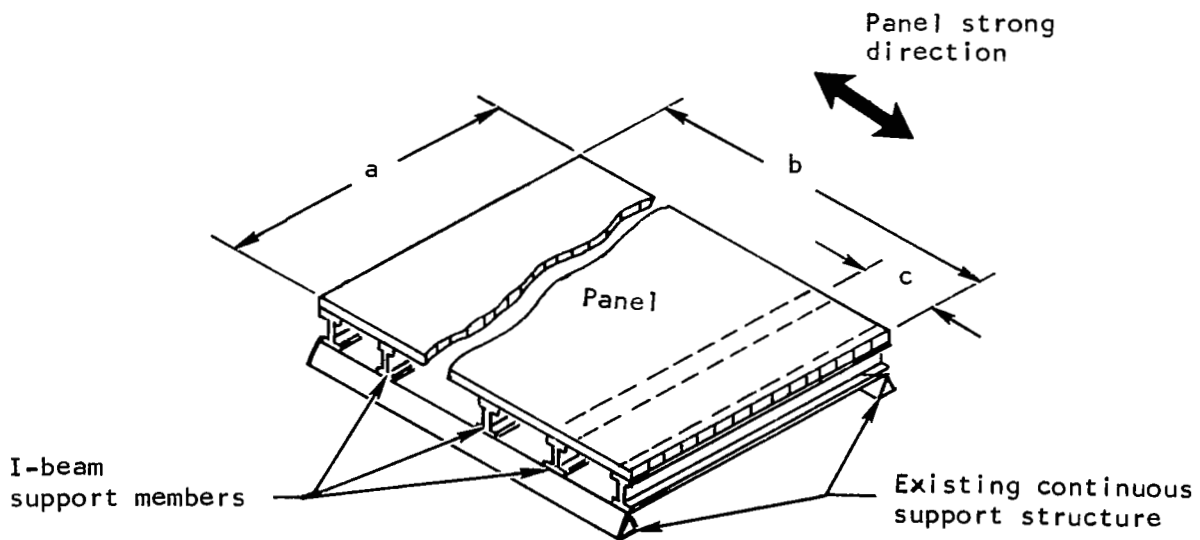


Figure 41. Beam Parameters vs Structural Index



a. Case I. - Panel configuration



b. Case II. - Panel and I-beam combination

Figure 42. Structural Arrangements

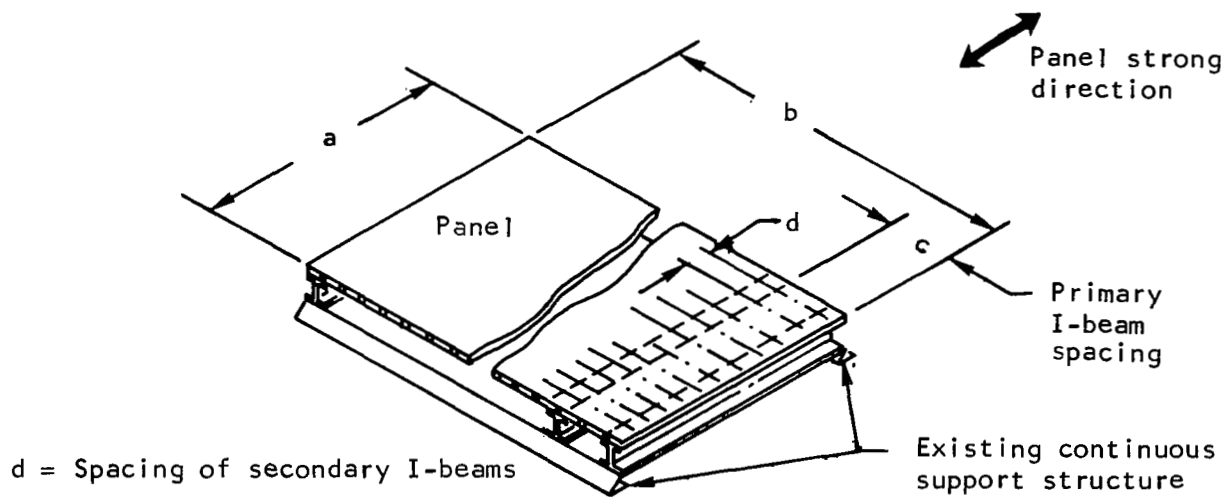


Figure 43. Case III.-Panel and Two-Dimensional I-Beam Array

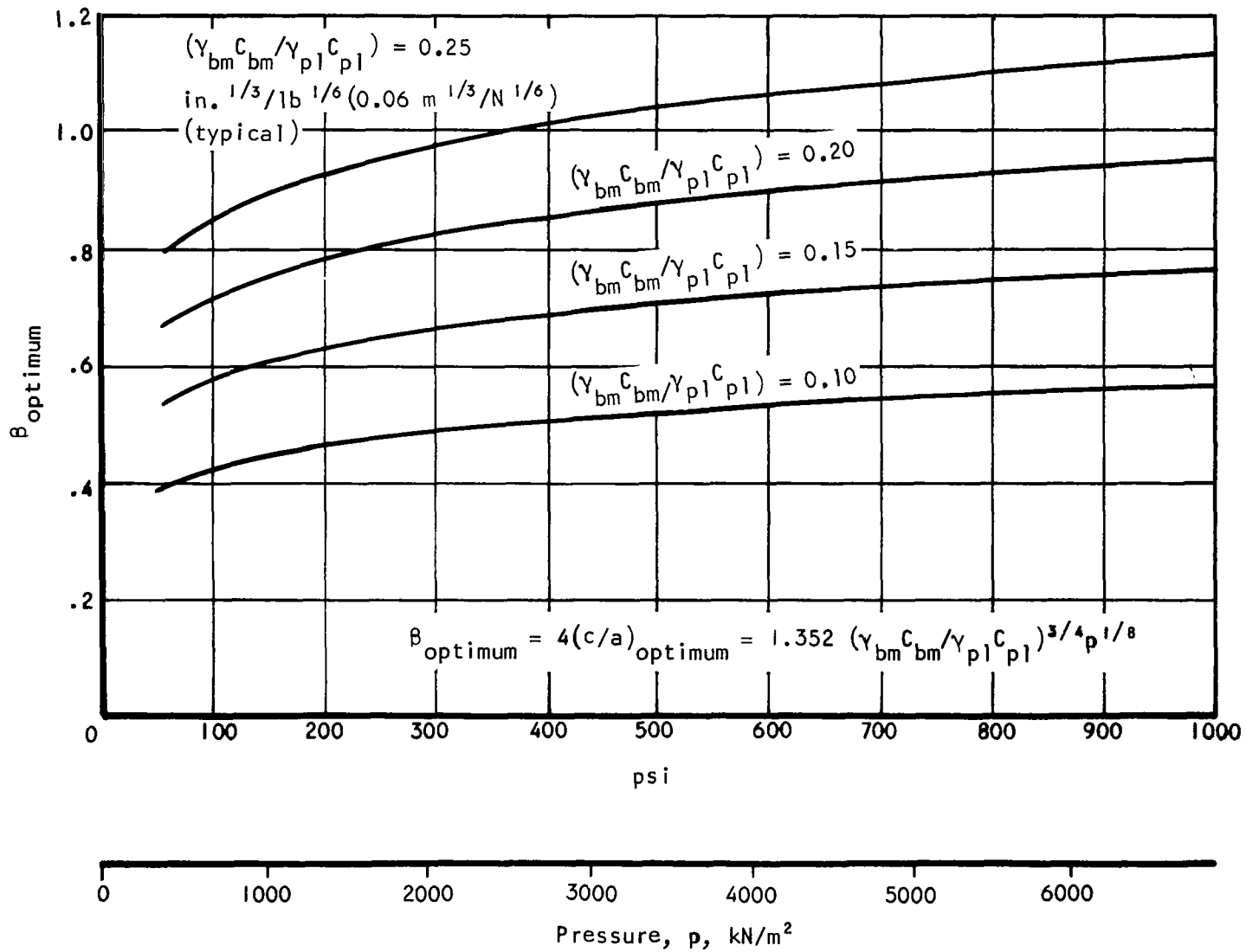


Figure 44. β vs Pressure for Several Values of $(\gamma_{bm} C_{bm} / \gamma_{pl} C_{pl})$

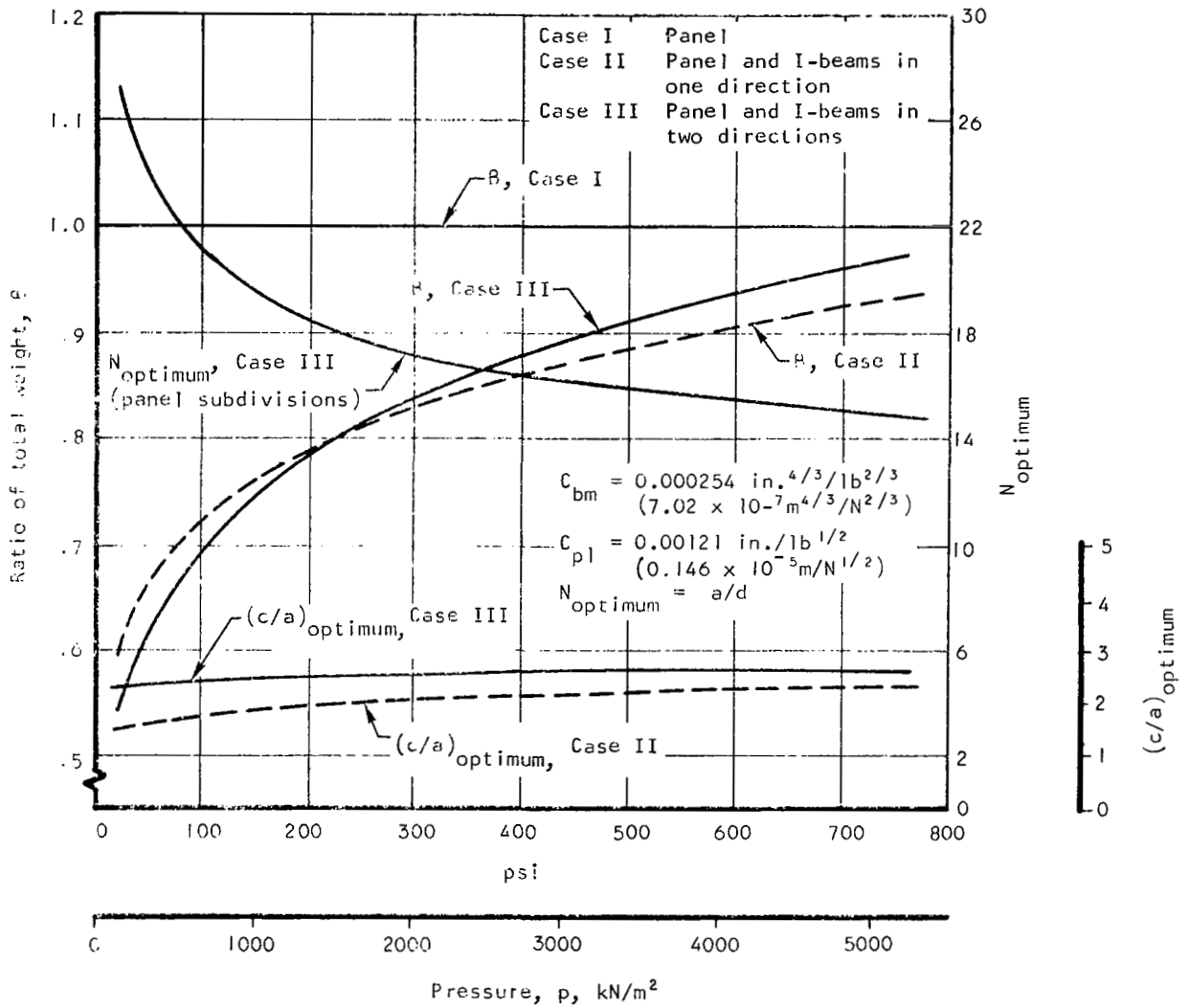


Figure 45. Comparative Panel Weights for Cases I, II, and III

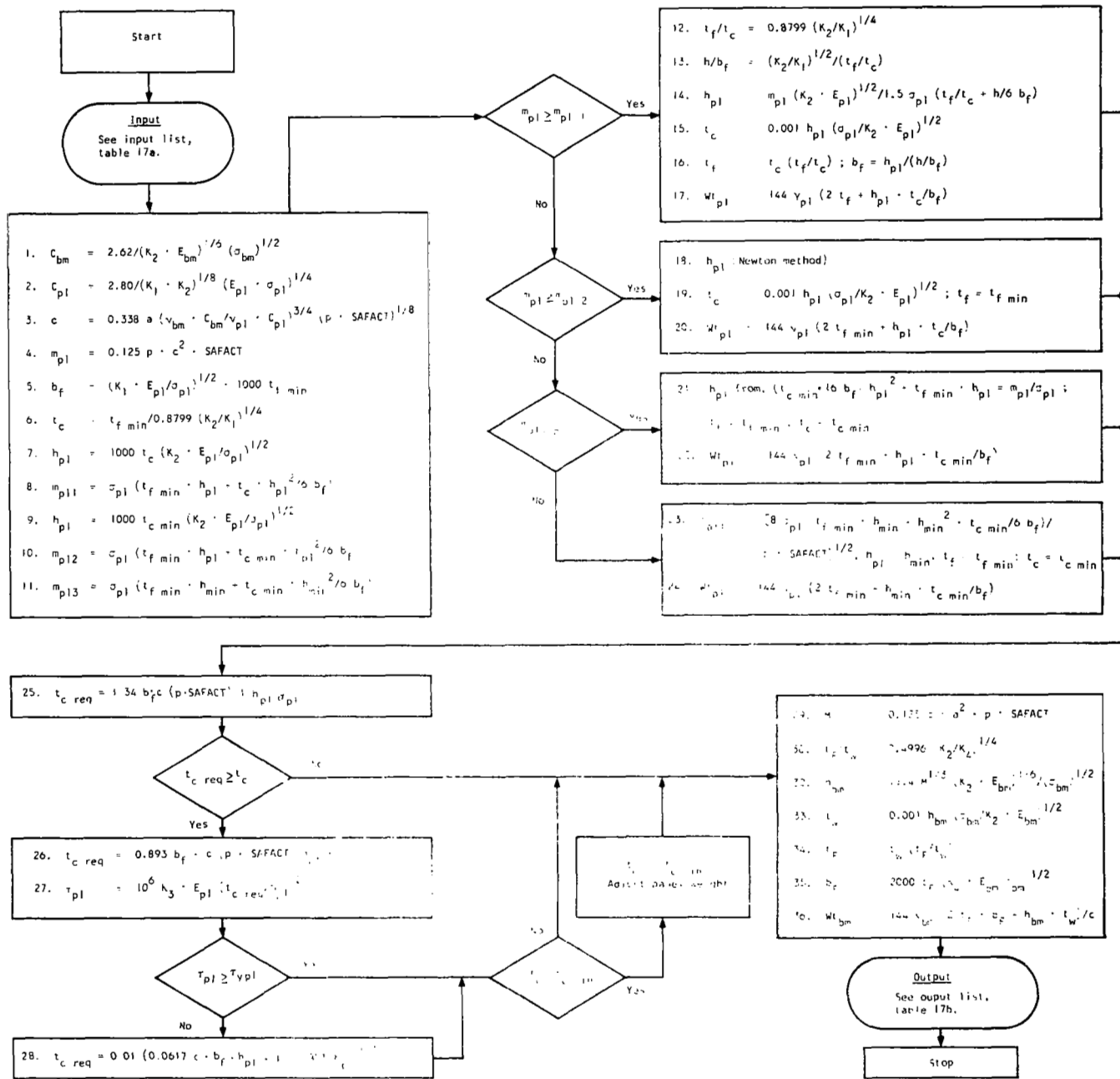


Figure 46. Computer Logic Diagram for Panel and Beam Weight Calculation

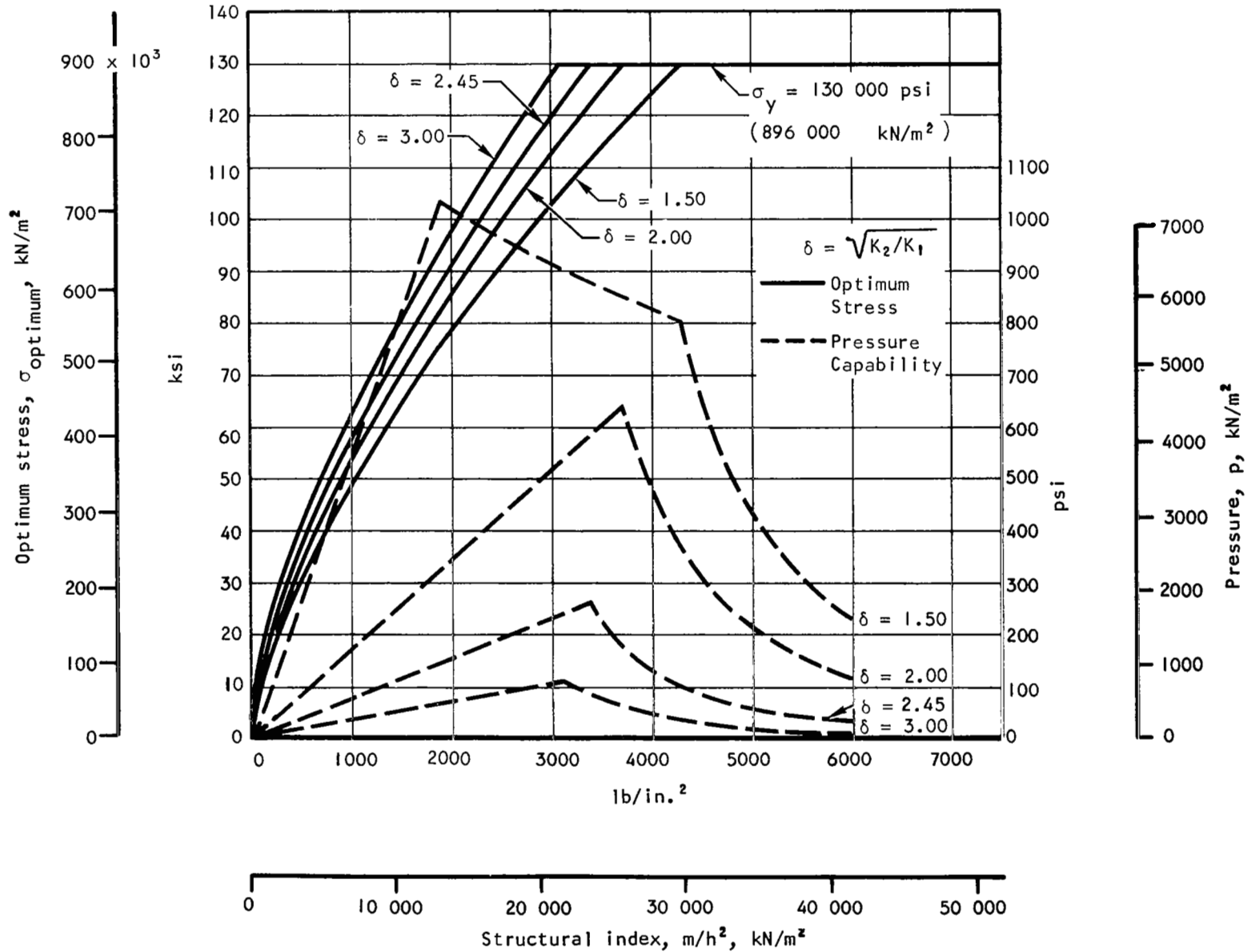


Figure 47. Rectangular-Web-Core Panel Optimum Stress and Pressure vs Structural Index

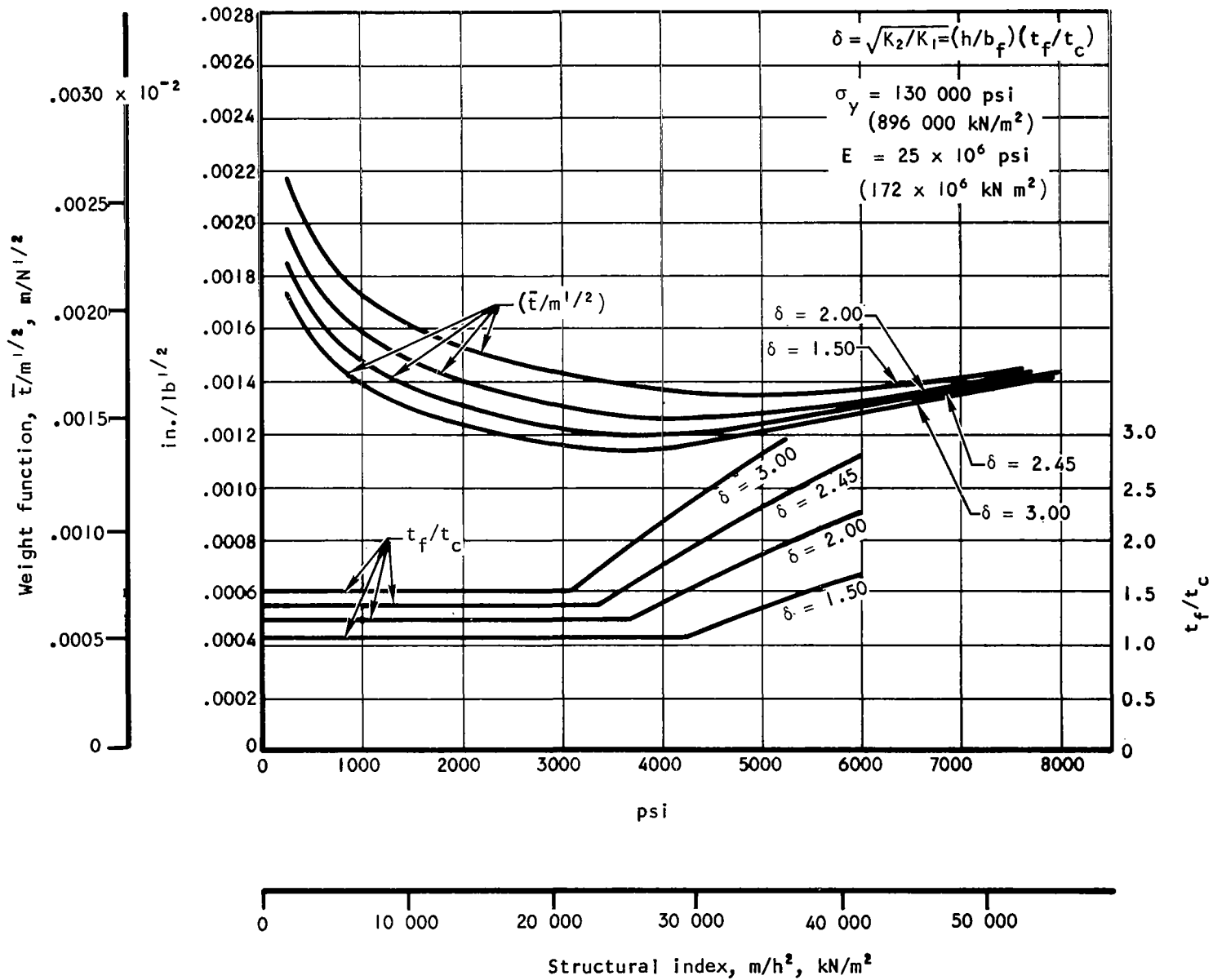


Figure 48. Weight Function vs Structural Index

Equivalent Notations for Sandwich Panels

	Regenerative panels program	NASA TN-3232
Faceplate buckling coefficient	K_f	K_s
Web buckling coefficient	K_c	--
Faceplate thickness	t_f	t_s
Web thickness	t_c	t_w
Web height	h	b_w
Web spacing	b_f	b_s

Also, the following relationships apply

$$K_1 = \pi^2 K_f / 12(1 - \nu^2) = 0.905 K_f$$

$$K_2 = \pi^2 K_c / 12(1 - \nu^2) = 0.905 K_c$$

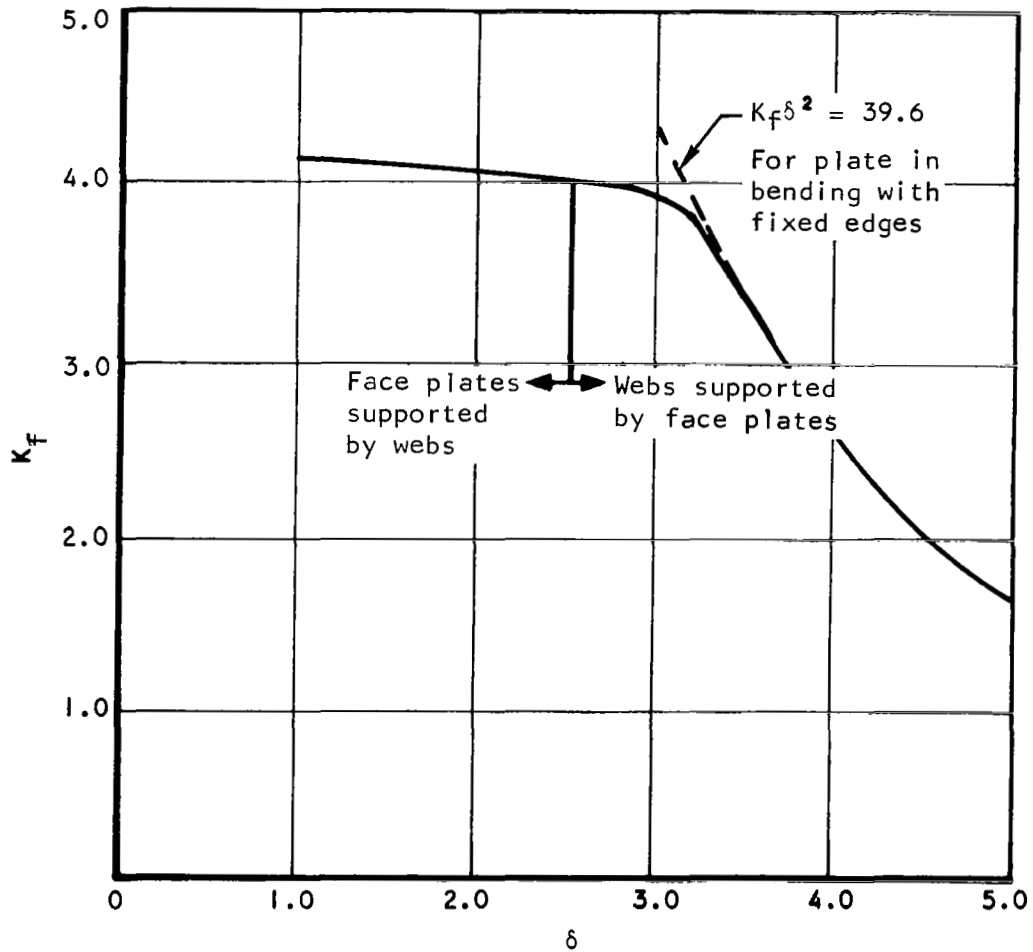


Figure 49. Web and Faceplate Buckling Interaction Curve

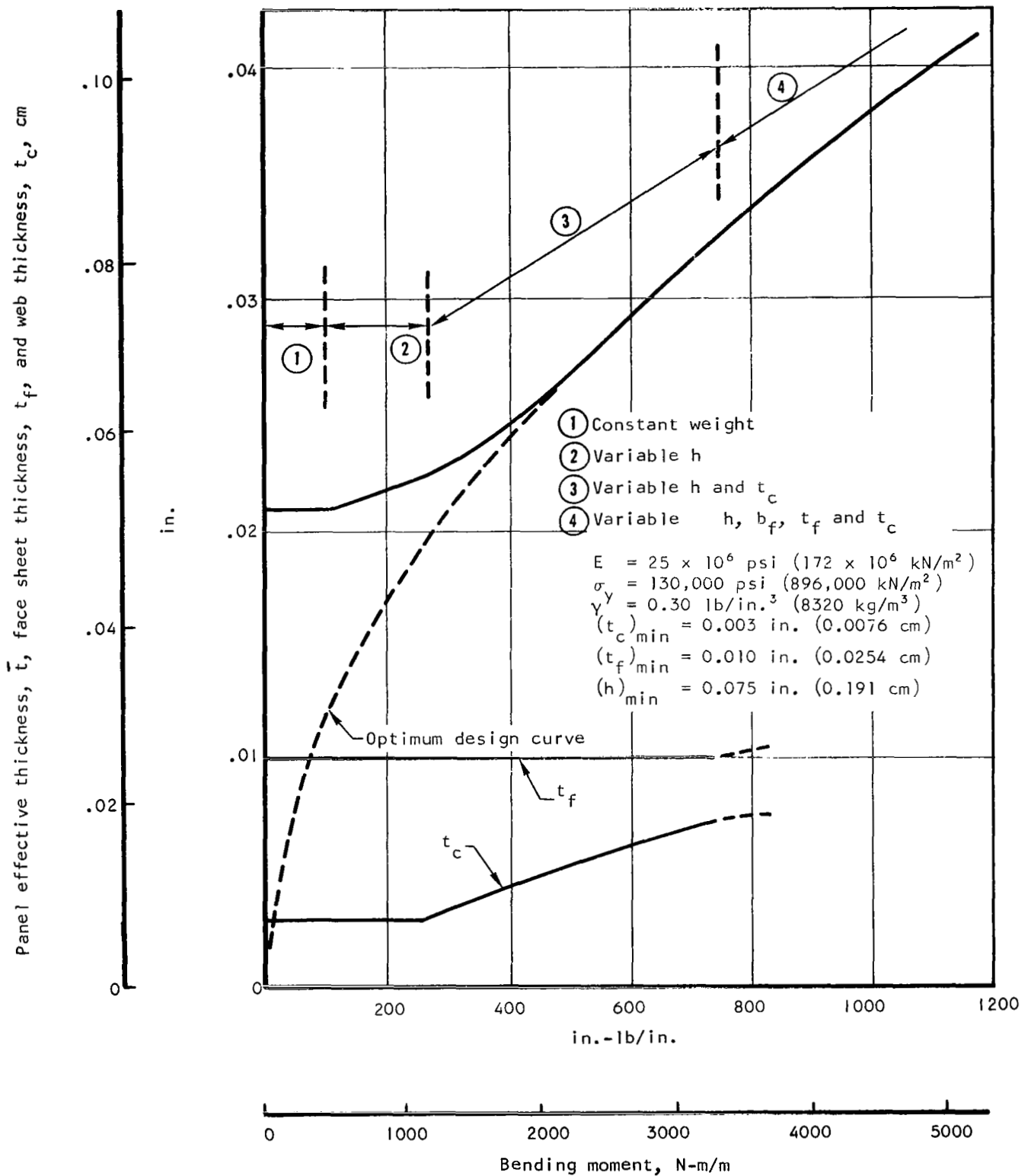


Figure 50. Minimum Panel Weight, Face Sheet Thickness, and Web Thickness vs Bending Moment

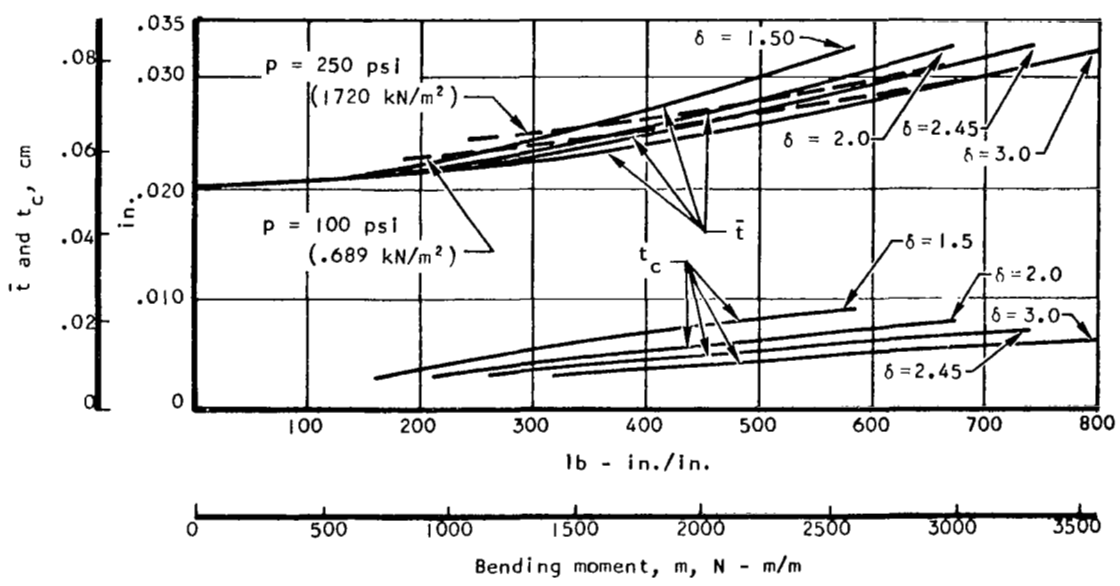
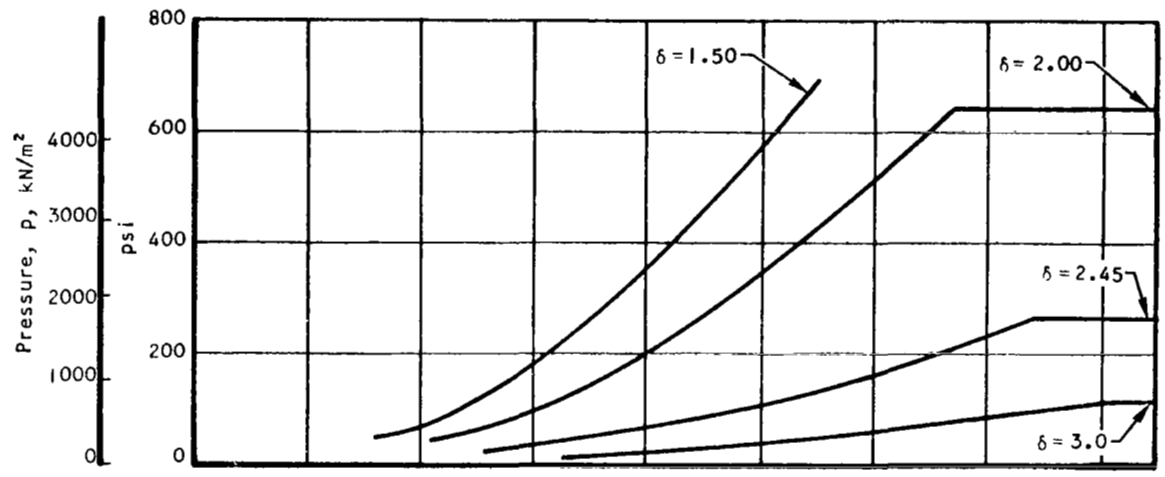


Figure 51. p , \bar{t} , and t_c vs Bending Moment, m

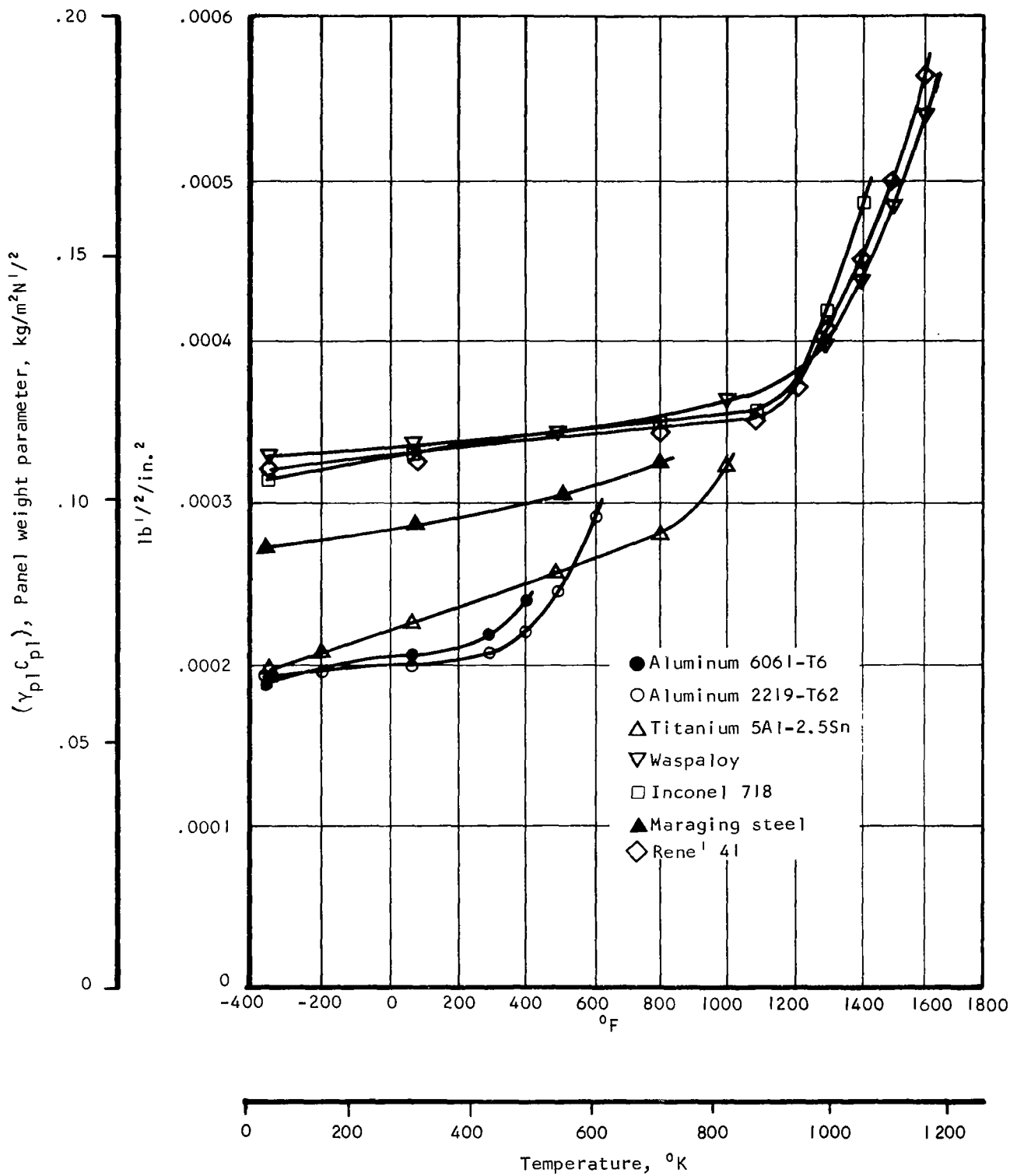


Figure 52. Panel Weight Parameter vs Temperature

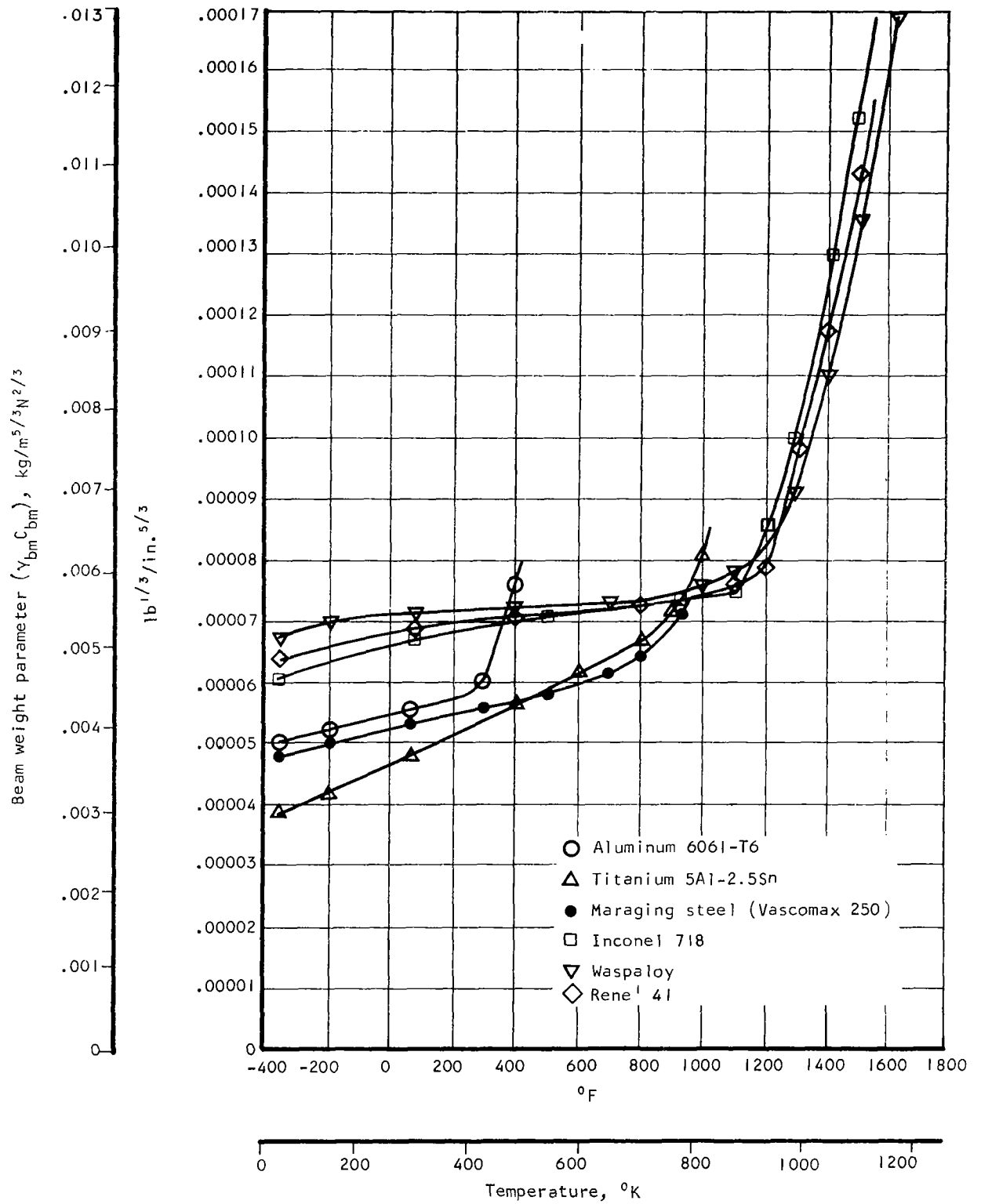


Figure 53. Beam Weight Parameter vs Temperature

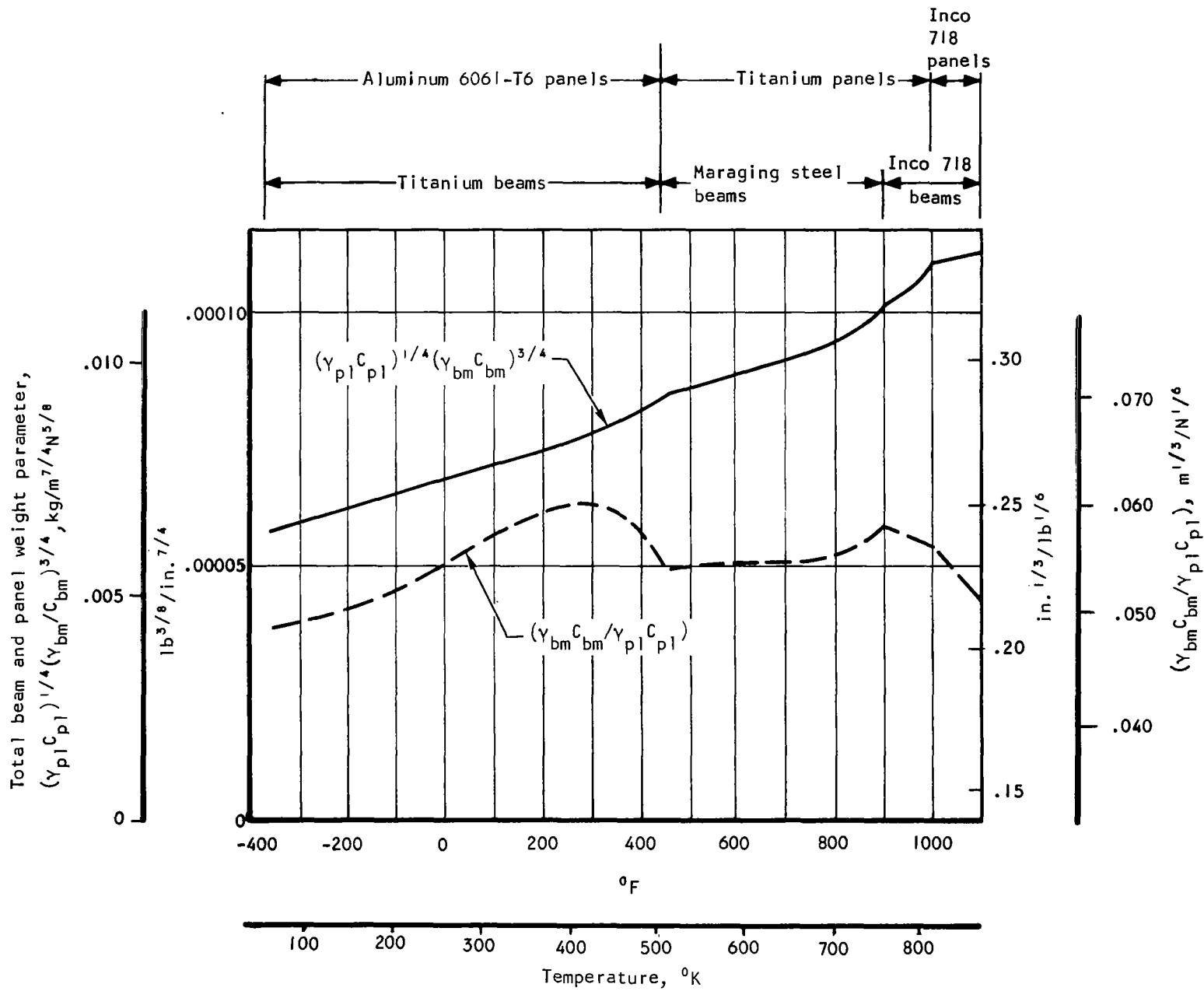


Figure 54. Total Weight Parameter, $(Y_{pl} C_{pl})^{1/4} (Y_{bm} C_{bm})^{3/4}$, and $(Y_{bm} C_{bm} / Y_{pl} C_{pl})$ vs Temperature

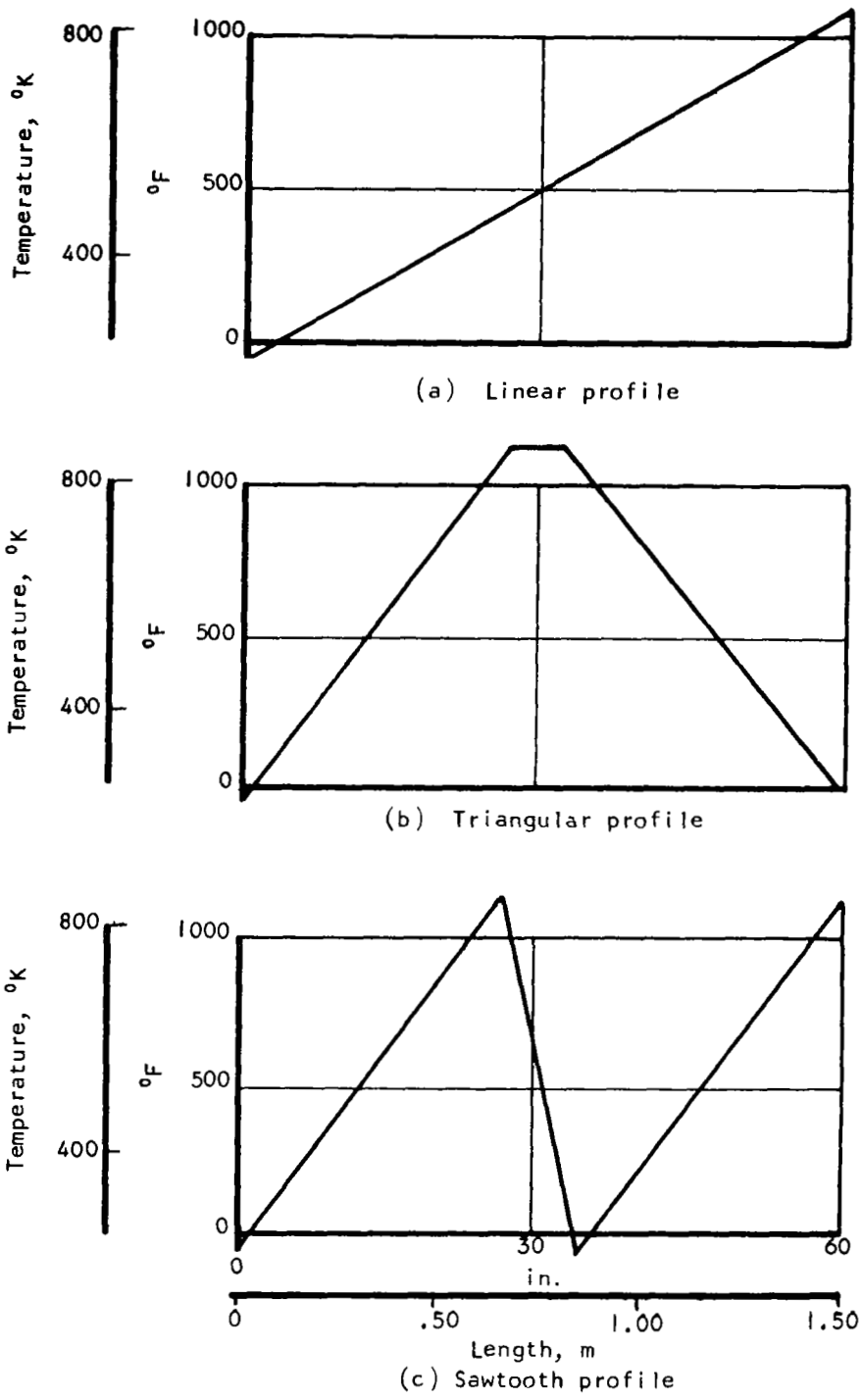
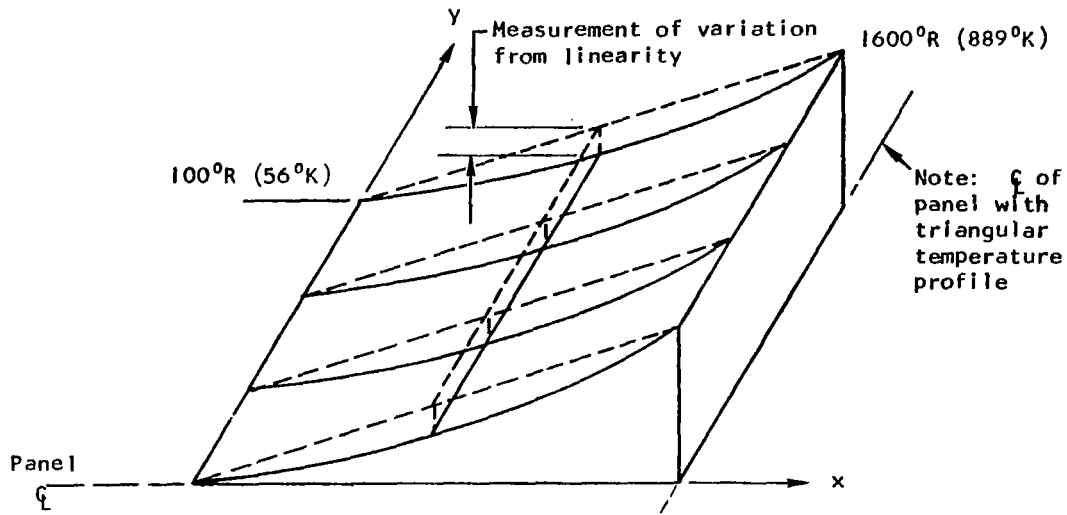
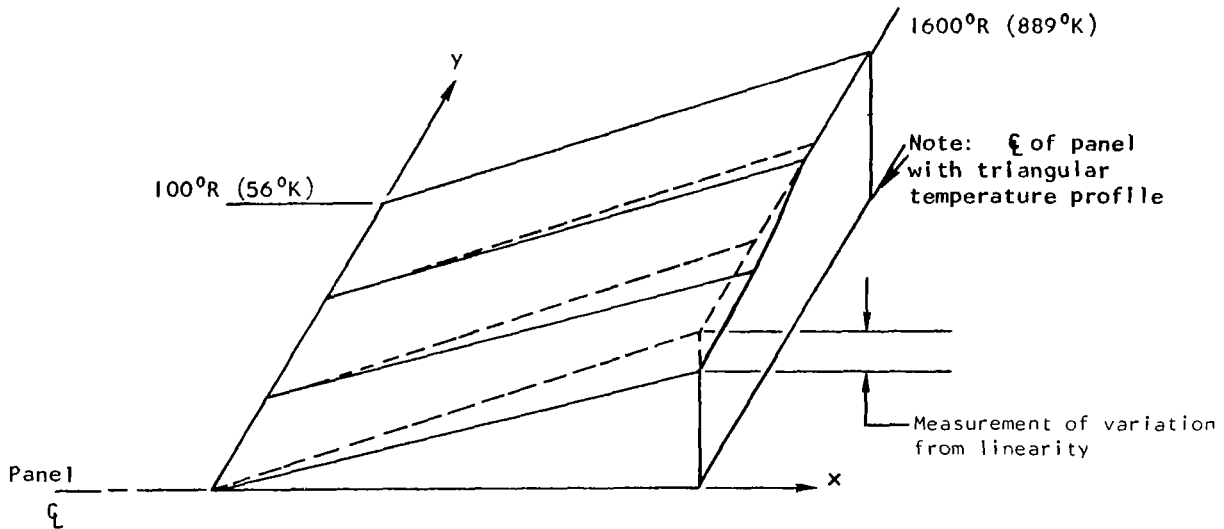


Figure 55. Temperature vs Axial Position in a 5-ft (1.52-m) Panel



a. Parabolic nonlinear increase in panel temperature (dotted lines show linear increase)



b. Linear increase in panel temperature with gaussian flow maldistribution across width (dotted lines show linear increase)

Figure 56. Nonlinear Panel Temperature Profiles (1/2 Panel Shown For Linear Profile and 1/4 Shown For Triangular Profile)

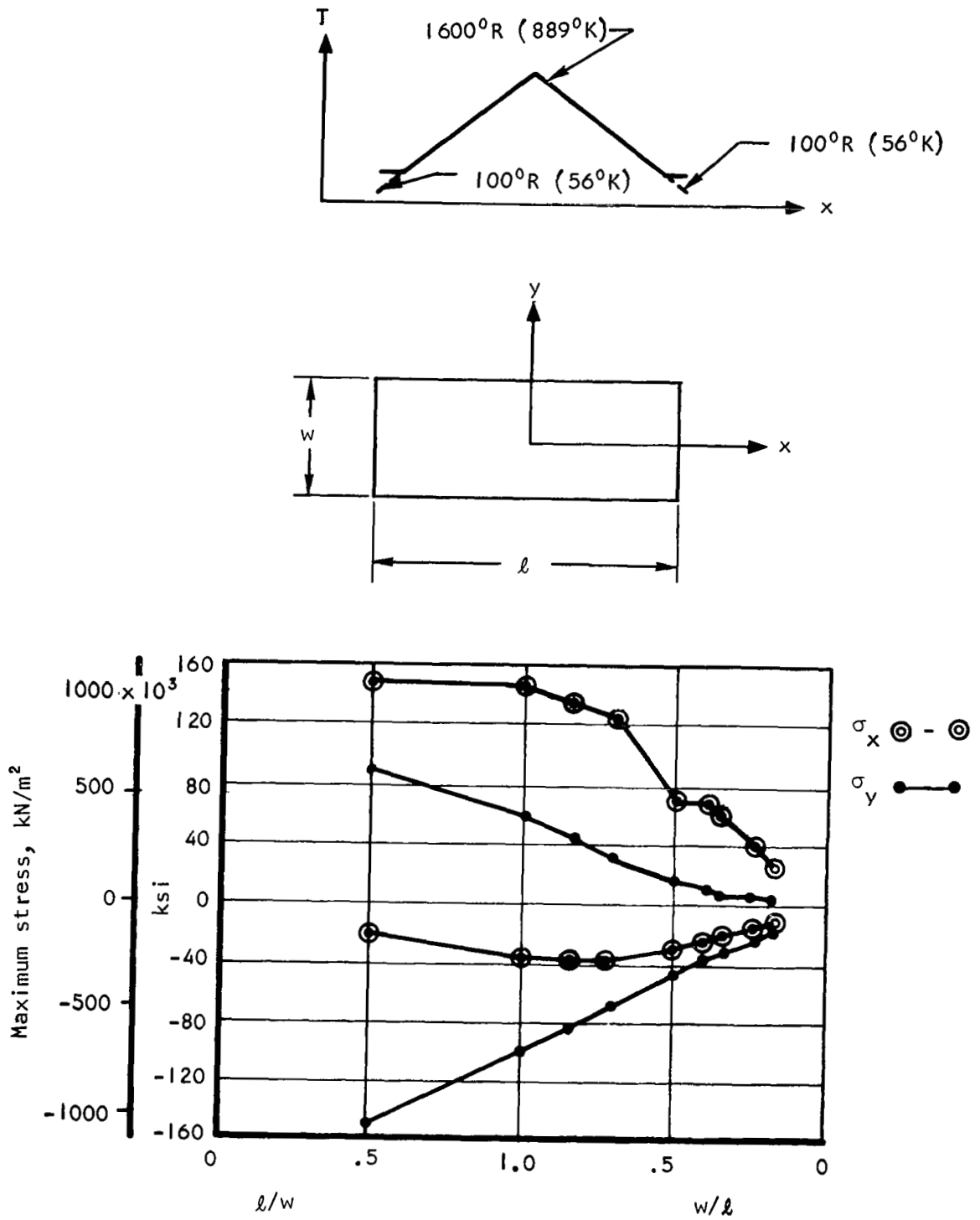


Figure 57. Maximum Tension and Compression Stresses for Triangular Temperature Profile vs Aspect Ratio

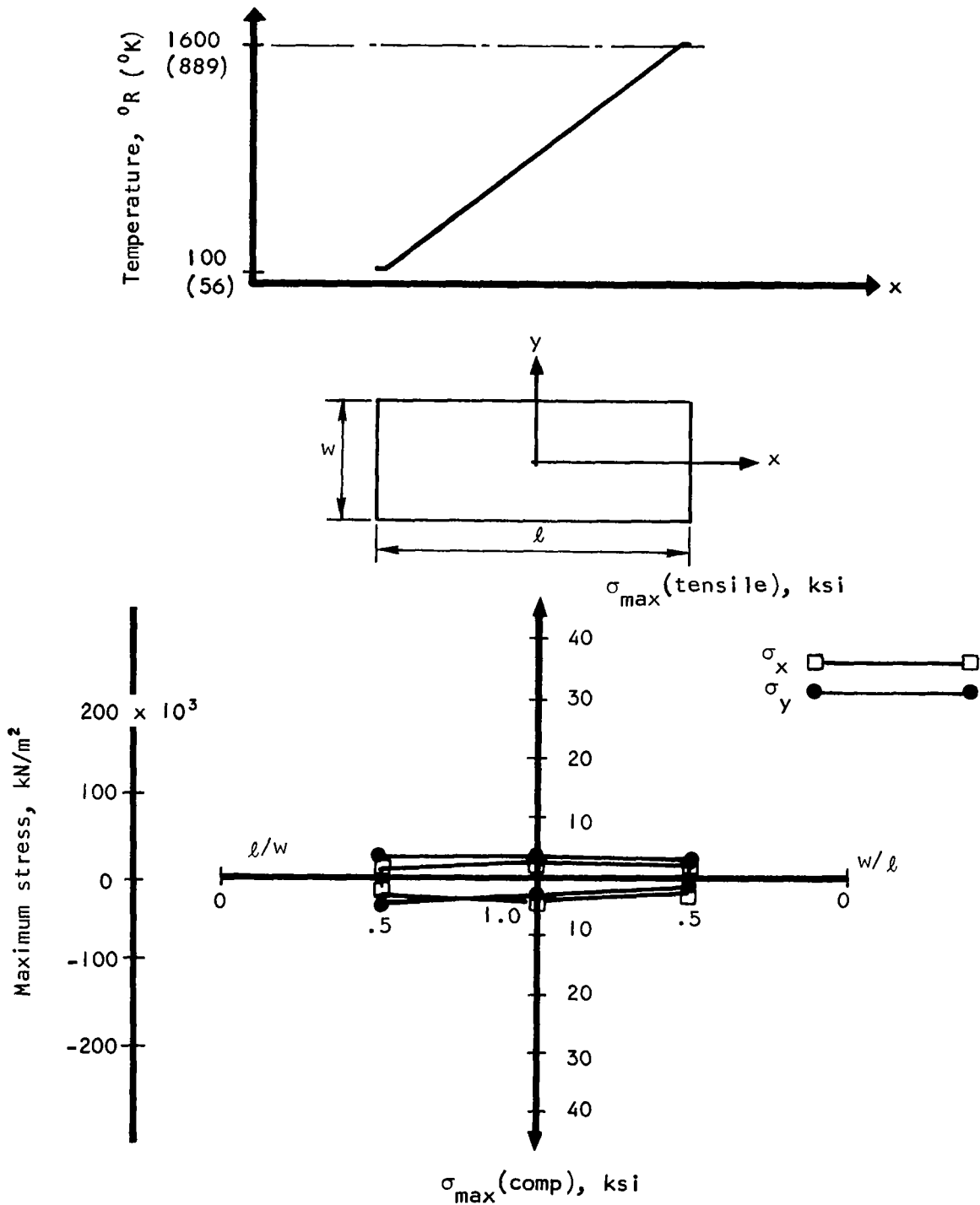


Figure 58. Maximum Tension and Compression Stresses for Linear Temperature Profile vs Aspect Ratio

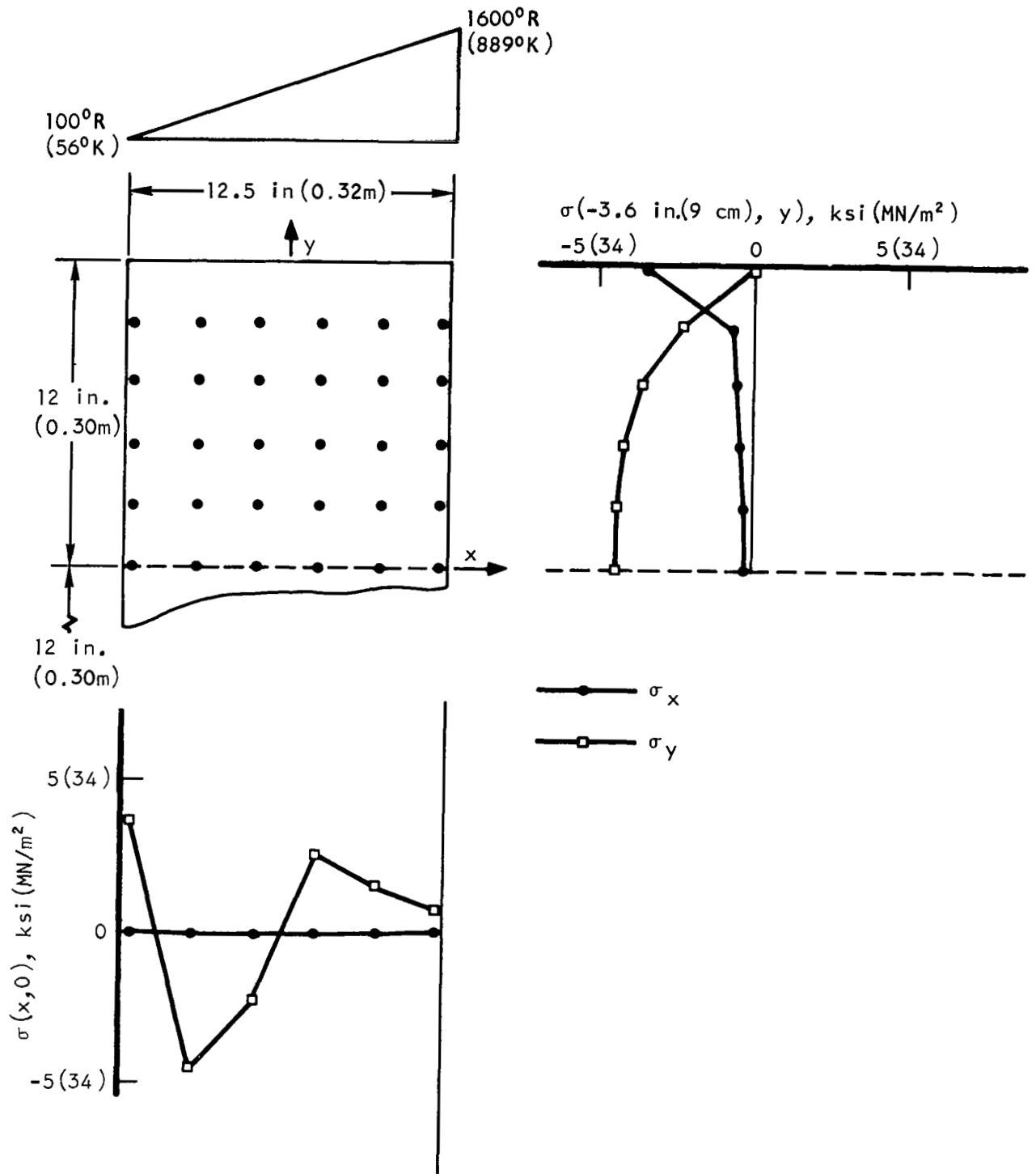
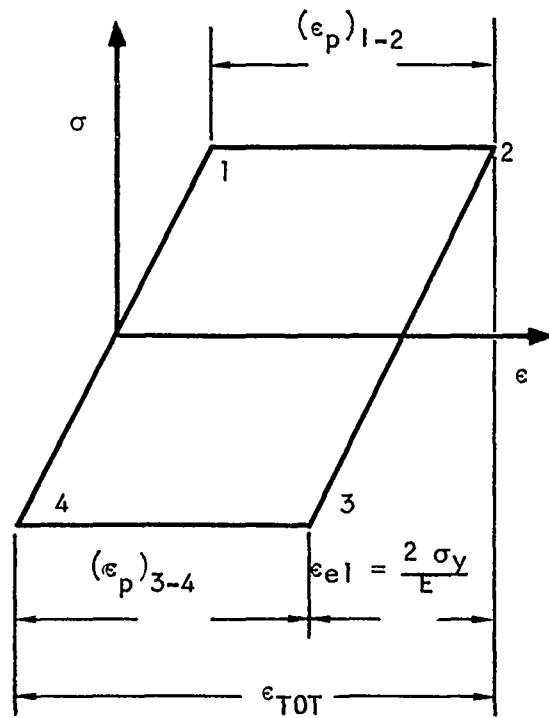


Figure 59. Typical Panel Layout and Stress Distribution, Linear Profile With 0.52 Aspect Ratio

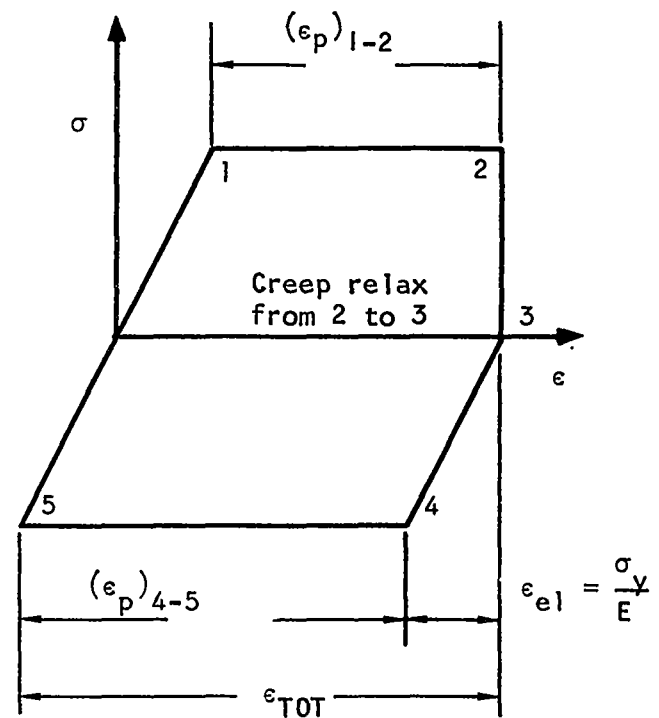


Cycle without creep

$$(\epsilon_p)_{1-2} = \epsilon_{TOT} - \frac{2\sigma_y}{E}$$

$$(\epsilon_p)_{3-4} = \epsilon_{TOT} - \frac{2\sigma_y}{E}$$

A-14751



Cycle with creep

$$(\epsilon_p)_{1-2} = \epsilon_{TOT} - \frac{2\sigma_y}{E}$$

$$(\epsilon_p)_{4-5} = \epsilon_{TOT} - \frac{\sigma_y}{E}$$

Figure 60. Typical Ideal Elastic-Plastic Load Cycles

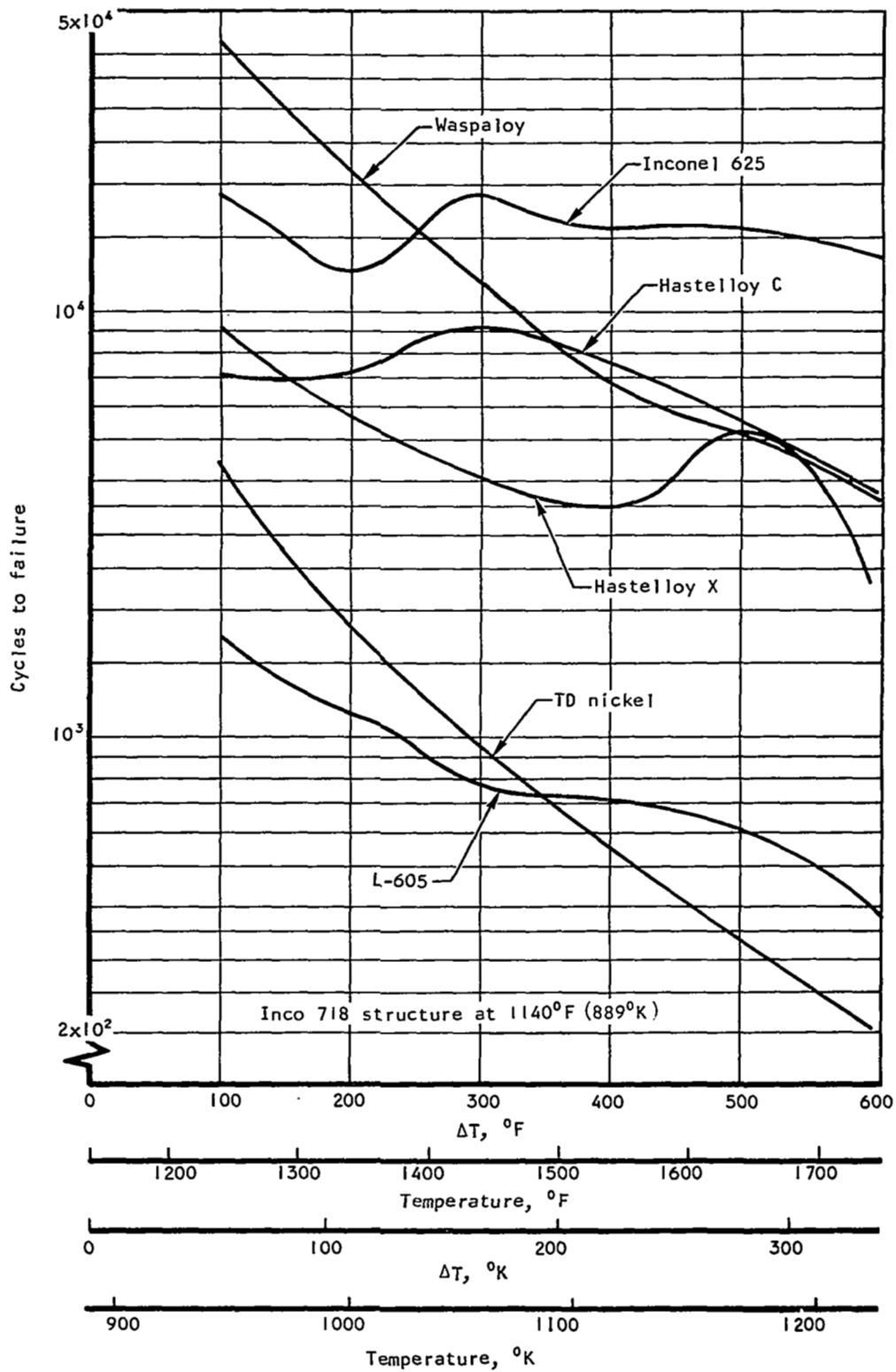


Figure 61. Cycles to Failure for Heat Exchanger Surface vs Temperature

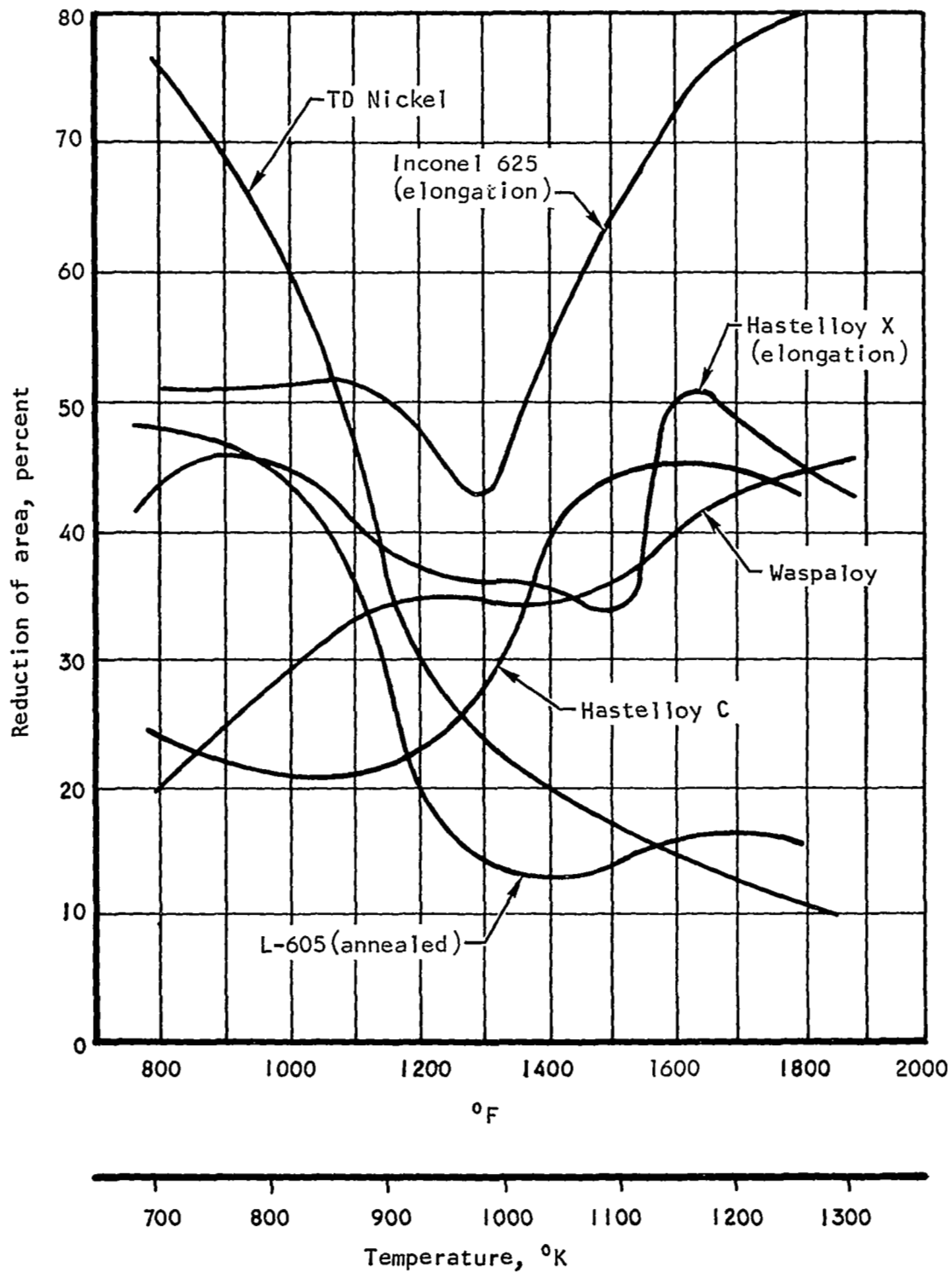


Figure 62. Ductility of Various Materials at Elevated Temperature (Data is Reduction in Area Except as Noted)

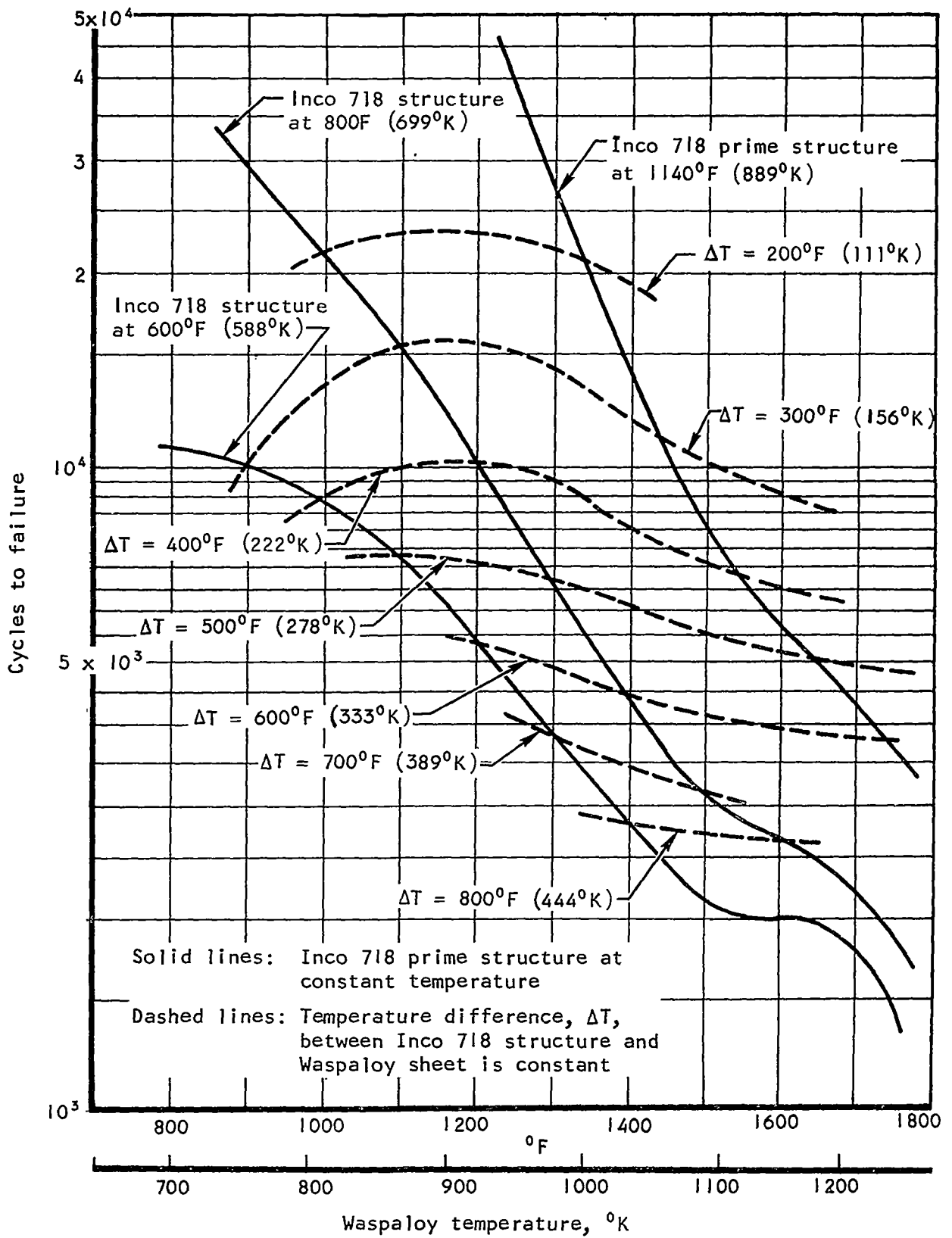


Figure 63. Cycles to Failure vs Temperature for a Waspaloy Heat Exchanger

- Note: 1. t_{fin} , in. (cm), as noted beside curves
 2. Fin geometry:
 $20(7.9)R0-h_{fin}-t_{fin}$ for offset
 $20(7.9)R-h_{fin}-t_{fin}$ for plain

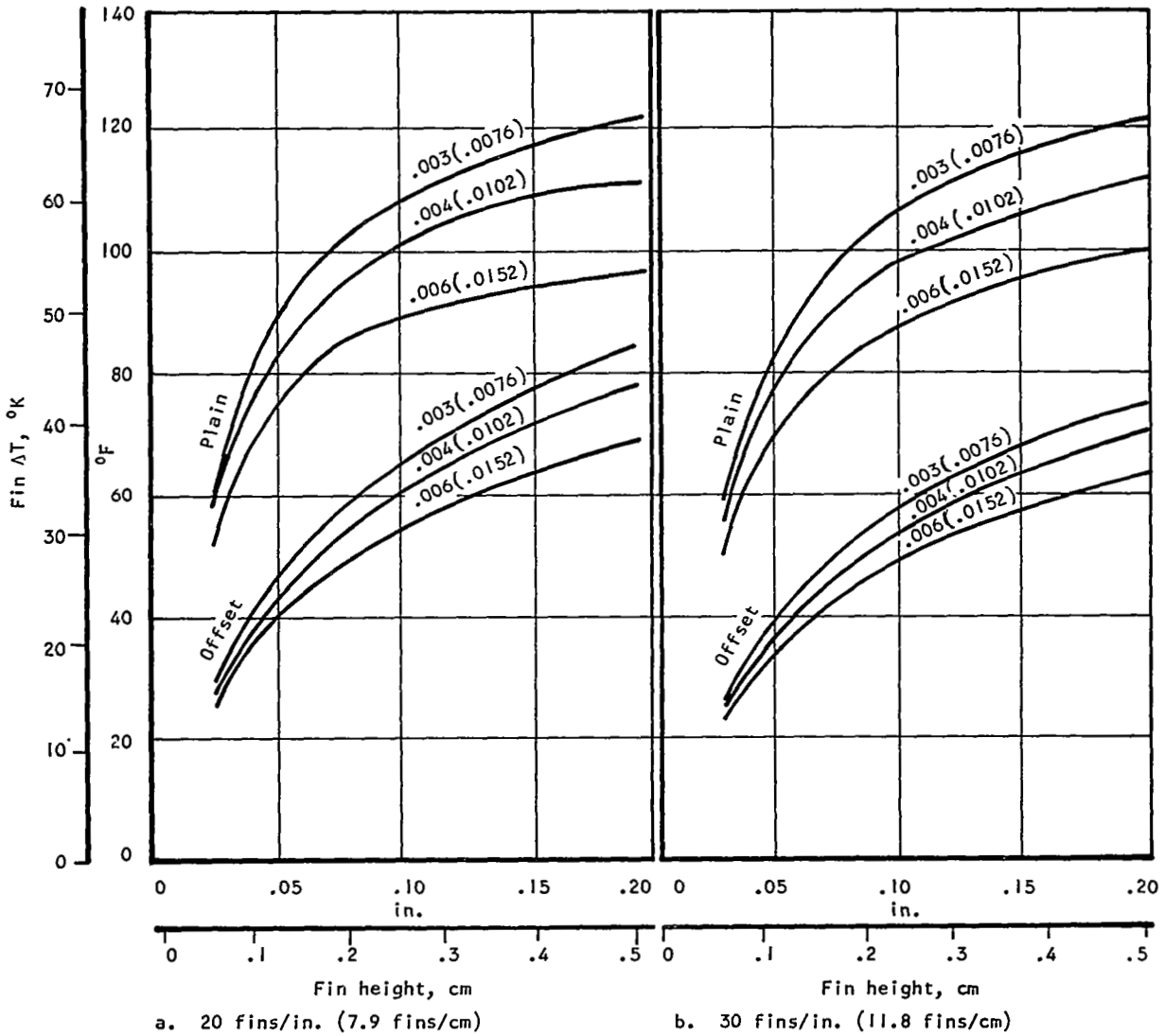


Figure 64. Fin ΔT vs Fin Height for a Heat Flux of 10 Btu/sec-ft² (114 kW/m²)

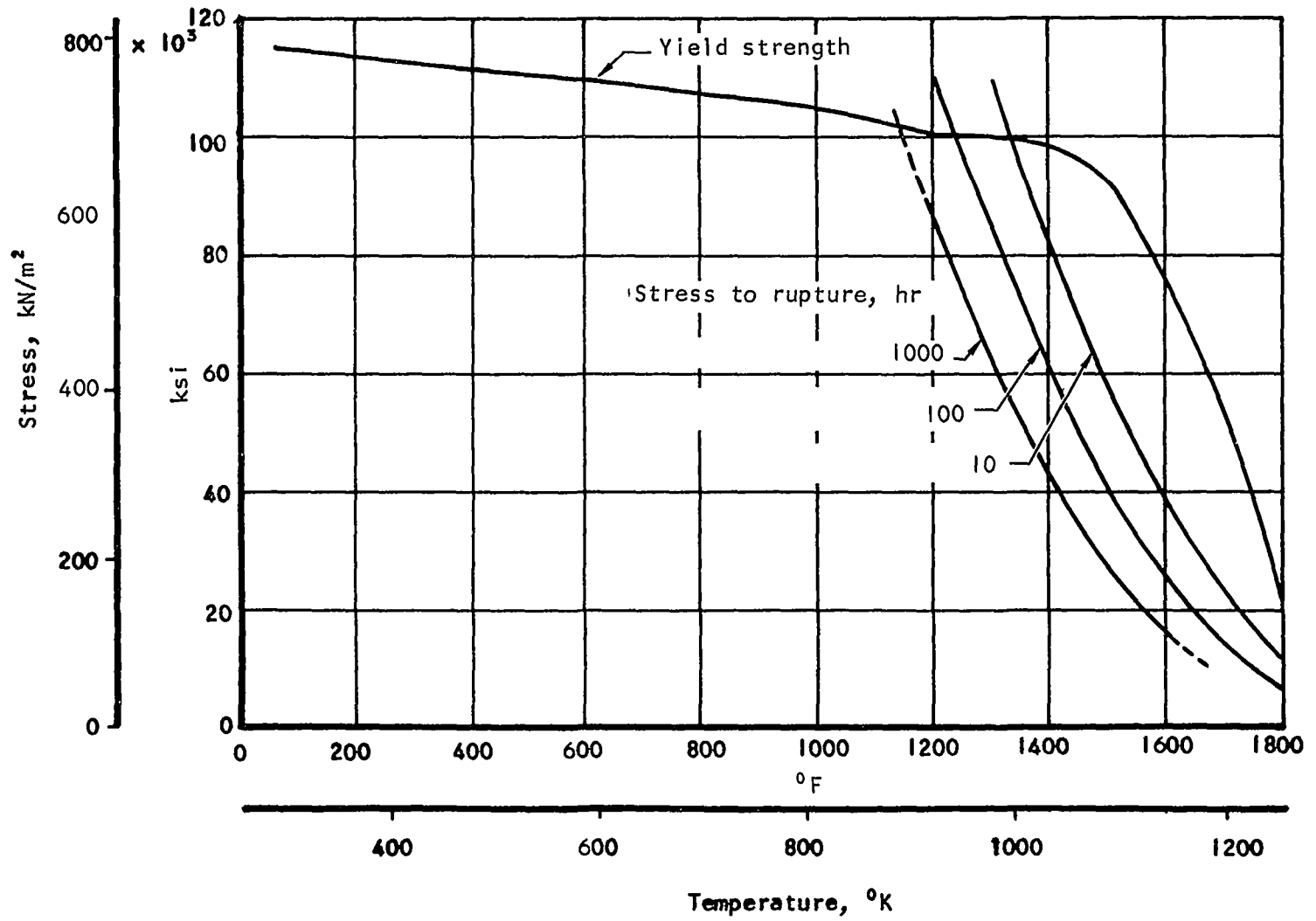


Figure 65. Waspaloy Strength Data vs Temperature

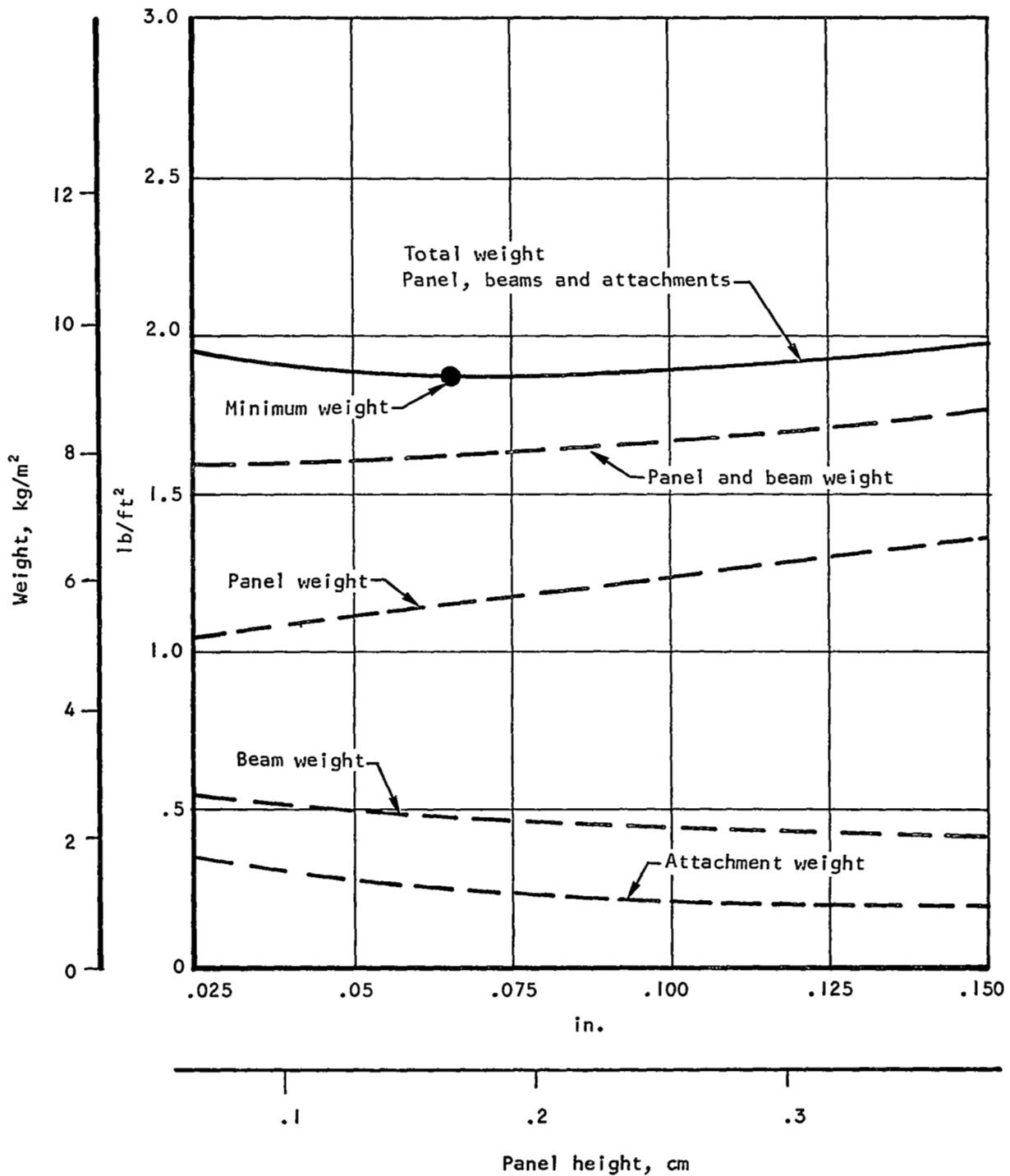


Figure 66. Concept 1 Weight vs Panel Height at 7 psi (48 kN/m²)

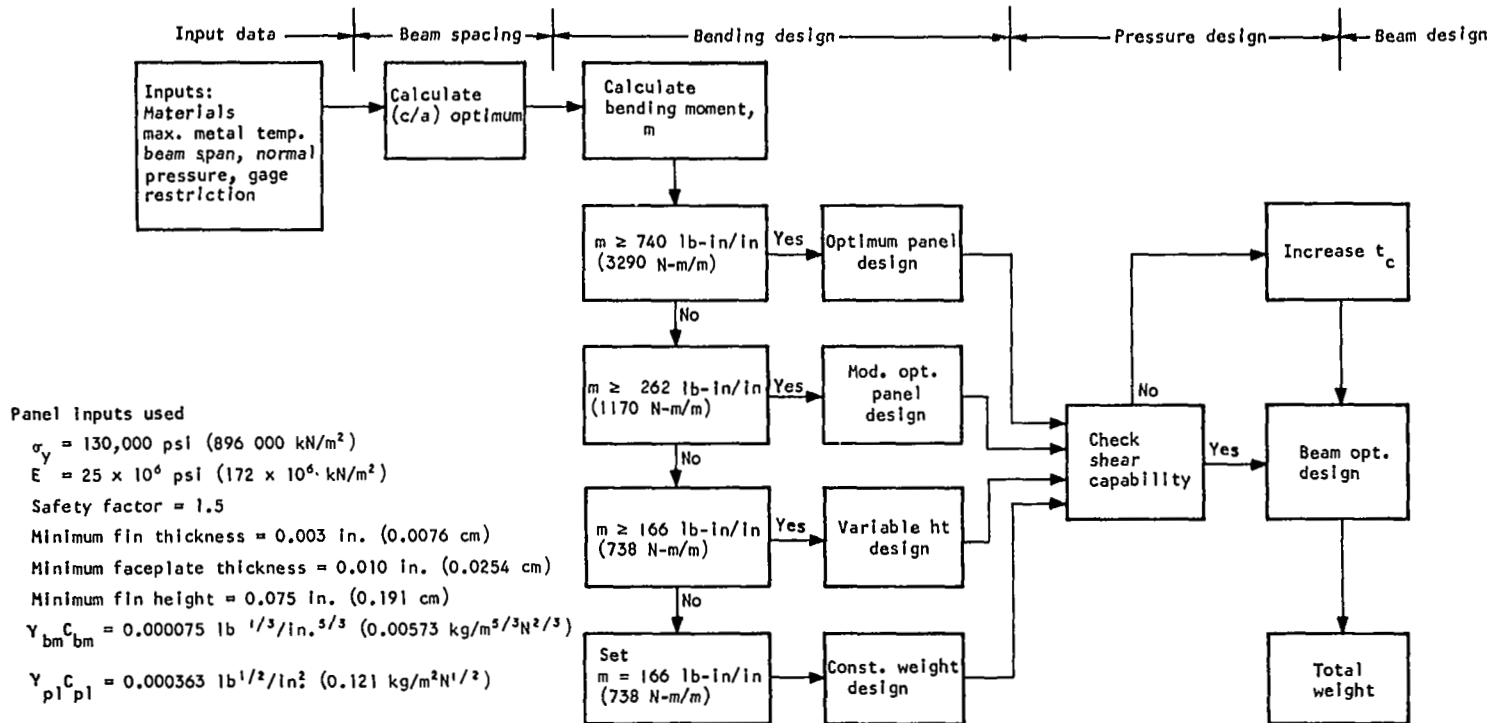


Figure 67. Structural Design Flow Diagram

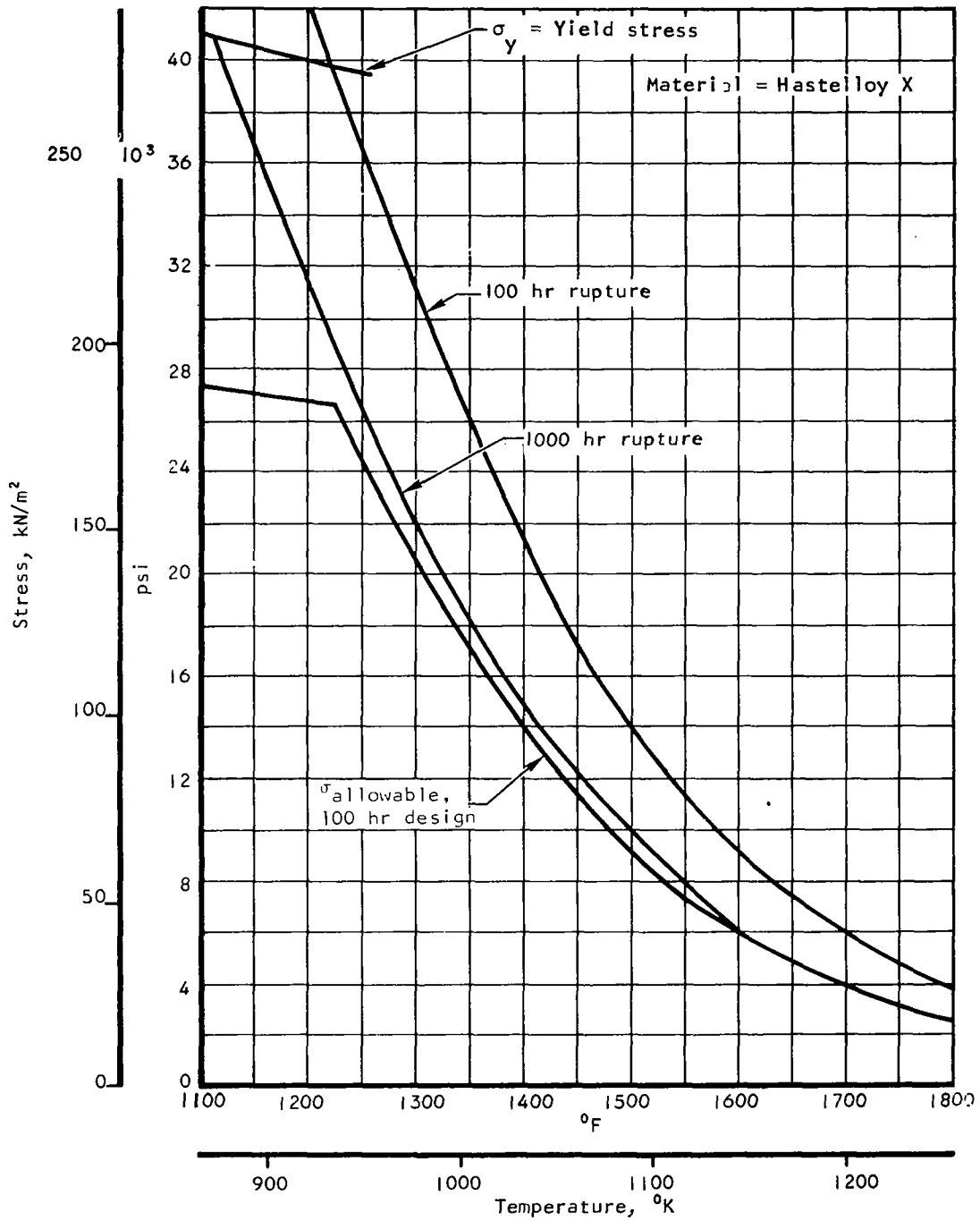


Figure 68. Fin Design Stress

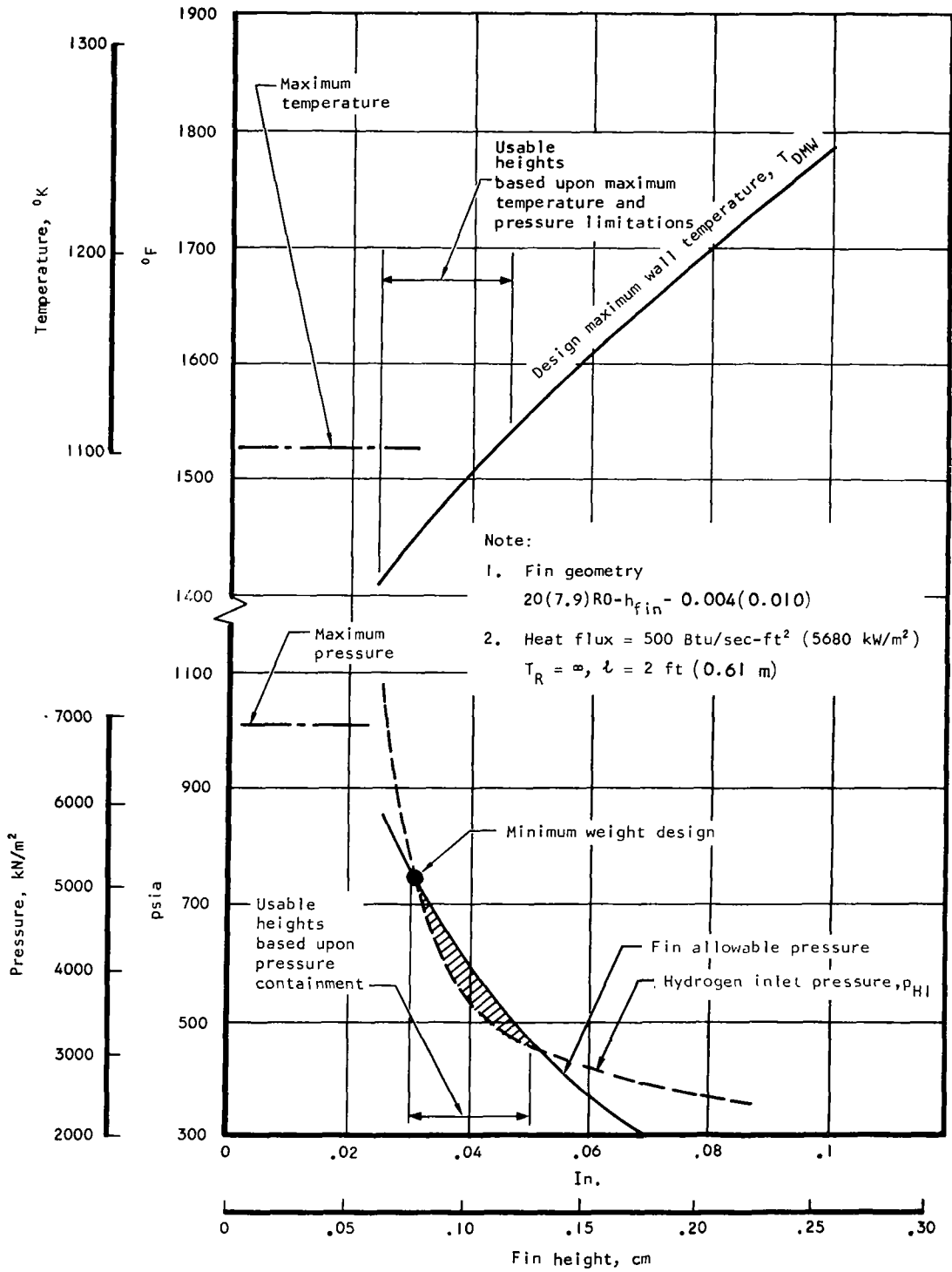


Figure 69. Heat Exchanger Design Curves

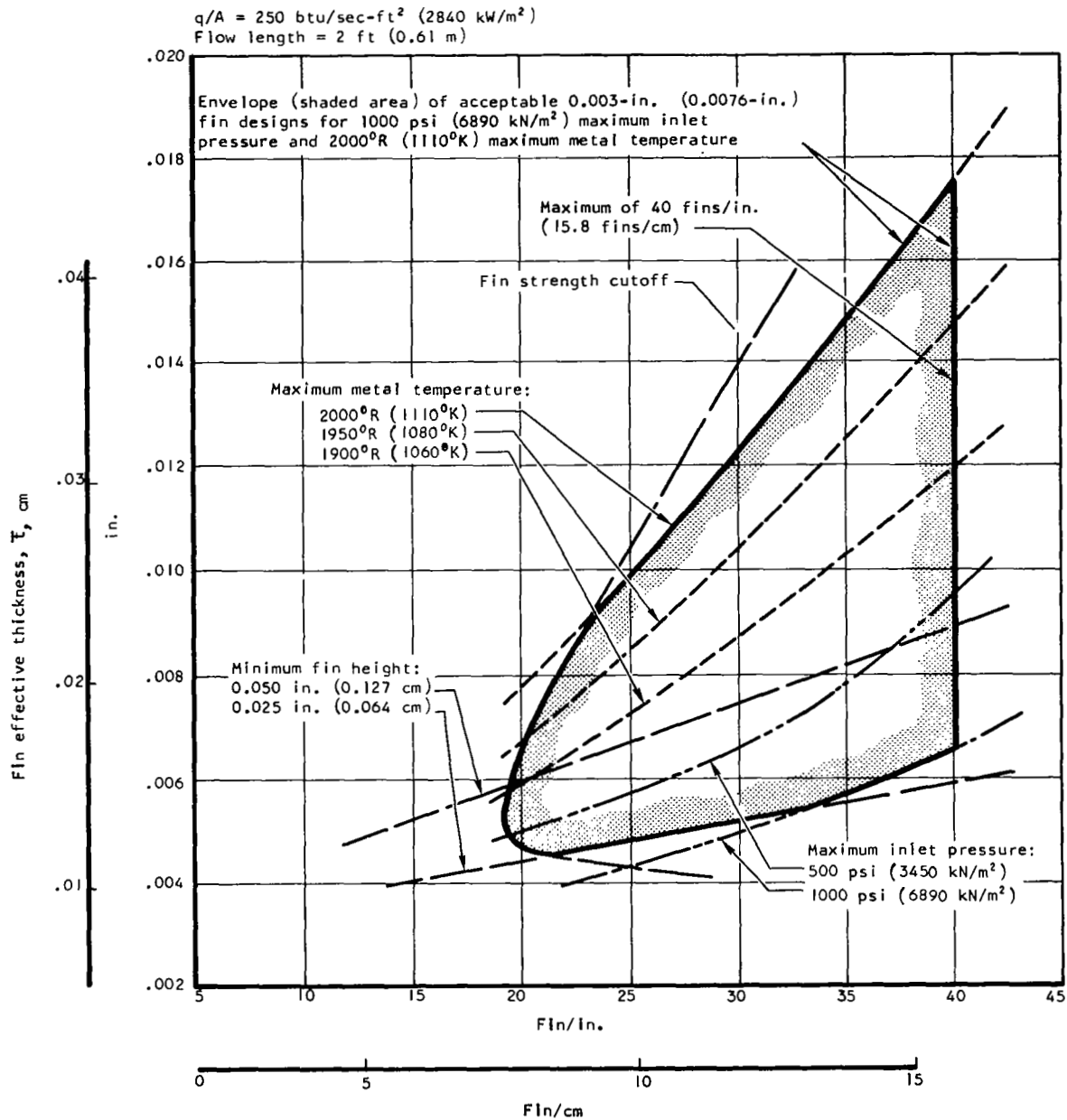


Figure 70. Envelope of Acceptable 0.003-in. (0.0076-cm) Fin Thickness Designs for a Heat Flux of 250 Btu/sec-ft² (2840 KW/m²)

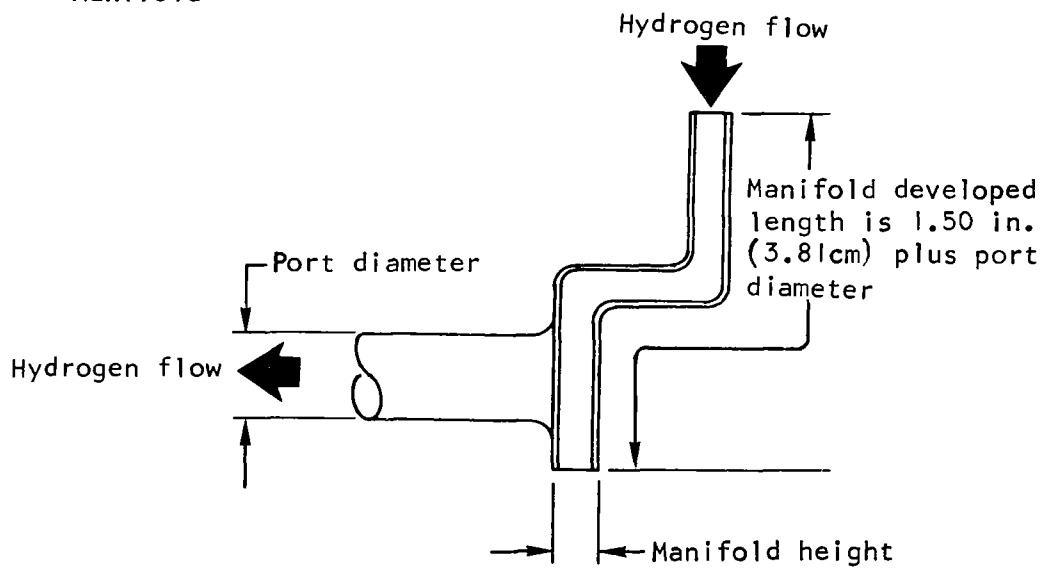
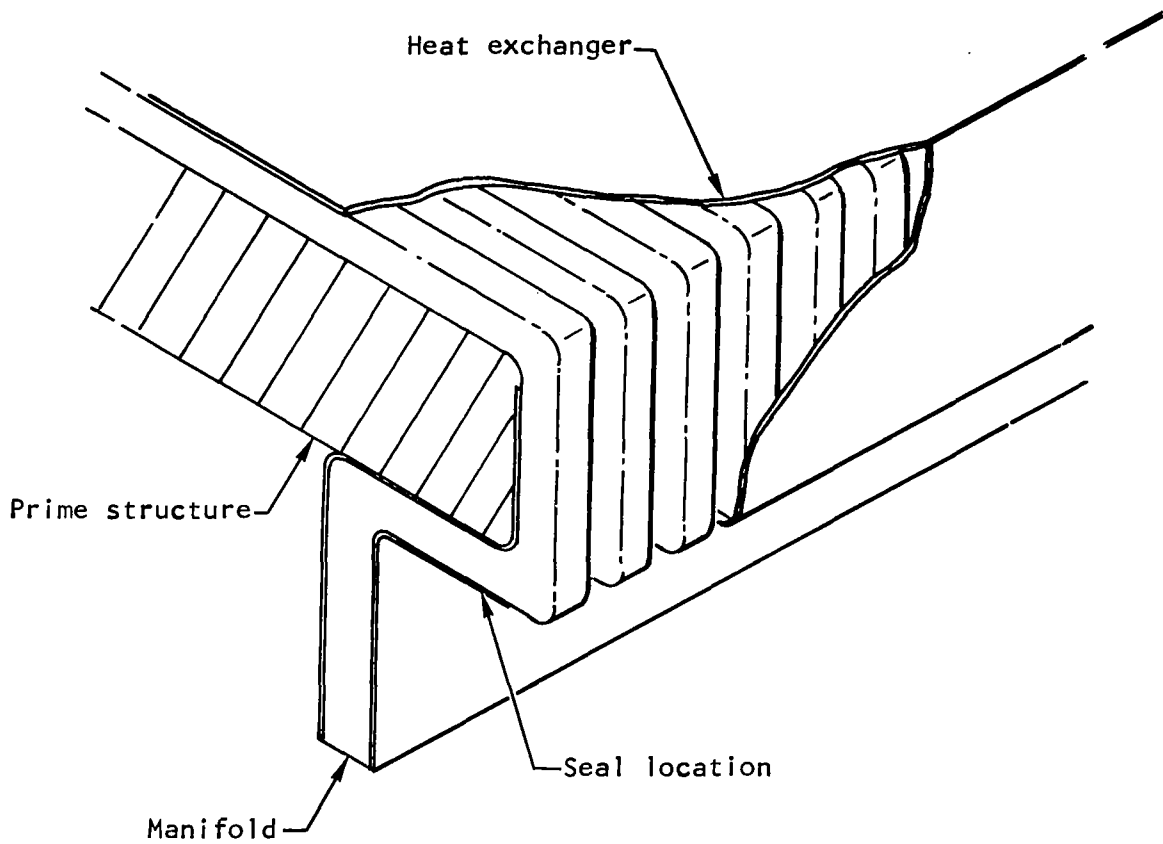


Figure 71. Manifold Arrangement

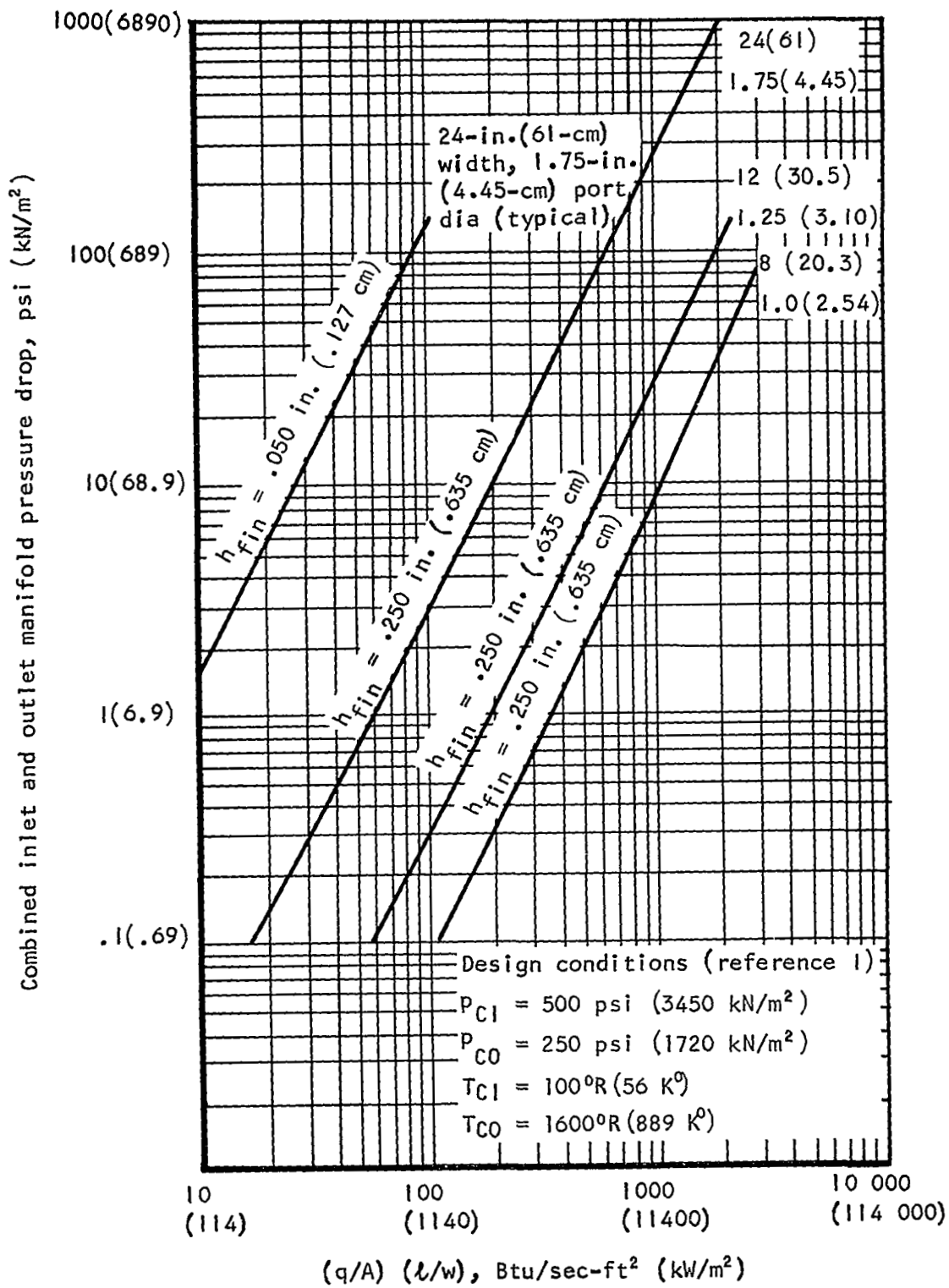
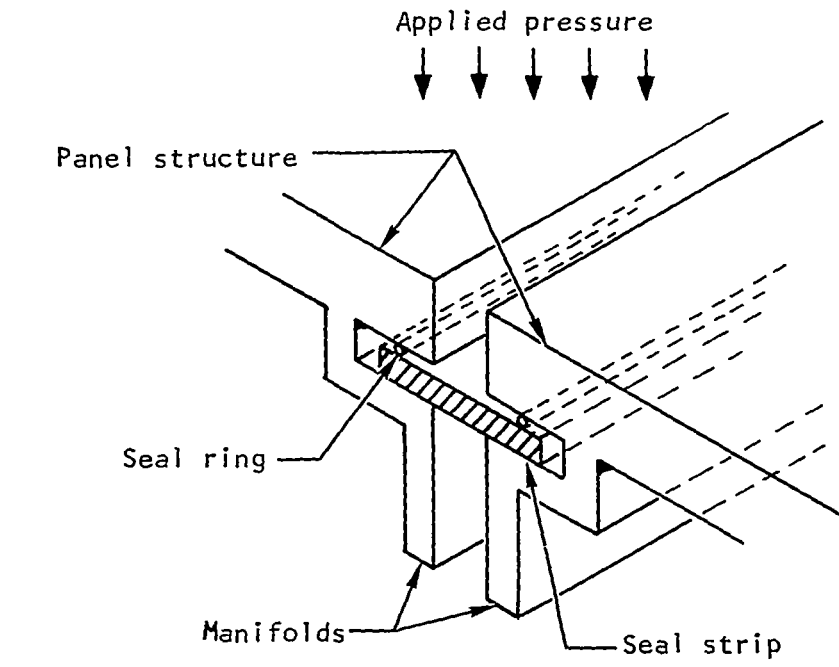
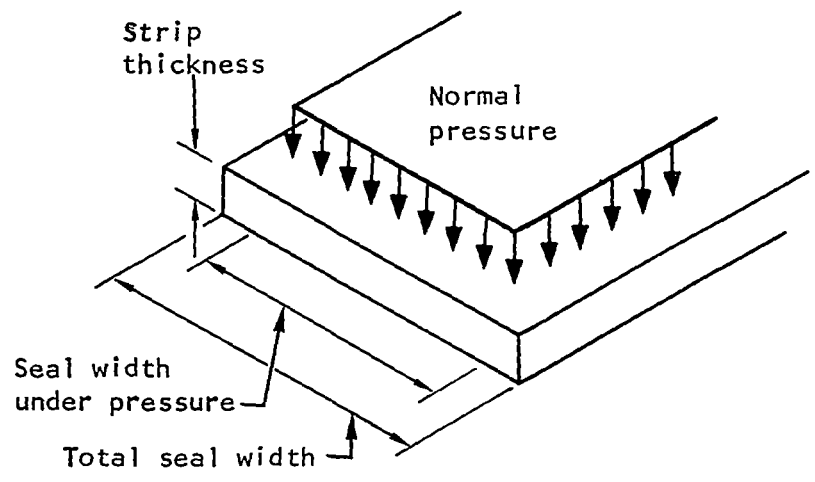


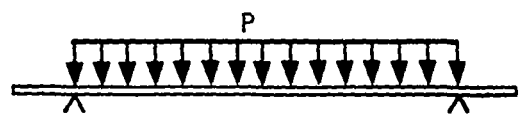
Figure 72. Total Manifold Pressure Drop vs $(q/A)(l/w)$ for Several Manifold Geometries with a Fin Geometry of $10(3.9)\text{R-}h_{fin} - 0.004(0.010)$



a. Seal and panel layout

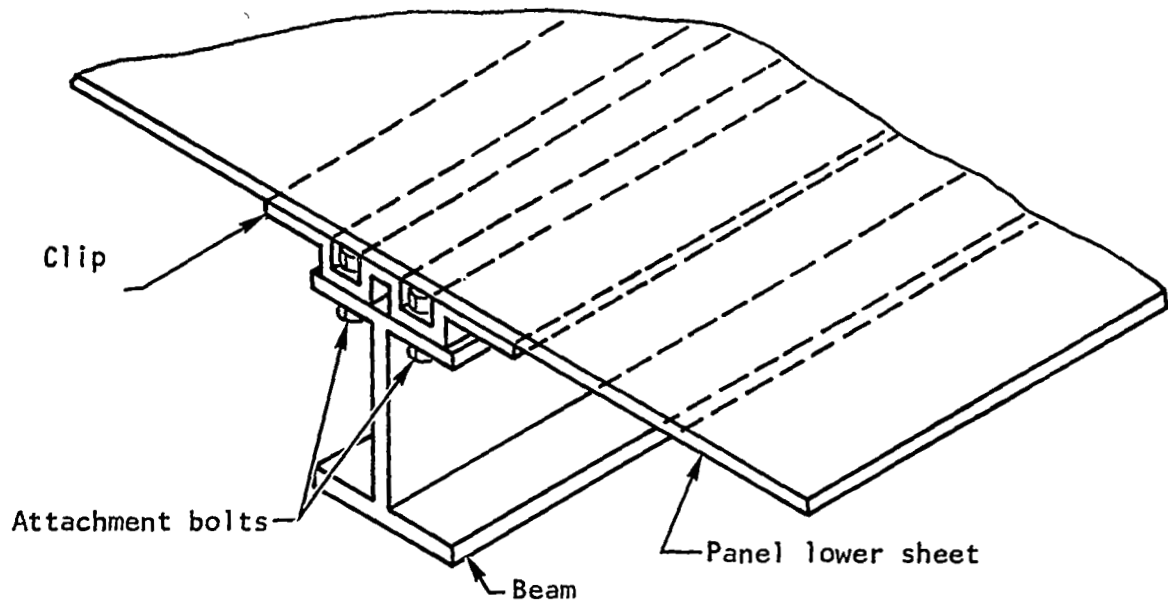


b. Seal schematic

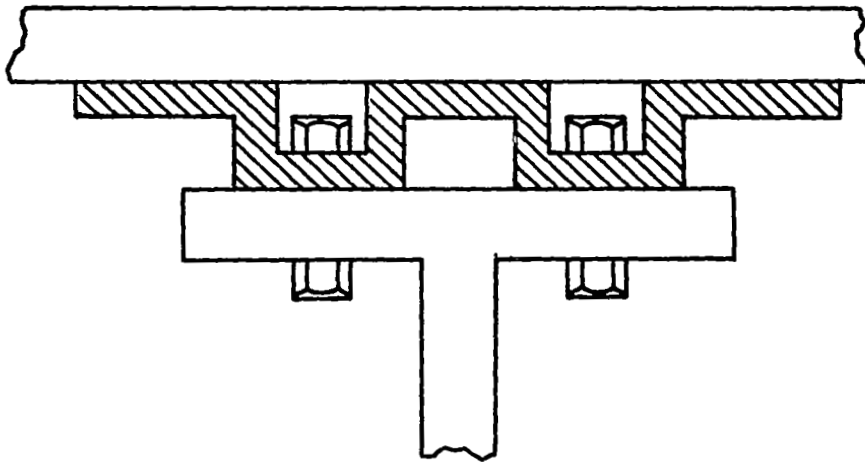


c. Seal loading and support diagram

Figure 73. Panel Seal Design



a. Overall view



b. Clip detail

Figure 74. Attachment Clip Design

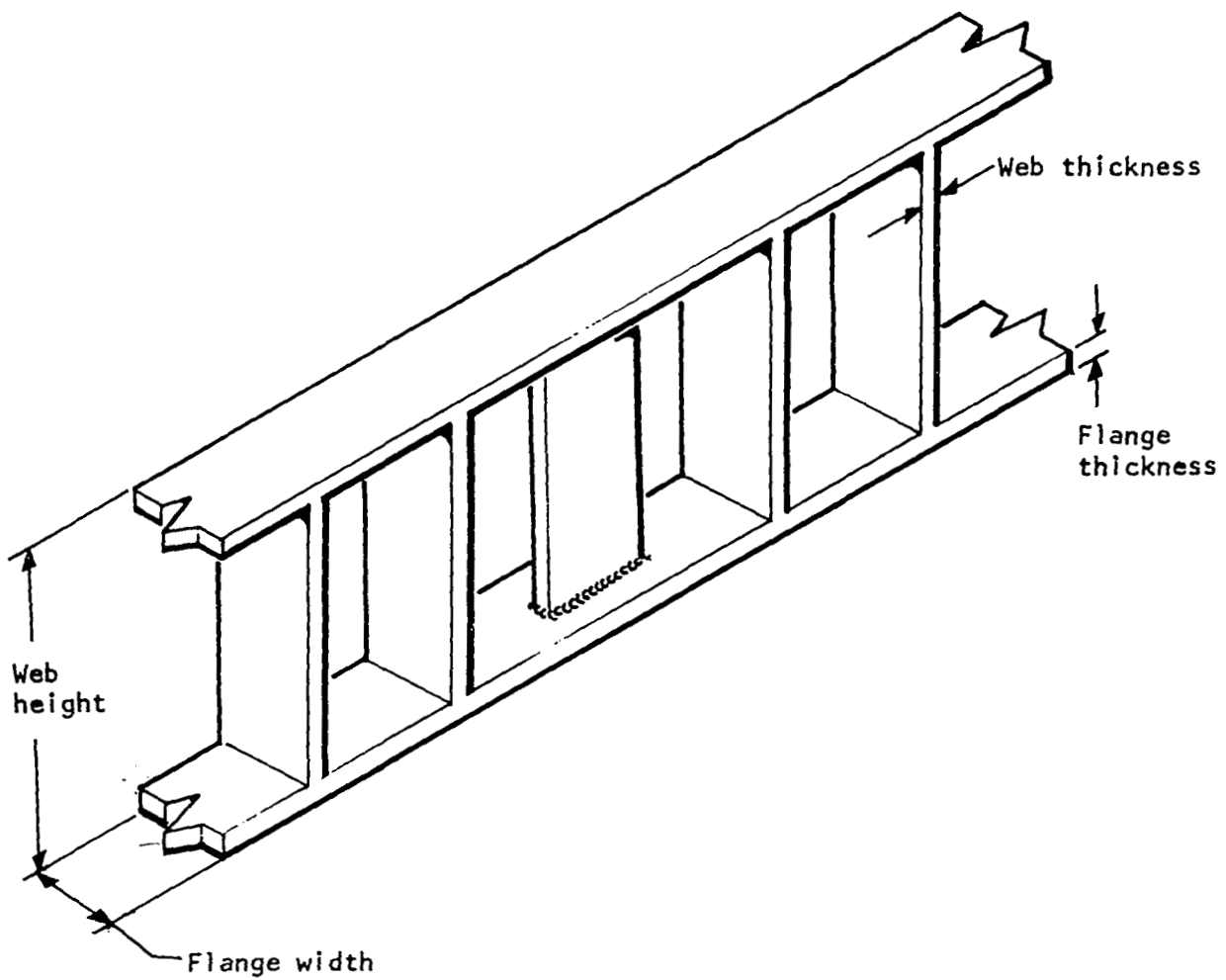


Figure 75. Spacer Beam Design Concept